Interreg - IPA CBC
Croatia - Serbia

Rescue

Renewable Energy Sources for smart sustainable health Centers, University Education and other public buildings

Study with recommendations for increasing RES use, establishing BEMS and EE improvement in public buildings in cross-border area

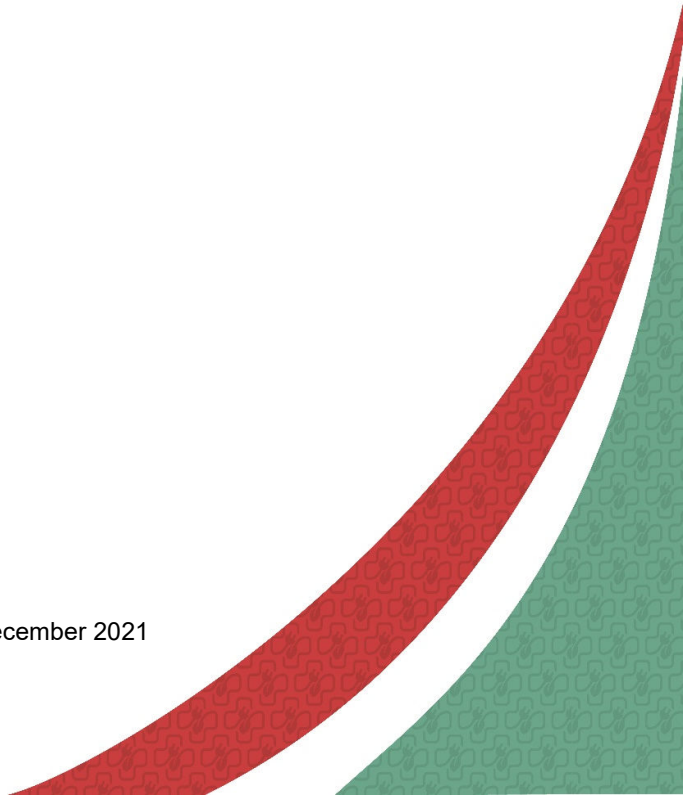

December 2021

Title page

Study with recommendations for increasing RES use, establishing BEMS and EE improvement in public buildings in cross-border area

Supported by: IPA Cross-border Cooperation Programme Croatia - Serbia 2014-2020

Project: Renewable energy sources for smart sustainable health centers, university education and other public buildings – RESCUE

Documentation type: Study

Abstract: This document presents a comprehensive study with recommendations for increasing RES use, establishing BEMS and EE improvement in public buildings in cross-border area. The study describes the available renewable energy sources that could be used for energy generation in the near vicinity of the public building. After exploring the demand and the potential, the study proposes the optimal configuration of the renewable energy and the smart building energy management systems that would significantly increase the public building efficiency while reducing the energy demand, bringing the public building one step closer to near zero-energy building.

Financing: **Project budget:** 1.936.989,91 € (EU IPA II funding 1.646.411,40 €)
FTN budget: 402.952,39 € (EU IPA II funding 342.509,53 €)

Project partners:
Faculty of Technical Sciences, Novi Sad
Clinical Centre of Vojvodina, Novi Sad
Faculty of Electrical Engineering, Computer Science and Information Technology, Osijek
Clinical Hospital Center, Osijek
Mechanical Engineering Faculty, Slavonski Brod

Signature:
Faculty of Technical Sciences, Trg Dositeja Obradovića 6, 21000 Novi Sad, Serbia

prof. dr Boris Dumnić, RESCUE project coordinator

Table of Contents

1. INTRODUCTION 17

2. THE MAIN FEATURES OF THE LOCATIONS AND THE BUILDINGS FOR THE EXEMPLARY FACILITIES 23

2.1. BUILDINGS FOR THE EXEMPLARY FACILITIES 23
2.1.1. FTN buildings 23
2.1.2. KCV buildings 24
2.1.3. FERIT buildings 27
2.1.4. KBCO buildings 29
2.1.5. UNISB building 33
2.2. CLIMATE CONDITIONS IN THE SURROUNDING AREA 36
2.2.1. FTN and KCV climate conditions 36
2.2.2. FERIT and KBCO climate conditions 37
2.2.3. UNISB climate conditions 41

3. CURRENT ENERGY DEMAND OVERVIEW FOR THE PUBLIC BUILDING 44

3.1. FTN BUILDINGS POWER SUPPLY AND ENERGY DEMAND 44
3.2. KCV BUILDINGS POWER SUPPLY AND ENERGY DEMAND 49
3.3. FERIT BUILDINGS POWER SUPPLY AND ENERGY DEMAND 62
3.4. KBCO BUILDINGS POWER SUPPLY AND ENERGY DEMAND 68
3.5. UNISB BUILDING POWER SUPPLY AND ENERGY DEMAND 71
3.5.1. The electrical infrastructure of the exemplary object and consumption analysis 71
3.5.2. The power supply of the "UNISB - Strojarski fakultet u Slavonskom Brodu, building in Ivan Gundulić Street 20a" 71
3.5.3. Analysis of the energy consumption 73
3.5.4. The thermal infrastructure of the exemplary object and consumption analysis 75
3.5.5. The analysis of the heat energy consumption 77

4. THE OVERVIEW OF THE POTENTIAL FOR THE AVAILABLE RENEWABLE ENERGY RESOURCES 78

4.1. FTN AND KCV POTENTIAL OF RENEWABLE ENERGY SOURCES 78
4.2. FERIT AND KBCO POTENTIAL OF RENEWABLE ENERGY SOURCES 91
4.2.1. Solar energy 92
4.2.2. Wind energy 94
4.2.3. Waste and biofuels 96
4.3. UNISB POTENTIAL OF RENEWABLE ENERGY SOURCES 98

5. PLANNED OPTIMAL RENEWABLE ENERGY SYSTEM TOPOLOGY AND BUILDING ENERGY MANAGEMENT SYSTEM FOR THE EXEMPLARY FACILITES 99

5.1. FTN RENEWABLE ENERGY SYSTEMS 99
5.1.1. Photovoltaic system 99
5.1.2. Solar tree 101
5.1.3. Photovoltaic based electric vehicle charging station 102
5.1.4. Renewable energy storage/supply system 104
5.1.5. Wind energy system 105
5.1.6. Heating, ventilation and air conditioning (HVAC) system 106
5.2. KCV RENEWABLE ENERGY SYSTEMS 107
5.3. FERIT RENEWABLE ENERGY SYSTEMS 114

5.3.1. Photovoltaic systems on the buildings roofs *115*
5.3.2. Renewable energy storage/supply system *121*
5.3.3. Wind energy system *122*
5.4. KBCO RENEWABLE ENERGY SYSTEMS 123
5.4.1. Photovoltaic systems on the buildings roofs *124*
5.4.2. Biodiesel generator and biodiesel production system *128*
5.5. UNISB RENEWABLE ENERGY SYSTEMS 129
5.5.1. Solar-Thermal systems *129*
5.5.2. Photovoltaic systems *130*
5.6. BUILDING ENERGY MANAGEMENT SYSTEMS 132

6. INSTALLED RENEWABLE ENERGY SYSTEMS FOR THE EXEMPLARY FACILITIES 137

6.1. FTN RENEWABLE ENERGY SYSTEMS 137
6.1.1. Photovoltaic system *137*
6.1.2. Solar tree *144*
6.1.3. Photovoltaic based electric vehicle charging station *146*
6.1.4. Renewable energy storage/supply system *149*
6.1.5. Wind energy system *153*
6.1.6. Heating, ventilation and air conditioning (HVAC) system *156*
6.2. KCV RENEWABLE ENERGY SYSTEMS 158
6.3. FERIT RENEWABLE ENERGY SYSTEMS 166
6.3.1. Photovoltaic systems on the buildings roofs *166*
6.3.2. Renewable energy storage/supply system *176*
6.4. KBCO RENEWABLE ENERGY SYSTEMS 178
6.4.1. Photovoltaic systems on the buildings roofs *178*
6.4.2. Biodiesel generator and biodiesel production system *185*
6.5. UNISB RENEWABLE ENERGY SYSTEMS 186
6.5.1. Technical description of Photovoltaic power plant UNISB, Gunduliceva 20A *186*
General data *186*
Connections (cables) *186*
Photovoltaic modules *187*
Inverter *188*
Lightning, overvoltage and surface protection *189*
Construction *189*
6.5.2. Technical description of thermotechnical system with heat pump and solar collectors at UNISB, Gunduliceva 20A *200*
General data *200*
Devices and assemblies of thermo-technical system *200*
Functionality and regulation of heating and cooling *201*

7. BUILDING ENERGY MANAGEMENT SYSTEMS FOR THE EXEMPLARY FACILITIES 210

7.1. FTN BUILDING ENERGY MANAGEMENT SYSTEM 210
7.2. KCV BUILDING ENERGY MANAGEMENT SYSTEM 213
7.3. FERIT BUILDING ENERGY MANAGEMENT SYSTEM 215
7.4. KBCO BUILDING ENERGY MANAGEMENT SYSTEM 219
7.5. UNISB BUILDING ENERGY MANAGEMENT SYSTEM 221
7.6. RESULTS 222

CONCLUSION 232

8. REFERENCES 233

List of figures

FIGURE 1.1 THE PREDICTION OF FOSSIL FUEL ENERGY RESERVES [1]. 17
FIGURE 1.2 CARBON DIOXIDE (CO_2) EMISSION BY A SPECIFIC TYPE OF FOSSIL FUEL [2]. ... 18
FIGURE 1.3 THE PREDICTION OF THE CO_2 EMISSION BASED ON DIFFERENT SCENARIOS [2]. 19
FIGURE 1.4 INVESTMENT IN DIFFERENT RENEWABLE ENERGY TECHNOLOGIES [6]. 20
FIGURE 1.5 WORLD NET ELECTRICITY GENERATION [8]. 21
FIGURE 2.1 LOCATION OF "MAŠINSKI INSTITUT" FACILITY. 23
FIGURE 2.2 THE MAIN ENTRANCE TO "MAŠINSKI INSTITUT". 24
FIGURE 2.3 PART OF "MAŠINSKI INSTITUT" WITH LABORATORIES FOR SCIENTIFIC RESEARCH. 24
FIGURE 2.4 FACILITIES IN THE KCV COMPLEX 25
FIGURE 2.5 MEDICAL REHABILITATION CLINIC INSIDE KCV COMPLEX 26
FIGURE 2.6 RADIOLOGY CLINIC INSIDE KCV COMPLEX 26
FIGURE 2.7 EMERGENCY CENTER FACILITY INSIDE KCV COMPLEX 27
FIGURE 2.8 LOCATION OF FACULTY OF ELECTRICAL ENGINEERING, COMPUTER SCIENCE AND INFORMATION TECHNOLOGY OSIJEK BUILDING IN TRPIMIROVA STREET [12] 28
FIGURE 2.9 LOCATION OF FACULTY OF ELECTRICAL ENGINEERING, COMPUTER SCIENCE AND INFORMATION TECHNOLOGY OSIJEK BUILDING IN CARA HADRIJANA STREET [12]. ... 28
FIGURE 2.10 THE MAIN ENTRANCE TO THE BUILDING IN TRPIMIROVA STREET. 29
FIGURE 2.11 THE MAIN ENTRANCE TO THE BUILDING IN CARA HADRIJANA STREET. 29
FIGURE 2.12 LOCATION OF KBCO COMPLEX IN HUTTLER STREET [12]. 31
FIGURE 2.13 NORTH SIDE OF THE CENTRAL KITCHEN BUILDING. 32
FIGURE 2.14 WEST SIDE OF THE BUILDING OF DEPARTMENT OF ONCOLOGY. 32
FIGURE 2.15 NORTH SIDE OF THE BUILDING OF DEPARTMENT OF DIAGNOSTICAL INTERVENTIONAL RADIOLOGY 33
FIGURE 2.16 LOCATION OF THE MECHANICAL ENGINEERING FACULTY BUILDING [12] 34
FIGURE 2.17 SITUATIONAL PLAN OF THE MECHANICAL ENGINEERING FACULTY FACILITY [12] 34
FIGURE 2.18 THE MAIN ENTRANCE TO FACILITY II OF MECHANICAL ENGINEERING FACULTY 35
FIGURE 2.19 PART OF MECHANICAL ENGINEERING FACULTY WITH PARKING AREA AND INSTALLED SOLAR THERMAL AND HEAT PUMP`S SYSTEMS 35
FIGURE 2.20 PART OF MECHANICAL ENGINEERING FACULTY WITH CLASSROOMS AND OFFICES WHERE THE THERMO-TECHNICAL (SOLAR THERMAL AND HEAT PUMPS) SYSTEM AND PHOTOVOLTAIC POWER PLANT ARE INSTALLED 35
FIGURE 2.21 ROSE WIND FOR NOVI SAD. 36

FIGURE 2.22 – MEAN ANNUAL WIND SPEED IN CROATIA (M/S) [14]. 38
FIGURE 2.23 MEAN ANNUAL POWER DENSITY IN CROATIA (W/M^2) [14]. 39
FIGURE 2.24 COMPARISON OF AIR TEMPERATURE TO THE AVERAGE FOR THE 1963 – 2018 PERIOD IN SLAVONSKI BROD 42
FIGURE 2.25 INSOLATION DURATION (H) IN SLAVONSKI BROD 43
FIGURE 3.1 TRANSFORMER STATION SINGLE LINE DIAGRAM. 45
FIGURE 3.2 ELECTRICAL ENERGY CONSUMPTION PER MONTH IN THE "MAŠINSKI INSTITUT" DURING 2018. 48
FIGURE 3.3 HEAT ENERGY CONSUMPTION PER MONTH IN THE "MAŠINSKI INSTITUT" DURING 2018. 49
FIGURE 3.10 ELECTRIC POWER CONSUMPTION IN "ZTS URGENTNI CENTAR" IN 2018 58
FIGURE 3.13 GRAPH OF THE THERMAL ENERGY CONSUMPTION OF THE OBJECT IN QUESTION 62
FIGURE 3.14 MAIN DISTRIBUTION CABINET SINGLE LINE DIAGRAM OF THE BUILDING IN TRPIMIROVA STREET. 63
FIGURE 3.15 SINGLE LINE DIAGRAM OF 10 KW PHOTOVOLTAIC PLANT ON THE BUILDING ROOF IN TRPIMIROVA STREET. 64
FIGURE 3.16 SINGLE LINE DIAGRAM OF THE POWER SUPPLY OF BUILDING IN CARA HADRIJANA STREET. 66
FIGURE 3.17 ELECTRICITY CONSUMPTION PER MONTH OF THE BUILDING IN TRPIMIROVA STREET DURING 2018. 68
FIGURE 3.18 ELECTRICITY CONSUMPTION PER MONTH OF THE BUILDING IN CARA HADRIJANA STREET DURING 2018. 68
FIGURE 3.19 KBCO COMPLEX POWER SUPPLY SCHEMATIC [16] 69
FIGURE 3.20 ELECTRICITY CONSUMPTION PER MONTH OF ALL KBCO FACILITIES DURING 2018. 70
FIGURE 3.21 TRANSFORMER STATION SINGLE LINE DIAGRAM 72
FIGURE 3.22 ELECTRICAL ENERGY CONSUMPTION PER MONTH IN THE "STROJARSKI FAKULTET U SLAVONSKOM BRODU, I. GUNDULIĆ STREET" DURING 2018 75
FIGURE 3.23 ANALYSIS OF GAS CONSUMPTION FOR FACULTY BUILDING AT IVAN GUNDULIĆ STREET 20A 77
FIGURE 4.1 THE PROJECTION OF THE CONSTRUCTION OF PLANTS FOR ELECTRICITY GENERATION USING RES UNTIL 2030 [17]. 78
FIGURE 4.2 THE TOTAL PLANNED PRODUCTION OF PRIMARY ENERGY FROM INDIVIDUAL RES FOR 2019. 79
FIGURE 4.3 GLOBAL IRRADIATION AND SOLAR ELECTRICITY POTENTIAL OF THE REPUBLIC OF SERBIA 80
FIGURE 4.4 GLOBAL IRRADIATION AND SOLAR ELECTRICITY POTENTIAL FOR THE OPTIMALLY-INCLINED PHOTOVOLTAIC MODULES OF THE REPUBLIC OF SERBIA [18]. 81

FIGURE 4.5 DAILY AVERAGE IRRADIANCE ON THE FIXED PLANE WITH SLOPE 0° AND AZIMUTH 0° FOR THE MONTH OF JULY, CITY OF NOVI SAD [18]. 83

FIGURE 4.6 DAILY AVERAGE IRRADIANCE ON THE FIXED PLANE WITH SLOPE 35°, AND AZIMUTH 0° FOR THE MONTH OF JULY, CITY OF NOVI SAD [18]. 85

FIGURE 4.7 DAILY AVERAGE TEMPERATURE FOR THE MONTH OF JULY, CITY OF NOVI SAD [18]. 87

FIGURE 4.8 MONTHLY AVERAGE IRRADIANCE ON THE FIXED PLANE WITH SLOPE 0°, AND AZIMUTH 0° FOR THE YEAR OF 2016, CITY OF NOVI SAD [18]..... 87

FIGURE 4.9 THE MORPHOLOGICAL COMPOSITION OF MUNICIPAL WASTE IN THE REPUBLIC OF SERBIA [20]. 89

FIGURE 4.10 SHARE OF INDIVIDUAL SECTORS IN THE TOTAL AMOUNT OF WASTE 90

FIGURE 4.11 GENERATED QUANTITIES OF HAZARDOUS AND NON-HAZARDOUS WASTE IN THE PERIOD 2010-2013 91

FIGURE 4.12 – ANNUAL GLOBAL SOLAR IRRADIATION ON HORIZONTAL SURFACE IN REPUBLIC OF CROATIA [22]. 92

FIGURE 4.13 – ANNUAL GLOBAL SOLAR IRRADIATION ON OPTIMALLY INCLINED SURFACE IN REPUBLIC OF CROATIA [22]. 93

FIGURE 4.14 MONTHLY MEAN VALUES OF WIND SPEED FOR 2015 AT THE WEATHER STATION IN ČEPIN NEAR OSIJEK..... 95

FIGURE 4.15 WIND SPEED FREQUENCY AT THE MICROLOCATION OF FERIT BUILDING IN TRPIMIROVA STREET 96

FIGURE 4.16 – ROSE OF WINDS FOR THE MICROLOCATION OF FERIT BUILDING IN TRPIMIROVA STREET 96

FIGURE 5.1 THE LOCATION FOR THE PV PLANT CONSTRUCTION. 100

FIGURE 5.2 BLOCK DIAGRAM OF THE PV PLANT. 100

FIGURE 5.3 ESTIMATED ELECTRICAL ENERGY PRODUCTION OF THE PV PLANT, LOCATED AT THE EXEMPLARY OBJECT..... 101

FIGURE 5.4 BLOCK DIAGRAM OF THE SOLAR TREE SYSTEM USED AS A GENERATOR FOR ASSISTIVE DEVICES CHARGING STATION. 102

FIGURE 5.5 ESTIMATED ELECTRICAL ENERGY PRODUCTION OF THE SOLAR TREE USED AS AN ASSISTIVE DEVICES CHARGING STATION, LOCATED AT THE EXEMPLARY OBJECT. 102

FIGURE 5.6 BLOCK DIAGRAM OF THE PHOTOVOLTAIC SYSTEM FOR THE ELECTRIC VEHICLE CHARGING POWER PRODUCTION. 103

FIGURE 5.7 ESTIMATED ELECTRICAL ENERGY PRODUCTION OF THE PV BASED SYSTEM USED TO CHARGE ELECTRIC VEHICLES, LOCATED AT THE EXEMPLARY OBJECT..... 104

FIGURE 5.8 BLOCK DIAGRAM OF THE ENERGY STORAGE/SUPPLY SYSTEM. 105

FIGURE 5.9 BLOCK DIAGRAM OF THE WIND POWER SYSTEM. 105

FIGURE 5.10 ESTIMATED ELECTRICAL ENERGY PRODUCTION OF THE WIND BASED SYSTEM. 106

FIGURE 5.11 BLOCK DIAGRAM OF THE HVAC SYSTEM. 107

FIGURE 5.12 BLOCK DIAGRAM OF THE PV PLANT ON THE RADIOLOGY CLINIC ROOF 108
FIGURE 5.13 ESTIMATED ELECTRICAL ENERGY PRODUCTION OF THE PV PLANT, LOCATED ON THE RADIOLOGY CLINIC ROOFTOP. 109
FIGURE 5.14 BLOCK DIAGRAM OF THE PV PLANT ON THE EMERGENCY CENTER ROOFTOP 109
FIGURE 5.15 ESTIMATED ELECTRICAL ENERGY PRODUCTION OF THE PV PLANT, LOCATED ON THE EMERGENCY CENTER ROOFTOP 110
FIGURE 5.16 BLOCK DIAGRAM OF THE PV PLANT ON KCV PARKING 110
FIGURE 5.17 ESTIMATED ELECTRICAL ENERGY PRODUCTION OF THE PV PLANT, LOCATED ON THE KCV PARKING 111
FIGURE 5.18 MONTHLY SOLAR IRRADIANCE ON THE LOCATION OF THE MEDICAL REHABILITATION CLINIC 112
FIGURE 5.19 BLOCK DIAGRAM OF SOLAR THERMAL SYSTEM LOCATED ON MEDICAL REHABILITATION CLINIC ROOF 112
FIGURE 5.20 SOLAR THERMAL ENERGY DELIVERED TO THE SYSTEM [KWH] 113
FIGURE 5.21 SYSTEM FOR BIO-DIESEL PRODUCTION FROM WASTE OIL 114
FIGURE 5.22 BLOCK DIAGRAM OF 75 KW PV SYSTEM ON BUILDING IN TRPIMIROVA STREET 115
FIGURE 5.23 PRELIMINARY 3D MODEL OF 75 KW PV SYSTEM ON BUILDING ROOF IN TRPIMIROVA STREET (WITH POSSIBLE WALL-MOUNTED MODULES DEPENDING ON ROOF SHADING) 116
FIGURE 5.24 BLOCK DIAGRAM OF 5 KW PV BASED E-BIKE CHARGING STATION. 117
FIGURE 5.25 ESTIMATED ELECTRICITY PRODUCTION OF 80 KW PV SYSTEMS ON BUILDING IN TRPIMIROVA STREET 118
FIGURE 5.26 BLOCK DIAGRAM OF 35 KW PV SYSTEM ON BUILDING IN CARA HADRIJANA STREET 118
FIGURE 5.27 PRELIMINARY 3D MODEL OF 35 KW PV SYSTEM ON BUILDING ROOF IN CARA HADRIJANA STREET 119
FIGURE 5.28 BLOCK DIAGRAM OF 5 KW PV BASED E-BIKE CHARGING STATION. 119
FIGURE 5.29 ESTIMATED ELECTRICITY PRODUCTION OF 40 KW PV SYSTEMS ON BUILDING IN CARA HADRIJANA STREET 121
FIGURE 5.30 BLOCK DIAGRAM OF THE ENERGY STORAGE/SUPPLY SYSTEM. 122
FIGURE 5.31 BLOCK DIAGRAM OF THE WIND POWER SYSTEM. 122
FIGURE 5.32 ESTIMATED ELECTRICITY PRODUCTION OF 6 KW WIND ENERGY SYSTEM LOCATED AT THE EXEMPLARY OBJECT IN TRPIMIROVA STREET. 123
FIGURE 5.33 BLOCK DIAGRAM OF THE PV SYSTEMS ON BUILDING OF CENTRAL KITCHEN 124
FIGURE 5.34 3D MODEL OF PV SYSTEM ON BUILDING OF CENTRAL KITCHEN 125

FIGURE 5.35 ESTIMATED ELECTRICITY PRODUCTION OF 110 KW PV SYSTEM OF CENTRAL KITCHEN 126
FIGURE 5.36 BLOCK DIAGRAM OF THE PV SYSTEM ON BUILDINGS OF DEPARTMENT OF ONCOLOGY AND DEPARTMENT OF DIAGNOSTICAL AND INTERVENTIONAL RADIOLOGY 127
FIGURE 5.37 3D MODEL OF PV SYSTEM ON BUILDINGS OF DEPARTMENT OF ONCOLOGY AND DEPARTMENT OF DIAGNOSTICAL AND INTERVENTIONAL RADIOLOGY 127
FIGURE 5.38 ESTIMATED ELECTRICITY PRODUCTION OF PV SYSTEM ON BUILDING IN CARA HADRIJANA STREET 128
FIGURE 5.39 PRINCIPAL SCHEMATIC OF SYSTEM FOR BIODIESEL PRODUCTION FROM WASTE OIL 128
FIGURE 5.40 BLOCK DIAGRAM OF BIODIESEL GENERATOR SYSTEM 129
FIGURE 5.41 3D MODEL OF PHOTOVOLTAIC AND SOLAR-THERMAL SYSTEM ON BUILDING IN I. GUNDULIĆ STREET 131
FIGURE 5.42 BASIC BLOCK DIAGRAM OF BUILDING ENERGY MANAGEMENT SYSTEM FOR FTN 133
FIGURE 5.43 BASIC BLOCK DIAGRAM OF BUILDING ENERGY MANAGEMENT SYSTEM FOR KCV 134
FIGURE 5.44 BASIC BLOCK DIAGRAM OF BUILDING ENERGY MANAGEMENT SYSTEM FOR FERIT BUILDING IN TRPIMIROVA STREET 135
FIGURE 5.45 BASIC BLOCK DIAGRAM OF KBCO BUILDING ENERGY MANAGEMENT SYSTEM 136
FIGURE 6.1 PV PLANT ON THE ROOFTOP OF THE FTN BUILDING 138
FIGURE 6.2 ABB SOLAR INVERTER 139
FIGURE 6.3 INSTALLED SOLAR TREE 144
FIGURE 6.4 GROWATT MIC3000TL-X INVERTER 144
FIGURE 6.5 SOLAR POWERED EV CHARGING STATION 147
FIGURE 6.6 EV CHARGER 147
FIGURE 6.7 EV CHARGER TECHNICAL DATA 148
FIGURE 6.8 THE INVERTER UNIT THAT CONNECTS PV SYSTEM FOR EV CHARGING STATION TO THE GRID 149
FIGURE 6.9 SUPERCAPACITORS WITHIN STORAGE-SUPPLY SYSTEM 150
FIGURE 6.10 BATTERY WITHIN STORAGE-SUPPLY SYSTEM 152
FIGURE 6.11 INSTALLED WIND SYSTEM AT THE ROOFTOP OF THE BUILDING 154
FIGURE 6.12 INSTALLED HVAC UNIT 156
FIGURE 6.13 PV SYSTEM ON THE RADIOLOGY CLINIC ROOF 159
FIGURE 6.14 LUXOR M120 PV MODULE TECHNICAL DATA 159
FIGURE 6.15 ABB PVS-50-TL SOLAR INVERTER 160

FIGURE 6.16 ELECTRIC CABINET FOR INTERCONNECTION AND MONITORING OF RADIOLOGY CLINIC PV PLANT 160

FIGURE 6.17 PV SYSTEM ON THE EMERGENCY CENTER ROOF 161

FIGURE 6.4 ELECTRIC CABINET FOR INTERCONNECTION AND MONITORING OF EMERGENCY CENTER PV PLANT 161

FIGURE 6.18 PV PLANT ON THE KCV PARKING 162

FIGURE 6.2 LUXOR M108 PV MODULE TECHNICAL DATA 162

FIGURE 6.19 SOLAR-THERMAL SYSTEM ON THE MEDICAL REHABILITATION CLINIC ROOF 163

FIGURE 6.20 TECHNICAL DATA FOR SOLAR COLLECTORS ON THE MEDICAL REHABILITATION CLINIC ROOF 163

FIGURE 6.21 INTERCONNECTION BETWEEN SOLAR-THERMAL AND EXISTING HEATING SYSTEM 164

FIGURE 6.22 BIO-DIESEL PRODUCTION SYSTEM 164

FIGURE 6.23 DIESEL GENERATOR SYSTEM IN KCV COMPLEX 165

FIGURE 6.24 ELECTRIC CABINET FOR SUPPLYING THE BIO-DIESEL PRODUCTION SYSTEM 165

FIGURE 6.25 BLOCK SCHEMATIC OF FERIT BUILDING POWER SYSTEM IN TRPIMIROVA STREET 167

FIGURE 6.26 ROOM 3-40 ALONG WITH RO-SE1, RO-SE2 CABINETS AND HYBRID INVERTES WITH LITHIUM BATTERY PACKS 168

FIGURE 6.27 FERIT PHOTOVOLTAIC SYSTEM MODULES ON BUILDING ROOF IN TRPIMIROVA STREET 169

FIGURE 6.28 WALL-MOUNTED INVERTERS AT THE 3RD FLOOR OF FERIT BUILDING IN TRPIMIROVA STREET 169

FIGURE 6.29 BLOCK SCHEMATIC OF FERIT BUILDING POWER SYSTEM IN CARA HADRIJANA STREET 170

FIGURE 6.30 FERIT PHOTOVOLTAIC SYSTEM MODULES ON BUILDING ROOF IN CARA HADRIJANA STREET 171

FIGURE 6.31 WALL-MOUNTED INVERTERS AT THE 1ST FLOOR OF FERIT BUILDING IN CARA HADRIJANA STREET 172

FIGURE 6.32 WIRING DIAGRAM OF HYBRID INVERTER GROWATT SPH 5000TL3-BH WITH BATTERY PACK 177

FIGURE 6.33 H48050 LITHIUM-ION BATTERY PACK WITH ENERGY CAPACITY OF 9.6 KWH (LEFT) AND ARK 7.6H-A1 LITHIUM-ION BATTERY PACK WITH ENERGY CAPACITY OF 7.68 KWH (RIGHT) INSTALLED AT THE DC SIDE OF THE HYBRID INVERTER GROWATT SPH 5000TL3-BH IN THE ROOM 3-40 OF FERIT BUILDING IN TRPIMIROVA STREET 177

FIGURE 6.34 SINGLE LINE DIAGRAM OF THE SUBSTATION TS 10/0.4 KV BOLNICA 3 (MATERNITE/GINEKOLOGIJA) IN KBCO [16] 182

FIGURE 6.35 SINGLE LINE DIAGRAM OF THE KBCO PHOTOVOLTAIC SYSTEMS [16] 183

FIGURE 6.36 PLACEMENT OF THE PHOTOVOLTAIC MODULES ON THE CENTRAL KITCHEN AND DEPARTMENT OF ONCOLOGY AND DEPARTMENT OF DIAGNOSTICAL AND INTERVENTIONAL RADIOLOGY BUILDING ROOF AT KBCO [16] 184

FIGURE 6.37 KBCO PHOTOVOLTAIC SYSTEM ON CENTRAL KITCHEN BUILDING ROOF 184

FIGURE 6.38 KBCO PHOTOVOLTAIC SYSTEM ON DEPARTMENT OF ONCOLOGY AND DEPARTMENT OF DIAGNOSTICAL AND INTERVENTIONAL RADIOLOGY BUILDING ROOF ... 185

FIGURE 6.39 KBCO 125 KW BIODIESEL GENERATOR 185

FIGURE 6.40 KBCO BIODIESEL PRODUCTION SYSTEM FROM WASTE OIL 186

FIGURE 6.41 PHOTOVOLTAIC POWER PLANT ON UNISB BUILDING IN I. GUNDULIĆ STREET 188

FIGURE 6.42 INVERTERS OF PHOTOVOLTAIC POWER PLANT ON UNISB BUILDING IN LABORATORY FOR RENEWABLE ENERGY SOURCES 189

FIGURE 6.43 BASE ROOF CONSTRUCTION (K2 SYSTEMS) OF PHOTOVOLTAIC POWER PLANT ON UNISB BUILDING IN I. GUNDULIĆ STREET 190

FIGURE 6.44 SITUATION MAP OF PHOTOVOLTAIC POWER PLANT ON UNISB BUILDING 191

FIGURE 6.45 PV ARRAYS OF PHOTOVOLTAIC POWER PLANT ON UNISB BUILDING IN I. GUNDULIĆ STREET (GROUND PLAN) 192

FIGURE 6.46 PV ARRAYS OF PHOTOVOLTAIC POWER PLANT ON UNISB BUILDING IN I. GUNDULIĆ STREET (FRONT PLAN, SOUTH SIDE) 193

FIGURE 6.47 PV ARRAYS OF PHOTOVOLTAIC POWER PLANT ON UNISB BUILDING IN I. GUNDULIĆ STREET (FRONT PLAN, EAST SIDE) 194

FIGURE 6.48 INVERTERS OF PHOTOVOLTAIC POWER PLANT ON UNISB BUILDING IN LABORATORY FOR RENEWABLE ENERGY SOURCES 194

FIGURE 6.49 CONNECTION SCHEME OF PHOTOVOLTAIC POWER PLANT OF UNISB BUILDING 195

FIGURE 6.50 SINGLE-POLE ELECTRIC SCHEME OF MAIN CABINET OF PHOTOVOLTAIC POWER PLANT UNISB 196

FIGURE 6.51 SINGLE-POLE ELECTRIC SCHEME OF MAIN CABINET OF PHOTOVOLTAIC POWER PLANT UNISB 197

FIGURE 6.52 SINGLE-POLE ELECTRIC SCHEME OF MAIN OUTDOOR CABINET (SSRO1) OF UNISB BUILDING 198

FIGURE 6.53 SINGLE-POLE ELECTRIC SCHEME OF HARDWARE FOR BEMS (PLC) - UNISB BUILDING 199

FIGURE 6.54 HEAT PUMPS INSTALLED IN FRONT OF THE UNISB BUILDING 202

FIGURE 6.55 VERTICAL INSULATED STORAGE TANK IN THE UNISB BUILDING 203

FIGURE 6.56 DEVICES OF THERMO-TECHNICAL SYSTEM IN THE UNISB BUILDING 204

FIGURE 6.57 FAN CONVERTERS OF THERMO-TECHNICAL SYSTEM IN THE UNISB BUILDING, G111 205

FIGURE 6.58 FAN CONVERTERS OF THERMO-TECHNICAL SYSTEM IN THE UNISB BUILDING, CORRIDOR 205
FIGURE 6.59 OUTDOOR THERMO-TECHNICAL SYSTEM OF THE UNISB BUILDING 206
FIGURE 6.60 SCHEME OF THERMO-TECHNICAL SYSTEM OF THE UNISB BUILDING 207
FIGURE 6.61 FAN CONVERTERS INSIDE THE UNISB BUILDING 208
FIGURE 6.62 CONNECTION SCHEME OF FAN CONVERTERS INSIDE THE UNISB BUILDING 209
FIGURE 7.1 INSTALLED SIEMENS SENTRON SMART POWER METES. 210
FIGURE 7.2 INSTALLED PLC UNIT WITH ADDITIONAL SIGNAL BOARDS. 211
FIGURE 7.3 SCADA SYSTEM WORKING STATION. 212
FIGURE 7.4 MAIN SCREEN IN SIEMENS SCADA SYSTEM. 212
FIGURE 7.5 . MAIN SCREEN IN INVIEW WEB SCADA SYSTEM. 213
FIGURE 7.6 SIEMENS SENTRON SMART POWER METER 213
FIGURE 7.7 SCADA SYSTEM FOR MONITORING AND CONTROL OF KCV SYSTEMS 214
FIGURE 7.8 SCADA SYSTEM WORKING STATION 215
FIGURE 7.9 FERIT BUILDING ENERGY MANAGEMENT SYSTEM SCHEMATIC 216
FIGURE 7.10 FERIT DATA LOGGER GROWATT SHINEMASTER 216
FIGURE 7.11 SINGLE-LINE DIAGRAM OF POWER QUALITY MONITORING IN FERIT BUILDING IN TRPIMIROVA STREET 218
FIGURE 7.12 PQ3 IN ELECTRICAL SWITCHBOARD RO-SE2 219
FIGURE 7.13 KBCO BUILDING ENERGY MANAGEMENT SYSTEM SCHEMATIC 220
FIGURE 7.14 KBCO DATA LOGGER SMA DATA MANAGER M 221
FIGURE 7.15 ELECTRIC CABINETS: PV SYSTEM (LEFT) AND THERMO-TECHNICAL SYSTEM (RIGHT) 222
FIGURE 7.16 KBCO PV SYSTEMS OVERVIEW 222
FIGURE 7.17 KBCO TOTAL YIELD OF PV SYSTEMS IN AUGUST 2021 223
FIGURE 7.18 FERIT OVERVIEW OF HYBRID INVERTER EQUIPPED WITH RENEWABLE ENERGY STORAGE 223
FIGURE 7.19 FERIT PV SYSTEM GENERATION PROFILE INSTALLED ON BUILDING ON DECEMBER 20 2021 224
FIGURE 7.20 LOCATION OF TEMPERATURE SENSORS INSIDE THE UNISB BUILDING AND THEIR WEEKLY MEASURED DATA 225
FIGURE 7.21 OUTPUT POWER OF UNISB PV POWER PLANT DURING CLOUDY DAY 225
FIGURE 7.22 DAILY GENERATED ELECTRIC ENERGY OF UNISB PV POWER PLANT DURING DECEMBER 2021 226
FIGURE 7.23 MONTHLY GENERATED ELECTRIC ENERGY OF UNISB PV POWER PLANT DURING 2021. 227

FIGURE 7.24 CONTINUOSLY MEASURED DATA OF OUTSIDE TEMPERATURE AT THE UNISB BUILDING DURING THE DAY 227

FIGURE 7.25 CONTINUOSLY MEASURED DATA OF INSOLATION AT UNISB BUILDING DURING THE DAY 228

FIGURE 7.26 MONTHLY AVERAGE MEASURED DATA OF INSOLATION AND TEMPERATURE AT UNISB BUILDING DURING 2021. 228

FIGURE 7.27 INSOLATION OF TYPICAL SUMMER DAY AT UNISB BUILDING 229

FIGURE 7.28 MONTHLY DATA OF ELECTRICITY GENERATION OF UNISB PV POWER PLANT MEASURED BY NETWORK ANALYZER 229

FIGURE 7.29 ENERGY PERCENTAGE MONTHLY SAVINGS BETWEEN 2020. AND 2021. (UNISB PV POWER PLANT IN FUNCTION) 230

FIGURE 7.30 ENERGY MONTHLY DATA DURING 2020. AND 2021. (UNISB PV POWER PLANT IN FUNCTION) 230

FIGURE 7.31 ENERGY MONTHLY SAVINGS BETWEEN 2020. AND 2021. (UNISB PV POWER PLANT IN FUNCTION) 231

List of tables

TABLE 2.1 THE MEAN VALUES OF MONTHLY, ANNUAL AND EXTREME VALUES OF CLIMATOLOGICAL VALUES FOR NOVI SAD (RIMSKI ŠANČEVI - 45°20 AND 19°51E, N. V. 84 M) 36

TABLE 2.2 MONTHLY MEAN AND EXTREME VALUES OF CLIMATOLOGICAL PARAMETERS FOR OSIJEK [15]. 40

TABLE 2.3 – AVERAGE VALUES OF CLIMATIC PARAMETERS FOR SLAVONSKI BROD 41

TABLE 3.1 AN OVERVIEW OF THE FEEDERS LOCATED ON THE LOW-VOLTAGE SIDE OF THE TRANSFORMER STATION. 46

TABLE 3.2 ELECTRICAL ENERGY CONSUMPTION IN THE "MAŠINSKI INSTITUT" DURING 2018. 47

TABLE 3.3 HEAT ENERGY CONSUMPTION FOR THE "MAŠINSKI INSTITUT" DURING 2018. 48

TABLE 3.12 – ELECTRICAL ENERGY CONSUMPTION OF THE BUILDINGS DURING 2018. 67

TABLE 3.13 – ELECTRICAL ENERGY CONSUMPTION OF ALL KBCO FACILITIES DURING 2018. 70

TABLE 3.14 ELECTRICAL ENERGY CONSUMPTION IN THE "STROJARSKI FAKULTET U SLAVONSKOM BRODU, I. GUNDULIĆ STREET" DURING 2018 74

TABLE 3.15 THE NUMBER OF RADIATORS ACCORDING TO THE ROOM PURPOSE 75

TABLE 4.1 YEARLY AVERAGE PARAMETERS FOR NOVI SAD ACCORDING TO THE GLOBAL SOLAR ATLAS [19]. 82

TABLE 4.2 DAILY AVERAGE IRRADIANCE ON THE FIXED PLANE WITH SLOPE 0° AND AZIMUTH 0° FOR THE MONTH OF JULY, CITY OF NOVI SAD [18]. 84

TABLE 4.3 DAILY AVERAGE IRRADIANCE ON THE FIXED PLANE WITH SLOPE 30° AND AZIMUTH 0° FOR THE MONTH OF JULY, CITY OF NOVI SAD [18]. 86

TABLE 4.4 MONTHLY AVERAGE IRRADIANCE ON THE FIXED PLANE WITH SLOPE 0° AND AZIMUTH 0° FOR THE YEAR OF 2016, CITY OF NOVI SAD [18] 88

TABLE 4.5 SHARE OF INDIVIDUAL SECTORS IN THE TOTAL AMOUNT OF WASTE GENERATED IN THE YEARS 2010-2013 [21]. 89

TABLE 4.6 – GLOBAL MONTHLY AND ANNUAL SOLAR IRRADIATION FOR OSIJEK [22]. 93

TABLE 4.7 THEORETICAL ANNUAL ENERGY POTENTIAL OF SOLID WASTE BIOMASS FOR OSIJEK-BARANJA COUNTY [23] 97

TABLE 4.8 ANNUAL THEORETICAL ENERGY POTENTIAL OF LIQUID BIOFUELS PRODUCTION IN OSIJEK-BARANJA COUNTY [23] 98

TABLE 5.1 SOLAR THERMAL SYSTEM PROPERTIES 113

TABLE 5.2 OVERVIEW OF SOLAR THERMAL ENERGY (ANNUAL VALUES) 113

TABLE 5.3 – TECHNICAL CHARACTERISTICS OF PV MODULES [26]. 117

TABLE 5.4 TECHNICAL CHARACTERISTICS OF PV MODULES [26]. 126

TABLE 5.5 TECHNICAL CHARACTERISTICS OF PHOTOVOLTAIC MODULES SUNCECO SEM 300W-HE 132

TABLE 6.1 PV MODULES TECHNICAL DATA 138
TABLE 6.2 ABB PVS-50-TL SOLAR INVERTER TECHNICAL CHARACTERISTICS 140
TABLE 6.3 TECHNICAL SPECIFICATION FOR PV MODULES USED TO BUILD THE SOLAR TREE 145
TABLE 6.4 TECHNICAL SPECIFICATION FOR INVERTER UNIT WITHIN SOLAR TREE SYSTEM 146
TABLE 6.5 TECHNICAL DATA ABOUT SUPERCAPACITOR SYSTEM 151
TABLE 6.6 TECHNICAL DATA ABOUT BATTERY SYSTEM. 153
TABLE 6.7 WIND SYSTEM TECHNICAL SPECIFICATION 155
TABLE 6.8 TECHNICAL SPECIFICATION FOR INSTALLED HVAC SYSTEM 158
TABLE 6.9 TECHNICAL CHARACTERISTICS OF GROWATT MID 20KTL3-X INVERTERS [28] 173
TABLE 6.10 TECHNICAL CHARACTERISTICS OF GROWATT 10000TL3-S INVERTERS [29] 174
TABLE 6.11 TECHNICAL CHARACTERISTICS OF GROWATT SPH 5000TL3-BH HYBRID INVERTERS [30] 175
TABLE 6.12 TECHNICAL CHARACTERISTICS OF PHOTOVOLTAIC MODULES LUXOR ECOLINE M60/320W [31] 176
TABLE 6.13 TECHNICAL CHARACTERISTICS OF 9.6 KWH LITHIUM-ION BATTERY PACK H48050 [32] 178
TABLE 6.14 TECHNICAL CHARACTERISTICS OF 7.68 KWH LITHIUM-ION BATTERY PACK ARK 7.6H-A1 [33] 178
TABLE 6.15 TECHNICAL CHARACTERISTICS OF SMA SUNNY TRIPOWER CORE1 INVERTERS [34] 179
TABLE 6.16 TECHNICAL CHARACTERISTICS OF SMA SUNNY TRIPOWER 20000TL INVERTERS [35] 180
TABLE 6.17 TECHNICAL CHARACTERISTICS OF PHOTOVOLTAIC MODULES SOLVIS SV60-300E [36] 181

1. Introduction

Energy consumption is constantly increasing since the global population rises and due to the development of industrial sectors, leaving fossil fuel reserves depleted and climate change seriously impacted. Fossil fuels are still dominantly employed for energy harvesting, but finite supply and numerous problems with energy exploitation imply that new solutions have to be incorporated in the energy production process.

Not only that fossil fuels reserves are limited, harder to locate and expensive to transport, but their negative influence on the environment requires active participation in increasing energy efficiency, finding and exploiting of alternate energy sources. The prediction of the finite energy reserves for coal, gas and oil, the most exploited fossil fuels [1], is given in Figure 1.1.

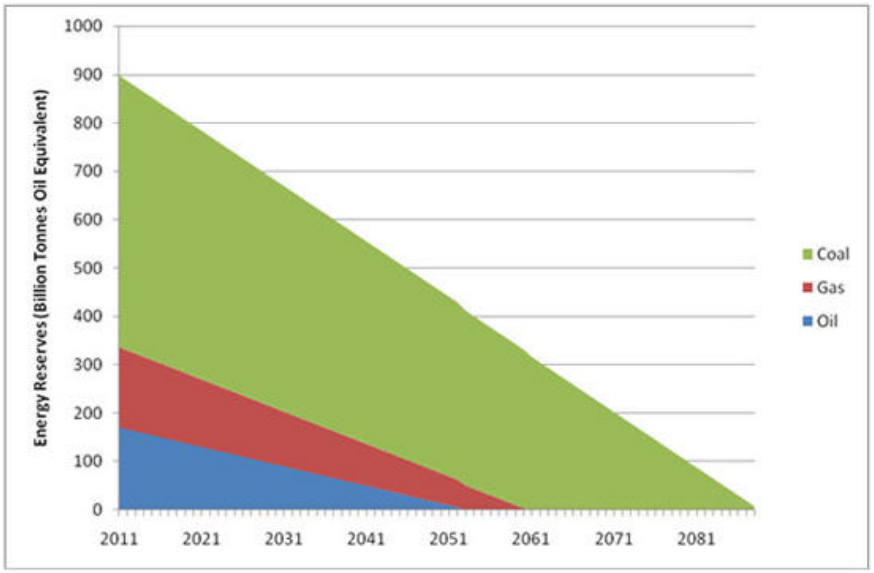

Figure 1.1 The prediction of fossil fuel energy reserves [1].

One of the biggest issues associated with the combustion of fossil fuels is carbon emission. In Figure 1.2 carbon dioxide (CO_2) emission by a specific type of fossil fuel is given [2]. It can be seen that industrial and economic growth in the last century has contributed to a significant increase in CO_2 concentration.

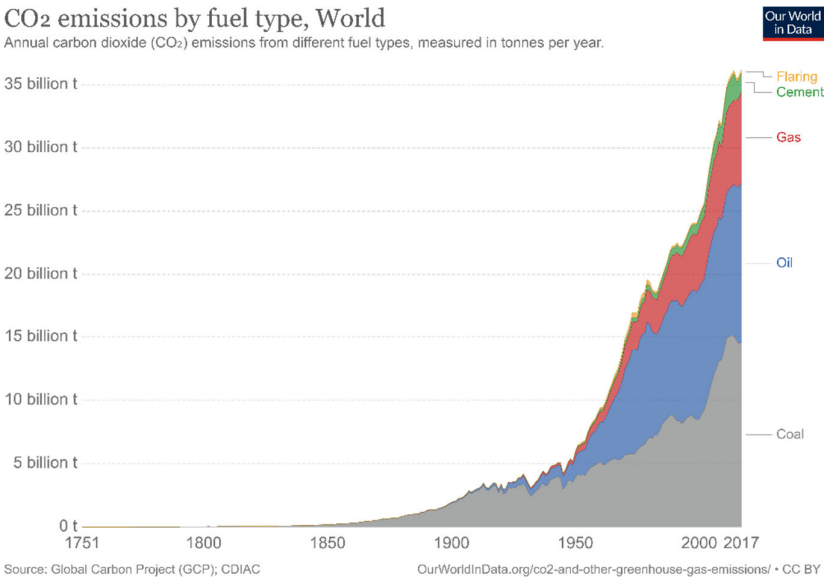

Figure 1.2 Carbon dioxide (CO_2) emission by a specific type of fossil fuel [2].

Carbon dioxide is a major greenhouse gas and thus extremely contributes to global warming, climate change and ocean acidification. Carbon dioxide concentration in the atmosphere has risen about 43% since the beginning of the industrial revolution in the mid-eighteenth century – half of that since 1980 [3]. In the high economic growth case, world CO_2 emissions increase at an average rate of 1.8% annually from 2006 to 2030, as compared with 1.4% in the reference case. For the OECD countries, the projected average increase in the high growth case is 0.6% per year, for the non-OECD countries, the average is 2.6% per year. In the low growth case, world CO_2 emissions increase by 1.0% per year from 2006 to 2030, with averages of 0.1% per year for the OECD countries and 1.8% per year for the non-OECD countries. In 2030, total energy-related CO_2 emissions worldwide range from a projected 36,930 Mt in the low growth case to 44,108 Mt in the high growth case, which is 19.4% higher than projected in the low growth case [4]. Figure 1.3 predicts CO_2 emission based on different scenarios [2]:

- No climate policies: projected future emissions if no climate policies were implemented; this would result in an estimated 4.1-4.8°C warming by 2100 (relative to pre-industrial temperatures);
- Current climate policies: projected warming of 3.1-3.7°C by 2100 based on currently implemented climate policies;
- National pledges: if all countries achieve their current targets/pledges set within the Paris climate agreement, it's estimated average warming by 2100 will be 2.6-3.2°C. This will go well beyond the overall target of the Paris Agreement to keep warming "well below 2°C";

- 2°C consistent: there is a range of emissions pathways that would be compatible with limiting average warming to 2°C by 2100. This would require a significant increase in the ambition of the current pledges within the Paris Agreement;
- 1.5°C consistent: there is a range of emissions pathways that would be compatible with limiting average warming to 1.5°C by 2100. However, all would require a very urgent and rapid reduction in global greenhouse gas emissions.

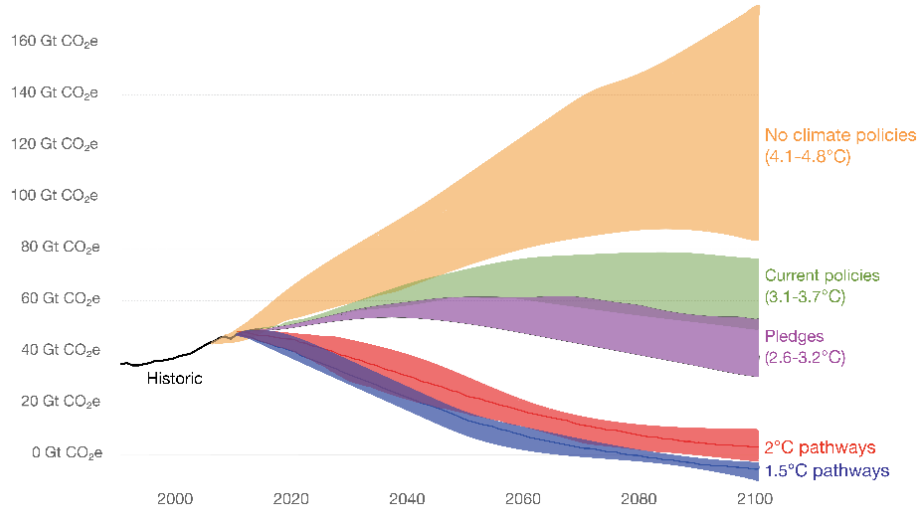

Figure 1.3 The prediction of the CO_2 emission based on different scenarios [2].

According to the HCWH (Health Care Without Harm) Europe climate report published in Dec 2016 [5], the health sector is a major emitter of greenhouse gasses. For example, in 2012, the total carbon footprint of England's public healthcare sector was 32 million tons of carbon dioxide equivalents (CO_2 equivalent refers to a combination of harmful greenhouse gases, not just carbon dioxide), accounting for 38% of public sector emissions in England. This serves to illustrate how the healthcare sector is contributing an enormous amount of harmful emissions, which in turn undermines the health of the same population the sector is meant to heal.

Based on these prognoses, it is clear that is necessary to implement a number of CO_2 restriction measures in order to achieve a decrease in the CO_2 concentration. One of the measures that can be taken is to increase the reduction of the used energy, for example, with the investment in new equipment that is more energy efficient. Another one is to use alternative energy sources that contribute less to greenhouse gas emissions.

Nowadays, higher energy efficiency is obtained using power electronics. Power electronic devices are present in almost every part of the power system since they enable the conversion of electric power and are used to control power flow and voltage. Power electronic devices are fast and reliable, can provide better power quality and add new functionalities and flexibility to the grid. Without them, the integration of renewable energy sources into the traditional power network could not be possible. Renewables use

technologies that are safe, reliable, affordable and widely available. In order to utilize the best resource locations, many renewable generators have to be located far from existing load canters which leads towards the expansion and decentralization of the power system.

In the last decade, the investment in renewables has drastically increased, which is depicted in Figure 1.4 (large hydropower is not included) [6]. These trends suggest that investors see solar and wind energy as the dominant renewable technologies of the future. The share of renewable energy in the power sector would increase from 25% in 2017 to 85% by 2050, mostly through growth in solar and wind power generation [7].

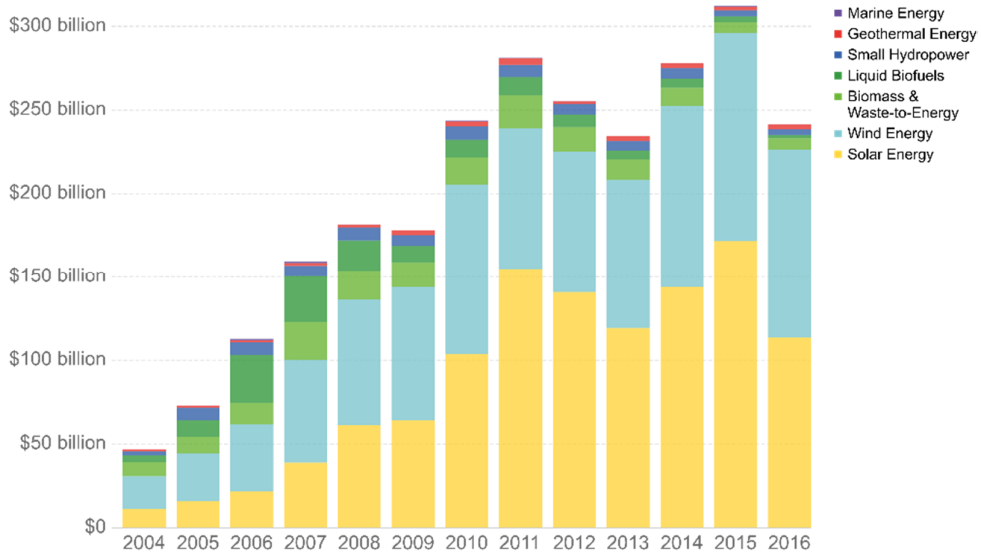

Figure 1.4 Investment in different renewable energy technologies [6].

Renewable energy technology should result in less global warming, improved public health through a reduction of air and water pollution, stable electricity price and contribute to the reliability and resilience of the grid. In addition, unlike fossil fuels, energy sources used by renewables are inexhaustible. Therefore, EIA (U.S. Energy Information Administration) projects that renewables will provide nearly half of world electricity by 2050, which is depicted in Figure 1.5 [8].

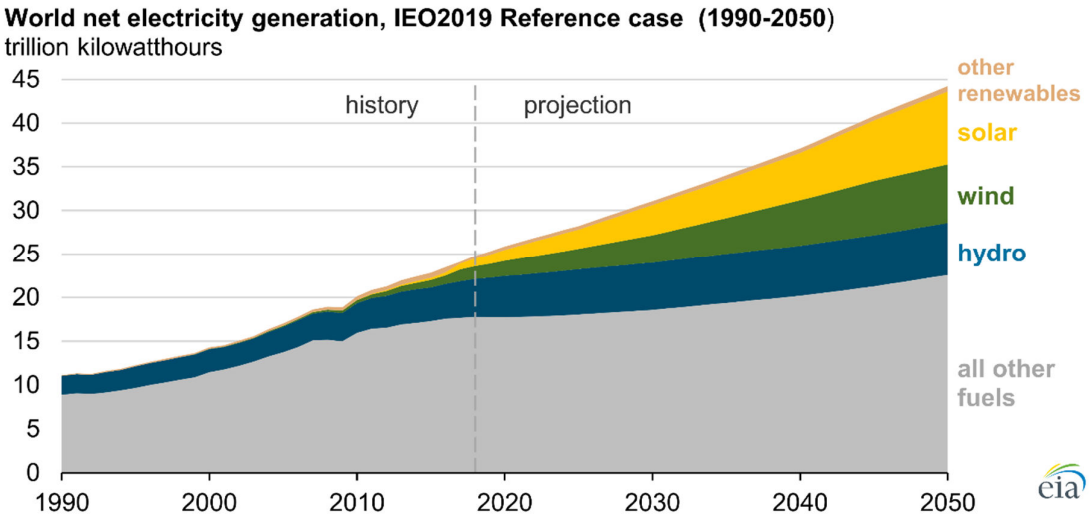

Figure 1.5 World net electricity generation [8].

Energy storage systems, such as batteries, supercapacitors, flywheels, thermal storages, etc., play a critical role in the transition of the global energy system toward 100% renewables. As the shares of solar photovoltaics and wind energy are going to increase significantly beyond 2030, the role of storage is crucial in providing an uninterrupted energy supply.

Following the CO_2 reduction tendency, vehicles that run on fossil fuels should be replaced with electric-powered vehicles. Although currently electric vehicles are more expensive than gasoline-powered vehicles, with time, the running or operating costs of an electric vehicle may be lower than a traditional car (as a result of efficiency gains and lower cost of electricity relative to liquid fuel), so we will begin to get some economic return on our initial investment.

The reduction of greenhouse gasses would help in the decrease in environmental pollution that has become a severe problem. Another measure that can be taken is waste management – a series of actions that aim to reduce the generation and promote the reuse and recycling of solid and hazardous waste. Another benefit that can be obtained is energy recovery. Energy recovery from waste is the conversion of non-recyclable waste materials into usable heat, electricity, or fuel.

Energy efficiency can be increased by reducing the energy consumption of public buildings. This results in substantial energy savings and therefore less usage of fossil fuels. This strategy is recognized and adopted by a number of countries worldwide. A zero-energy building would be a preeminent goal. Of course, this is not possible without the renewables which should cover a part of energy necessities. In order to monitor and control the energy consumption of buildings, Building Energy Management Systems (BEMS) are crucial. BEMS provide real-time remote monitoring and integrated control of a wide range of connected systems, allowing modes of operation, energy use, environmental conditions and so on to be monitored and allowing to optimize performance and comfort. To function correctly they

must be properly designed, installed and commissioned and must have a user interface that is easy to operate.

These issues are addressed in various laws and directives in both Republic of Croatia and Republic of Serbia. As a candidate country to become a member state of the European Union, Republic of Serbia should harmonize its laws with the EU, i.e. with EU directives on energy efficiency, where some steps have already been taken. The Energy Efficiency Directive 2012/27/EU is pursuing the overall objective of the energy efficiency target of saving 20% of the Union's primary energy consumption by 2020, and of making further energy efficiency improvements after 2020 [9]. The amending directive (2018/2002) [10] was agreed to update the policy framework to 2030 and beyond. The key element of the amended directive is an energy efficiency target for 2030 of at least 32.5%. The directive allows for a possible upward revision in the target in 2023, in case of substantial cost reductions due to economic or technological developments. It also includes an extension to the energy savings obligation in end-use, introduced in the 2012 directive. Under the amending directive, EU countries will have to achieve new energy savings of 0.8% each year of final energy consumption for the 2021-2030 period. Another important directive is Directive 2010/31/EU on the energy performance of buildings [11]. This directive introduces a framework for improving the energy efficiency of buildings and proposes a plan in which all new buildings are nearly zero-energy buildings by 31 December 2020.

Regarding the abovementioned, it is clear how important is to invest in and implement new technologies that enable higher energy efficiency and thus reduce the impact on climate change and provide energy savings. In order to achieve this, it is necessary to analyse the energy performance profile and determine which elements are critical. This document provides an overview of the configuration of the planned renewable energy systems, realised building energy management systems and it possibilities.

This document compromises the following sections:

- the second section offers insight into the main geographical, meteorological and other features of the public buildings for the exemplary facilities;
- the third section examines current energy demand for the exemplary facilities;
- the fourth section investigates the potential for utilization of renewable energy;
- the fifth section described planned optimal renewable energy system topology and building energy management system for the exemplary facilities;
- the sixth section gives an overview of installed renewable energy systems for the exemplary facilities;
- the seventh section gives an overview of building energy management systems for the exemplary facilities.

2. The main features of the locations and the buildings for the exemplary facilities

2.1. Buildings for the exemplary facilities

2.1.1. FTN buildings

"Mašinski institut" facility is located within the campus of the University of Novi Sad and represents one of the nine buildings of the Faculty of Technical Sciences. The facility is located in the South Bačka District, which is one of seven administrative districts of the autonomous province of Vojvodina, Serbia. "Mašinski institut" is located in Liman I, part of the city of Novi Sad, at Vladimir Perić Street No. 2. The geographical coordinates of the facility are north latitude 45° 14' 44.82" and east longitude 19° 51' 01.59", as shown in Figure 2.1 (*source: google.com/maps*).

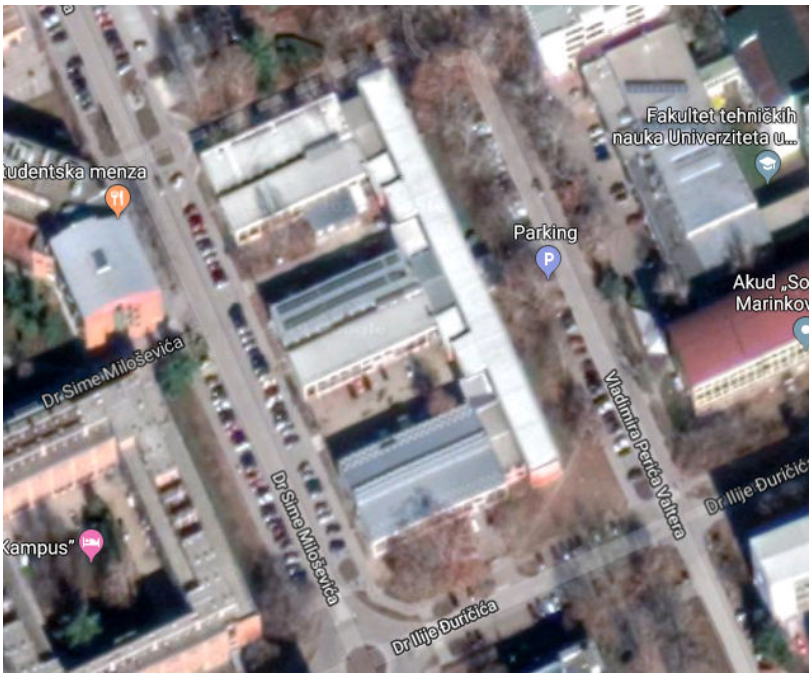

Figure 2.1 Location of "Mašinski institut" facility.

"Mašinski institut" consists of a two-story building equipped with laboratories, with a total area of 7225 m^2. The facility is divided into 98 offices, 42 laboratories, 9 computer laboratories and 24 classrooms. The main entrance to the building, as well as part of the building with laboratories and classrooms, are given in Figure 2.2 and Figure 2.3, respectively.

Figure 2.2 The main entrance to "Mašinski institut".

Figure 2.3 Part of "Mašinski institut" with laboratories for scientific research.

2.1.2. KCV buildings

Clinical Center of Vojvodina (hereinafter KCV) is hospital complex offering the tertiary level medical services to patients of the Vojvodina province. Additionally, it is the only emergency center and inpatient hospital for the region of South Backa. It is located in the city of Novi Sad, more precisely in Hajduk Veljkova No. 1-9 Street. Figure 2.4 shows the geographical arrangement of the facilities inside KCV complex.

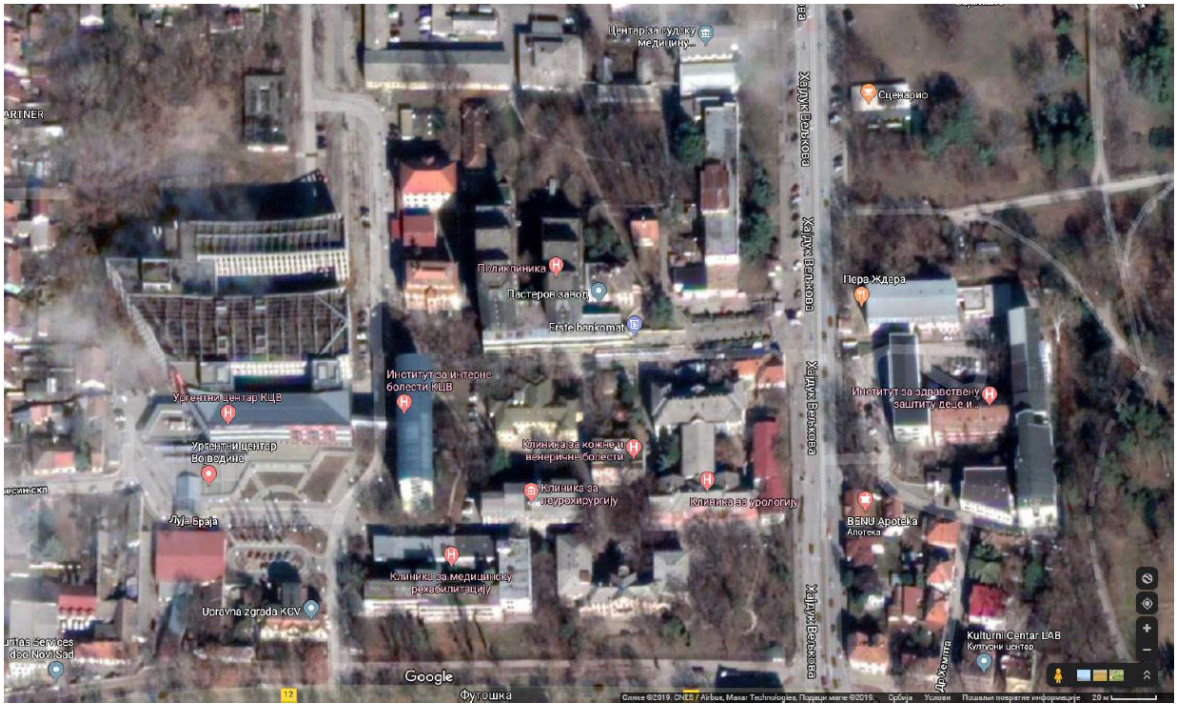

Figure 2.4 Facilities in the KCV complex

The KCV complex consists of 26 different facilities, which are dedicated to different purposes ranging from medical care and rehabilitation to education and medical training. Facilities that are of interest for this study are Medical Center for Rehabilitation, Radiology clinic and Emergency center.

The Medical Rehabilitation Clinic, shown in Figure 2.5 is an institution of national importance since it employs a high number of medical professionals that use the latest medical methodologies for treating sick or injured patients with threatening or temporary disabilities.

The Radiology Center (Radiology Clinic), shown in Figure 2.6 is one of the most significant institutions of this kind in Serbia and region. With few dozens of employed specialists and subspecialists as well as modern equipment, this facility offers services in the field of diagnostic and interventional radiology.

Figure 2.5 Medical Rehabilitation Clinic inside KCV complex

Figure 2.6 Radiology Clinic inside KCV complex

The Emergency Center facility, shown in Figure 2.7, is one of the most advanced facilities of this kind in the Republic of Serbia and region. With modern medical equipment and highly competent medical personal, it offers high quality medical care in accordance with the most recent medical standards. It incorporates surgical and non-surgical blocks, diagnostic and emergency blocks, which enables rapid response in patient treatment.

Figure 2.7 Emergency Center facility inside KCV complex

2.1.3. FERIT buildings

Faculty of Electrical Engineering, Computer Science and Information Technology occupies two buildings, first in the street Kneza Trpimira 2B and second in campus of Josip Juraj Strossmayer University of Osijek (Cara Hadrijana 10B). Faculty buildings are located in city of Osijek in Slavonia-Baranja County. Geographical locations of buildings are North latitude 45° 33' 24.82'', East longitude 18° 41' 44.24'' for building in Trpimirova street and North latitude 45° 33' 23.88'', East longitude 18° 42' 42.85'' for building in Cara Hadrijana street.

Faculty building in Trpimirova street is located at k.č.br. 5985/9, K.O. Osijek, as shown in situation in Figure 2.8 Near the faculty building, Student Center, high school center and recreational center are located while few blocks away, old town of Osijek - fortress Tvrđa (citadel) is situated. Faculty building in Cara Hadrijana street is located at k.č.br. 6660/1, k.o. Osijek, as shown in situation in Figure 2.9. Faculty building is a part of Josip Juraj Strossmayer University of Osijek campus alongside few other faculties. Near the building, Clinical Hospital Center Osijek is situated.

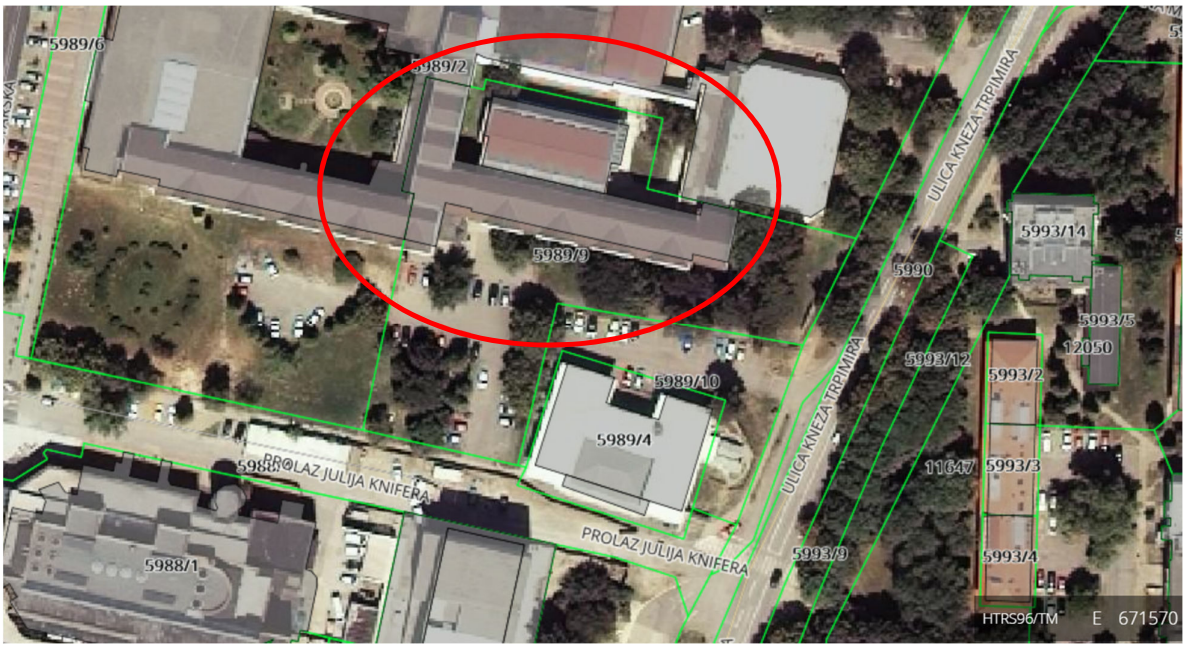

Figure 2.8 Location of Faculty of Electrical Engineering, Computer Science and Information Technology Osijek building in Trpimirova street [12].

Figure 2.9 Location of Faculty of Electrical Engineering, Computer Science and Information Technology Osijek building in Cara Hadrijana street [12].

Both Faculty buildings are a three-story building equipped with offices, classrooms and laboratories. Besides that, building in Cara Hadrijana has basement floor while building in Trpimirova does not. Totally, both Faculty buildings are equipped with 27 laboratories, of

which 9 computer laboratories, 18 classrooms and 52 offices. Total area of Faculty building in Trpimirova is 4500 m^2 while for the building in Cara Hadrijana street is 3700 m^2. Figure 2.10 and Figure 2.11 show main entrance to the Trpimirova street and Cara Hadrijana street buildings.

Figure 2.10 The main entrance to the building in Trpimirova street.

Figure 2.11 The main entrance to the building in Cara Hadrijana street.

2.1.4. KBCO buildings

Clinical Hospital Center Osijek (KBCO) started operation as a Clinical Hospital Osijek in 1874. During 20th century, hospital experiences massive expansion in spatial and personnel view. At the end of the 20th century, hospital turns into clincal-hospital center we know today. Currently, medically speaking, KBCO includes 26 organisational units, 17 clinics, 7 departments and 1 emergency center and 2 general purpose medical units (hospital pharmacy and central ordering).

KBCO occupies multiple locations in city of Osijek and its surroundings. KBCO functions in major clinical-hospital complex in Huttler street, Department of Eye Diseases which occupies 2 smaller facilities in Europske Avenije street and Department of Physical Medicine and Rehabilitation which occupies complex of building in Bizovac near Osijek. This study will focus only on clinical-hospital complex of buildings at the address Josipa Huttlera 4, Osijek. KBCO complex in Huttler street is located in the eastern part of Osijek in Slavonia-Baranja County. Geographical location of the complex is North latitude 45° 33' 19.79'', East longitude 18° 42' 45.5''.

KBCO complex in Huttler street is located on multiple cadastral parcels as shown in Figure 2.12. Near the complex, Josip Juraj Strossmayer University of Osijek campus is located, as well as building of the Faculty of Electrical Engineering, Computer Science and Information Technology Osijek in Cara Hadrijana street.

In this study, building on which renewable energy systems will be installed will be in focus. These buildings represent central kitchen (red squared in Figure 2.12), building of Department of Oncology (blue squared in Figure 2.12) and building of Department of Diagnostical and Interventional Radiology (green squared in Figure 2.12).

Figure 2.12 Location of KBCO complex in Huttler street [12].

Central kitchen is general-purpose facility used for preparation of food and diets of KBCO users. North side of the building in given in Figure 2.13.

The Department of Radiology and Oncology was established in 1932. The present building began to be built in 1968 and was commissioned in 1970 under the name "Department of Radiology and Oncology". At the end of 1973, the department was divided into: Department of Radiodiagnosis and Department of Oncology and Radiotherapy. Prior to becoming independent, the department integrated its activities in both the diagnostic treatment of patients and the implementation of therapeutic procedures in accordance with available equipment. By dividing the department into the diagnostic and therapeutic part, the equipment is rebuilt to extend the range of diagnostic procedures (ultrasound, computer tomography, magnetic resonance imaging, mammograms and specific therapeutic devices: CO bomb, linear accelerator, simulators for planning treatment procedures). West side of the building of Department of Oncology is given in Figure 2.14, while north side of the building of Department of Diagnostical and Interventional Radiology is given in Figure 2.15.

Figure 2.13 North side of the central kitchen building.

Figure 2.14 West side of the building of Department of Oncology.

Figure 2.15 North side of the building of Department of Diagnostical Interventional Radiology

2.1.5. UNISB building

The Mechanical Engineering Faculty in Slavonski Brod is a part of the University of Slavonski Brod. The Faculty is located at the Brodsko-Posavska County which is one of 20 counties in Croatia. Brodsko-Posavska County is located in the South of Slavonija Region which is one (East) of 5 Croatia's Non-Administrative regions. The analyzed facility of Faculty is located at Ivan Gundulić Street No. 20a. The geographical coordinates of the building are north latitude 45° 9' 18.73" and east longitude 18° 1' 19.54", as shown in Figure 2.16.

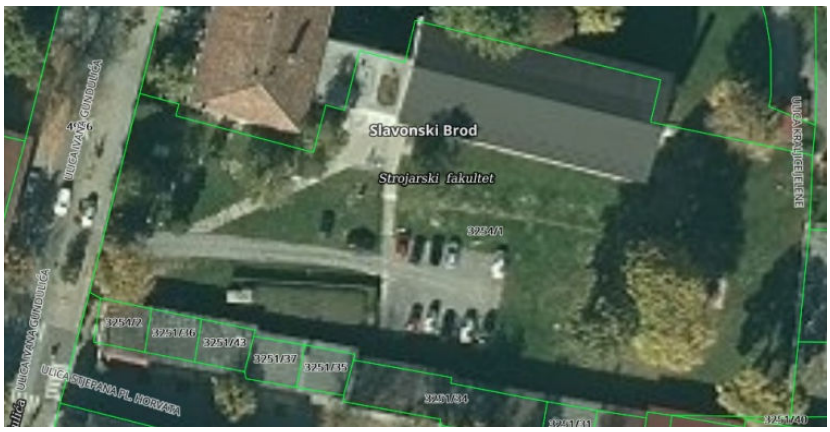

Figure 2.16 Location of the Mechanical Engineering Faculty building [12]

The facility of Faculty is located at k.č.br. 3254/1, K.O. Slavonski Brod, as shown in the situational plan given in Figure 2.17. Near the facility is a facility of Pedagogical Faculty in Slavonski Brod.

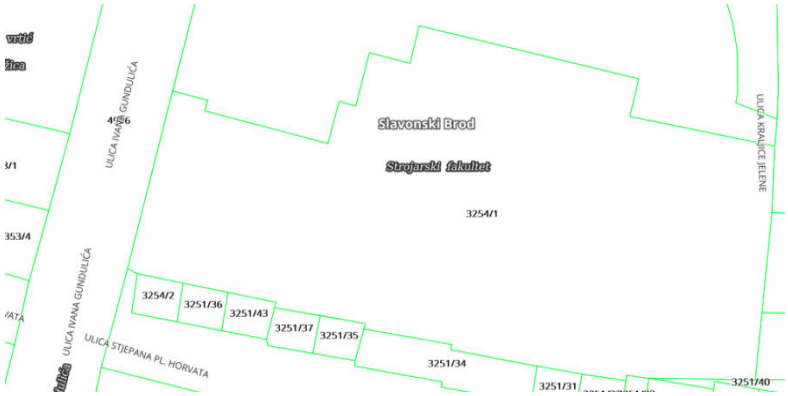

Figure 2.17 Situational plan of the Mechanical Engineering Faculty facility [12]

The building of Faculty is equipped with laboratories, with a total area of 1404 m^2. The facility is divided into 22 offices, 4 laboratories, 4 computer laboratories and 2 classrooms. The main entrance to the building, part of the building with laboratories and classrooms, as well as the roof of the Mechanical Engineering Faculty facility, where the photovoltaic power plant is located and installed thermo-technical devices in front of the building given in the figures below (Figure 2.18, Figure 2.19, Figure 2.20).

Figure 2.18 The main entrance to facility II of Mechanical Engineering Faculty

Figure 2.19 Part of Mechanical Engineering Faculty with parking area and installed solar thermal and heat pump`s systems

Figure 2.20 Part of Mechanical Engineering Faculty with classrooms and offices where the thermo-technical (solar thermal and heat pumps) system and photovoltaic power plant are installed

2.2. Climate conditions in the surrounding area

2.2.1. FTN and KCV climate conditions

Moderately continental climate characterized by cold winters and warm summers and continental climate with well-distributed rainfall is changing in the territory of Vojvodina. During the autumn and winter, there is a chance of an endemic strong and cold wind ("košava"), which lasts three to ten days and can cause some damage during heavy snowfall. Figure 2.21 shows the rose wind for Novi Sad, from which it is possible to recognize that the dominant wind in this area is the Košava, which blows from the east-southeast and west-northwest.

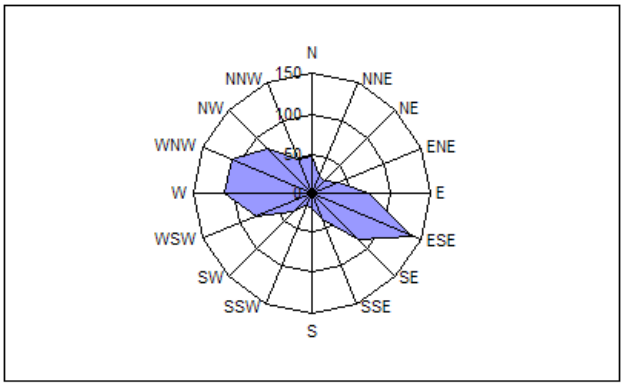

Figure 2.21 Rose wind for Novi Sad.

Table 2.1 shows the mean values of monthly, annual and extreme values of climatological values in the period from 1981 to 2010 (according to data of the Republic Hydro-meteorological Institute). Novi Sad is at an average altitude of 80 m, with an average temperature of 11.4 ℃ during the year, and with an average temperature of 0.2 ℃ in January and 21.9 ℃ in July. The lowest measured temperature was -27.6 ℃, while the highest measured temperature was 41.6 ℃. The annual average rainfall is 647.3 mm and the average number of days with snow cover is 39. The average amount of solar radiation during the year on an area of 1 square meter is 129.2 kWh/m^2.

Table 2.1 The mean values of monthly, annual and extreme values of climatological values for Novi Sad (Rimski Šančevi - 45°20 and 19°51E, n. v. 84 m)

	Jan	Feb	Mar	Apr	May	Jun	Jul	Aug	Sept	Oct	Nov	Dec	Year
	Temperature [℃]												
Mean maximum value	3.7	6.1	12.0	17.7	23.0	25.8	28.1	28.3	23.6	18.0	10.5	4.8	16.8
Mean minimum value	-3.1	-2.4	1.5	6.2	11.3	14.1	15.5	15.3	11.4	6.9	2.2	-1.5	6.5
Normal value	0.2	1.6	6.4	11.8	17.3	20.1	21.9	21.6	16.9	11.8	5.9	1.5	11.4
Absolute maximum	18.7	22.3	28.3	30.8	34.0	37.6	41.6	40.0	37.4	29.2	25.0	21.0	41.6
Absolute minimum	-27.6	-24.2	-19.9	-6.2	1.8	4.8	7.5	7.0	2.5	-6.2	-13.8	-24	-27.6

Mean number of frost days	22	18	10	2	0	0	0	0	0	2	9	18	81
Mean number of tropical days	0	0	0	0	1	6	11	11	2	0	0	0	32
Average relative moisture [%]	85	79	71	67	66	69	68	68	72	76	82	86	74
Hours of daily light													
Average	64.8	99.0	156.4	190.1	250.8	269.4	303.6	285.8	205.7	158.9	92.4	58.4	2135
Number of clear days	3	5	5	5	5	6	11	12	9	8	4	3	75
Number of cloudy days	14	10	9	7	5	5	3	3	5	6	11	15	94
Radiation [kWh/m^2]	53.1	71.8	131	161	173	180	201	198	146	113	76.3	45.9	129.2
Precipitation [mm/m^2]													
Mean monthly sum	39.1	31.4	42.5	49.2	63.0	91.4	64.3	57.5	53.8	52.7	53.8	48.8	647.3
Maximum daily sum	31.8	23.2	32.6	40.2	91.8	67.6	68.7	68.0	48.8	59.0	54.9	37.6	91.8
Mean number of days >=0,1 mm/m^2	12	10	11	12	13	12	10	9	10	9	11	13	132
Mean number of days >=10 mm/m^2	1	1	1	1	2	3	2	2	2	2	2	1	20
Number of days with snow	13	10	3	0	0	0	0	0	0	0	3	9	39

2.2.2. FERIT and KBCO climate conditions

Continental Croatia is characterized by temperate continental climate and throughout the whole year it is marked by very variable atmospheric conditions because of circulation zone of mid-latitudes. Main feature of the climate is a diversity of weather situations with intense and frequent interchanges during the year caused by low or high air pressure moving complexes, usually like vortices hundreds and thousands of kilometers in diameter. Furthermore, continental Croatia climate is also modified by the Mediterranean maritime influence, which weakens by distancing towards the east. The next, more local than regional, factor that influences the climate is orography which, on the windward side of the orographic obstacle, makes easier the amplification of short-term heavy precipitation while on the leeward side generates appearance of precipitation shadow. Finally, these conditions also depend on the current season [13].

Stationary anticyclonic weather types with low clouds or fog and a very gentle air flow are beneficial for frost occurrence during the winter. On contrary, fast-moving cyclonic weather types (cyclone and trough) in spring result in frequent and unforeseen weather changes, varying from cold to warm, calm to windy or dry to rainy periods. During summer, small air pressure gradient results in a cooling night breeze blowing down mountain slopes interrupted by cold fronts passing through bringing fresh Atlantic air. Consequently, this results in strong air mixing, increased wind, thunder and showers from dense clouds with vertical development. Autumn is distinguished by intervals of calm anticyclonic weather, but there are also rainy days caused by passing cyclones. Autumn starts with warm and sunny days and fresh nights with much dew and low fog while at the ending conditions transform to cold, foggy, and gloomy [13].

Crucial source of information for Croatia's wind energy potential estimation is the wind atlas. Maps given in Figure 2.22 an Figure 2.23 show average wind speed (m/s) and mean wind power density (W/m²) maps at 10 m and 80 m above ground. Given maps are a result of atmospheric numerical model and represent an average value in a grid cell of 2 km x 2 km [14].

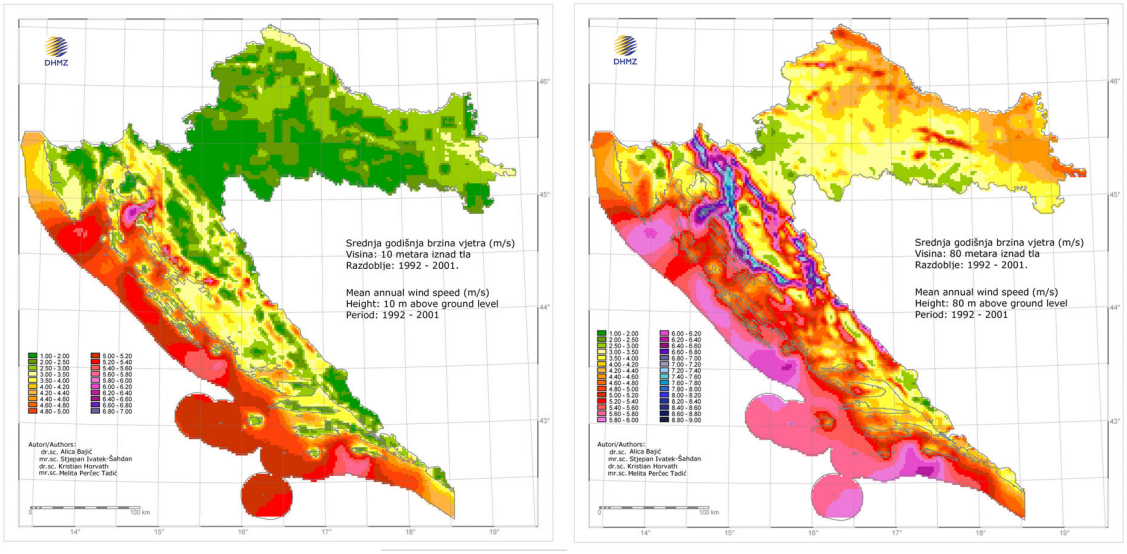

e

Figure 2.22 – Mean annual wind speed in Croatia (m/s) [14].

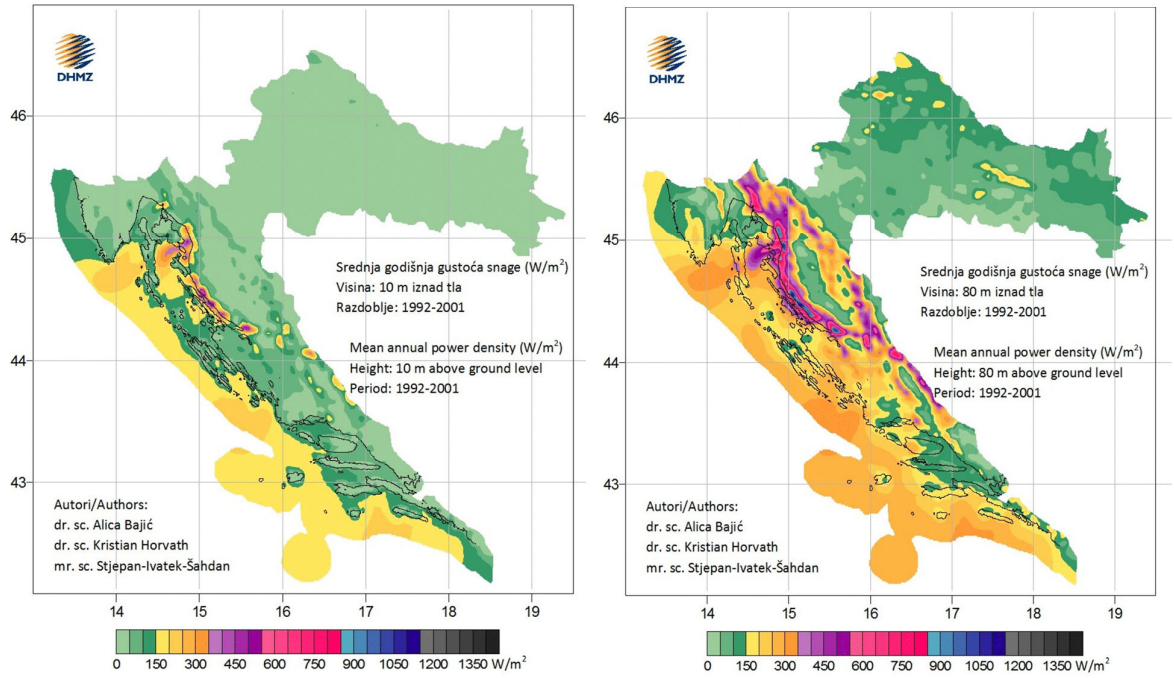

Figure 2.23 Mean annual power density in Croatia (W/m^2) [14].

Table 2.2 shows monthly mean and extreme values of climatological parameters in the period from 1999 to 2018 (according to data of the Croatian Meteorological and Hydrological Service). Osijek is at an average altitude of 90 m, with an average temperature of 11℃ during the year, and with an average temperature of -0.6℃ in January and 21.7℃ in July. The lowest measured temperature was -27.1℃ in July, while the highest measured temperature was 40.3℃ in August and September. The total annual average rainfall is 692.9 mm and the average number of days with snow cover is 23.

Table 2.2 Monthly mean and extreme values of climatological parameters for Osijek [15].

	Jan	Feb	Mar	Apr	May	Jun	Jul	Avg	Sept	Oct	Nov	Dec
Temperature [°C]												
Mean	-0.6	1.3	6.3	11.6	16.6	19.8	21.7	20.9	16.7	11.3	5.8	1.3
Absolute maximum	19	23	26.9	30.9	36	39.6	40.3	40.3	37.4	30.5	25.8	21.3
Absolute minimum	-27.1	-26.4	-21.0	-6.8	-3.0	1.0	4.7	5.1	-1.2	-8.6	-15.7	-23.2
Daylight hours [h]												
Total	59.7	86.3	142.9	182.1	226.5	247.1	276.3	261.6	191.8	150.4	75.1	52.0
Rainfall												
Volume [mm]	45.4	42.7	45.7	57.8	70.3	82.4	61.3	58.8	55.5	59.5	59.8	53.7
Maximum snow height [m]	52	93	49	22	-	-	-	-	-	-	40	60
Number of days												
Clear	3	4	5	5	5	6	9	11	9	7	3	2
Foggy	6	4	2	1	0	0	1	1	2	4	6	7
Rainy	7	7	10	12	13	12	10	9	9	10	11	10
With frost	7	7	7	2	0	0	0	0	0	3	6	8
With snow	6	6	3	1	0	0	0	0	0	0	2	5
Icy day ($t_{min} \leq -10°C$)	4	3	0	0	0	0	0	0	0	0	0	2
Frosty day ($t_{min} < 0°C$)	9	4	1	0	0	0	0	0	0	0	1	6
Cold day ($t_{min} < 0°C$)	23	18	11	2	0	0	0	0	0	2	8	19

Warm day (t_{max} ≥ 25°C)	0	0	0	2	11	18	24	23	12	2	0	0
Hot day (t_{max} ≥ 30°C)	0	0	0	0	2	6	11	10	3	0	0	0

2.2.3. UNISB climate conditions

UNISB has a very similar climate conditions to Osijek because of its geographical proximity described in section 2.2.2. Comparison to the average for the 1963 – 2018 period in Slavonski Brod (according to data of the Croatian Meteorological and Hydrological Service). The average values of climatic parameters, climate normals, give an insight into the climatic characteristics of the area. By comparing climatic parameters for different 30-year periods, one can gain insight into the climatic conditions of an area or their variability can be an indication of climate change. In Table 2.3 are shown average values of climatic parameters while Figure 2.24 shows comparison of air temperature to the average for the period od 1963 to 2018 in Slavonski Brod.

Table 2.3 – Average values of climatic parameters for Slavonski Brod

1961–1990

		I	II	III	IV	V	VI	VII	VIII	IX	X	XI	XII	Z/W	P/Sp	Lj/Su	J/A	Veg	G/An
Temperatura zraka Air temperature																				
t	(°C)	-1.1	1.7	6.1	11.1	15.8	19.0	20.6	19.9	16.1	10.7	5.4	0.7	0.5	11.0	19.8	10.7	17.1	10.5	
T_{max}	(°C)	18.7	21.9	27.4	31.4	35.2	37.0	39.2	38.8	34.5	30.2	25.2	23.0	23.0	35.2	39.2	34.5	39.2	39.2	
T_{min}	(°C)	-27.8	-23.0	-14.0	-4.5	-1.7	1.7	6.1	4.7	-3.1	-5.8	-13.7	-22.0	-27.8	-14.0	1.7	-13.7	-4.5	-27.8	
t_{max}	(°C)	2.5	6.2	11.9	17.2	22.0	25.0	27.1	26.7	23.3	17.3	10.0	4.2	4.3	17.0	26.3	16.9	23.6	16.1	
t_{min}	(°C)	-4.8	-2.4	0.8	5.0	9.3	12.5	13.6	13.2	9.9	5.3	1.3	-2.6	-3.2	5.0	13.1	5.5	10.6	5.1	
$t_{min\ 5cm}$	(°C)	-5.6	-3.9	-1.3	2.7	7.0	10.6	11.7	10.8	8.0	3.5	-0.1	-3.7	-4.4	2.8	11.1	3.8	8.5	3.3	
$t_{min\ 5cm\ min}$	(°C)	-28.6	-26.0	-19.0	-8.5	-5.0	-1.7	0.6	3.0	-7.0	-9.8	-18.5	-23.3	-28.6	-19.0	-1.7	-18.5	-8.5	-28.6	
$t_{max/a}$ / t_{min}	(°C)																			
t_{min} ≤-10°C	(d)	4.6	1.8	0.6	0.0	0.0	0.0	0.0	0.0	0.0	0.0	0.3	2.1	8.5	0.6	0.0	0.3	0.0	9.4	
t_{max}<0°C	(d)	9.8	3.4	0.8	0.0	0.0	0.0	0.0	0.0	0.0	0.0	0.4	6.0	19.1	0.8	0.0	0.4	0.0	20.4	
t_{min}<0°C	(d)	26.1	19.3	12.0	2.2	0.2	0.0	0.0	0.0	0.2	3.3	10.8	22.5	67.1	14.4	0.0	14.2	2.6	96.5	
t_{max}≥25°C	(d)	0.0	0.0	0.3	2.0	8.9	16.1	21.8	20.9	11.2	2.5	0.1	0.0	0.0	11.2	58.9	13.8	81.0	83.8	
t_{max}≥30°C	(d)	0.0	0.0	0.0	0.1	0.8	3.5	8.2	7.5	2.1	0.0	0.0	0.0	0.0	0.9	19.2	2.2	22.2	22.3	
t_{min}≥20°C	(d)	0.0	0.0	0.0	0.0	0.0	0.1	0.2	0.2	0.1	0.0	0.0	0.0	0.0	0.0	0.4	0.0	0.4	0.4	
$t_{min\ 5cm}$<0°C	(d)	26.5	21.3	17.6	8.0	1.2	0.1	0.0	0.0	0.7	7.4	13.6	23.5	70.5	26.7	0.1	21.7	10.0	119.9	
Temperaturni zbroj iznad pragova 5°C i 10°C Temperature sum above the thresholds 5°C and 10°C																				
$t_{5°C}$	(°C)	4.1	17.5	80.0	184.1	328.6	411.2	474.9	461.9	346.3	198.1	63.0	12.9	33.6	592.7	1348.0	607.4	2257.0	2581.7	
$t_{5°C\ max}$	(°C)	22.7	91.4	147.4	258.6	411.4	491.7	544.3	535.1	451.5	347.3	186.8	65.3	116.0	743.0	1554.2	778.0	2523.1	2979.9	
$t_{5°C\ min}$	(°C)	0.0	0.0	19.5	92.7	253.0	362.6	417.0	370.8	257.0	85.5	3.2	0.0	3.1	411.1	1209.4	468.8	1966.2	2251.7	
$t_{10°C}$	(°C)	0.1	1.7	13.7	62.8	178.2	261.2	319.9	306.9	197.3	72.5	10.8	1.2	3.0	252.7	888.0	280.6	1304.3	1424.3	
$t_{10°C\ max}$	(°C)	2.5	14.2	38.9	125.5	258.2	341.7	388.3	380.1	301.6	199.8	71.1	22.1	33.2	378.2	1094.2	429.8	1630.7	1762.0	
$t_{10°C\ min}$	(°C)	0.0	0.0	0.0	17.4	101.4	212.6	261.9	215.8	109.7	5.3	0.0	0.0	0.0	127.0	749.4	157.5	1085.8	1157.4	
Temperatura tla Soil temperature																				
t_{5cm}	(°C)	0.3	2.0	6.0	11.7	17.2	21.2	22.9	22.0	18.1	12.4	6.4	2.0	1.4	11.7	22.0	12.3	18.8	11.8	
$t_{5cm\ max}$	(°C)	3.5	6.0	9.3	17.8	21.2	24.0	26.2	23.7	21.3	16.4	9.4	4.2	6.0	21.2	26.2	21.3	26.2	26.2	
$t_{5cm\ min}$	(°C)	-6.1	-3.4	2.2	8.7	14.1	19.1	20.1	19.3	15.6	9.2	2.6	-2.9	-6.1	2.2	19.1	2.6	8.7	-6.1	
t_{30cm}	(°C)	1.4	2.6	5.8	11.3	16.2	20.1	22.0	21.8	18.5	13.3	7.8	3.2	2.4	11.1	21.3	13.1	18.3	12.0	
$t_{30cm\ max}$	(°C)	3.7	5.7	9.0	14.2	19.0	22.7	24.5	23.3	21.0	16.9	11.0	5.4	5.7	19.0	24.5	21.0	24.5	24.5	
$t_{30cm\ min}$	(°C)	-4.4	-0.8	1.6	8.7	13.8	18.4	19.8	19.4	16.3	10.8	4.5	-0.9	-4.4	1.6	18.4	4.5	8.7	-4.4	
Oborina Precipitation																				
R	(mm)	48.9	42.7	50.8	59.4	73.3	84.8	82.5	69.1	59.1	52.0	63.6	57.5	148.7	183.5	236.2	174.8	428.1	743.6	
R_{max}	(mm)	120.7	119.4	118.0	114.9	179.5	142.6	262.2	168.7	171.6	155.0	127.7	123.3	308.5	292.1	462.2	271.5	621.4	928.2	
R_{min}	(mm)	4.8	8.4	4.8	21.0	9.7	25.8	25.5	4.8	9.5	0.1	10.5	3.9	43.6	94.0	107.9	79.0	299.1	540.7	
R_{dmax}	(mm)	28.4	25.5	29.8	42.5	65.5	52.4	76.8	51.0	64.0	58.6	38.3	35.8	35.8	65.5	76.8	64.0	76.8	76.8	
$R_{d≥0.1mm}$	(d)	13.3	12.1	13.0	13.4	13.3	14.1	10.2	10.4	9.4	9.6	12.7	14.8	40.0	39.6	34.7	31.7	70.7	146.1	
$R_{d≥1mm}$	(d)	7.8	7.8	8.6	9.2	9.7	10.3	7.8	7.1	6.7	6.5	9.3	9.9	25.4	27.5	25.1	22.5	50.7	100.6	
$R_{d≥5mm}$	(d)	3.5	3.1	3.3	3.9	4.7	5.2	4.5	4.1	3.7	3.3	4.3	3.9	10.6	11.9	13.9	11.3	26.2	47.5	
$R_{d≥10mm}$	(d)	1.3	1.3	1.5	1.9	2.3	2.7	2.7	2.6	2.1	1.7	1.9	1.4	4.0	5.6	7.9	5.6	14.1	23.2	
$R_{d≥20mm}$	(d)	0.2	0.1	0.3	0.4	0.6	1.2	1.2	0.9	0.6	0.4	0.5	0.3	0.6	1.4	3.3	1.5	4.9	6.8	
$R_{d≥50mm}$	(d)	0.0	0.0	0.0	0.0	0.0	0.0	0.1	0.0	0.0	0.1	0.0	0.0	0.0	0.0	0.2	0.1	0.2	0.3	
$S_{≥1cm}$	(d)	14.2	8.5	2.7	0.1	0.0	0.0	0.0	0.0	0.0	0.0	0.0	2.2	8.5	31.1	2.8	0.0	2.2	0.1	36.3
$S_{≥10cm}$	(d)	7.1	4.4	0.6	0.0	0.0	0.0	0.0	0.0	0.0	0.0	0.5	3.8	15.3	0.6	0.0	0.5	0.0	16.4	
$S_{≥30cm}$	(d)	2.3	0.9	0.0	0.0	0.0	0.0	0.0	0.0	0.0	0.0	0.0	0.5	3.7	0.0	0.0	0.0	0.0	3.7	
$S_{≥50cm}$	(d)	0.0	0.1	0.0	0.0	0.0	0.0	0.0	0.0	0.0	0.0	0.0	0.2	0.3	0.0	0.0	0.0	0.0	0.3	
S_{max}	(cm)	47	55	24	4	0	0	0	0	0	0	15	68	68	24	0	15	4	68	
Isparavanje Evaporation																				
EV	(mm)																			
EVmax	(mm)																			
EVmin	(mm)																			
PET	(mm)	10	17	31	52	77	99	115	104	70	40	21	12	39	160	318	131	517	648	
ET	(mm)	10	17	31	52	77	96	109	94	64	39	21	12	39	160	299	124	492	622	

1971–2000

		I	II	III	IV	V	VI	VII	VIII	IX	X	XI	XII	Z/W	P/Sp	Lj/Su	J/A	Veg	G/An
Temperatura zraka Air temperature																				
t	(°C)	-0.2	1.9	6.5	11.0	16.1	19.3	21.0	20.4	16.1	10.6	5.0	1.1	0.9	11.2	20.2	10.6	17.3	10.7	
T_{max}	(°C)	18.7	21.9	27.4	29.0	34.6	35.1	38.6	39.6	34.5	30.2	25.6	23.0	23.0	34.8	39.6	34.5	39.6	39.6	
T_{min}	(°C)	-26.1	-23.0	-12.9	-5.5	-0.8	1.7	6.0	4.7	-3.0	-7.4	-13.7	-20.5	-26.1	-12.9	1.7	-13.7	-5.5	-26.1	
t_{max}	(°C)	3.5	6.9	12.5	17.1	22.2	25.2	27.4	27.2	23.1	17.0	9.5	4.8	5.0	17.3	26.6	16.5	23.7	16.4	
t_{min}	(°C)	-3.8	-2.6	0.9	4.9	9.4	12.7	14.0	13.7	9.9	5.4	1.0	-2.4	-3.0	5.0	13.4	5.5	10.8	5.2	
$t_{min\ 5cm}$	(°C)	-4.8	-4.4	-1.4	2.3	6.9	10.6	11.8	11.1	7.9	3.7	-0.4	-3.5	-4.2	2.6	11.2	3.7	8.4	3.3	
$t_{min\ 5cm\ min}$	(°C)	-27.5	-26.0	-16.5	-8.5	-5.0	-1.7	0.6	3.0	-7.0	-9.8	-18.5	-21.5	-27.5	-16.5	-1.7	-18.5	-8.5	-27.5	
$t_{max/a}$ / t_{min}	(°C)																			
t_{min} ≤-10°C	(d)	2.9	1.9	0.5	0.0	0.0	0.0	0.0	0.0	0.0	0.2	2.2	7.0	0.5	0.0	0.2	0.0	7.7		
t_{max}<0°C	(d)	7.9	3.1	0.6	0.0	0.0	0.0	0.0	0.0	0.0	0.8	4.8	15.9	0.6	0.0	0.8	0.0	17.2		
t_{min}<0°C	(d)	25.4	19.8	12.1	2.6	0.1	0.0	0.0	0.0	0.1	3.6	11.5	21.8	67.4	14.8	0.0	15.2	2.8	97.0	
t_{max}≥25°C	(d)	0.0	0.0	0.4	2.1	9.6	16.5	22.6	22.1	11.1	2.2	0.0	0.0	0.0	12.1	61.2	13.4	84.0	86.6	
t_{max}≥30°C	(d)	0.0	0.0	0.0	0.0	0.8	4.0	8.8	8.7	1.7	0.0	0.0	0.0	0.0	0.8	21.5	1.8	24.0	24.1	
t_{min}≥20°C	(d)	0.0	0.0	0.0	0.0	0.1	0.4	0.4	0.0	0.0	0.0	0.0	0.0	0.0	0.0	0.9	0.0	0.9	0.9	
$t_{min\ 5cm}$<0°C	(d)	26.4	21.8	18.0	9.0	1.1	0.1	0.0	0.0	0.6	7.2	14.3	22.9	71.4	28.0	0.1	21.9	10.7	121.1	
Temperaturni zbroj iznad pragova 5°C i 10°C Temperature sum above the thresholds 5°C and 10°C																				
$t_{5°C}$	(°C)	5.8	19.4	85.2	181.3	332.8	418.4	485.7	478.7	345.0	197.1	58.9	13.4	38.7	599.2	1382.8	601.0	2241.9	2621.8	
$t_{5°C\ max}$	(°C)	22.7	89.0	160.0	275.6	424.8	484.3	568.4	640.1	451.5	284.3	169.3	65.3	116.0	734.8	1670.7	799.3	2553.4	3060.4	
$t_{5°C\ min}$	(°C)	0.0	0.0	19.5	92.7	225.3	362.6	417.0	370.8	257.0	85.5	3.2	0.0	3.5	411.1	1209.4	468.8	1966.2	2251.7	
$t_{10°C}$	(°C)	0.1	1.4	15.8	61.5	181.4	268.4	330.7	323.7	195.8	74.9	9.7	1.5	3.0	258.7	922.8	280.4	1361.5	1464.8	
$t_{10°C\ max}$	(°C)	2.5	11.1	38.9	139.9	269.9	334.2	411.4	485.1	301.6	141.1	44.5	22.1	33.2	387.4	1210.6	407.8	1688.1	1794.7	
$t_{10°C\ min}$	(°C)	0.0	0.0	0.0	17.4	81.1	212.8	281.9	215.8	108.7	5.3	0.0	0.0	0.0	127.0	749.4	157.5	1085.8	1157.4	
Temperatura tla Soil temperature																				
t_{5cm}	(°C)	0.9	2.4	6.6	11.7	17.8	21.5	23.3	22.7	18.2	12.4	6.3	2.2	1.8	12.0	22.5	12.3	19.2	12.2	
$t_{5cm\ max}$	(°C)	3.5	6.0	10.1	14.5	21.2	24.0	26.2	27.5	21.3	14.8	10.0	4.2	6.0	21.2	27.5	21.3	27.5	27.5	
$t_{5cm\ min}$	(°C)	-1.2	-0.7	2.2	8.6	13.9	19.5	21.5	19.3	15.6	9.2	2.6	-0.8	-1.2	2.2	19.3	2.6	8.6	-1.2	
t_{30cm}	(°C)	1.7	2.5	6.2	11.1	16.8	20.5	22.6	22.5	18.5	13.3	7.8	3.4	2.5	11.4	21.8	13.2	18.7	12.2	
$t_{30cm\ max}$	(°C)	4.2	5.7	9.8	13.9	19.7	23.8	25.4	26.4	21.0	16.2	10.8	5.6	5.7	19.7	26.4	21.0	26.4	26.4	
$t_{30cm\ min}$	(°C)	-1.7	-0.5	2.5	8.3	13.2	18.6	20.8	19.4	16.2	10.3	4.5	1.2	-1.7	2.5	18.6	4.5	8.3	-1.7	
Oborina Precipitation																				
R	(mm)	47.3	38.5	45.8	55.9	69.4	82.4	87.8	67.9	62.9	68.3	68.4	53.4	137.9	171.1	238.1	199.6	426.3	748.1	
R_{max}	(mm)	111.7	83.6	98.8	101.8	179.5	164.5	262.2	141.2	173.8	183.4	127.7	113.3	223.5	292.1	462.2	358.2	621.4	992.2	
R_{min}	(mm)	12.4	3.3	10.5	23.8	9.7	25.3	8.4	10.9	9.5	4.1	10.5	3.9	43.8	94.0	123.8	79.0	250.9	511.3	
R_{dmax}	(mm)	36.8	29.6	30.4	28.1	45.0	64.2	76.8	48.4	42.4	58.6	36.0	34.3	36.8	45.0	76.8	58.6	76.8	76.8	
$R_{d≥0.1mm}$	(d)	12.0	11.1	12.1	13.4	12.5	13.8	10.4	10.1	9.7	11.0	12.4	13.7	36.8	37.9	34.4	33.1	70.0	142.2	
$R_{d≥1mm}$	(d)	7.3	7.2	7.8	9.2	9.2	10.4	7.9	7.2	7.4	7.8	8.8	9.0	23.6	26.2	25.4	23.7	51.2	98.8	
$R_{d≥5mm}$	(d)	3.5	2.7	3.0	3.9	4.2	5.3	4.6	4.1	4.2	4.1	4.8	3.6	9.7	11.2	14.0	13.0	26.4	48.0	
$R_{d≥10mm}$	(d)	1.5	1.2	1.4	1.9	2.1	2.5	3.1	2.5	2.2	2.2	2.3	1.3	3.9	5.4	8.1	6.7	14.3	24.2	
$R_{d≥20mm}$	(d)	0.1	0.1	0.2	0.2	0.6	0.9	1.3	0.9	0.6	0.7	0.5	0.3	0.5	1.1	3.2	1.8	4.7	6.6	
$R_{d≥50mm}$	(d)	0.0	0.0	0.0	0.0	0.0	0.0	0.0	0.0	0.0	0.0	0.0	0.0	0.0	0.1	0.1	0.1	0.1	0.2	
$S_{≥1cm}$	(d)	11.2	7.3	1.8	0.2	0.0	0.0	0.0	0.0	0.0	0.0	2.7	7.4	26.3	2.0	0.0	2.7	0.2	30.6	
$S_{≥10cm}$	(d)	4.1	3.0	0.3	0.0	0.0	0.0	0.0	0.0	0.0	0.4	1.7	9.1	0.3	0.0	0.4	0.0	9.5		
$S_{≥30cm}$	(d)	0.3	0.5	0.0	0.0	0.0	0.0	0.0	0.0	0.0	0.0	0.1	0.9	0.0	0.0	0.0	0.0	0.9		
$S_{≥50cm}$	(d)	0.0	0.0	0.0	0.0	0.0	0.0	0.0	0.0	0.0	0.0	0.0	0.0	0.0	0.0	0.0	0.0	0.0	0.0	
S_{max}	(cm)	34	51	24	4	0	0	0	0	0	0	15	36	51	24	0	15	4	51	
Isparavanje Evaporation																				
EV	(mm)																			
EVmax	(mm)																			
EVmin	(mm)																			
PET	(mm)	11	18	33	51	79	101	117	109	69	39	20	12	41	163	327	128	526	659	
ET	(mm)	11	18	33	51	79	98	111	95	63	38	20	12	41	163	304	121	497	629	

		1961–1990																	1971–2000													
		I	II	III	IV	V	VI	VII	VIII	IX	X	XI	XII	Z/W	P/Sp	LJ/Su	J/A	Veg	G/An	I	II	III	IV	V	VI	VII	VIII	IX	X	XI	XII	Z/W	P/Sp	LJ/Su	J/A	Veg	G/An
Vlažnost zraka Air humidity																																					
U	(%)	87.0	81.7	74.5	71.5	73.7	74.7	73.4	75.7	79.1	81.7	86.1	88.2	85.6	73.2	74.6	82.3	74.7	78.9	87.1	80.9	73.1	72.0	73.6	74.7	73.7	75.6	79.6	82.4	86.3	88.6	85.5	72.9	74.7	82.8	74.9	79.0
Umin	(%)	31.0	13.0	5.0	6.0	18.0	23.0	24.0	21.0	16.0	15.0	28.0	31.0	13.0	5.0	21.0	15.0	6.0	5.0	31.0	13.0	5.0	6.0	18.0	23.0	25.0	21.0	18.0	15.0	28.0	31.0	13.0	5.0	21.0	15.0	6.0	5.0
U>80%	(d)	16.5	8.9	5.1	4.4	3.5	3.0	2.3	2.5	3.1	6.0	13.4	17.8	43.2	13.0	7.8	22.5	18.8	86.5	16.5	7.9	4.9	4.5	3.8	3.4	2.6	2.8	3.2	7.4	13.3	17.3	41.7	13.1	8.8	23.9	20.3	87.5
U<30%	(d)	0.0	0.3	3.0	3.8	1.4	0.7	0.7	1.0	1.3	0.8	0.1	0.0	0.3	8.2	2.4	2.2	8.8	13.1	0.0	0.4	2.9	3.3	1.7	0.6	0.7	1.3	0.7	0.8	0.1	0.0	0.9	0.4	7.9	2.7	1.6	8.4	12.5
e	(hPa)	5.2	5.9	7.0	9.3	13.1	16.4	17.8	17.3	14.4	10.7	8.0	6.0	5.7	9.8	17.1	11.0	14.7	10.9	5.5	5.9	7.0	9.2	13.3	16.6	18.1	17.8	14.5	10.8	7.8	6.1	5.9	9.9	17.5	11.0	14.9	11.1
Sunčevo zračenje Solar radiation (1961-1980)																				**Sunčevo zračenje** Solar radiation															
G_{0°	(MJm^{-2})	128	192	346	474	609	633	653	571	427	278	134	90	410	1429	1857	838	3367	4535																		
$G_{45^\circ S}$	(MJm^{-2})	200	271	414	482	550	542	573	555	496	389	199	132	603	1446	1669	1084	3197	4802																		
Trajanje sijanja Sunca Insolation duration																				**Trajanje sijanja Sunca** Insolation duration															
SS	(h)	1.6	2.7	4.3	5.7	7.0	7.6	8.6	8.1	6.4	4.4	2.2	1.4	1.9	5.6	8.1	4.3	7.2	5.0	1.8	3.2	4.6	5.8	7.2	7.9	8.7	8.2	6.3	4.2	2.2	1.6	2.2	5.9	8.3	4.3	7.4	5.2
SS_{rel}	(%)																																				
SS_{max}	(h)	3.2	6.0	6.5	8.0	8.7	9.1	10.6	10.2	9.0	6.7	3.7	2.9	3.1	6.8	9.1	5.3	8.0	5.7	3.8	6.0	6.3	7.3	9.3	11.4	10.6	11.0	9.0	6.1	3.9	2.9	3.7	7.3	10.6	5.3	8.9	6.3
SS_{min}	(h)	0.5	0.6	2.2	3.8	4.5	5.9	6.1	6.2	4.5	2.7	0.1	0.5	0.9	4.1	6.8	3.1	6.2	4.4	0.5	0.6	2.6	3.8	4.5	5.9	6.1	6.2	4.5	2.7	0.1	0.6	0.9	4.1	6.8	3.1	6.2	4.4
Naoblaka Cloudiness																				**Naoblaka** Cloudiness															
N (10/10)		7.8	7.3	6.8	6.5	6.2	6.0	4.8	4.6	5.2	6.1	7.8	8.1	7.7	6.5	5.1	6.3	5.5	6.4	7.6	6.7	6.3	6.3	5.8	5.6	4.7	4.4	5.1	6.1	7.4	7.6	7.3	6.1	4.9	6.2	5.3	6.1
N_{max} (10/10)		9.4	9.3	8.5	7.8	7.7	7.2	7.5	6.5	6.8	8.0	9.6	9.7	8.8	7.6	6.2	7.4	6.6	7.0	9.4	9.3	8.2	7.8	7.7	7.2	7.5	6.5	7.2	8.0	9.6	9.5	8.5	7.3	6.2	7.4	6.6	7.0
N_{min} (10/10)		5.9	4.3	4.7	4.9	4.8	5.0	3.3	2.6	2.3	3.8	5.9	6.1	6.1	5.4	4.2	5.3	4.8	5.7	4.5	4.1	4.7	4.9	4.1	2.6	3.3	1.8	2.3	4.3	5.9	5.8	5.3	4.9	3.0	5.2	4.0	5.1
N<2/10		1.6	1.9	3.1	3.4	3.3	3.1	7.0	8.7	6.5	3.8	1.7	1.2	4.7	9.7	18.8	12.0	32.0	45.2	2.0	3.3	3.6	3.3	3.8	3.6	7.1	8.8	5.8	3.5	1.9	1.9	7.2	10.6	19.5	11.2	32.4	48.5
N<2/10 max		5	8	9	11	10	7	13	18	19	10	5	4	16	22	32	24	51	71	10	12	9	11	10	13	13	21	17	10	5	7	22	22	38	22	56	82
N<2/10 min		0	0	0	0	0	0	1	0	0	0	0	0	0	2	11	3	16	23	0	0	0	0	0	0	1	0	0	0	0	0	0	3	9	3	16	23
N>8/10		18.0	14.9	13.3	11.0	9.7	8.4	5.7	5.8	7.6	10.3	16.7	19.6	52.5	34.1	19.8	34.6	48.2	141.1	17.6	13.1	11.0	10.2	8.3	7.0	5.2	4.9	6.9	10.7	15.9	17.6	48.3	29.6	17.1	33.5	42.6	128.5
N>8/10 max		29	24	24	18	18	15	15	11	13	19	27	28	68	50	31	49	66	178	29	24	21	18	18	15	15	10	14	19	27	28	68	47	31	49	66	178
N>8/10 min		9	3	3	4	3	2	2	0	1	2	9	10	37	21	11	24	31	107	6	3	3	4	2	0	2	0	0	4	7	10	26	12	2	21	17	72
Meteorološke pojave Weather phenomena																				**Meteorološke pojave** Weather phenomena															
magla/fog		15.6	10.6	6.1	3.6	5.4	7.0	8.0	10.4	15.3	17.5	15.1	15.4	41.7	15.1	25.4	47.9	49.6	130.1	15.4	10.6	6.2	4.7	6.1	7.7	9.1	11.2	16.2	17.4	15.2	15.8	41.8	16.9	28.1	48.7	55.0	135.5
magla/fog max		26	21	20	11	13	18	20	23	27	27	24	26	65	43	53	77	103	232	26	21	20	11	13	18	20	23	27	27	24	26	65	43	53	77	103	232
magla/fog min		7	3	0	0	0	0	0	0	2	5	0	5	16	0	3	15	10	47	5	2	0	0	1	1	0	0	0	8	7	3	17	4	3	18	7	44
tuča/hail		0.0	0.0	0.0	0.1	0.3	0.2	0.2	0.1	0.1	0.0	0.0	0.0	0.0	0.4	0.5	0.1	1.0	1.0	0.0	0.0	0.1	0.0	0.2	0.2	0.3	0.2	0.1	0.1	0.0	0.0	0.1	0.3	0.7	0.2	1.0	1.2
tuča/hail max		0	0	1	1	1	1	1	1	1	0	0	1	1	2	2	1	2	3	1	0	1	1	1	1	1	2	1	1	0	1	1	2	2	1	3	3
tuča/hail min		0	0	0	0	0	0	0	0	0	0	0	0	0	0	0	0	0	0	0	0	0	0	0	0	0	0	0	0	0	0	0	0	0	0	0	0
grm/thun		0.1	0.1	0.4	2.3	5.8	7.6	6.9	6.7	2.0	0.7	0.4	0.2	0.4	8.5	21.3	3.1	31.3	33.3	0.1	0.1	0.5	1.9	5.1	6.8	6.3	6.1	2.1	1.0	0.3	0.2	0.5	7.5	19.2	3.5	28.3	30.7
grm/thun max		1	1	2	8	12	14	14	13	6	4	2	2	2	15	30	7	45	48	1	1	2	6	10	16	14	12	6	5	2	2	2	15	30	8	43	47
grm/thun min		0	0	0	0	1	3	2	2	0	0	0	0	0	1	14	0	18	20	0	0	0	0	1	2	2	1	0	0	0	0	0	1	9	0	18	20
rosa/dew		1.4	3.0	11.3	18.9	22.2	22.2	25.1	25.9	24.5	22.8	11.6	3.4	7.9	52.4	73.2	58.9	138.7	192.3	2.9	4.8	12.8	18.8	23.0	22.1	25.8	25.9	24.5	23.4	12.9	4.8	12.5	54.5	73.8	60.9	140.1	201.8
rosa/dew max		21	19	25	26	30	28	31	31	30	31	25	20	34	71	87	81	164	247	21	19	25	26	30	28	31	31	30	30	25	20	34	71	87	81	164	247
rosa/dew min		0	0	0	10	13	13	8	19	16	11	2	0	0	26	50	33	98	126	0	0	0	7	6	2	8	3	13	7	3	0	0	14	13	25	39	54
mraz/frost		11.1	10.2	10.0	3.6	0.3	0.0	0.0	0.0	0.3	4.9	9.3	11.5	32.8	13.9	0.0	14.6	4.2	81.2	14.8	13.7	11.2	3.9	0.2	0.0	0.0	0.0	0.3	5.1	10.0	13.8	42.3	15.3	0.0	15.4	4.4	73.0
mraz/frost max		26	22	17	11	3	0	0	0	2	17	22	23	63	24	0	30	14	108	26	24	17	11	1	0	0	0	2	12	22	28	71	26	0	30	14	108
mraz/frost min		0	0	3	0	0	0	0	0	0	0	1	0	8	3	0	2	0	14	3	3	3	0	0	0	0	0	0	0	0	0	19	5	0	2	0	51
inje/rime		5.6	1.7	0.3	0.0	0.0	0.0	0.0	0.0	0.0	0.2	1.3	3.5	10.8	0.3	0.0	1.4	0.0	12.5	4.8	1.8	0.3	0.0	0.0	0.0	0.0	0.0	0.0	0.2	1.3	3.3	9.9	0.3	0.0	1.5	0.0	11.7
inje/rime max		20	7	3	0	0	0	0	0	0	3	7	10	28	3	0	8	0	31	18	7	3	0	0	0	0	0	0	3	7	10	28	3	0	8	0	31
inje/rime min		0	0	0	0	0	0	0	0	0	0	0	0	0	0	0	0	0	0	0	0	0	0	0	0	0	0	0	0	0	0	0	0	0	0	0	0
Tlak zraka Air pressure																				**Tlak zraka** Air pressure															
p	(hPa)	1009.1	1008.8	1005.6	1002.7	1004.0	1004.4	1005.2	1005.2	1007.5	1009.0	1007.7	1008.2	1008.0	1004.1	1004.9	1008.1	1004.8	1006.3	1010.4	1008.4	1006.3	1002.7	1004.2	1004.5	1004.9	1005.4	1007.0	1008.7	1008.4	1009.3	1009.3	1004.4	1004.9	1008.0	1004.8	1006.7
p max	(hPa)	1033.2	1030.7	1030.3	1023.4	1018.6	1018.2	1016.0	1016.1	1023.8	1026.0	1029.4	1035.8	1035.8	1030.3	1018.2	1029.4	1023.8	1035.8	1029.4	1031.1	1030.3	1023.5	1018.8	1019.0	1018.0	1016.1	1023.6	1028.3	1029.4	1032.1	1034.0	1030.3	1019.0	1029.4	1023.6	1034.0
p min	(hPa)	975.7	964.7	977.0	976.1	981.2	989.2	995.2	987.0	984.6	976.8	977.7	960.5	960.5	976.1	995.2	976.8	995.2	960.5	975.7	964.7	977.0	978.3	981.2	988.8	995.2	987.6	982.5	977.8	977.7	960.5	960.5	977.0	995.2	977.7	995.2	980.5
Vjetar Wind																				**Vjetar** Wind															
v_b	(ms^{-1})	1.8	2.0	2.4	2.4	2.0	1.9	1.7	1.7	1.5	1.6	1.7	1.9	1.9	2.3	1.7	1.6	1.9	1.9	2.0	2.2	2.6	2.6	2.2	2.1	1.9	1.8	1.7	1.8	1.9	2.0	2.1	2.5	1.9	1.8	2.1	2.1
v_b max	(ms^{-1})	15.4	13.1	12.5	13.5	12.0	12.0	16.8	12.0	12.0	12.0	13.0	13.1	15.4	13.5	16.8	13.0	16.8	16.8	15.4	16.9	18.4	20.3	14.3	14.2	16.8	14.2	15.9	16.9	18.5	13.6	16.9	20.3	16.8	18.5	20.3	20.3
v_{max}	(ms^{-1})	30.0	25.4	23.3	29.7	25.1	23.1	31.1	29.6	28.0	23.0	25.6	27.7	30.0	29.7	31.1	28.0	31.1	31.1	30.0	26.0	25.7	29.7	25.6	26.1	38.3	29.6	28.0	27.0	27.2	27.7	30.0	29.7	38.3	28.0	38.3	38.3
Osjet ugode Thermal sensation																				**Osjet ugode** Thermal sensation															
$PhET_{7h}$	(°C)	-8.7	-8.4	-2.5	4.9	12.5	17.1	18.3	15.4	9.3	3.0	-2.1	-6.2	-7.8	5.0	16.9	3.4	12.9	4.4	-7.6	-7.4	-2.5	4.4	12.5	16.9	18.2	15.7	9.2	3.4	-2.1	-6.0	-7.0	4.8	16.9	3.5	12.8	4.6
$PhET_{14h}$	(°C)	-1.8	-0.6	9.3	15.8	23.2	27.7	31.1	30.2	25.0	16.1	6.3	-0.2	-0.9	16.1	29.7	15.8	25.5	15.2	-0.9	0.9	9.6	15.9	23.2	28.0	31.2	31.2	24.8	15.9	6.1	0.3	0.1	16.3	30.1	15.6	25.7	15.5
$PhET_{21h}$	(°C)	-7.4	-6.8	0.0	4.9	10.2	13.7	15.3	14.5	10.7	5.0	-0.6	-5.1	-6.4	5.1	14.5	5.1	11.6	4.5	-6.3	-5.6	0.1	4.9	10.4	14.1	15.8	15.3	10.9	5.4	-0.6	-4.8	-5.5	5.2	15.0	5.2	11.9	5.0

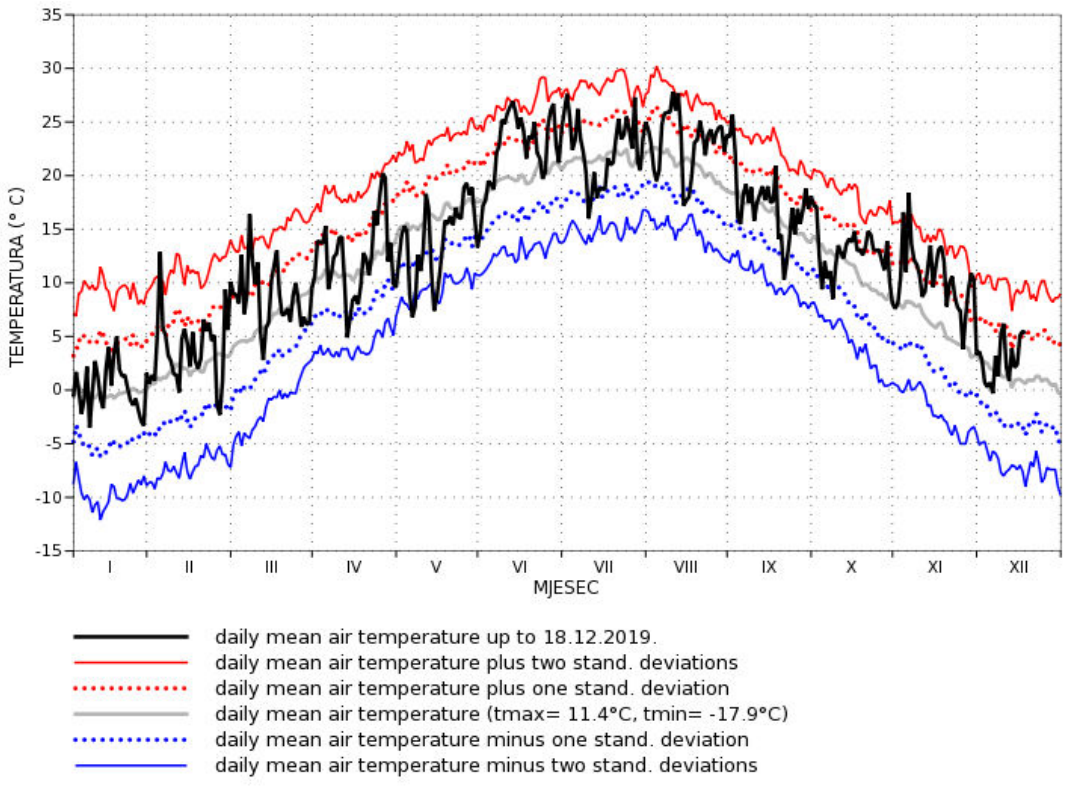

Figure 2.24 Comparison of air temperature to the average for the 1963 – 2018 period in Slavonski Brod

Figure 2.25 show months insolation duration (h) for last 4 years comparison with average monthly duration in 1961. – 1990. period for Slavonski Brod.

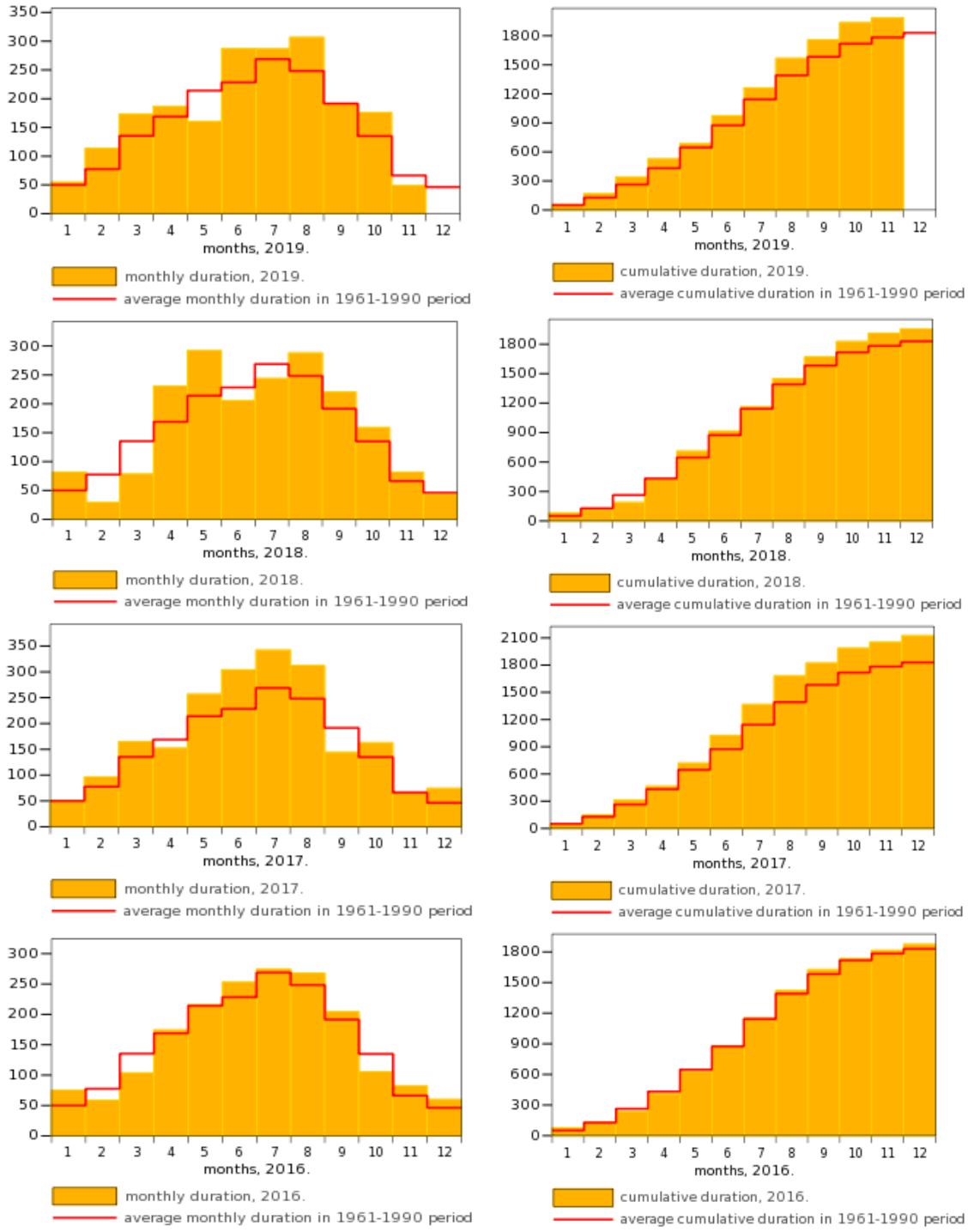

Figure 2.25 Insolation duration (h) in Slavonski Brod

3. Current energy demand overview for the public building

In order to implement different strategies for the increase of energy efficiency, it is necessary to analyze the electrical installation infrastructure of the object, as well as existent power supply units and the consumption of electrical energy in the exemplary objects.

3.1. FTN buildings power supply and energy demand

“Mašinski institut” is supplied from the transformer station located within the object. The transformer station is placed in the ground level of the object, near the main entrance, in a hallway on the right side of the building called the “G” sector. The transformer station is called “TS Mašinski fakultet” and a three-phase oil transformer with a nominal power of 630 kVA, a turn ratio of 10/0.4 kV/kV and a Yy0 transformer connection was used for the object power supply.

Aluminum cable with the 3x150 mm2 cross-section was used as a high-voltage cable. On the low-voltage side copper busbar 3x(2x80x5) + 1x(80x5) mm2 was used. The main circuit breaker is set to the nominal value of the 1250 A. Single line diagram of the transformer station is illustrated in Figure 3.1.

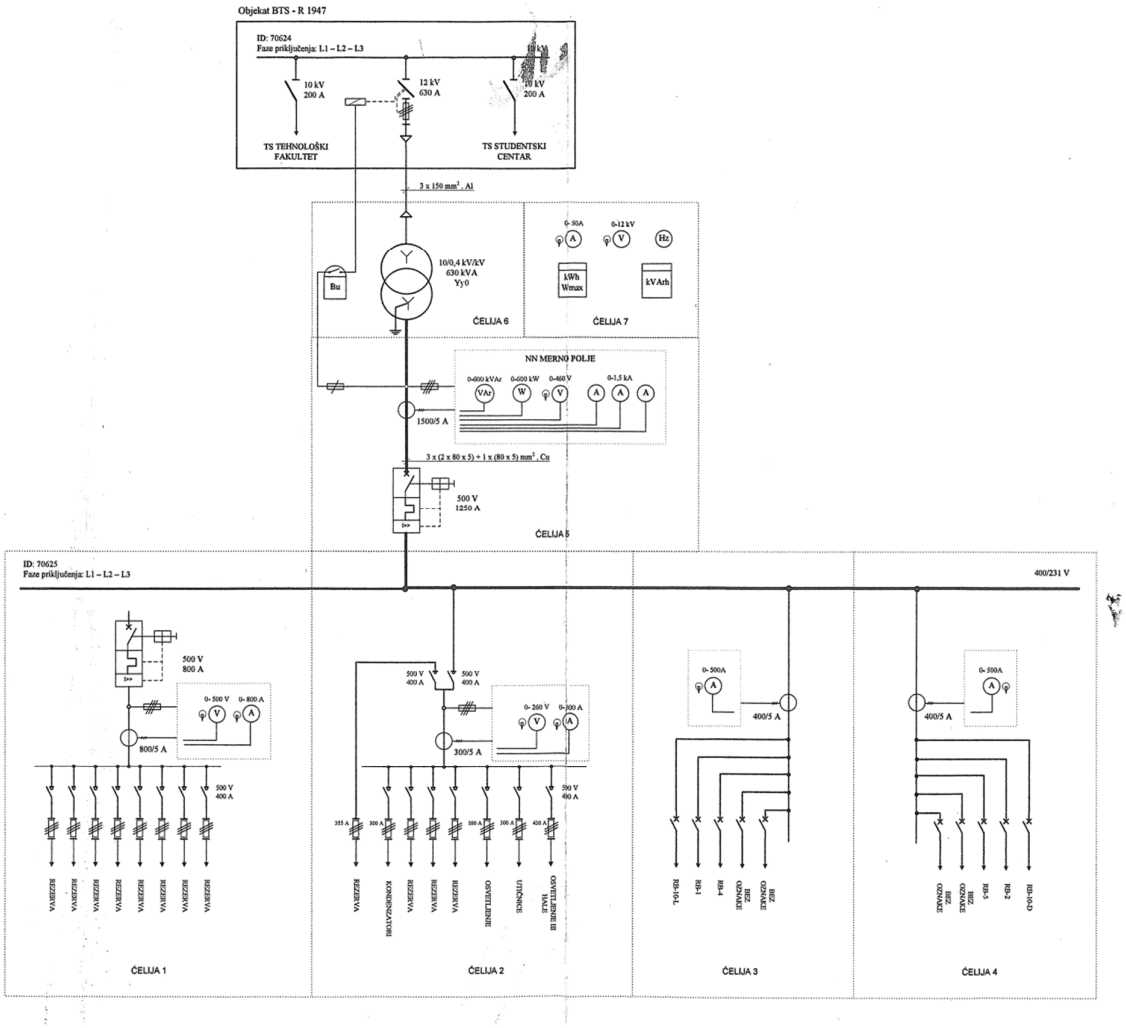

Figure 3.1 Transformer station single line diagram.

Table 3.1 shows all outgoing feeders on the low-voltage side of the transformer, together with the cross-sections of the cable lines. These feeders are used to supply different blocks of the "Mašinski institut". The low-voltage side of the transformer is constituted from five cells and the main circuit breaker with the nominal current 1250 A is placed in the first cell.

In the second cell, five feeders are located and three of them have a reserve function. Feeders RB-2 and RB-3 are connected to the circuit breaker with nominal current 320 A and cable type PP00-Y 4x185mm^2 is used. Feeder RB-10-D has reserve function and is supplied with the PP00-Y 4x150mm^2 cable. Two more feeders have the same function and one is supplied from the 320 A circuit breaker, while the other is supplied from the contactor.

In the third cell, five outgoing feeders, supplied from the circuit breakers with nominal current 320 A, are located. For the feeder RB-10-L cable type PP00-Y 4x150mm^2 was

used and for the feeders RB-1 and RB-4 the type PP00-Y 4x185mm^2 was employed. Two remaining feeders withe the cable type PP00-Y 4x150mm^2 are used as a reserve.

In the fourth cell, there are eight feeders and only one is used as a reserve. For the reserve feeder, as a protective element, fuse with nominal current 200 A and gG characteristics is used. The second feeder is protected with fuse with nominal current 100 A and gG characteristics and the used cable type is PP00-Y 4x50mm^2. The fuse with current 200 A and gG characteristic and cable PP00-Y 4x185mm^2 were used for the third feeder and for the fourth feeder 35 A, gG fuse and cable PP00-Y 4x16mm^2. The fifth and sixth feeder are protected with 200 A, gG fuse and the used cable type is NAYY-J 4x50mm^2. The same fuse was used for the protection of the seventh feeder, but here the cable type is NAYY-J 4x70mm^2. The fifth cell is the reserve.

Table 3.1 An overview of the feeders located on the low-voltage side of the transformer station.

Cell	Breaker mark	Nominal breaker current [A]	Cable type	Note
2	RB-10-D	Breaker not installed	PP00-Y 4x150mm2	Reserve
2	RB-2	320	PP00-Y 4x185mm2	
2	RB-5	320	PP00-Y 4x185mm2	
2	-	320	PP00-Y 4x150mm2	Reserve
2	-	Breaker not installed		Reserve
3	RB-10-L	320	PP00-Y 4x150mm2	
3	RB-1	320	PP00-Y 4x185mm2	
3	RB-4	320	PP00-Y 4x185mm2	
3	-	320	PP00-Y 4x150mm2	Reserve
3	-	320	PP00-Y 4x150mm2	Reserve
4	-	200A gG	PP00-Y 4x185mm2	Feeder 1 - Reserve
4	-	100 A gG	PP00-Y 4x50mm2	Feeder 2
4	-	200A gG	PP00-Y 4x185mm2	Feeder 3
4	-	35A gG	PP00-Y 4x16mm2	Feeder 4
4	-	200A gG	NAYY-J 4x50mm2	Feeder 5
4	-	200A gG	NAYY-J 4x50mm2	Feeder 6
4	-	200A gG	N2XH-J 4x70mm2	Feeder 7
5	-			Feeder 8 - Reserve

All active feeders are employed to supply different areas in the “Mašinski institut” (such as laboratories, teaching rooms, offices, etc.) through the distribution cabinets placed in the various locations in the object. Regarding the installation time and maintenance of the distribution cabinets, different conditions of the cabinets were noticed during the visual inspection of the object. Some cabinets completely lost functionality and became inefficient and thus represent a danger for both the users and the equipment.

To address appropriate measures for the enhancement of energy efficiency, it is necessary to analyze the energy consumption in the exemplary object. A detailed analysis is given for the period from January 2018 to December 2018.

Table 3.12 shows an overview of the power energy consumption from January 2018 to December 2018.

Table 3.2 Electrical energy consumption in the "Mašinski institut" during 2018.

	Consumption in higher tariff [kWh]	Consumption in lower tariff [kWh]	Total consumption [MWh]	Total energy cost [RSD]	Total cost with taxis without VAT [RSD]	Total cost [RSD]
Jan 2018	25,442.4	7,366.4	32.809	171,580.95	276,429.79	331,715.75
Feb 2018	21,521.6	5,973.6	27.495	144,201.81	240,571.87	288,686.24
Mar 2018	29,407.0	8,091.0	37.498	211,150.76	324,373.94	389,248.73
Apr 2018	27,434.0	6,653.0	34.087	193,501.91	302,708.14	363,249.77
May 2018	34,020.0	6,536.0	40.556	233,287.24	353,784.49	424,541.39
Jun 2018	35,978.0	5,747.0	41.725	242,181.41	366,443.76	439,732.51
Jul 2018	24,285.0	5,614.0	29.899	170,219.81	272,310.88	326,773.06
Avg 2018	28,278.0	7,498.0	35.776	201,945.80	313,364.77	376,037.72
Sep 2018	23,552.0	6,725.0	30.277	170,062.97	272,469.86	326,963.84
Oct 2018	30,208.0	7,613.0	37.821	273,839.66	393,852.96	472,623.55
Nov 2018	26,482.0	7,491.0	33.973	244,164.42	355,571.26	426,685.51
Dec 2018	29,142.0	6,497.0	35.639	259,922.54	375,589.15	450,706.98
Total	335,750.0	81,805.0	417.555	2,516,059.28	3,847,470.88	4,616,965.06

Table 3.12 shows the trend of energy consumption increase, especially during the winter period when additional heating is needed and also during the summer when additional cooling is needed. Slight consumption decline is visible during January and February, during the examination period, when no teaching is arranged, and also in July, August and September when there are no curricular activities in the Faculty during the vacation period. In Figure 3.17 energy consumption per month, expressed in MWh, in the period from January 2018 to December 2018.

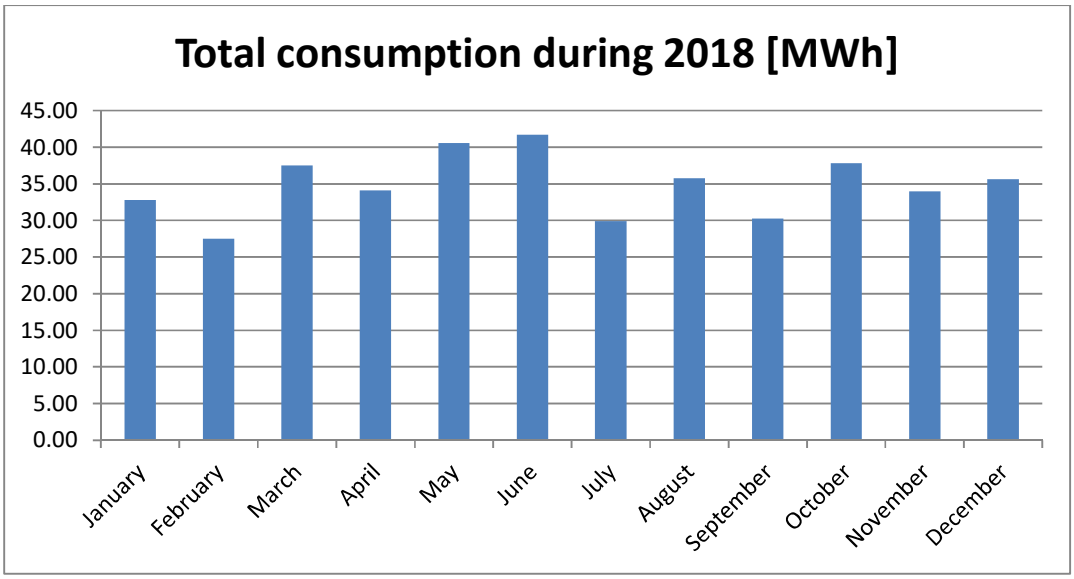

Figure 3.2 Electrical energy consumption per month in the "Mašinski institut" during 2018.

It can be seen that the highest energy consumption was in June. This is probably because the weather conditions lead to the substantial use of air-conditioning systems. During July, the consumption was the somewhat lower since most of the employees started to take their vacation in this period. During the winter, the highest consumption was in December since the semester was ongoing. Moreover, in this period, additional heating devices were employed since temperatures were low. The lowest consumption was in February, when there are no teaching activities. Also, the average temperature for this month was higher than usually.

The thermal infrastructure of the "Mašinski institut" is connected to the district heating system of the utility company "Novosadska toplana" through two heat substations with two separate meters. The main heating energy source is natural gas and delivered power is charged per kWh.

In order to adequately investigate the thermal energy balance of the exemplary object, the analysis of the delivered heat energy in the period from January 2018 to December 2018. This period includes the heating season, as well as the period when the heating is not activated.

Total energy consumption per month, considering the period from January 2018 to December 2018 is given in Table 3.3.

Table 3.3 Heat energy consumption for the "Mašinski institut" during 2018.

Month	Consumed energy 1st substation [kWh]	Consumed energy 2nd substation [kWh]	Total consumption 1st + 2nd [kWh]	Total cost [RSD]
Jan 2018	102,930.00	98,080.00	201,010.00	1,756,764.61

Feb 2018	86,620.00	84,190.00	170,810.00	1,582,027.41
Mar 2018	88,120.00	86,180.00	174,300.00	1,602,220.55
Apr 2018	42,580.00	43,660.00	86,240.00	1,092,705.39
May 2018	0.00	0.00	0.00	593,720.75
Jun 2018	0.00	0.00	0.00	593,720.75
Jul 2018	0.00	0.00	0.00	593,720.75
Aug 2018	0.00	0.00	0.00	593,720.75
Sep 2018	0.00	0.00	0.00	593,720.75
Oct 2018	9,920.00	14,800.00	24,720.00	736,750.67
Nov 2018	39,950.00	40,070.00	80,020.00	1,005,003.28
Dec 2018	79,630.00	76,590.00	156,220.00	1,415,721.28
Total	449,750.00	443,570.00	893,320.00	12,159,796.98

Figure 3.3 illustrates the heat energy consumption per month, during 2018. The chart shape is characteristic of the remotely controlled system that is active only during the heating season (October – April). It can be seen that the highest consumption is in January, when the outside temperature is very low, while there is no heat energy consumption during the summer. Therefore, during the summer only installed power is charged.

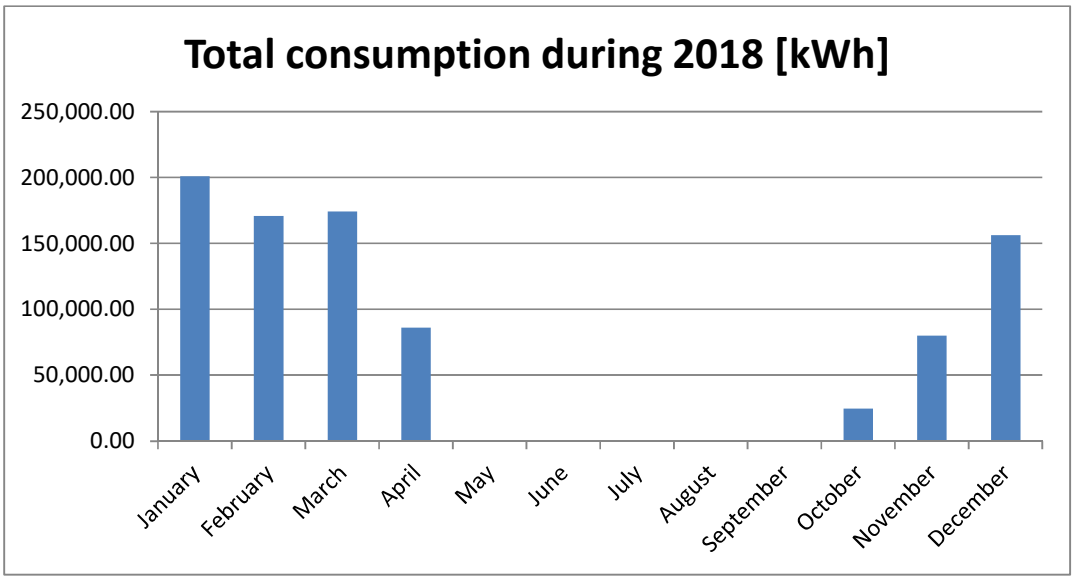

Figure 3.3 Heat energy consumption per month in the "Mašinski institut" during 2018.

3.2. KCV buildings power supply and energy demand

The facility of the Medical Rehabilitation Clinic is powered by a transformer station located in the courtyard of the Clinical Center of Vojvodina. The transformer station is

located in a separate facility, near the Technical Services Department. The transformer station is called "TS Klinička Bolnica". The power supply of the facility in the transformer station was achieved by the use of two three-phase oil transformers with a power of 10/0.4 kV / kV 630 kVA, and one three-phase oil transformer with a power of 10/0.4 kV / kV.

The high voltage side consists of 7 fields, divided into two segments. The first segment consists of three fields, namely: “Trafo polje 1”, “Merna ćelija” and “Trafo polje 2”. The transformer boxes 1 and 2 have switchgear and protective equipment for the protection and manipulation of the on / off switch of the 630 kVA transformer. In the measuring cell, the equipment for measuring consumption of all facilities connected to the low voltage side of "TS Klinička Bolnica" is located. The second segment of the high voltage section consists of 4 fields (or cells). The first field represents the junction cell, and this cell represents the connection between the first and second segments of the high voltage section. It is equipped with appropriate switching and protection equipment. The second and third cells are identical and represent excerpts to the substations "TS Zagrebačka" and "TS Medicinski fakultet". They are also equipped with appropriate switching and protection equipment. The last, fourth cell is a classic transformer cell equipped with switchgear and protective equipment to protect and manipulate the on / off switch of a third 250 kVA transformer. In Figure Figure 3.4 a single-pole diagram of the high-voltage segment of the substation is shown.

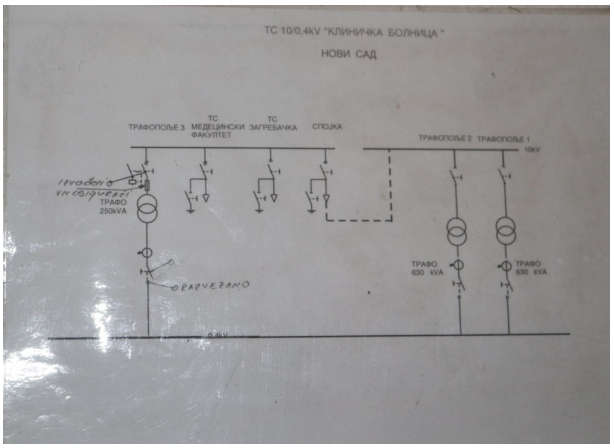

Figure 3.4 Single-pole diagram of the high-voltage segment of the substation

The low voltage side of the substation consists of 5 fields (or cells) interconnected by copper bus bars. Table 3.4 gives an overview of the low-voltage side of the transformer station "TS Klinička Bolnica", as well as cross sections of the used low-voltage cable lines that supply certain objects.

The first, third and fifth fields are identical and are made up of a group of main switches for the statements given in Table 3.4. The second and fourth fields represent transformers 1 and transformers 2. The fields are equipped with main switches and measuring instruments.

In the event of a power failure by the electricity distribution system, the transformer station "TS Klinička Bolnica" is also connected to the diesel power unit, which assumes the role of electricity supply to the facilities connected to the said substation.

Table 3.4 Overview of the low voltage side of the transformer station "TS Klinička Bolnica"

Tap No.	Clinics	Cable type	Current limiters
1	Psychiatry Clinic	PP00 4x120 mm^2	3x200 A
2	Clinic of Neurology		
3	Clinic for Nephrology	PP00 4x150 mm^2	3x250 A
4	Gastroenterology Clinic		
5	Endocrinology Clinic		
6	Hematology Clinic		
7	Infectious Diseases Clinic	PP00-A 4x(1x240) mm^2	3x200 A
8	Rehabilitation Clinic	PP00 4x150 mm^2	3x200 A
9	Technical service	2xPP00 5x16 mm^2	3x80 A
10	Procurement + Garage Workshops	PP00 4x150 mm^2	3x250 A
11	Department of Pathology	PP00 4x35 mm^2	3x100 A
12	Boiler room	PP00 4x120 mm^2	3x160 A
13	Part of outdoor lighting	PP00 4x16 mm^2	3x25 A
14	CT on radiology	PP00 4x150 mm^2	3x250 A

The facility in question has premises for different purposes, containing different types of consumers. One of the most important consumers of electricity, especially in offices and exam rooms, are computers, whereby around 50 units are in the facility.

For cooling, ventilation and temperature control purposes, air conditioners are most commonly used in the premises of the facility, which can also be a major consumer of electricity (especially in periods when climatic conditions require longer operation). The object in question contains a total of 38 air conditioners of the latest generation and 8 air conditioners of the older design. The capacity of individual capacity of newer air conditioners is 9000 BTU, while for old air conditioners it was not possible to determine the capacity of capacity. The facility of the medical rehab clinic also has one central climate. Central climate is of special design and is located in the hydrotherapy room, where it is used to regulate the ventilation of the pool.

In addition to the above-mentioned premises, the Medical Rehabilitation Clinic has 7 kinesiotherapy rooms, 4 electrotherapy rooms and 2 occupational therapy rooms. Occupational therapy is part of a therapeutic-rehabilitation program and includes manual, creative, recreational, social, educational and other activities, with the aim of achieving a specific function, mental attitude or behavior in the patient. Kinesiotherapy is an area of physical therapy that deals with the application of movement for the purpose of healing, with the aim of establishing the optimal functioning of parts and the organism as a whole.

Electrotherapy represents the use of numerous modalities of electric current, which are obtained by means of modern electronic devices for therapeutic purposes.

Kinesiotherapy and occupational therapy rooms, with the exception of air conditioning, are not equipped with significant electricity consumers. While electrotherapy rooms have special electronic devices used for therapeutic purposes.

Significant consumers of electricity in the clinic's facility are water heaters, boilers and elevators for the transportation of persons and materials. The Medical Rehabilitation Clinic has 3 boilers with 80 l capacity of 2 kW, 2 boilers with capacity of 10 l with capacity of 2 kW and 2 lifts for transportation of patients and staff, as well as one small lift for transportation of materials.

Figure 3.5 shows a graphical representation of electricity consumption by month for “TS Klinička Bolnica“, whereby the consumption is expressed in megawatt hours (MWh), from September 2018 to August 2019.

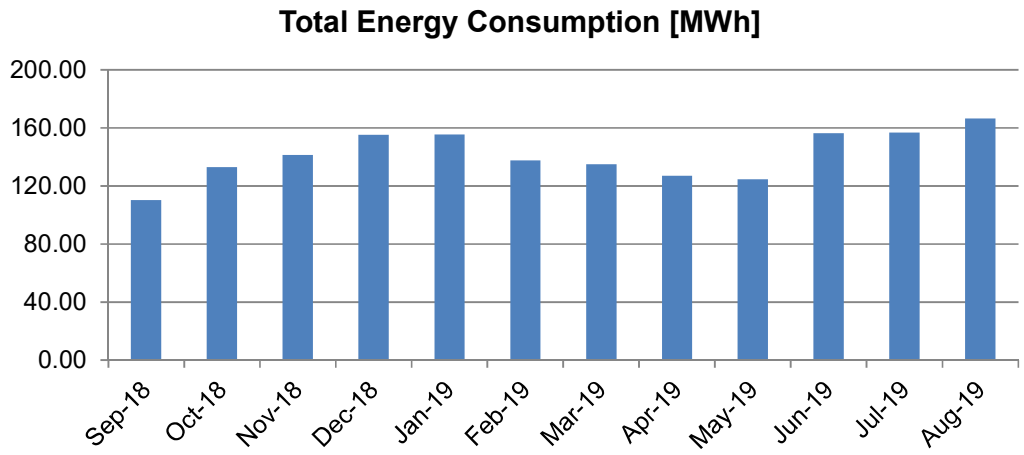

Figure 3.5 Overview of the electrical energy consumption for “TS Klinička Bolnica“

The graphs clearly show that the highest electricity consumption is in July. The reason for this can be found in the fact that during this period the climatic conditions were such that the use of the air conditioners was necessary. In winter, the highest power consumption was in December.

The Radiology clinic is powered from two transformer station namely “TS Poliklinika” and “TS Kotlarnica”. Both transformer stations are located in the courtyard of the Clinical Center of Vojvodina. The high voltage side consists of 5 fields, namely: “Trafo”, “Merna”, “Dovodno polje”, “Odvodno polje” and “Rezerva”. The transformer box has switchgear and protective equipment for the protection and manipulation of the on/off switch of the 1000 kVA transformer. In the measuring cell the equipment for measuring consumption of all facilities connected to the low voltage side of "TS Kotlarnica" is located.

Power transformer in “TS Kotlarnica” is three phase 20/0.4 kV/kV oil transformer with rated power of 1000 kVA. Cooling of the transformer is oil natural air natural (ONAN) which means that windings are cooled with natural flow of the oil while the transformer dish is cooled by natural flow of the air. Winding connection is Dy5 which is standard for a distribution transformers.

The low voltage side of the transformer station consists of 4 fields shown in Figure 3.6, interconnected by copper bus bars. Table 3.5 gives an overview of the low-voltage side of the transformer station "TS Kotlarnica", as well as cross sections of the used low-voltage cable lines that supply certain objects and accompanying current limiters.

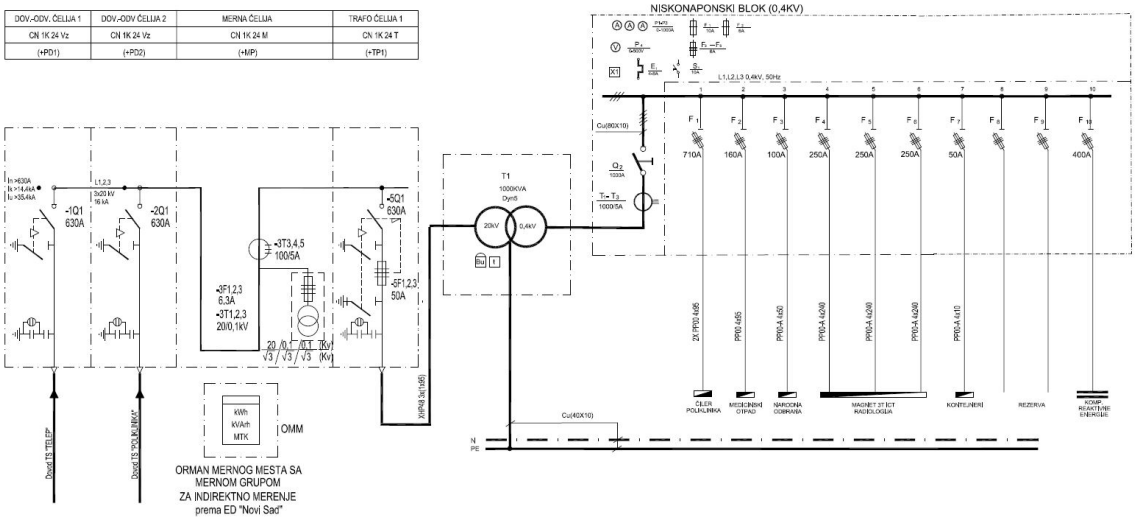

Figure 3.6 Single-pole diagram of the “TS Kotlarnica”

The high voltage side in the “TS Poliklinika” consists of 5 fields, namely: “Transformator 1”, “Transformator 2”, “Merenje celija”, “Dovod 1” and “Dovod 2”. The transformer boxes 1 and 2 have switchgear and protective equipment for the protection and manipulation of the on/off switch of the 1000 kVA transformer. In the measuring cell the equipment for measuring consumption of all facilities connected to the low voltage side of "TS Kotlarnica" is located.

Figure 3.7 gives a single-pole diagram of the high-voltage segment of the “TS Poliklinika” where all 5 substation fields can be clearly seen.

Table 3.5 Overview of the low voltage side of the transformer station "TS Kotlarnica"

Tap No.	Facility	Cable type	Current limiters
1	Chiller in Policlinic facility	PP00 2x(4x150) mm^2	3x710 A
2	Medical waste	PP00 4x95 mm2	3x160 A

3	Population protection	PP00-A 4x50 mm2	3x100 A
4	MRI scanners and CT scanners in Radiology clinic	PP00-A 4x240 mm2	3x250 A
5			
6			
7	Containers	PP00 4x10 mm2	3x50 A
8	Reserve	PP00 4x120 mm2	3x160 A
9		PP00 4x120 mm2	3x160 A
10	Reactive power compensation	PP00 4x150 mm2	3x400 A

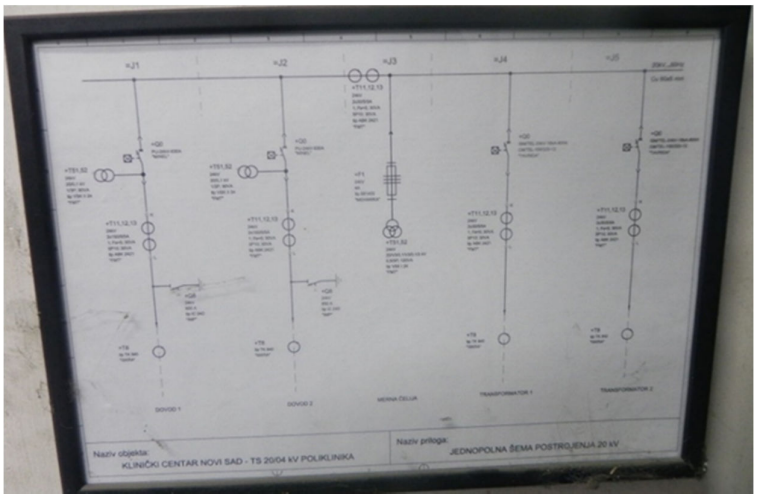

Figure 3.7 Single-pole diagram of the high-voltage segment of the "TS Poliklinika"

Two power transformers in "TS Poliklinika" are three phase 20/0.4 kV/kV oil transformers with rated power of 1000 kVA. Cooling of the transformer is oil natural air natural (ONAN) which means that windings are cooled with natural flow of the oil while the transformer dish is cooled by natural flow of the air. Winding connection is Dy5 which is standard for a distribution transformers. The low voltage side of the transformer station consists of 12 fields, and they are interconnected with the copper bus bars. Table 3.6 gives an overview of the low-voltage side of the transformer station "TS Poliklinika", as well as cross sections of the used low-voltage cable lines that supply certain objects and accompanying current limiters.

Table 3.6 Overview of the low voltage side of the transformer station "TS Poliklinika"

Tap No.	**Clinics**	**Cable type**	**Current limiters**
1	Policlinic Facility	PP00 3x150 mm^2	3x400 A
2	Surgery admission	PP00 3x150 mm^2	3x400 A
3	Kitchen	PP00 3x150 mm^2	3x400 A
4	Dialysis Department	PP00 3x150 mm^2	3x400 A
5	Policlinic Facility	PP00 4x150 mm^2	3x400 A
6			

7			
8	MRI Scanner	PP00 4x120 mm^2	3x400 A
9	Lighting system	PP00 4x150 mm^2	3x400 A
10	Pathology Department	PP00 4x70 mm^2	3x160 A
11	Sterilization	PP00 4x185 mm^2	3x400 A
12	Infectious diseases clinic	PP00 4x150 mm^2	3x400 A

The facility of the Emergency Center is powered from a transformer station located in the courtyard of the Clinical Center of Vojvodina. The transformer station is located in a separate facility. The transformer station is called "ZTS Urgentni Centar". The power supply of the Emergency Center was achieved with the use of two identical three-phase dry transformer. Two power transformers in “ZTS Urgentni Centar” are three-phase 20/0.4 kV/kV oil transformers with rated power of 1600 kVA working in parallel. Cooling of the transformers is air natural (AN) which means that windings of the dry transformer without enclosure are cooled with natural flow of the air. Winding connection is Dy5 which is standard for a distribution transformer. The “TS Urgentni Centar” facility is complex and contains a high number of compactly integrated protective, manipulative and measuring equipment. High voltage segment in “ZTS Urgentni Centar” is shown in Figure 3.8.

In the event of a power failure in the electricity distribution system, the transformer station "ZTS Urgentni Centar" is also connected to the diesel power unit, which assumes the role of electricity supply to the facilities connected to this substation. All diesel generator stations are accompanied with appropriate ATS units which means that immediately after the power outage occurs the diesel generators are automatically activated.

The “ZTS Urgentni Centar” is also equipped with the reactive power compensation system. Two electrical cabinets designated as “Polje kompenzacije TRAFO 1” and “Polje kompenzacije TRAFO 2” contain all necessary switch, protective and measuring equipment as well as capacitor blocks that are required to achieve power factor correction. First electrical cabinet is responsible for the first and latter for the second dry transformer reactive power compensation.

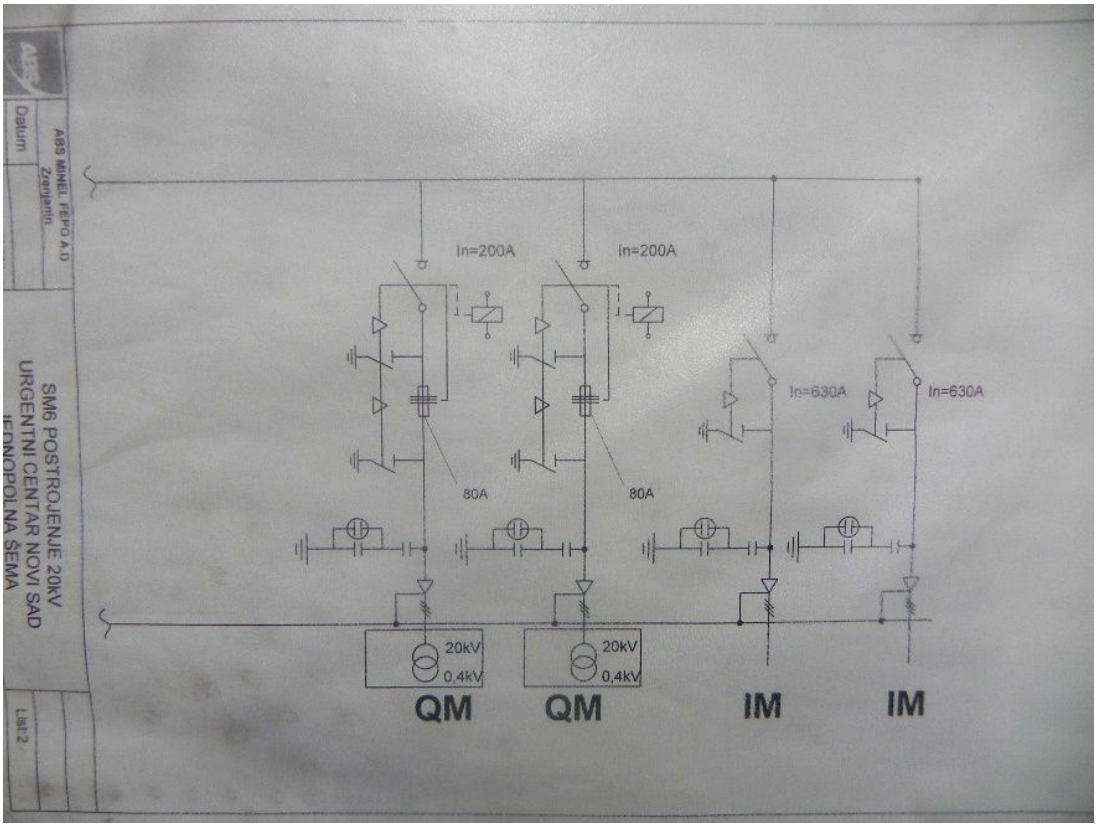

Figure 3.8 Single-pole diagram of the high-voltage segment in "TS Urgentni Centar"

The low voltage side of the transformer station is very complex. Separate electrical cabinet is used to only supply lighting system in the building as well as for the decorative lighting system on the exterior walls of the Emergency Center. Table 3.7 gives an overview of the low-voltage side of the transformer station "ZTS Emergency Center", as well as cross sections of the used low-voltage cable lines that supply consumers.

Table 3.7 Overview of the available taps at low voltage side of the transformer station "ZTS Urgentni centar"

Tap No.	Clinics	Cable type	Current limiters
1	Two CT scanners	PP00 4x150 mm^2	3x400 A
2	Three X-Ray scanners		
3	Lighting system	PP00 4x150 mm^2	3x400 A
4	Reserve	PP00 4x95 mm^2	3x160 A
5			

Radiology Clinic and Emergency Center both have premises for different purposes, containing different types of consumers however, some of the biggest consumers that herein are of interest are similar. One of the most important consumers of electricity,

especially in offices and exam rooms, are computers and typical working station equipped with personal computer.

For cooling, ventilation and temperature control purposes, air conditioners are most commonly used in the premises of both facilities. These can be a major consumer of electricity (especially in periods when climatic conditions require longer operation). The capacity of newer air conditioners is 9000 BTU, while for old air conditioners it was not possible to determine the capacity. Most common type of consumer that fall into the category of high power consumers are CT scanners, MRI scanners and X-Ray scanners used for diagnostic purposes in both institutions. In Table 3.8 an overview of the biggest power consumers is shown as well as transformer station from which the particular consumer is supplied.

Table 3.8 Overview of the biggest consumers in Emergency Center and Radiology clinic

Qty.	Consumer type	Power supply	Location	Power rating
2	CT scanner	ZTS Urgentni Centar	Emergency Center	65 kVA
3	X-Ray scanner			100 kVA
1	CT scanner	TS Kotlarnica	Radiology Clinic	100 kVA
1	CT scanner	TS Klinicka bolnica		80 kVA
1	CT scanner	TS Poliklinika		100 kVA
1	MRI scanner			88 kVA
1	MRI scanner			100 kVA
1	X-Ray scanner			65 kVA
1	X-Ray scanner			60 kVA
2	X-Ray scanner			50 kVA

From Figure 3.9 it can be inferred that during year electric energy consumption from “TS Poliklinika” is fairly constant with maximum consumption of around 300 MWh in January, March and August, and minimal consumption around 210 MWh in October.

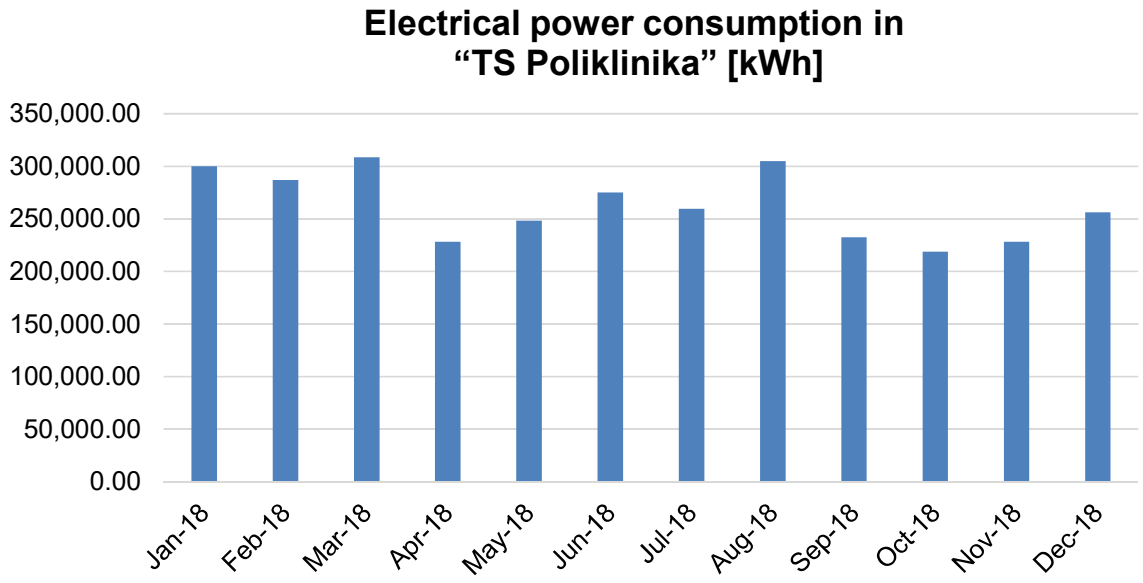

Figure 3.9 Electric power consumption in “TS Poliklinika” in 2018

From Figure 3.10 it can be inferred that during year electric energy consumption from “ZTS Urgentni Centar” is varies slightly with maximum consumption of around 250 MWh in August and minimal consumption around 149 MWh in February.

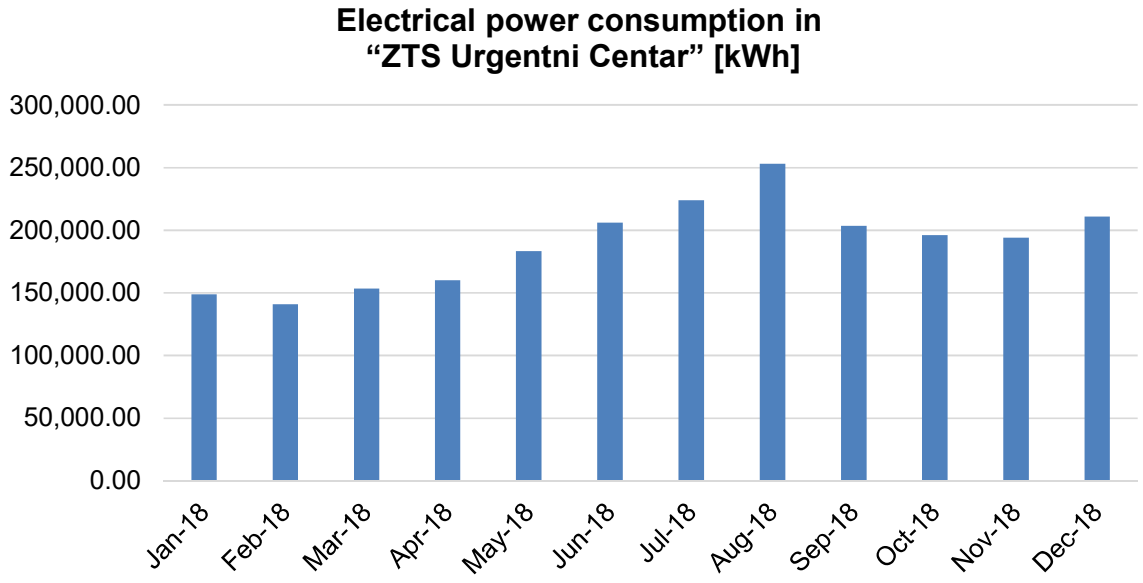

Figure 3.10 Electric power consumption in “ZTS Urgentni Centar” in 2018

From Figure 3.11 it can be inferred that during year electric energy consumption from "TS Kotlarnica" is varies noticeably with maximum consumption of around 51 MWh in August and minimal consumption around 11 MWh in April.

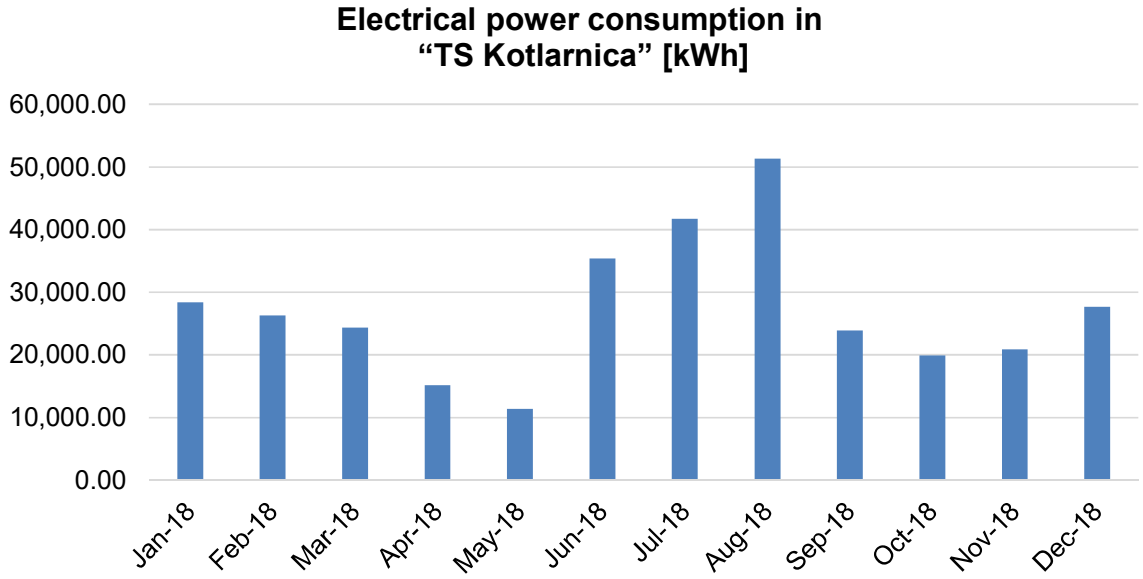

Figure 3.11 Electric power consumption in "TS Kotlarnica" in 2018

Until September 2019, the thermal energy infrastructure of the Medical Rehabilitation Clinic was connected to its own boiler room, which used fuel oil to heat the facility. In addition to rehabilitation, the boiler room is also used to heat other facilities within the clinical center. In order to increase reliability and reduce the cost of heating the facility, in September 2019, the Medical Rehabilitation Clinic was connected to the district heating system of the public utility company „Novosadska Toplana". Natural gas is used as the main energy source for heat production, and the energy supplied is charged per kWh.

Inside the building, radiator-type heating devices are used for heat transfer and space heating, which are usually located below the windows. A visit to the Medical Rehabilitation Clinic facility concluded that the facility was heated using two types of radiators - cast and panel radiators. Cast radiators vary in dimensions in height and length. The variation in the length of the structure is the result of a different number of pipes, i.e. ribs (which are welded one after the other regularly). At the Medical Rehabilitation Clinic, radiators have between 8 and 30 ribs, depending on the space in which they are installed.

Panel radiators belong to flat plate radiators, but they are made of smooth or profiled sheet steel, which in the simplest form has a heating plate through which the heating fluid (hot water) passes. Panel radiators are newer type and are installed in the hydrotherapy space.

Table 3.9 shows the number of radiators used by room type, as well as the type of radiator present in the object in question. The total number of radiators used within the facility of the Medical Rehabilitation Clinic, is also shown in the table.

Table 3.9 Number of heaters by type and premises

Radiator type	Premises	Number of pieces
Cast	Examine rooms	**26**
Cast	Offices	**26**
Cast	Therapy rooms	**30**
Cast	Hospital rooms	**35**
Cast	Corridors	**32**
Cast	Toilets	**27**
Panel	Hydrotherapy	**6**
Cast	Storage rooms	**32**
Total	Cast	**208**
	Panel	**6**
Total		**214**

Table 3.10 shows the fuel oil consumption of the entire boiler room from September 2018 to August 2019.

Table 3.10 Total fuel oil consumption of boiler room KCV

Month	Delivered fuel oil [kg]	Total [RSD]
September 2018	75.000,00	5.532.300,00
October 2018	101.160,00	7.848.228,24
November 2018	150.440,00	11.605.161,60
December 2018	225.440,00	15.749.612,16
January 2019	198.820,00	13.195.781,04
February 2019	251.360,00	17.602.124,88
Mart 2019	125.280,00	9.065.260,80
April 2019	147.480,00	10.831.689,84
Maj 2019	99.940,00	7.358.632,80
Jun 2019	75.040,00	5.397.301,20
July 2019	99.720,00	7.158.979,68
August 2019	99.220,00	6.910.033,20
Total	**1.648.900,00**	**118.255.105,44**

Table 3.11 shows the total consumption of fuel oil by months between September 2018 and August 2019 for the entire boiler room of the Clinical Center. In cooperation with the KCV technical service, the calculation of fuel oil estimates for the facility in question was made.

Table 3.11 Total fuel oil consumption for the KCV

Month	Amount of fuel oil consumed [kg]	Total [RSD]
September 2018	10.591,00	781.234,52
October 2018	15.299,00	1.186.896,42

November 2018	18.325,00	1.413.737,10
December 2018	26.269,00	1.835.257,42
January 2019	27.039,00	1.794.956,98
February 2019	22.810,00	1.597.429,92
Mart 2019	20.369,00	1.473.900,84
April 2019	15.014,00	1.102.628,16
Maj 2019	13.598,00	1.001.247,94
Jun 2019	11.177,00	803.939,26
Jul 2019	11.362,00	815.609,81
August 2019	11.419,00	795.173,48
Total	**203.272,00**	**14.602.011,84**

A visual representation (graph) of the heating energy consumption - fuel oil is given in Figure 3.12, where it can be seen that fuel oil consumption varies over months. It is easy to see that during the winter months the consumption is the highest, during the heating season, while in the other months the consumption is lower, because then the thermal energy is used only to heat the space of the hydrotherapy pool. Graphs show that the highest spending was recorded in January 2019, while in September 2018 it was the lowest. Monthly consumption is also influenced by the amount of fuel oil from the previous month. Therefore, in some months a smaller amount of fuel oil was purchased due to the stocks remaining from the previous month.

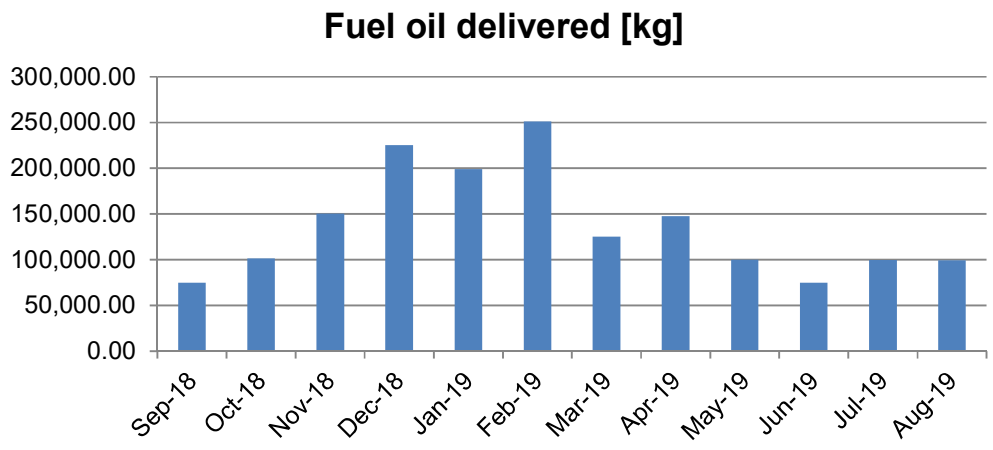

Figure 3.12 Fuel oil consumption graph

A visual representation (graph) of the thermal energy consumption is given in Figure 3.13 where it can be seen that the highest consumption is during the heating season, while in other months the consumption is approximately constant.

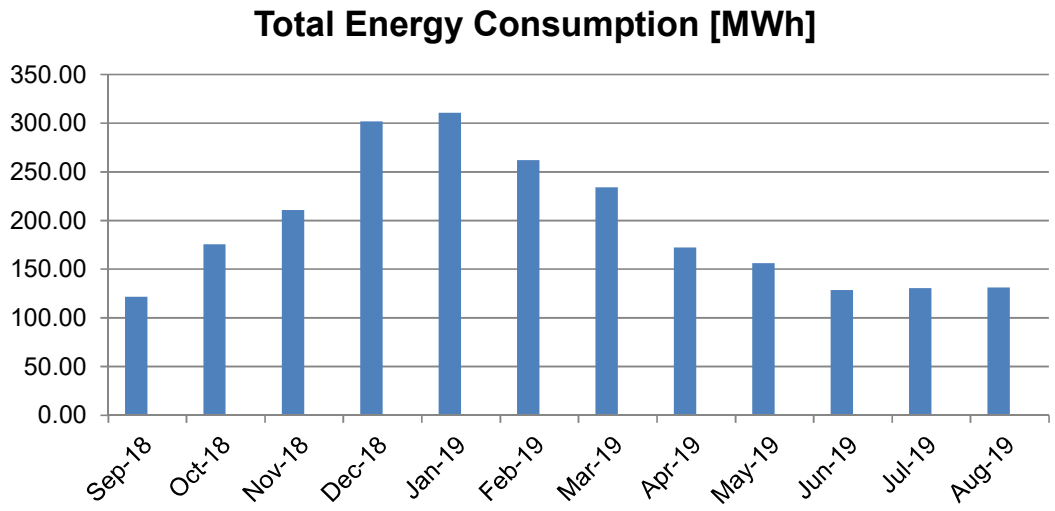

Figure 3.13 Graph of the thermal energy consumption of the object in question

3.3. FERIT buildings power supply and energy demand

Building in Trpimirova street is supplied from the low voltage distribution network. Point of common coupling of building and network is integrated cabinet placed outside, on the wall of the building equipped with electricity meter. Metering cabinet and main distribution cabinet are connected PP00-Y 4 x 35 + 25 mm^2 with cooper cable. Main fuses are rated at 200 A with gL characteristic. In the main distribution cabinet of the building, 4 low voltage feeders lead to building loads. Each feeder is protected with 35 A fuse with gL characteristic and uses PP00-Y 5 x 16 mm^2 copper cable. Single line diagram of main distribution cabinet is given in Figure 3.14.

Considering that the object was connected to the power grid infrastructure during the object construction period, the document that provides the permission for the object connection was not available for this study at the time of creation.

Furthermore, 10 kW photovoltaic system was installed on the building roof in Trpimirova street and integrated into electric power network. AC side of the photovoltaic system inverter is connected by PP00-A 4 x 16 mm^2 + P/F 16 mm^2 cable to the metering cabinet (distribution network). Single line diagram of photovoltaic system is given in Figure 3.15.

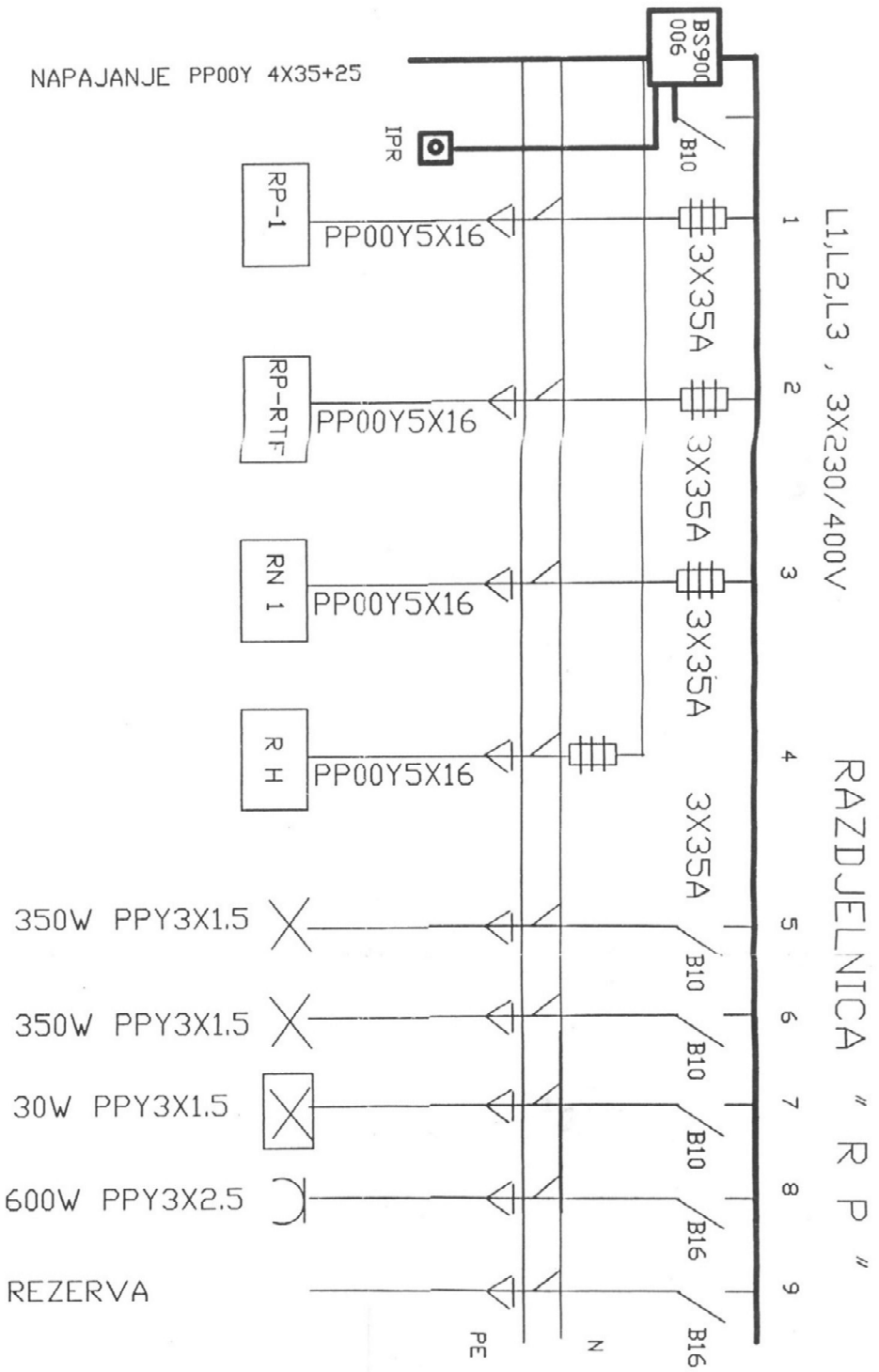

Figure 3.14 Main distribution cabinet single line diagram of the building in Trpimirova street.

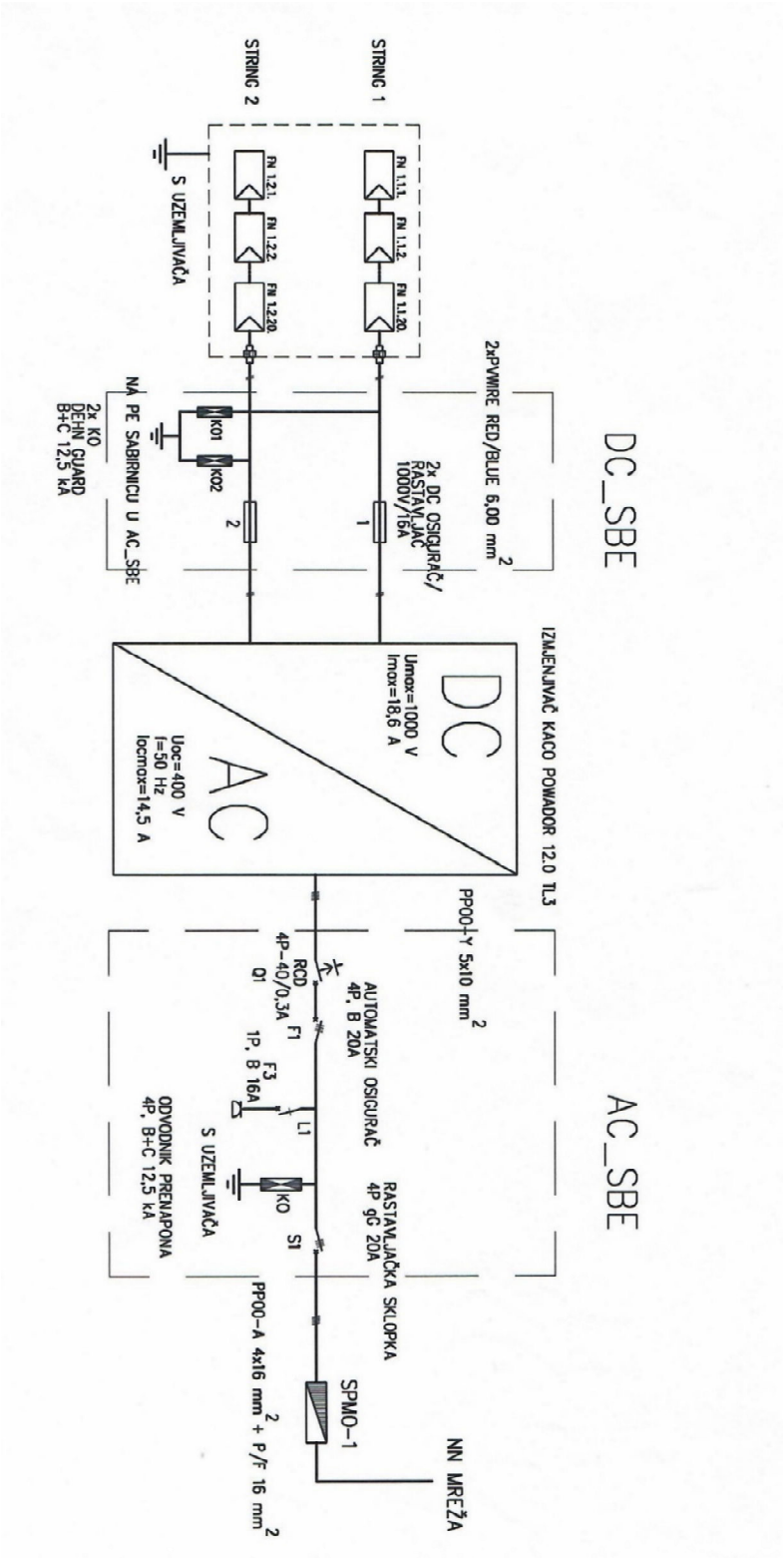

Figure 3.15 Single line diagram of 10 kW photovoltaic plant on the building roof in Trpimirova street.

Building in Cara Hadrijana street is supplied from the low voltage distribution network. Point of common coupling of building and network is integrated cabinet placed outside, on the wall of the building equipped with electricity meter. Metering cabinet and main distribution cabinet are connected with XP00-A 2 x (4 x 185 mm2) cable. Main fuses are rated at 630 A with gG characteristic. In the main distribution cabinet of the building, 6 low voltage feeders lead to other building cabinets and 1 reserve feeder for elevator which is not yet constructed. Feeders are protected with various rated currents from 25 A to 280 A with gG characteristic and use various cables which are given in Figure 3.16.

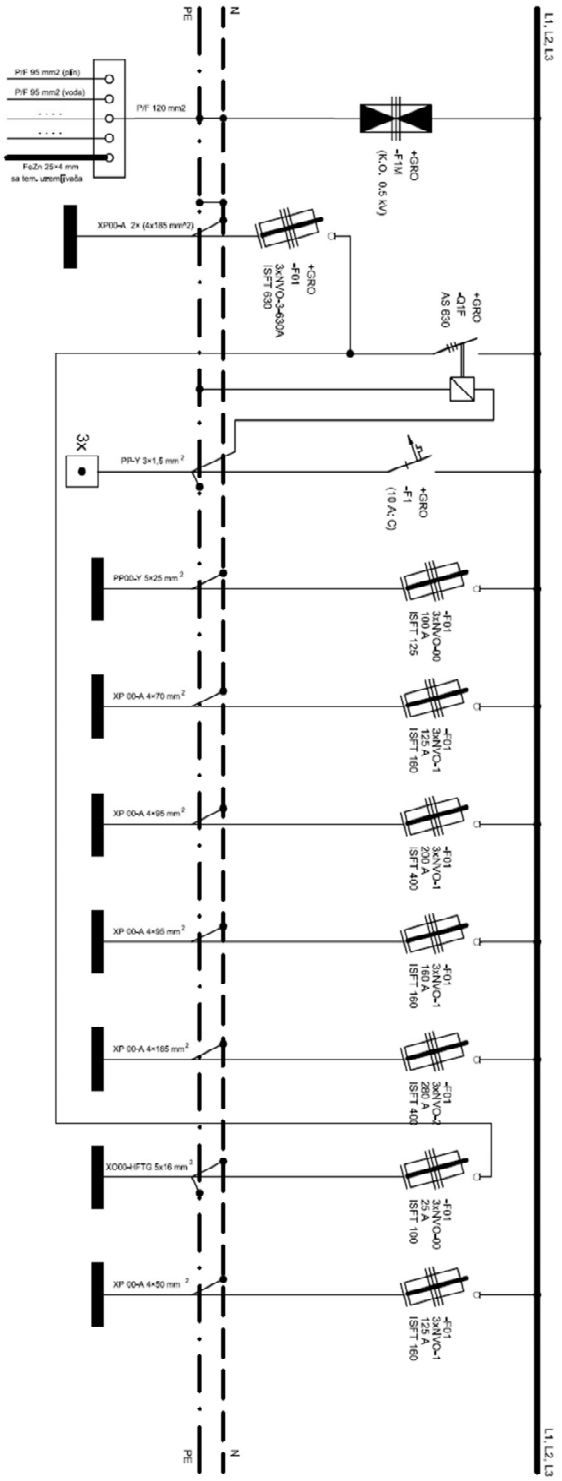

Figure 3.16 Single line diagram of the power supply of building in Cara Hadrijana street.

In order to establish appropriate measures for the enhancement of energy efficiency, it is necessary to analyze the energy consumption in the exemplary objects. A detailed analysis is given for the period from January 2018. to December 2018. This period is chosen as a reference since it covers the entire student year, calendar year and all seasons. During the analysis, all relevant parameters for the energy consumption were taken from the electricity bills for the exemplary object.

Table 3.12 shows an overview of the electricity consumption and electricity cost from January to December 2018 for both buildings. Net electricity consumption of the building in Trpimirova street is resulting from total building consumption reduced by electricity production from 10 kW photovoltaic system on the roof of the building in Trpimirova street. Building in Cara Hadrijana street is represented by total consumption only.

Table 3.12 – Electrical energy consumption of the buildings during 2018.

	Building in Trpimirova street		**Building in Cara Hadrijana street**	
	Net consumption [MWh]	**Total cost [HRK]**	**Total consumption [MWh]**	**Total cost [HRK]**
Jan 2018	19.416	17,846.00	6.577	6,068.00
Feb 2018	18.248	16,743.00	6.517	5,890.00
Mar 2018	19.693	19,278.00	8.605	7,375.00
Apr 2018	17.751	17,763.00	7.769	7,062.00
May 2018	20.389	20,642.00	8.031	7,250.00
Jun 2018	20.554	21,985.00	6.976	6,626.00
Jul 2018	18.024	18,413.00	7.011	6,259.00
Aug 2018	15.49	15,436.00	6.185	5,915.00
Sep 2018	17.056	17,094.00	7.534	7,032.00
Oct 2018	20.388	20,635.00	8.964	8,054.00
Nov 2018	21.16	21,249.00	9.45	8,264.00
Dec 2018	19.161	18,865.00	9.333	8,259.00
Total	227.33	225,949.40	92.953	84,055.58

Table 3.12 shows the relatively constant electricity consumption during the year for building in Trpimirova street while the electricity consumption of building in Cara Hadrijana street has variability during the year. Slight consumption decline is visible during the August and September during the examination and vacation period when no teaching and exams are arranged. From the October to December, electricity consumption in building in Cara Hadrijana street is higher. Analyzing the annual electricity bills, total

electricity consumption of both buildings was 320,283.43 kWh with the total cost of 310,004.98 HRK.

Graphical interpretation of the electricity consumption is depicted in Figure 3.17 and Figure 3.18 which show energy consumption per month, expressed in MWh, in the period from January to December 2018 for buildings in Trpimirova and Cara Hadrijana street, respectively.

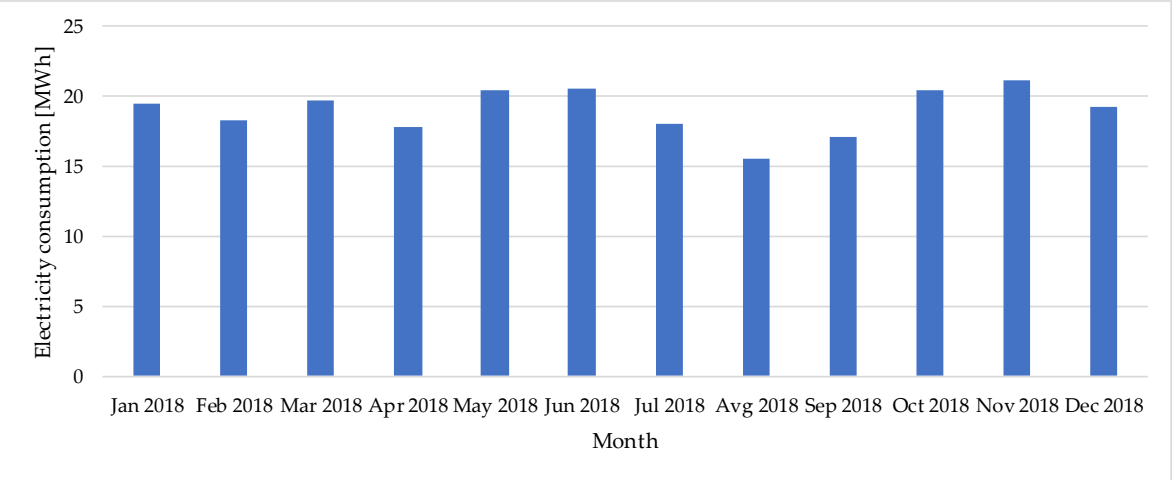

Figure 3.17 Electricity consumption per month of the building in Trpimirova street during 2018.

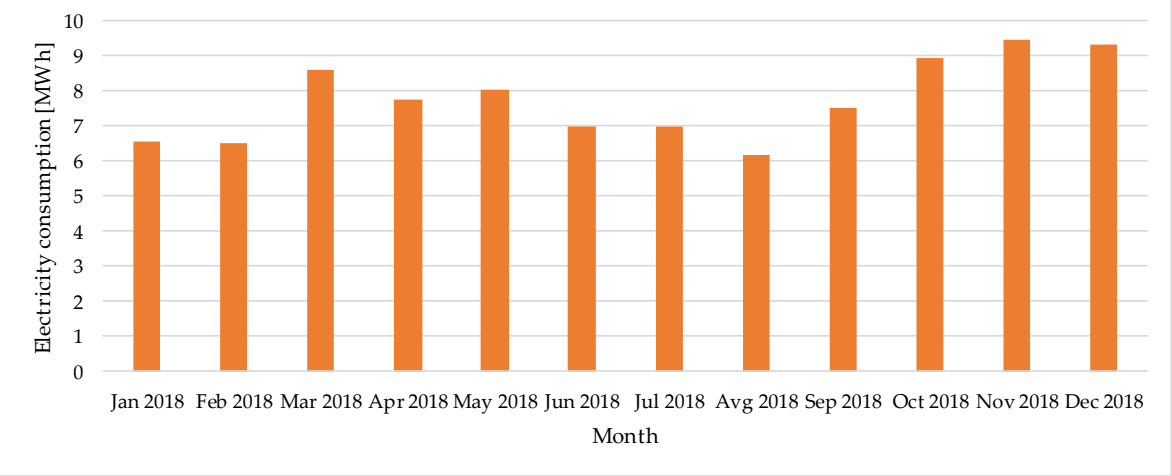

Figure 3.18 Electricity consumption per month of the building in Cara Hadrijana street during 2018.

3.4. KBCO buildings power supply and energy demand

KBCO complex supplies from 10 kV distribution system using four 10/0.4 kV substations. Schematic of the KBCO complex power supply system along with surrounding 10 kV distribution network is given in Figure 3.19.

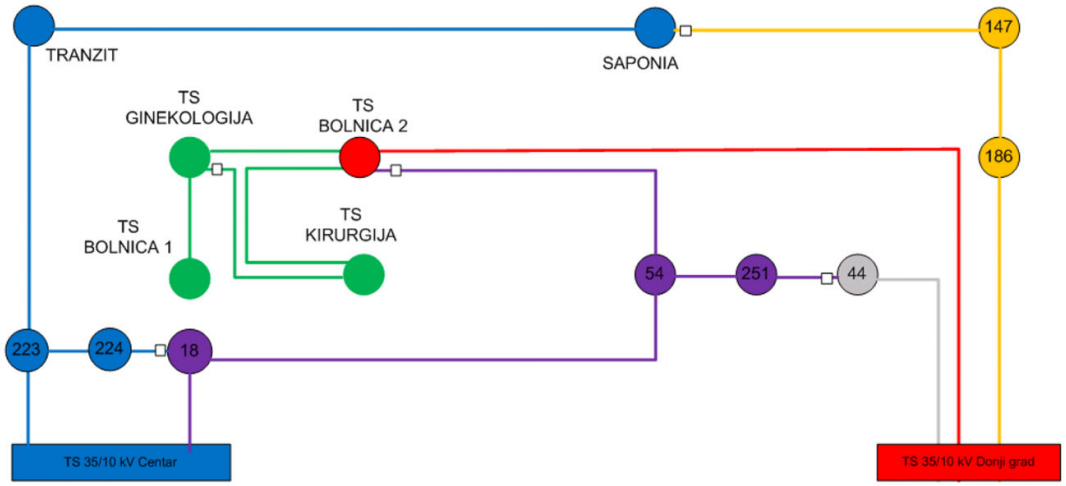

Figure 3.19 KBCO complex power supply schematic [16]

In order to establish appropriate measures for the enhancement of energy efficiency, it is necessary to analyze the energy consumption in the exemplary objects. A detailed analysis is given for the period from January 2018. to December 2018. This period is chosen as a reference since it covers the entire year, calendar year and all seasons. During the analysis, all relevant parameters for the energy consumption were taken from the electricity bills for all KBCO facilities. Electricity consumption of the KBCO complex in Huttler street is measured at PCC at the 10 kV feeder.

Table 3.12Table 3.13 shows an overview of the electricity consumption and electricity cost from January to December 2018 for all KBCO facilities. Most of the total electricity is consumed by KBCO complex in Hutller street where renewable energy sources systems will be installed. It is expected that all produced electricity is going to be consumed directly by consumption of the KBCO complex buildings so there is no need for additional energy storage systems.

Table 3.13 – Electrical energy consumption of all KBCO facilities during 2018.

	Total consumption [MWh]	Total cost [HRK]
Jan 2018	715.392	508,213.00
Feb 2018	662.873	479,547.00
Mar 2018	716.018	506.647.00
Apr 2018	698.288	507,260.00
May 2018	795.443	583,280.00
Jun 2018	933.263	694,318.00
Jul 2018	1043.97	760,847.00
Aug 2018	976.59	15,436.00
Sep 2018	702.008	548,075.00
Oct 2018	747.278	562,559.00
Nov 2018	729.128	562,702.00
Dec 2018	714.75	562,702.00
Total	9435.001	5,784,939.00

Table 3.13 shows variable electricity consumption during the year for all KBCO facilities. Consumption increase is visible during the summer months (June to August) during the hot weather conditions. Analyzing the annual electricity bills, total electricity consumption of all KBCO facilities is 9435.001 MWh with the total cost of 5,784,939.00 HRK. Graphical interpretation of the electricity consumption of all KBCO facilities in 2018 is depicted in Figure 3.20.

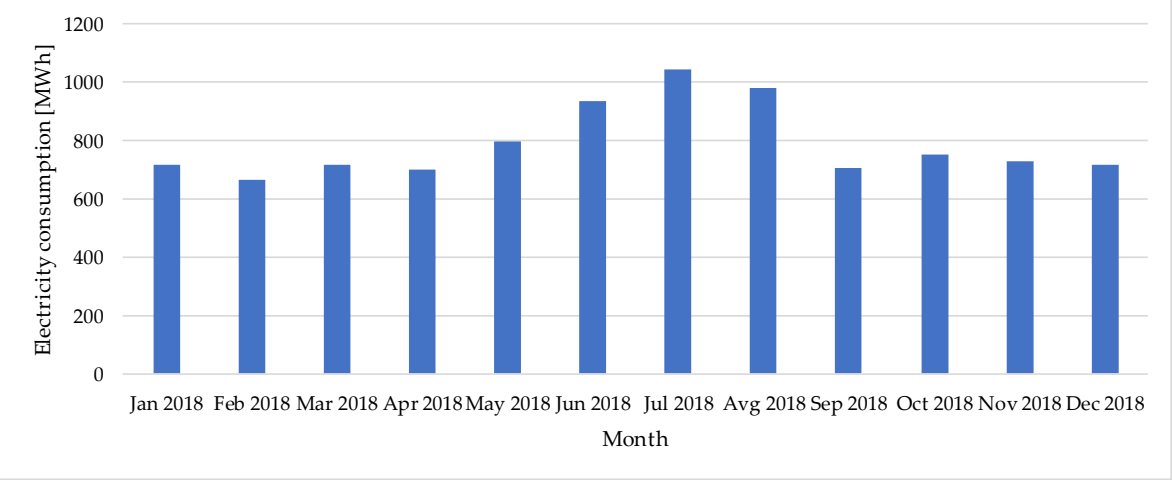

Figure 3.20 Electricity consumption per month of all KBCO facilities during 2018.

3.5. UNISB building power supply and energy demand

3.5.1. The electrical infrastructure of the exemplary object and consumption analysis

In order to implement different strategies for the increase of energy efficiency, it is necessary to analyze the electrical installation infrastructure of the UNISB object, as well as existent power supply units and the consumption of electrical energy in the exemplary object.

Here, “UNISB - Strojarski fakultet u Slavonskom Brodu, building in Ivan Gundulić Street 20a”, as a part of the building complex of the Mechanical Engineering Faculty in Slavonski Brod, will be referred to as exemplary object.

3.5.2. The power supply of the “UNISB - Strojarski fakultet u Slavonskom Brodu, building in Ivan Gundulić Street 20a”

This building is supplied from the public transformer station located within the yard of the object, ownership of the HEP group – Croatian Electricity Board. The transformer station is located outside near the main entrance where there is also freestanding distribution cabinet with meter for recording electricity consumption of the object (approved peak power was 29.9 kW and now it is 71 kW). The transformer station is called “TS Gundulić Street” and a three-phase oil transformer with a nominal power of 1000 kVA, a turn ratio of 10/0.4 kV and a Dyn5 transformer connection was used for the object power supply.

Aluminum cable 3 x (XHE 49A 1x150 mm^2) was used as a high-voltage cable. On the low-voltage side copper busbar 3x(2x80x5) + 1x(80x5) mm^2 was used. The main circuit breaker is set to the nominal value of the 1600 A. Single line diagram of the transformer station is illustrated in Figure 3.21.

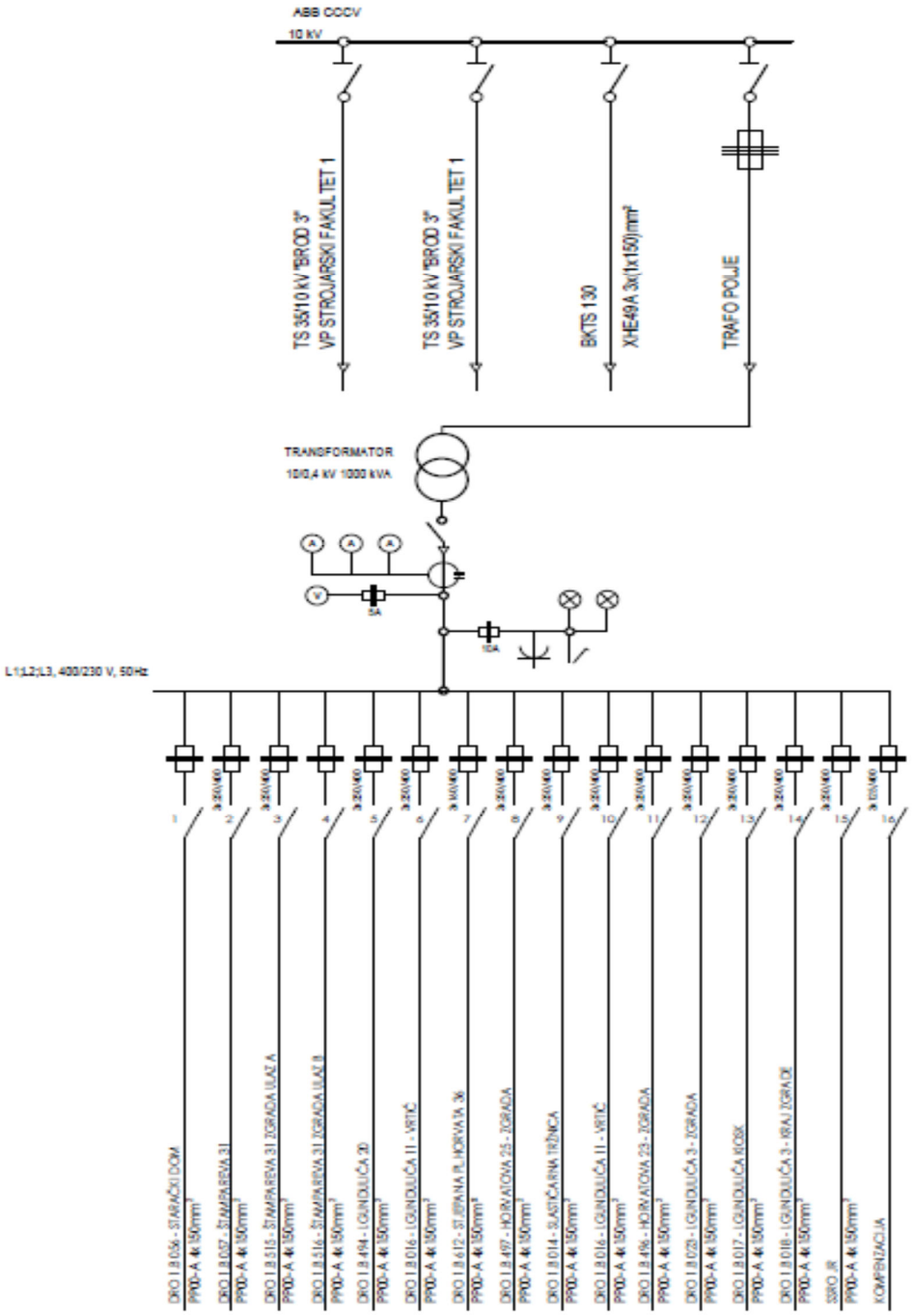

Figure 3.21 Transformer station single line diagram

Figure 3.21 shows all outgoing feeders on the low-voltage side of the transformer, together with the cross-sections of the cable lines. Feeder 5 is used to supply building of Strojarski fakultet, Ivan Gundulić Street 20a. The low-voltage block of the transformer station is protected by the main circuit breaker with the nominal current 1600 A. Low-voltage block has 15 low voltage feeders (+compensation). Low voltage block feeder 5 is

power supply of the freestanding electric cabinet in the south-west part of the yard of the analyzed building, connected to group of objects (including analyzed object) by cable type PP00-Y 4x150 mm^2. It is protected by fuse with nominal current 250 A and gG characteristics. A cable, type XP00-A 4 x 150 mm^2 makes electric connection between freestanding electric cabinet next to transformer substation (SSPMO) to main freestanding distribution cabinet of the building located in front of the building (SSRO1). Building is connected to SSRO1 by electric cable XP00-A 4x70 mm^2 to main cabinet of the building (GRO) located in the hallway of the building, directly at the entrance to the building. That main electric cabinet houses the main fuses of the building, electric installation of the building busbars and fuses. Photovoltaic power plant is connected from Laboratory for renewable energy sources G116 (inverters) to SSRO1 by electric cables XP00-A 4x70 mm^2 and FG16OR16 1x35 mm^2.

Considering that the object was connected to the power grid infrastructure during the object construction period (the year 1963.), the document that provides the permission for the object connection was not available for this study at the time of creation.

3.5.3. Analysis of the energy consumption

In order to establish appropriate measures for the enhancement of energy efficiency, it is necessary to analyze the energy consumption in the exemplary object. A detailed analysis is given for the period from January 2018. to December 2018. This period is chosen as a reference since it covers the entire student year, calendar year and all seasons. During the analysis, all relevant parameters for the energy consumption were taken from the electricity bills for the exemplary object.

Table 3.14 shows an overview of the power energy consumption from January 2018. to December 2018.

Table 3.14 Electrical energy consumption in the "Strojarski fakultet u Slavonskom Brodu, I. Gundulić Street" during 2018

	Consumption in higher tariff E1 [kWh]	Consumption in lower tariff E2 [kWh]	Total consumption [MWh]	Total energy cost [HRK]	Total cost with VAT taxis [HRK]
January 2018	3363	1324	4687	4359.61	4926.36
February 2018	3060	1254	4314	3900.60	4407.68
Mart 2018	3477	1450	4927	4380.09	4949.50
April 2018	2916	1385	4301	3802.07	4296.34
May 2018	2948	1246	4194	3805.38	4300.08
June 2018	2584	1214	3798	3448.51	3896.81
July 2018	2027	1117	3144	2813.76	3179.55
August 2018	1617	1002	2619	2290.19	2587.92
September 2018	2399	1172	3571	3232.79	3653.05
October 2018	2644	1162	3806	3516.77	3973.95
November 2018	3121	1150	4271	3989.00	4507.57
December 2018	2991	1419	4410	3924.20	4434.34
Total 2018	*33147*	*14895*	*48042*	*43462.96*	*49113.15*

Table 3.14 shows the trend of energy consumption increase, especially during the winter period. Slight consumption decline is visible during the January and February during the examination period when no teaching is arranged and Mart as beginning of the summer semester, while the lowest consumption is in August when there are no activities in the Faculty during the vacation period. In Figure 3.22 energy consumption per month, expressed in kWh is presented in the period from January 2018. to December 2018.

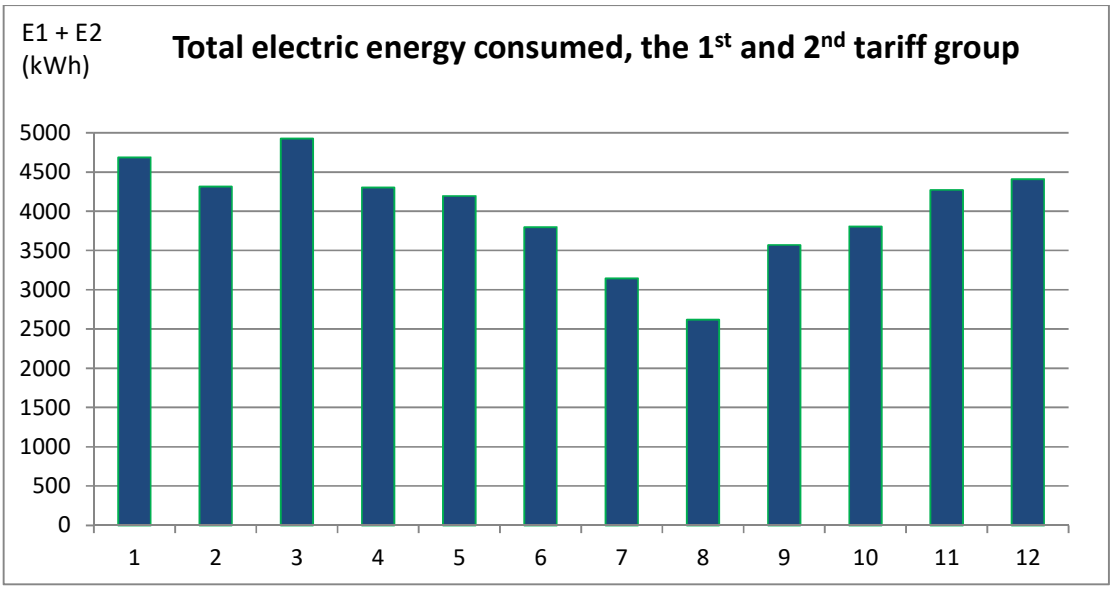

Figure 3.22 Electrical energy consumption per month in the "Strojarski fakultet u Slavonskom Brodu, I. Gundulić Street" during 2018

It can be seen that the highest energy consumption was in March. During August, the consumption was the lowest since most of the employees take their vacation in this period. During the winter, the highest consumption was in January caused by usage of electrical heating devices (cold walls of the building after winter holidays).

3.5.4. The thermal infrastructure of the exemplary object and consumption analysis

The main heating energy source of the Mechanical Engineering Faculty facility II is natural gas and delivered power is charged per kWh. The exemplary object is supplied with one heat station. In the exemplary object, for the transmission of the heat power and space heating radiators are used. Usually, they are placed beneath the windows. Through the visual inspection of the Mechanical Engineering Faculty, it is concluded that one type of radiators were installed. It is a cast iron radiators. The height and length of the cast iron radiators vary. This is because there is a different number of tubes that are connected in series. Depending on the room they are built-in, the number of tubes in the cast iron radiators is between 5 and 40. In their simplest form, the heating fluid (warm water) is circulating through the tubes. The dimensions of the cast iron radiators in the exemplary object vary only in the length – 110 cm, 180 cm, 240 cm or 260 cm. The height of the cast iron radiators is 60 cm or 80 cm while the depth is 10 cm. In Table 3.15 the number of radiators located in different rooms is presented, together with the total number of radiators.

Table 3.15 The number of radiators according to the room purpose

Rooms	Number of radiators
Cabinets	33
Classrooms	12
Computer classrooms	14
Laboratories	10
Server room	1
Library and Reading room	7
Hallways	7
Toilets	3
Total number	87

3.5.5. The analysis of the heat energy consumption

An analysis of gas consumption for consumers (buildings of Strojarski fakultet) was conducted by the Mechanical Engineering Faculty in Slavonski Brod, specifically for the faculty building at Ivan Gundulić Street 20A, Slavonski Brod for 2018. Figure 3.23 shows the annual states of gas counters for each month in the given period. The gas consumption is multiplied by a correction factor of 1.086893 until August 2018, after which the correction factor 1.125969, and ultimately the consumption is expressed in kWh. During 2018. gas consumption was over 150,000 kWh per year.

Brod-plin d.o.o. Str. 1
Datum: 23.08.2019

ANALITIKA POTROŠNJE PLINA ZA POTROŠAČA
7450 STROJARSKI FAKULTET SLAVONSKI BROD

GODINA: 2018

Tarifna grupa / model:TG2 Poduzetništvo TM5

Datum očitanja	Brojilo	Staro stanje (m3)	Novo stanje (m3)	Utrošeno (m3)	Faktor korekcije	Utrošeno (m3)	Utrošeno (kWh)
Opskrbljivač:	**87814 MEĐIMURJE-PLIN d.o.o.**						
31.01.2018	288275	85165	87557	2392	1,086893	2600	25180
28.02.2018	288275	87557	90401	2844	1,086893	3091	30083
31.03.2018	288275	90401	92825	2424	1,086893	2635	25574
30.04.2018	288275	92825	93362	537	1,086893	584	5639
31.05.2018	288275	93362	93362	0	1,086893	0	0
30.06.2018	288275	93362	93362	0	1,086893	0	0
31.07.2018	288275	93362	93362	0	1,086893	0	0
31.08.2018	288275	93362	93362	0	1,086893	0	0
30.09.2018	288275	93362	93381	19	1,125969	21	204
31.10.2018	288275	93381	94313	932	1,125969	1049	10121
30.11.2018	288275	94313	96107	1794	1,125969	2020	19578
31.12.2018	288275	96107	99476	3369	1,125969	3793	36712
	Ukupno:			**14311**		**15793**	**153091**

Figure 3.23 Analysis of gas consumption for faculty building at Ivan Gundulić Street 20A

4. The overview of the potential for the available renewable energy resources

4.1. FTN and KCV potential of renewable energy sources

The Republic of Serbia has significant RES potential, which is estimated at 5.65 Mtoe per year. More than 60% of the total potential is biogas potential, whose use is estimated at approximately 30% (1.54 Mtoe), while hydropower has a share of 30% and more than half is utilized (909 ktoe). In order to achieve the mandatory national targets for the share of renewable energy in gross final consumption, the installation of higher electricity production using wind, biomass and sun are envisaged, as well as a higher RES share in heat production. The projection of the construction of plants for electricity generation using RES until 2030 is presented in Figure 4.1.

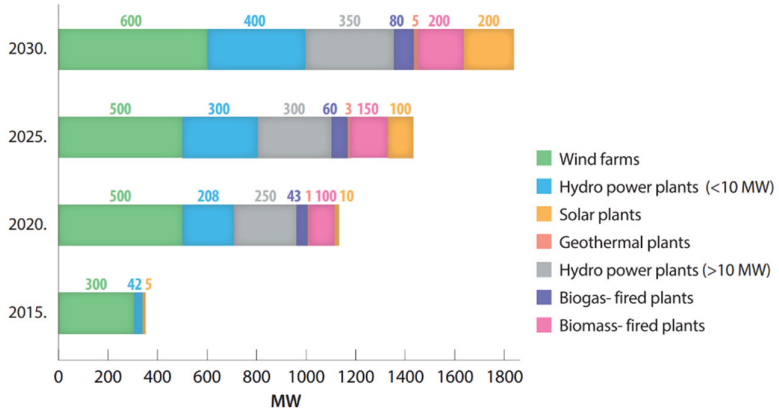

Figure 4.1 The projection of the construction of plants for electricity generation using RES until 2030 [17].

According to the Energy Balance of the Republic of Serbia for 2019, the total planned production of primary energy from RES in 2019 is 1.997 Mtoe, accounting for 18.9% of the total domestic production. The estimated participation of individual RES is shown in Figure 4.2. It can be observed that wind energy accounts for 5%, while solar and geothermal energy accounts for only 1%, which is extremely small given their estimated potential.

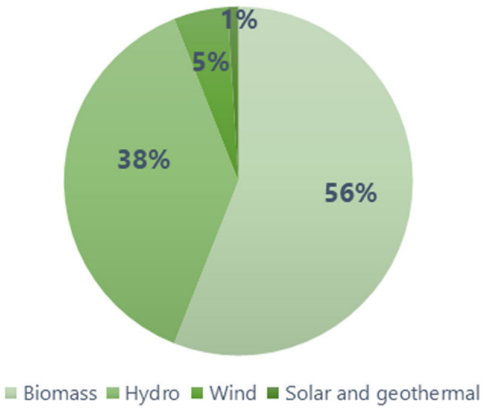

Figure 4.2 The total planned production of primary energy from individual RES for 2019.

Solar energy can be used to generate electricity or heat energy. The average annual global solar radiation in the Republic of Serbia is 30% higher than in Western European countries. In most parts, the number of hours of solar radiation is between 1500 and 2200 hours per year, which is higher than the most European countries. According to calculations of the scientific tool Photovoltaic Geographical Information System (PVGIS) for the EU member states and other European countries, the average value of global horizontal irradiation of the Republic of Serbia is approximately 1353 kWh/m^2. The minimum average value of the global horizontal irradiation is 1042 kWh/m^2, while the maximum is 1660 kWh/m^2. Global irradiation and solar electricity potential for the horizontally mounted photovoltaic modules is given in the Figure 4.3.

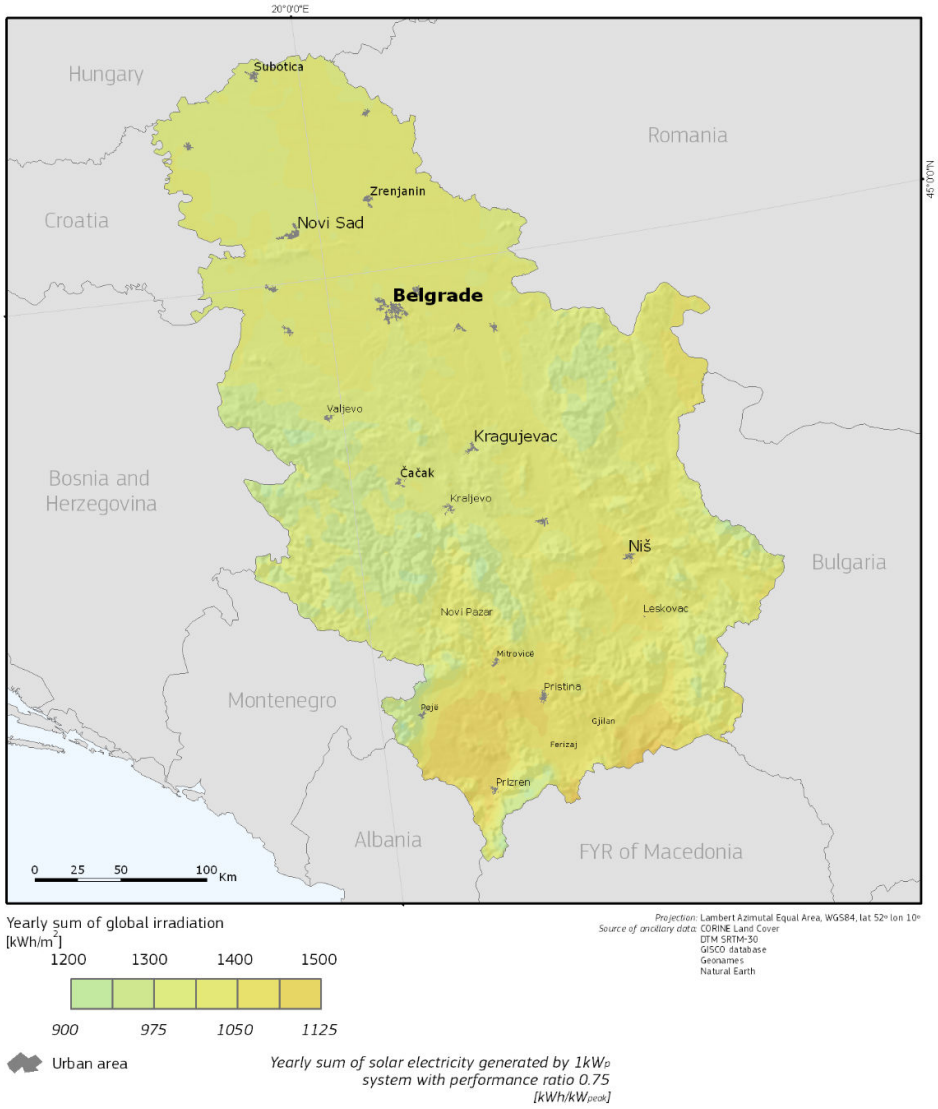

Figure 4.3 Global irradiation and solar electricity potential of the Republic of Serbia

Global irradiation and solar electricity potential for the optimally-inclined photovoltaic modules of the Republic of Serbia are shown in the Figure 4.4. The average value of global irradiation is approximately 1531 kWh/m^2, where the minimum average value is 1190 kWh/m^2, while the maximum is 1925 kWh/m^2.

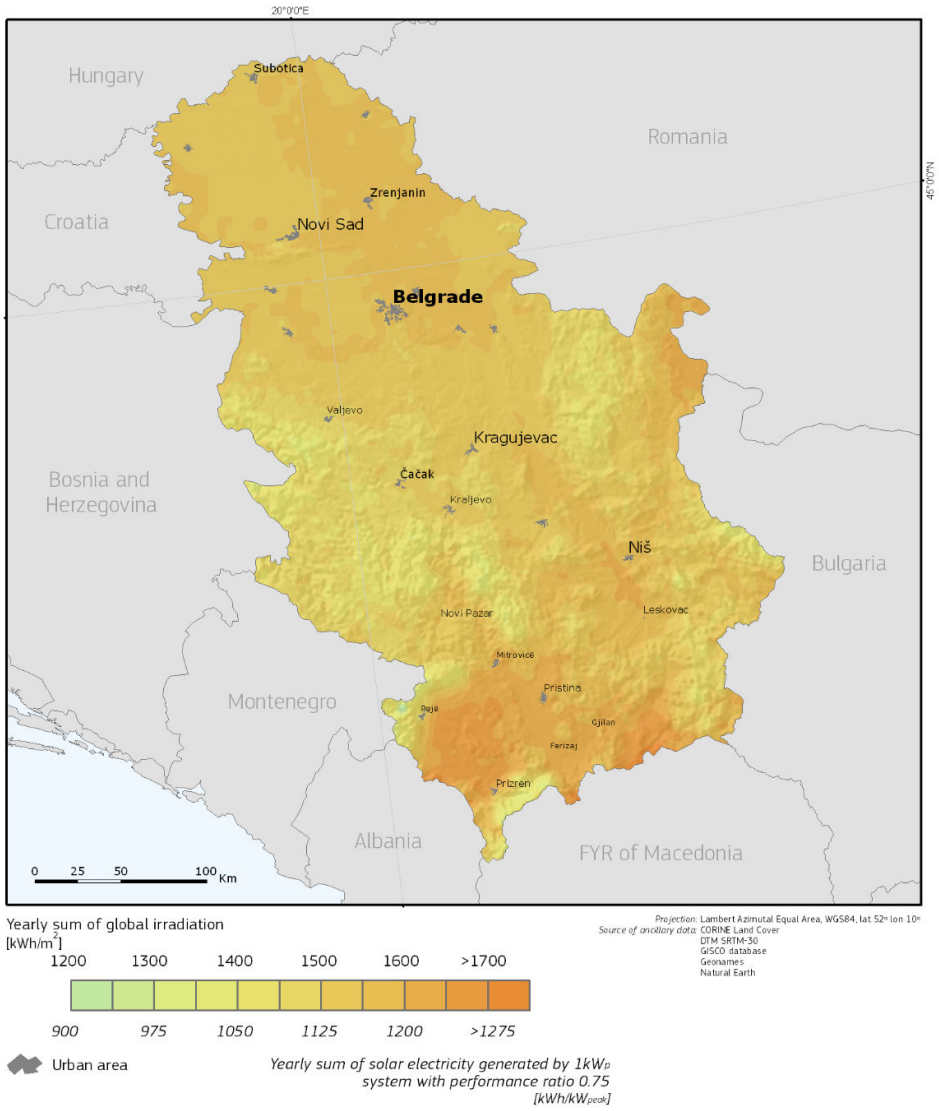

Figure 4.4 Global irradiation and solar electricity potential for the optimally-inclined photovoltaic modules of the Republic of Serbia [18].

In the Autonomous Province of Vojvodina, the average value of GHI ranges between 1294 kWh/m^2 in the north and 1335 kWh/m^2 in the south, or an average value of 1300 kWh/m^2. Depending on the season in sunny conditions, the intensity of global radiation in the midday hours can vary from 200 to 1000 W/m^2. The ratio of direct and diffuse radiation depends on geographical and microclimatic conditions. The ratio accounts from 40% to 60% and it is slightly higher in the winter period.

According to the Global Solar Atlas the city of Novi Sad has average global horizontal irradiation of 1337 kWh/m^2 per year, or 3662 kWh/m^2 per day, while the optimum tilt of photovoltaic (PV) modules is 34°, as shown in Table 4.1.

Table 4.1 Yearly average parameters for Novi Sad according to the Global Solar Atlas [19].

Glossary	Description	Value
Specific photovoltaic power output	Yearly average value of photovoltaic electricity (AC) delivered by a PV system and normalized to 1 kWp of installed capacity	1278 kWh/kWp
Direct normal irradiation	Average yearly sum of direct normal irradiation	1222 kWh/m2
Global horizontal irradiation	Average annual sum of global horizontal irradiation	1336 kWh/m2
Diffuse horizontal irradiation	Average yearly sum of diffuse horizontal irradiation	627 kWh/m2
Global titled irradiation at optimum angle	Optimum tilt of fix-mounted PV modules facing towards Equator set for maximizing GTI input	1547 kWh/m2
Air temperature	Average yearly air temperature at 2 m above ground	12.5 °C
Optimum tilt of PV modules	Optimum tilt of fix-mounted PV modules facing towards Equator set for maximizing global titled irradiation input	35/180°

Due to changes in the elevation angle of the Sun during the day, month and year, the value of the radiated energy that reaches the surface changes. More energy is received only by the surface at which the angle changes and adjusts to the position of the Sun each month, or even more if the receiving surface follows the Sun's trajectory daily. Nevertheless, the optimal slope of the collector should be 30-40°. The optimum slope for the summer period is 20-30° and for winter is about 60°. Therefore, in the given statistics different values for slope are chosen for the fixed plane.

For this analysis purposes PVGIS program is used. Daily average irradiance on the fixed plane with slope 0° and 35°, and azimuth 0° for the month of July, city of Novi Sad, are shown in Figure 4.5 and Figure 4.6 respectively. The results of this calculation consist of hourly values of the average solar irradiance for the month of July, given in W/m^2. The optional temperature graph, presented in Figure 4.7, shows the average air temperature each hour for the month of July. The minimum daily temperature for the month of July is 18°, while the maximum is 27.5°.

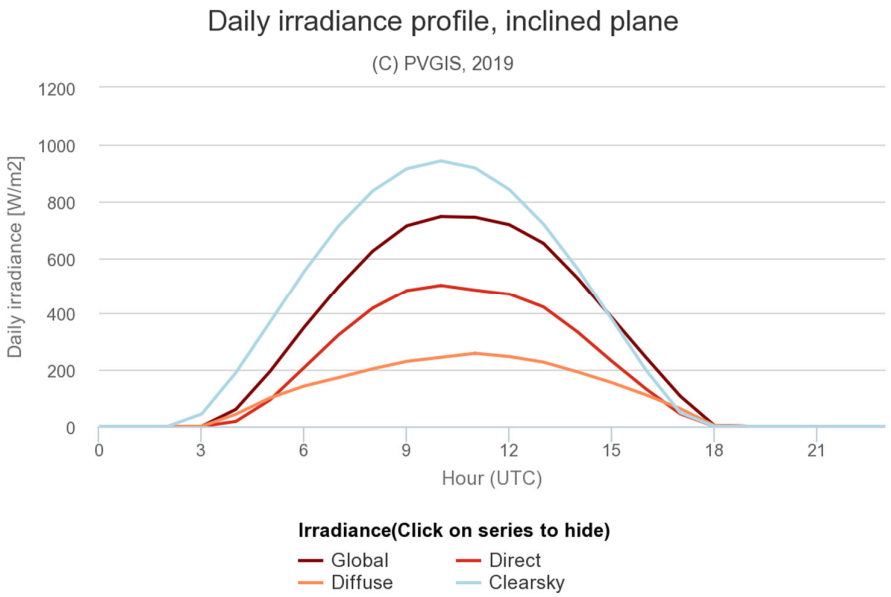

Figure 4.5 Daily average irradiance on the fixed plane with slope 0° and azimuth 0° for the month of July, city of Novi Sad [18].

The maximum global irradiance in case of the fixed plane with slope 0° is 745 kWh/m^2, while the maximum global clear-sky irradiance is 941 kWh/m^2. In Table 4.2 are given the average values of the global irradiance (G), direct irradiance (Gb), diffuse irradiance (Gd) and global clear-sky irradiance (Gcs) for the specific time period of the month of July.

Table 4.2 Daily average irradiance on the fixed plane with slope 0° and azimuth 0° for the month of July, city of Novi Sad [18].

Time	G [W/m^2]	Gb [W/m^2]	Gd [W/m^2]	Gcs [W/m^2]
00:45	0	0	0	0
01:45	0	0	0	0
02:45	0	0	0	0
03:45	0	0	0	44
04:45	60	17	43	190
05:45	194	94	101	369
06:45	351	208	143	550
07:45	495	323	172	711
08:45	622	419	203	835
09:45	712	482	230	914
10:45	745	501	244	941
11:45	742	484	258	916
12:45	716	469	247	840
13:45	650	423	227	718
14:45	526	334	192	559
15:45	385	230	155	379
16:45	243	132	111	199
17:45	107	44	63	48
18:45	3	0	3	0
19:45	0	0	0	0
20:45	0	0	0	0
21:45	0	0	0	0
22:45	0	0	0	0
23:45	0	0	0	0

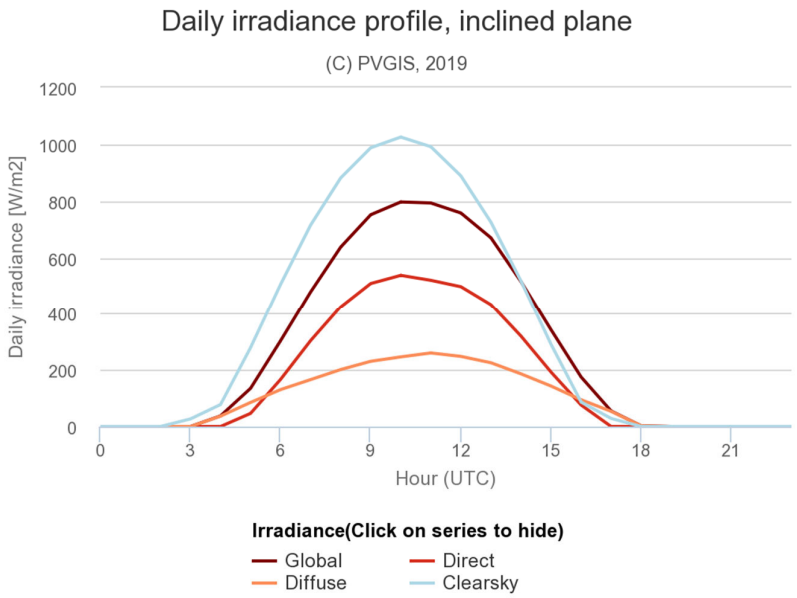

Figure 4.6 Daily average irradiance on the fixed plane with slope 35°, and azimuth 0° for the month of July, city of Novi Sad [18].

The maximum global irradiance in case of the fixed plane with slope 30° is 803 kWh/m2, while the maximum global clear-sky irradiance is 1034 kWh/m2. In Table 4.3 the average values of the global irradiance (G), direct irradiance (Gb), diffuse irradiance (Gd) and global clear-sky irradiance (Gcs) for the specific time period of the month of July are given.

Table 4.3 Daily average irradiance on the fixed plane with slope 30° and azimuth 0° for the month of July, city of Novi Sad [18].

Time	G [W/m^2]	Gb [W/m^2]	Gd [W/m^2]	Gcs [W/m^2]
00:45	0	0	0	0
01:45	0	0	0	0
02:45	0	0	0	0
03:45	0	0	0	27
04:45	37	0	37	78
05:45	135	46	85	279
06:45	303	167	130	505
07:45	478	304	166	715
08:45	637	425	201	881
09:45	751	508	230	988
10:45	796	537	246	1025
11:45	793	519	260	991
12:45	757	497	248	888
13:45	670	433	225	725
14:45	515	319	186	517
15:45	342	192	143	290
16:45	175	76	95	86
17:45	55	0	54	29
18:45	3	0	3	0
19:45	0	0	0	0
20:45	0	0	0	0
21:45	0	0	0	0
22:45	0	0	0	0
23:45	0	0	0	0

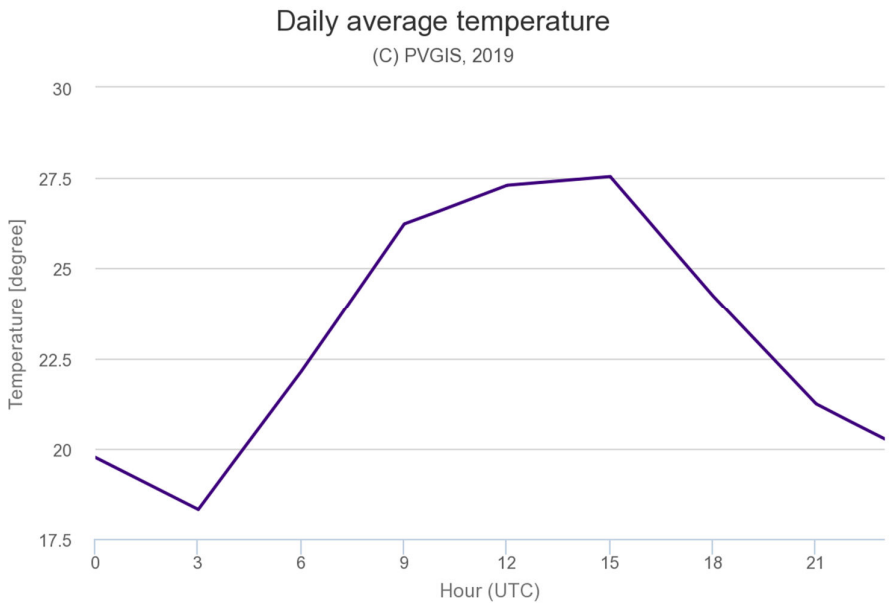

Figure 4.7 Daily average temperature for the month of July, city of Novi Sad [18].

Monthly average irradiance on the fixed plane with slope 0° and azimuth 0° for the year of 2016, city of Novi Sad, are shown in Figure 4.8. In Table 4.4 the monthly average values of the global horizontal irradiaton, direct normal irradiaton and global irradiation optimum angle of the year 2016 are given.

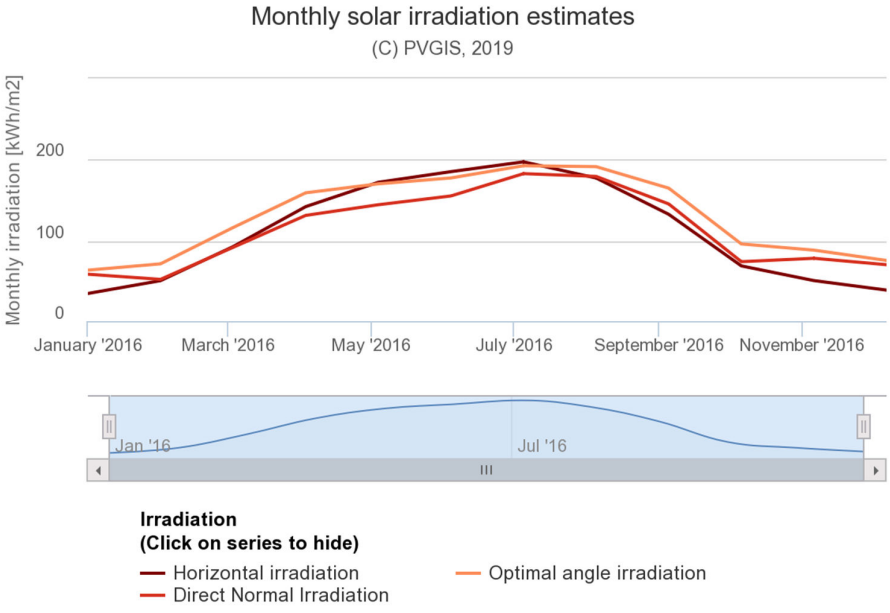

Figure 4.8 Monthly average irradiance on the fixed plane with slope 0°, and azimuth 0° for the year of 2016, city of Novi Sad [18].

The maximum monthly average value of the global horizontal irradiation is approximately 200 kWh/m^2 in month of July, whereas the minimum value is 35 kWh/m^2 in month of January.

Table 4.4 Monthly average irradiance on the fixed plane with slope 0° and azimuth 0° for the year of 2016, city of Novi Sad [18].

Month	Global horizontal irradiation [kWh/m^2]	Direct normal irradiation [kWh/m^2]	Global irradiation optimum angle [kWh/m^2]
January	35.15	58.9	63.9
February	50.95	52.56	71.67
March	92.93	92.01	116.41
April	142.15	131.36	159.2
May	172.17	144.49	170.26
June	185.26	155.32	177.49
July	197.34	182.81	192.57
August	177.43	179.39	191.42
September	132.69	145.45	164.93
October	69.14	74.35	96.19
November	51.04	78.52	88.56
December	39.32	70.62	75.84

Approximately 55% of the total energy consumed in households in Serbia as well as in Vojvodina is used in the form of electricity. A significant part of this energy is used for heating the sanitary water. Utilizing solar energy can help reduce the cost of heating hot water by about 60 to 70% during the year. According to the Serbian Energy Efficiency Agency estimates, Serbia's energy consumption could be reduced by more than 50% with more efficient heating and energy efficiency improvements in the industry.

Depending on system efficiency the Republic of Serbia has the potential to produce from 700 to 900 kWh of energy per square meter of solar thermal collector annually, which is high in comparison with the countries with a good reputation for energy solar usage. In the Republic of Serbia, 3.3 kWh could be produced per square meter and would be most effectively used in the tourism, health sector and households, primarily for heating hot water.

In the Republic of Serbia and Autonomous Province of Vojvodina, the use of solar energy for heating domestic hot water or space is almost negligible, although there has been an increase in the implementation with the support of state institutions, donations and financing from users in the past years. Greater use of solar systems in the Republic of Serbia is prevented mainly by the lack of state support for individuals as well as poor public awareness. The enormous savings of conventional energy would be achieved if each household had at least one unit of the solar collector to heat the domestic hot water. Viewed within the state's electricity system, this would represent a significant burden on the system.

The technically usable energy potential for the conversion of solar energy to thermal energy (for hot water preparation and other purposes) is estimated at 0.194 Mtons per year, assuming the application of solar thermal collectors to 50% of available facilities in the country.

The current situation in local self-governments of the Republic of Serbia is characterized by unreliable and incomplete data on the amount of municipal waste generation. The quantities of municipal waste annually were calculated on the basis of waste measurements in the reference to local governments. The urban population generates an average of 1 kg of municipal waste per citizen per day, while the rural population generates 0.7 kg of waste per citizen per day. Based on the census, the urban population is 57%, while 43% is rural. On average, a resident of the Republic of Serbia generates 0.87 kg of municipal waste per day or 318 kg per year. The population of 7 443 183 produces about 2 374 374 tons of waste a year. In Figure 4.9, the morphological composition of municipal waste in the Republic of Serbia. According to a report from the Environmental Protection Agency on waste management in 2011-2017, a total of 2.15 Mtons of waste was generated in 2017, of which municipal public utility companies collected 1.80 Mtons, or 83,7%. Most municipal waste is landfilled and only 3% is officially recycled.

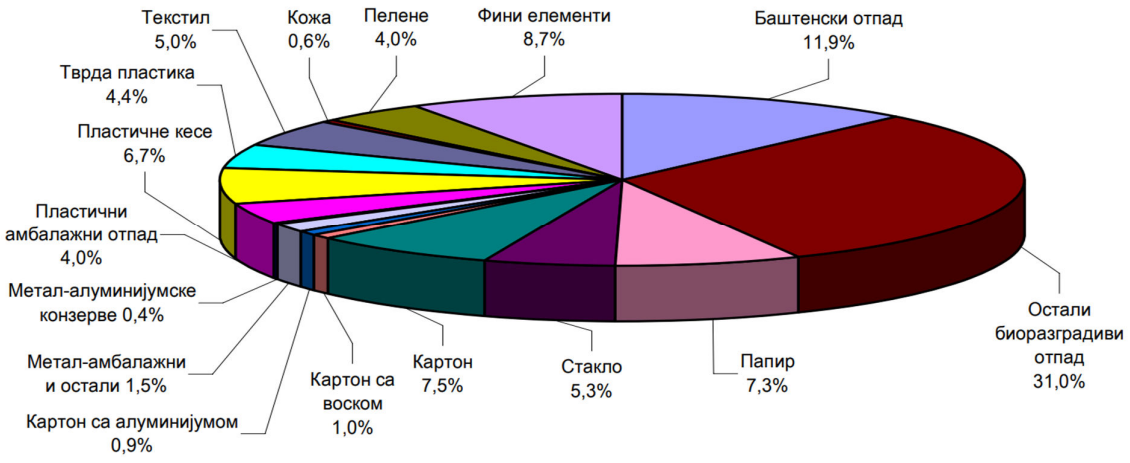

Figure 4.9 The morphological composition of municipal waste in the Republic of Serbia [20].

According to the results of statistical surveys on waste conducted at the Statistical Office of the Republic of Serbia in the period 2010-2013, the generated waste quantities recorded an increase. Table 4.5 and Figure 4.10 show the share of individual economic sectors in the total amount of waste generated in the years 2010-2013.

Table 4.5 Share of individual sectors in the total amount of waste generated in the years 2010-2013 [21].

Year	2010	2011	2012	2013
Total	**33 615 918**	**49 004 760**	**55 002 585**	**58 388 403**
Mining	26 460 274	41 522 482	47 896 363	50 807 563
Manufacturing industry	1 135 357	1 126 609	759 832	821 286
Electricity, gas and steam supply	6 020 287	6 355 668	5 744 350	6 199 079
Water supply and wastewater management	-	-	-	33 106
Construction	-	-	363 706	328 235
Service sectors	-	-	238 336	199 132

In 2013, Mining accounted for 87% of the total amount with 50 Mtons, followed by Electricity, gas and steam supply at 10.6% or 6 Mtons, Manufacturing by 1.4% or 750 000 tons and the remaining 1% is waste generated by other Service sectors. The largest increase in waste generated compared to the previous year was recorded in 2011, at 45.8%. Although the scope of the survey was expanded in 2012 and 2013, the largest increase in generated waste compared to the previous year remained in 2011.

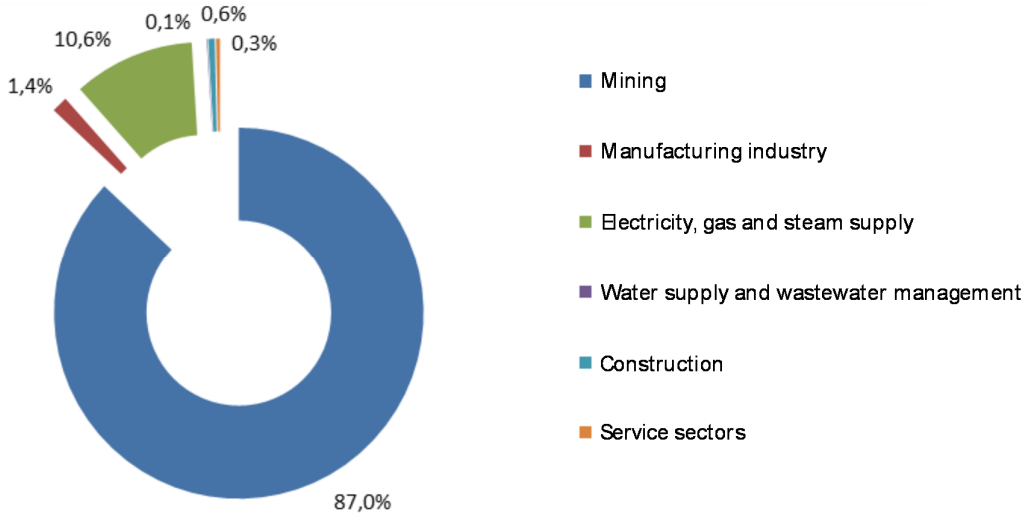

Figure 4.10 Share of individual sectors in the total amount of waste

Generated quantities of hazardous and non-hazardous waste in the period of 2010-2013, presented in Figure 4.11 also recorded an increase.

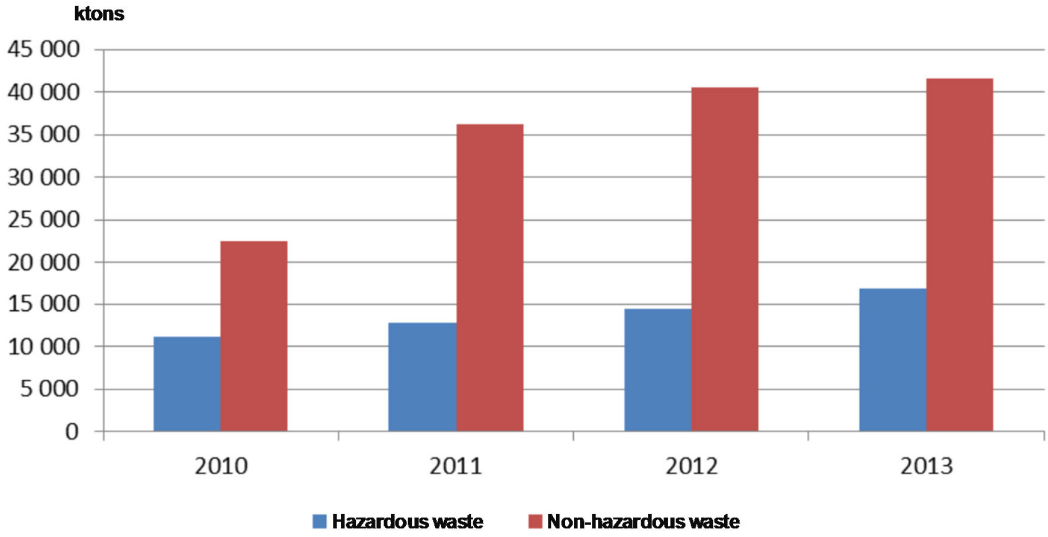

Figure 4.11 Generated quantities of hazardous and non-hazardous waste in the period 2010-2013

Mineral and combustion wastes are the most represented types of waste in the total amount of waste generated in observed years. Other types of waste were changing their share depending on the sectors covered by the survey. Until 2011, in addition to the aforementioned types of waste, vegetable waste, acid, base or saline waste as well as metallic iron waste were generated in large quantities. In 2012 and 2013, with the inclusion of the Construction and Services sectors in the scope of the survey, there were changes in the structure and an increase in the types of mineral waste generated in the bulk by the Construction (Land and Iron Metals) sector, as household and similar waste generated largely by the service sectors. There is no exact data on the quantities of waste oils generated on the territory of the Republic of Serbia. It is estimated that about 50,000 tons of various mineral oils are consumed annually. In addition, it is estimated that around 10,000 - 15,000 tons of motor and other oils and lubricants are consumed annually in the city of Belgrade. There is no regulated waste oil collection system in the territory of the Republic of Serbia. Waste oil collection and recovery capacities are approximately 25,000 t per year. Some operators carry out collection and temporary storage. To a lesser extent, the collection and regeneration of self-produced oil and the regeneration of oil by private entrepreneurs are present. Part of the waste oil is exported for final disposal, and part of the waste oil is illegally collected and disposed of, most often for energy purposes. There is a growing trend of organized collection and collection of edible waste oils. They are most commonly used for biodiesel production. There are also certain capacities for the treatment of oil emulsions by ultrafiltration and the subsequent disposal of the resulting oil concentrate by solidification. Cement plants have the capacity to use waste oils for energy purposes.

4.2. FERIT and KBCO potential of renewable energy sources

4.2.1. Solar energy

Because of its favourable geographical location, Republic of Croatia has large solar energy potential. Annual global solar irradiation on horizontal surface is given in Figure 4.12. Global irradiation and solar electricity potential for the optimally inclined photovoltaic (PV) modules of the Republic of Croatia are shown in Figure 4.13. It is visible that continental areas have slightly lower annual solar irradiated energy. Nevertheless, continental part, in which Osijek is situated has great solar energy potential.

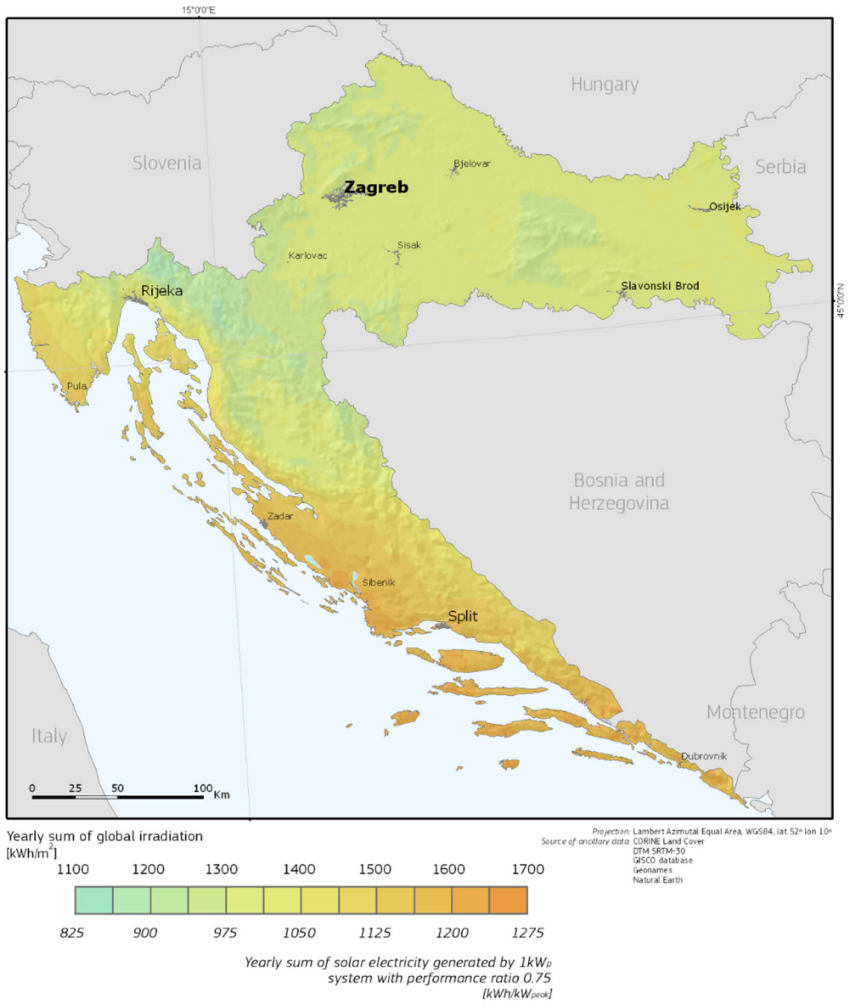

Figure 4.12 – Annual global solar irradiation on horizontal surface in Republic of Croatia [22].

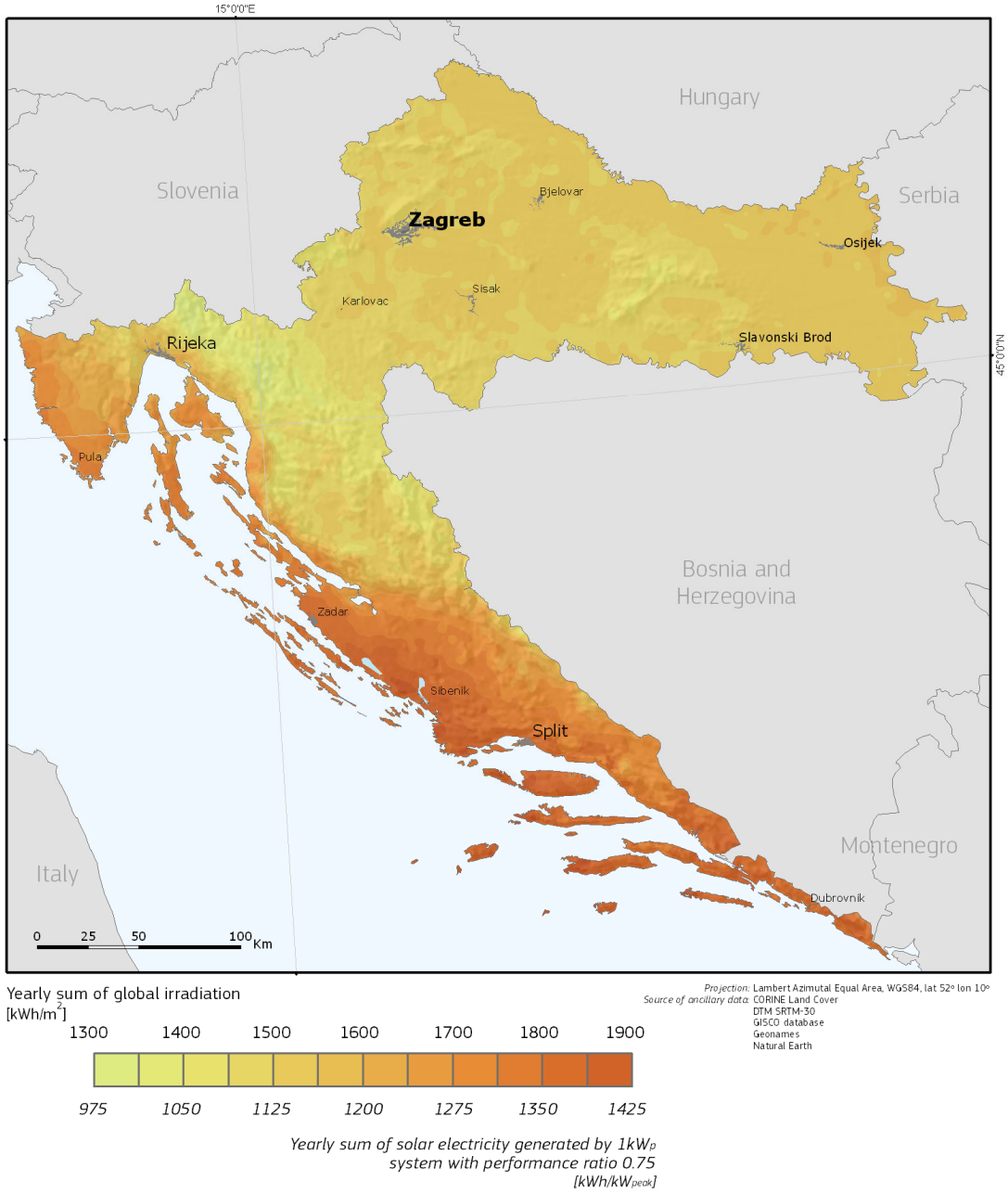

Figure 4.13 – Annual global solar irradiation on optimally inclined surface in Republic of Croatia [22].

Average annual solar irradiation on horizontal plane in Osijek region is around 1282 kWh/m2 while annual optimal inclination angle of PV modules and solar thermal collectors is 34° [22]. Highest solar irradiation occurs in summer months (June – August) while the lowest occur in winter months (November - January). Distribution of global solar irradiation for every month and annual solar irradiation for Osijek is given in Table 4.6.

Table 4.6 – Global monthly and annual solar irradiation for Osijek [22].

Month	Global
	kWh/m^2
January	40.8
February	41.78
March	90.86
April	133.58
Max	172.2
June	198.09
July	187.46
August	138.18
September	116.22
October	92.04
November	42.67
December	28.21
Total	1,282.09

Due to changes in the elevation angle of the Sun during the day, month and year, the value of the radiated energy that reaches the surface changes. More energy is received only by the surface at which the angle changes and adjusts to the position of the Sun each month, or even more if the receiving surface follows the Sun's trajectory daily. Nevertheless, the optimal slope of the collector should be 30-40°. The optimum slope for the summer period is 20-30° and for winter is about 60°.

4.2.2. Wind energy

In order to harness wind energy, one of the important factors is the existing road and railway structure and the accessibility of the terrain on which wind farms are planned. Also important is the existence and coverage of the territory with medium and high voltage power grid. Such infrastructure factors, necessary for successful connection of wind power plants, include the existence of suitable transformer stations and the possibility of connection to them. The most significant parameters for wind turbine performance are speed and direction of the wind at the site. Therefore, wind energy potential will be analysed with two separate measurements, first from weather station of Croatian Meteorological and Hydrological Service located in village Čepin near Osijek and second located at the roof of the building in Trpimirova street.

Measurements of wind speed in 2015, taken by weather station in Čepin near Osijek, are given in Figure 4.14. Highest mean wind speed occurs in March and April while the lowest in December.

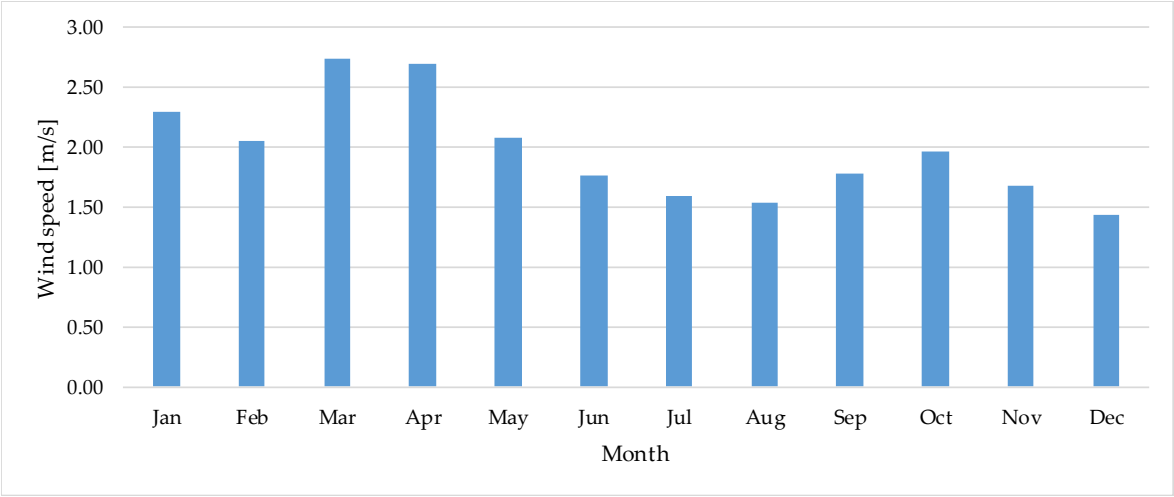

Figure 4.14 Monthly mean values of wind speed for 2015 at the weather station in Čepin near Osijek.

In order to asses wind energy potential for certain region or microlocation, wind speed measurements in surrounding area are needed. For this purpose, measurements taken by weather station located on the roof of the faculty building in Trpimirova street are also analysed. Figure 4.15 shows frequency distribution of wind speed based on 1-hour average values in 2018. It is visible from the figure that the highest frequency of wind speed occurs from 0 to 1 m/s.

Furthermore, to analyse the direction of the wind on the microlocation, rose of winds is constructed (Figure 4.16). It is visible that the most frequent wind speed direction is between East and South while the most frequent is South-East.

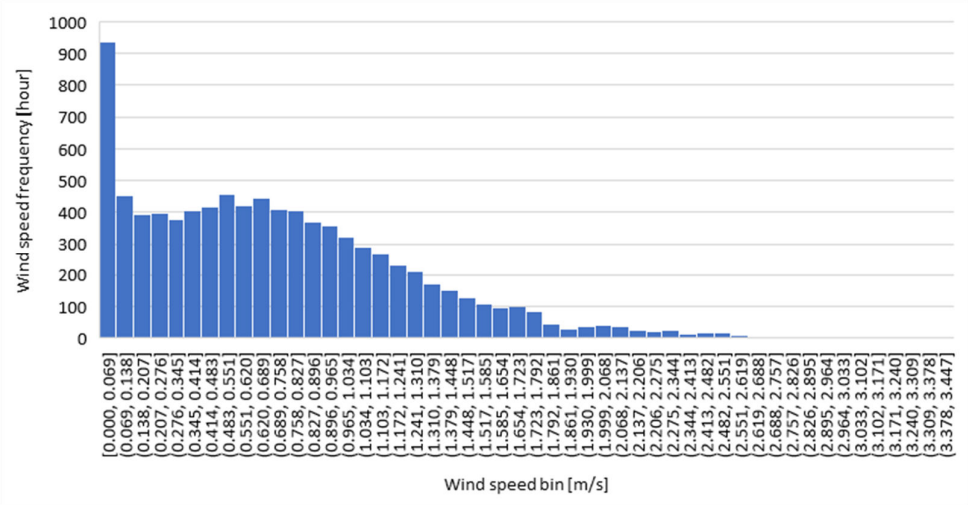

Figure 4.15 Wind speed frequency at the microlocation of FERIT building in Trpimirova street

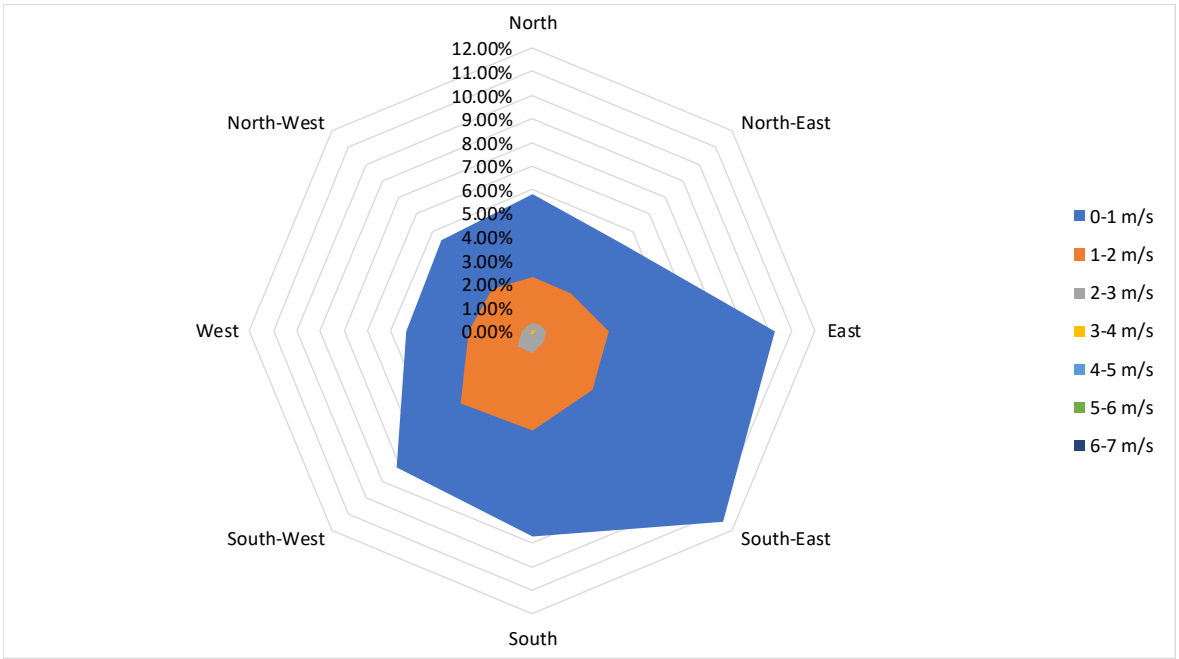

Figure 4.16 – Rose of winds for the microlocation of FERIT building in Trpimirova street

4.2.3. Waste and biofuels

Solid waste biomass is considered as biodegradable part of municipal waste, food industry and other related industries. Furthermore, solid waste biomass can origin from

wood industry. Theoretical annual energy potential of solid waste biomass for Osijek-baranja county is given in Table 4.7 [23].

Table 4.7 Theoretical annual energy potential of solid waste biomass for Osijek-baranja county [23]

Raw material type	Available waste [t/year]*	Theoretical energy potential [MWh/year]	Theoretical energy potential [TJ/year]
Slaughterhouse waste	4,651	23,255	84.7**
Wood industry waste	321	1,509	5.4
Biodegradable part of municipal waste	39,210	26,467	95.3**

*source: Waste logs for period of 2008-2010 (Agency for environmental protection), ** Registri otpada za razdoblje 2008-2010. (Agencija za zaštitu okoliša), ** obtained by biogas production technology

Liquid biofuels bioethanol and biodiesel can are produced by hydrolysis and esterification of vegetable oils with alcohol. In Osijek-Baranja county, corn and sugar beet can be used for production of bioethanol while rapeseed and soy can be used for biodiesel production.

Apart from agriculture crops, there are other ways of biodiesel production. There is a growing trend of organized collection and collection of edible waste oils used for food preparation in large public facilities. They can be easily used for biodiesel production. There are also certain capacities for the treatment of oil emulsions by ultrafiltration and the subsequent disposal of the resulting oil concentrate by solidification. Cement plants have the capacity to use waste oils for energy purposes.

Theoretical annual energy potential of bioethanol production from corn and sugar beet and biodiesel production from rapeseed and soy is given in Table 4.8 for Osijek-Baranja county [23].

Table 4.8 Annual theoretical energy potential of liquid biofuels production in Osijek-Baranja county [23]

Raw material type	Raw material mass [t/year]*	Biofuel quantity [t/year]	Lower heating value [GJ/t]	Theoretical energy potential [GWh/year]
Bioethanol				
Corn (a.v.)**	1,100,032	330,962	27	2,482
Sugar beet	8,048,159	623,887	27	4,679
Biodiesel				
Rapeseed	463,911	189,351	37	1,946
Soy	421,738	79,874	37	821

* Calculation is based on average yield of agriculture culture from Statistical anniversaries of Republic of Croatia for the period 2006 to 2008 and data of available agriculture land for cultivation of energy crops;
** a.v. – average value between dry milling and wet milling process

4.3. UNISB potential of renewable energy sources

Like in a case of climate conditions, Slavonski Brod has a very similar potential of renewable energy sources like Osijek, described in section 4.2.

Heat energy potentials of the renewable energy sources planned to mount on building of Strojarski fakultet are based on microclimatic conditions (air temperature, relative humidity, wind velocity, sun irradiation) in the area of Slavonski Brod. During the winter and summer time stable functionality of the heat pump provides up to maximum thermal power with high efficiency (COP). Low air temperatures (-7°C to -10°C) occur very rarely and the maximum outdoor air temperature in summer is up to + 33°C / + 35°C. The lowest and highest outside air temperatures have a rare frequency and their cumulative values are in a short period of time. During that period COP decrease, but rated power of heat pump remains constant.

5. Planned optimal renewable energy system topology and building energy management system for the exemplary facilites

In this section, regarding the features of the location and building for the exemplary objects and considering conducted analysis of the energy demand and potential for renewable energy sources, the recommendation for the optimal renewable energy system, as well as topology of the smart building energy system are proposed. This system would improve the energy efficiency of the exemplary object and provide higher reliability and better performance on the energy flow control.

5.1. FTN renewable energy systems

Renewable energy sources are incorporated into traditional power systems to increase the energy efficiency, reduce the power share coming from the fossil fuels and dependency from the utility grid.

According to the analysis of the renewables potential of the exemplary object, the following systems are suitable for installation:

- Photovoltaic system;
- Solar tree;
- Photovoltaic based electric vehicle charging station;
- Renewable energy storage/supply system;
- Wind energy system;
- Heating, ventilation and air conditioning (HVAC) system.

5.1.1. Photovoltaic system

Since the conditions for the utilization of solar energy are exceptional, the photovoltaic (PV) power plant should be constructed on the rooftop of the exemplary object. The precise location is depicted in Figure 5.1. The exemplary object is divided into three sectors and the PV plant is going to be placed on the rooftop on one of the sectors.

Figure 5.1 The location for the PV plant construction.

The installed power of the PV plant is 50 kW. The block diagram of the PV system is given in Figure 5.2.

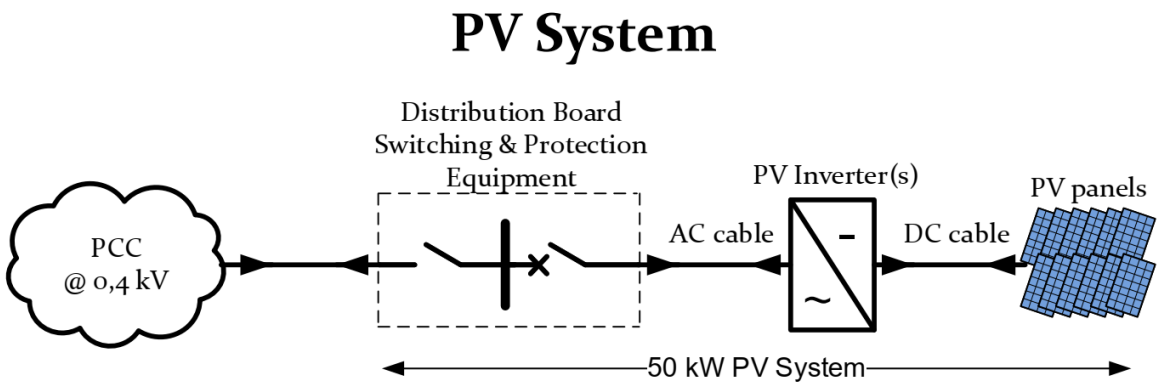

Figure 5.2 Block diagram of the PV plant.

PV strings, i.e. a series of the PV panels, are directly connected to three-phase inverter unit(s) which transform the DC voltage from the output of PV strings to AC voltage. The DC cables that connect PV strings with the inverters are planned for external mounting. The inverter(s) have built-in DC/DC converters with the algorithm for the maximum power

point tracking. Other electrical equipment such as protective and switching devices are placed inside the distribution board. The point between the board and the distribution power grid is called the point of common coupling (PCC) and the voltage level in the PCC is 0.4 kV.

Using the PVGIS software tool, it is possible to predict the total production of electrical energy of the PV plant monthly and is depicted in Figure 5.13. The total estimated value of the energy produced annually is 54.44 MWh.

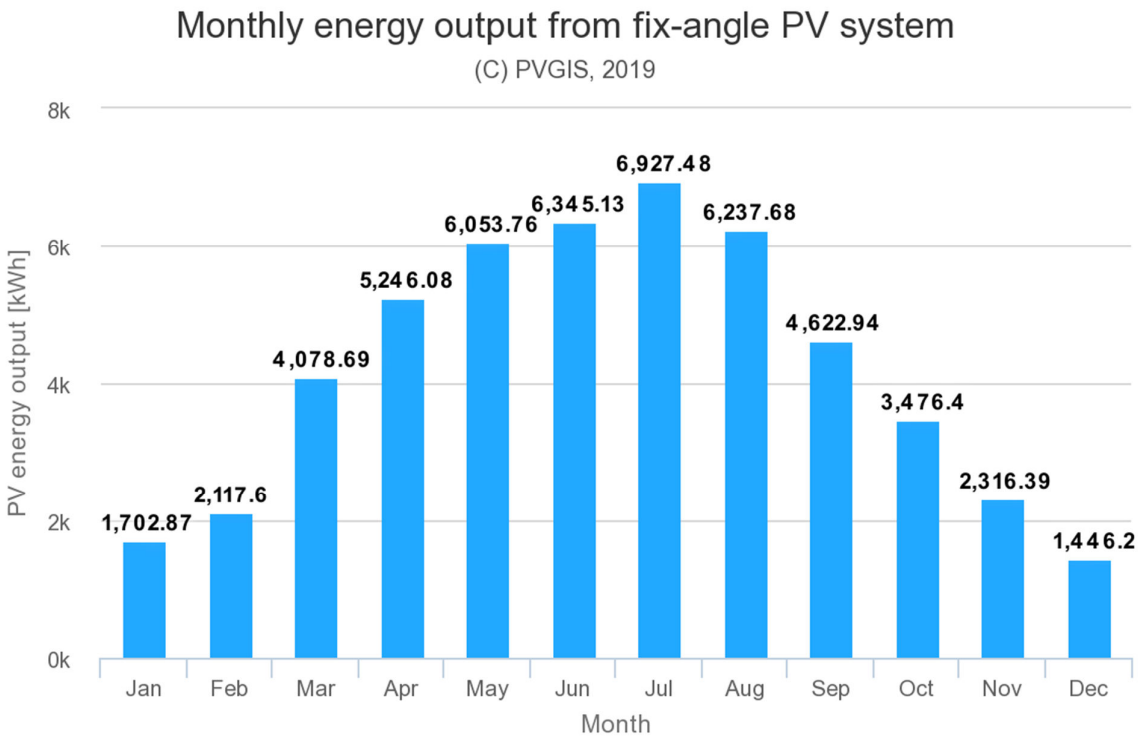

Figure 5.3 Estimated electrical energy production of the PV plant, located at the exemplary object.

5.1.2. Solar tree

To utilize available solar energy resources, a solar tree that can be used as assistive devices charging station will be located at the “Mašinski institut”, between two building sectors. Solar panels will be placed on a solar tree since it is aesthetically attractive, enhances the landscape and architecture and yet behaves as a functional power generator.

The installed power of the solar tree system is 2 kW. The block diagram of this system is depicted in Figure 5.24.

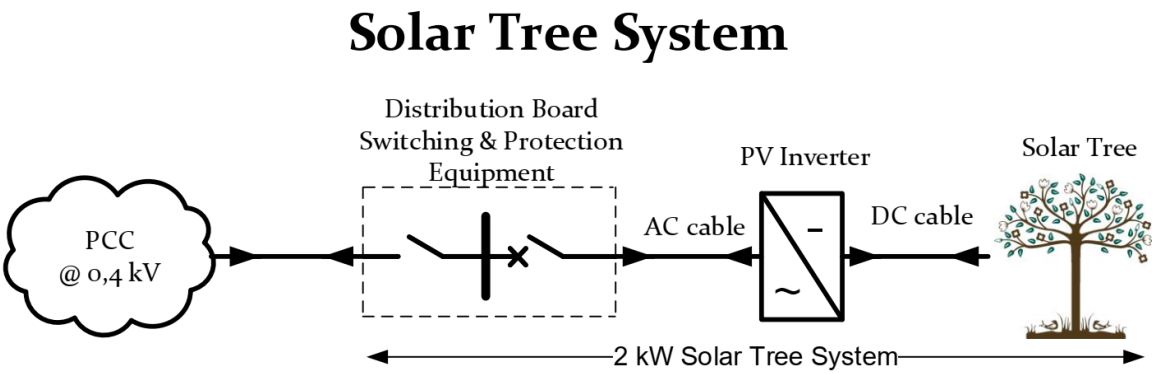

Figure 5.4 Block diagram of the solar tree system used as a generator for assistive devices charging station.

The solar tree is directly connected to the inverter unit that transforms the DC voltage from the output of PV panels placed on the solar tree to AC voltage. Electrical equipment such as protective and switching devices is placed inside the distribution board. The voltage level in the PCC is 0.4 kV.

Using the PVGIS software tool, it is possible to predict the total production of electrical energy of the solar tree monthly, which is depicted in Figure 5.5. The total estimated value of the energy produced annually is 2.18 MWh.

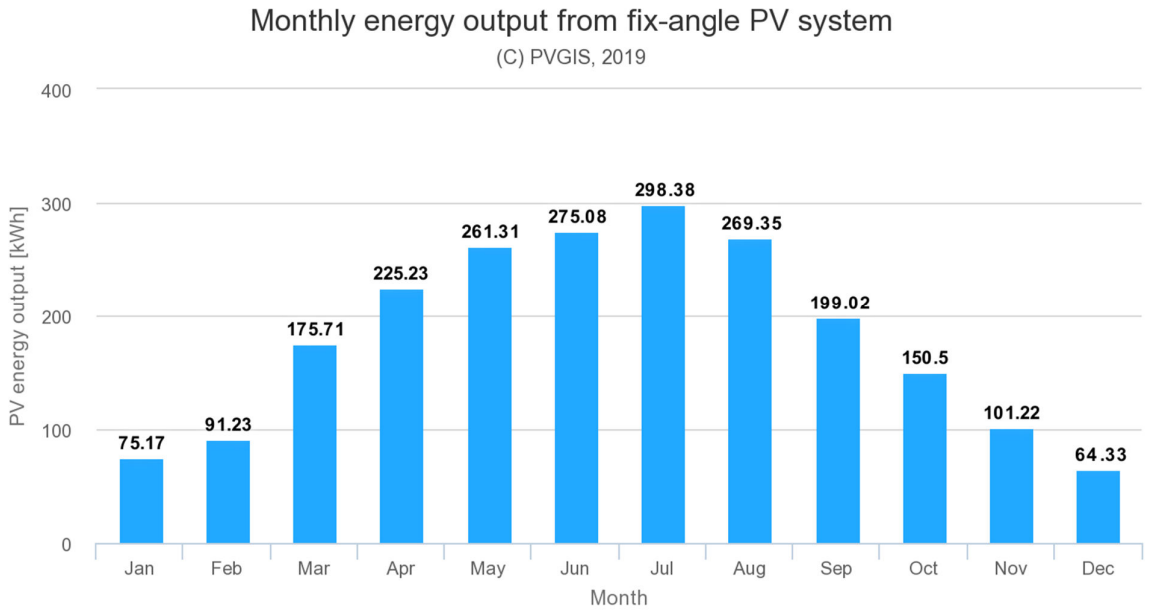

Figure 5.5 Estimated electrical energy production of the solar tree used as an assistive devices charging station, located at the exemplary object.

5.1.3. Photovoltaic based electric vehicle charging station

Solar energy is the ideal candidate to fuel green, electric mobility since it provides CO_2 -free electricity that can be used to drive electric vehicles. Looking at the physics, solar is complementary to electric mobility, particularly in certain use cases like day charging at workplaces or combined with battery capacity at home. By maximizing self-consumption ratios of solar electricity generated on-site, the EV owner reduces the need to consume energy from the grid, saving on their electricity bill while also reducing grid congestion.

Regarding the importance of the integration of electric vehicles, as well as the significance of clean mobility with solar energy as a cost-competitive and scalable candidate, a photovoltaic based electric vehicle charging station is going to be constructed in the exemplary object. The installed power of the EV charging station is 3 kW. The block diagram of this PV system used to produce power for EV charging is illustrated in Figure 5.6.

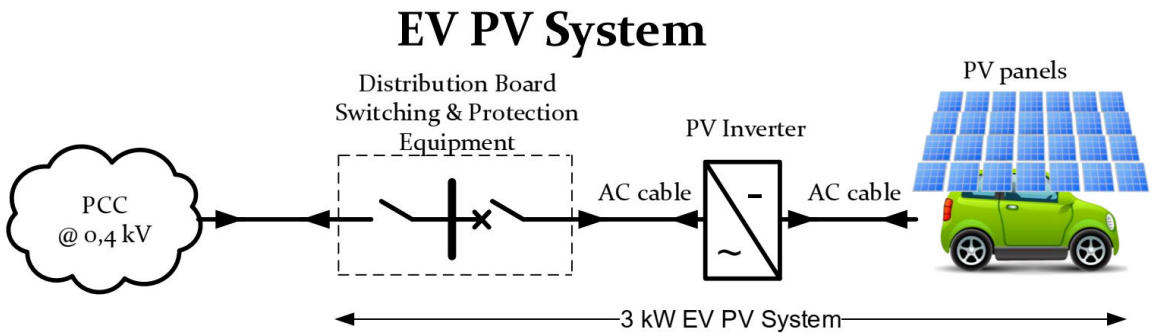

Figure 5.6 Block diagram of the photovoltaic system for the electric vehicle charging power production.

PV system used to power an electric vehicle is directly connected to the inverter unit that transforms the DC voltage from the output of the charging station to AC voltage. Electrical equipment such as protective and switching devices is placed inside the distribution board. The voltage level in the PCC is 0.4 kV.

Using the PVGIS software tool, it is possible to predict the total production of electrical energy of the PV based system that can be used for charging monthly, which is depicted in Figure 5.7. The total estimated value of the energy produced annually is 3.28 MWh.

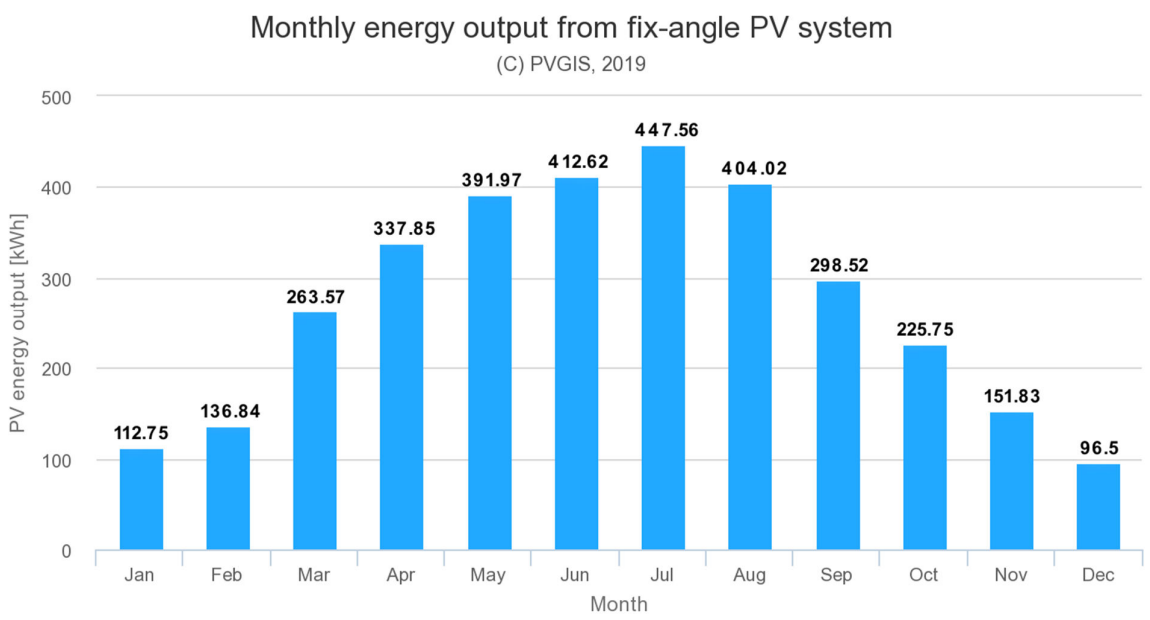

Figure 5.7 Estimated electrical energy production of the PV based system used to charge electric vehicles, located at the exemplary object.

5.1.4. Renewable energy storage/supply system

Energy storage/supply technologies are used in modern grids in order to enhance the reliability of renewable energy sources, improve the resilience of the grid and resolve its issues, as well as realize the benefits of smart grids and optimizing generation to suit demand. They are usually accompanied by renewable energy sources. Due to the highly intermittent nature of the renewables, sometimes it is possible that consumers do not need all the energy produced by the source or there is not enough energy as required. Therefore, energy storage/supply systems can be used to store energy when the amount generated exceeds the demand and inject power into the system during shortages. Furthermore, they can be used for the peak shaving application, i.e. to cover the peak load.

Therefore, a renewable energy based storage/supply system is going to be installed at the exemplary object in order to provide stabilizing the power output while also enhancing the reliability of the system. The block diagram of the energy storage/supply system is given in Figure 5.30. The bi-directional power converter is used as an interface between the storage/supply system and the grid. Switching and protection equipment is placed in the distribution board. The installed power of the bi-directional converter used in the system is 35 kW. The storage/supply system comprises the battery storage system, as well as the supercapacitor system. Batteries present an advanced technique for storing electrical energy in electrochemical form and have a wide range of use. Supercapacitors have a high energy storage capacity due to their high power ability and since the stored energy has to be used very quickly, they are able to provide peak shaving and thus improve the power profile.

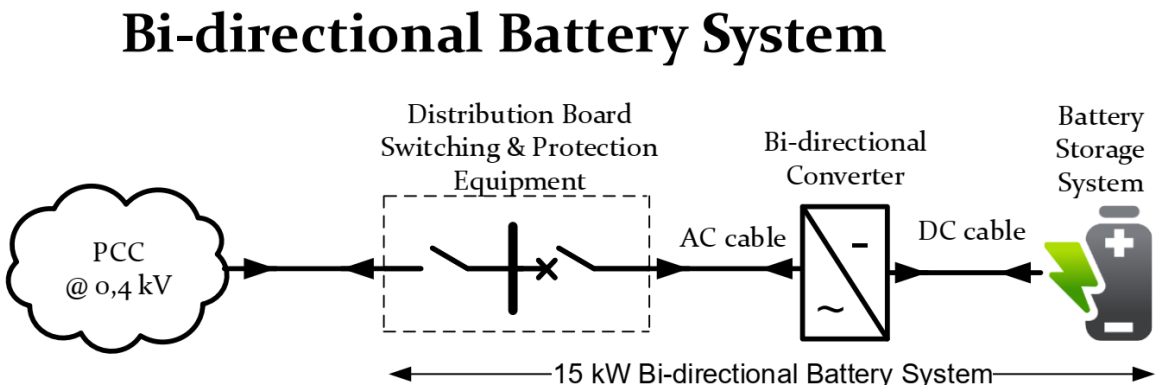

Figure 5.8 Block diagram of the energy storage/supply system.

The battery of the electric vehicles can also be used as a storage/supply unit and can enable different grid support functionalities. This is a state-of-art concept that is very interesting to the researches and certainly could become a new tool for electric utilities in the next decade.

5.1.5. Wind energy system

The exemplary public building is located in the region with good potential for wind energy development, especially in higher height levels. However, since the area is urbanized, there are limited options when it comes to wind energy due to the surrounding buildings, trees and other obstacles. Another important issue is the size of the wind turbine. Wind turbines can be noisy and require consistent, non-turbulent winds of certain speeds that are uncharacteristic of urban environments. However, due to the technology improvements wind turbines should be self-starting, ultra-quiet, provide smooth torque, and be highly efficient so usable energy can be delivered at modest wind speeds.

Therefore, a small wind power system is planned to be constructed on the rooftop of the “Mašinski institut”. Rooftops are elevated above the ground, where it is windier and the electricity is generated right where it is needed. The installed power of the system is 2kW. The block diagram of the wind power system is given in Figure 5.31.

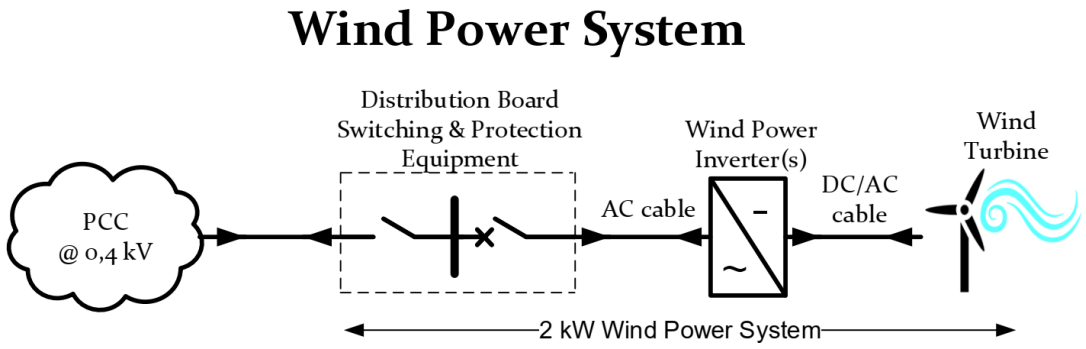

Figure 5.9 Block diagram of the wind power system.

The wind turbine is directly connected to the three-phase inverter unit(s) which transform the DC voltage from the output of wind turbine to AC voltage. Protective and switching devices are placed inside the distribution board. The voltage level in the PCC is 0.4 kV.

A free online tool from REUK.co.uk is used to estimate the amount of electricity that can be generated by a wind turbine with a known rotor diameter, in a location with a particular average wind speed. The prediction is that the energy produced annually is 1.06 MWh and estimated monthly output of the system is depicted in Figure 5.10.

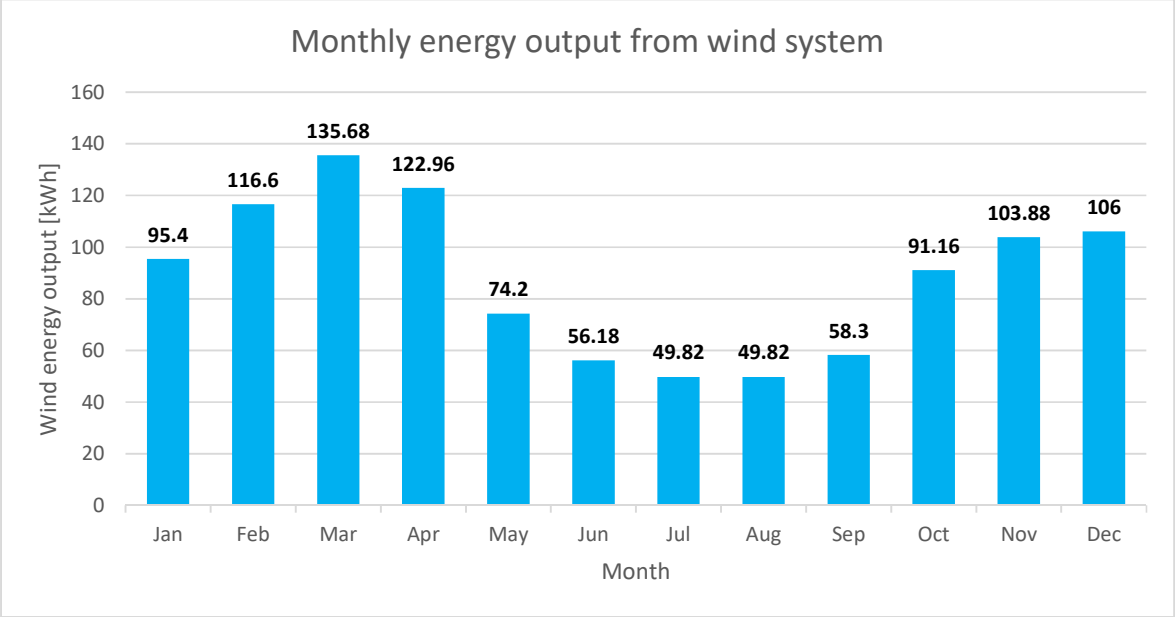

Figure 5.10 Estimated electrical energy production of the wind based system.

5.1.6. Heating, ventilation and air conditioning (HVAC) system

The exemplary object is primarily dedicated to research and teaching activities of a large number of employees and students. All parts of the building are at disposal almost the entire day, and thus thermal comfort and acceptable indoor air quality are extremely important. Moreover, considering the cost of the heating energy that is consumed in the object, the reduction of the heating bill price is beneficial. Therefore, heating, ventilation, and air conditioning system (HVAC) is an adequate solution to this problem. HVAC systems provide significant energy-saving benefits, have a positive environmental impact, can improve air quality by constantly exchanging the indoor air with fresh, offer superior humidity control and a variety of other options.

Therefore, the HVAC system is going to be installed in the exemplary object. The system is dedicated to the air conditioning of several laboratories. It is intended to provide better insulation of that part of the building in order to achieve greater system efficiency.

Energy-efficient windows and doors should provide insulation for the winter, decrease air conditioning use in the summer, and eliminate overall uneven heating and cooling.

The installed power of the HVAC system is 55 kW. The efficiency of its components depends on the relation between HVAC size and facility size, local climate, operation time and the type of the fuel HVAC uses. It is decided that the central HVAC system, based on air heat pump, with fan coils units. Thus, the volume of this combined system is reduced, and the outdoor ventilation is produced to properly condition the desired zone. The appropriate thermal medium is responsible for carrying the thermal load in a building by 80–90 %, while air medium conditions the remainder.

The block diagram the HVAC system connection to the grid is depicted in Figure 5.11. The system is directly connected to the PCC point at voltage level 0.4 kV, and complete equipment dedicated to the switching and protection is placed inside a distribution board. The HVAC system uses the thermal energy from different mediums – air, water, etc. If that thermal energy is not enough to fulfill all requirements, the remaining energy for heating/cooling process is taken from the grid.

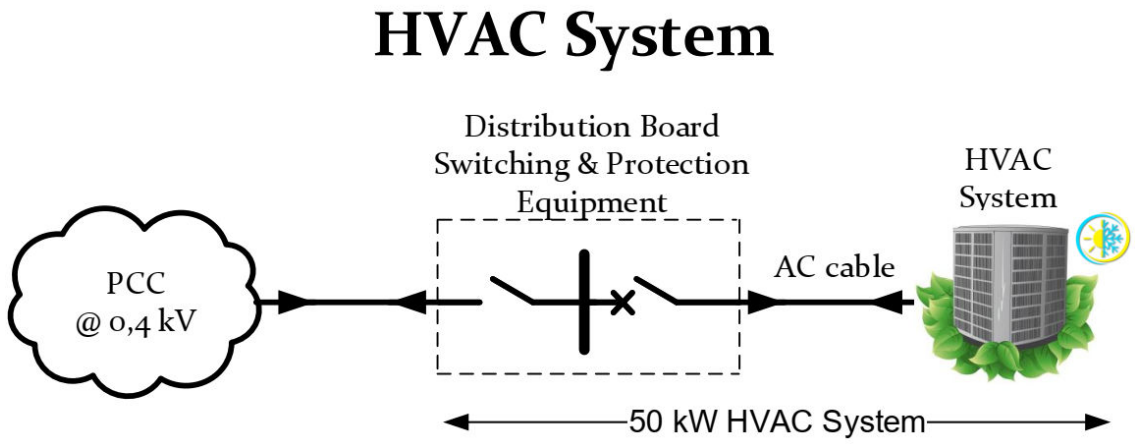

Figure 5.11 Block diagram of the HVAC system.

5.2. KCV renewable energy systems

One of the possible strategies for the increase in energy efficiency is to incorporate renewable energy sources into traditional power systems. If the power is partially produced by the renewables, the power share coming from the fossil fuels is decreased and thus greenhouse gas emission is reduced. Furthermore, the reduction in the energy provided by the power grid would lead to a significant money savings. Also, reduced risk of loss from grid blackouts is another benefit regarding less dependence of the object on the energy coming from the grid. This concept provides sustainable renewable energy to the grid and reduces the need for grid expansion.

According to the analysis of the renewables potential of the exemplary objects, the following systems are going to be constituted:

- Photovoltaic system on the roof of Radiology clinic;

- Photovoltaic system on the roof of Emergency center;
- Photovoltaic system on the parking inside KCV complex;
- Solar thermal system on the roof of Medical Rehabilitation clinic;
- Charging station for electric vehicles and assistive devices;
- Biodiesel backup generator system with biodiesel production;
- Building energy management system.

Radiology clinic has flat roof making the PV power plant construction and utilization completely justified. The installed power of the PV plant is 50 kW, the panel slope is 10 degrees and azimuth angle is 90 degrees. The block diagram of the PV system on the rooftop of the Radiology clinic is given in Figure 5.12.

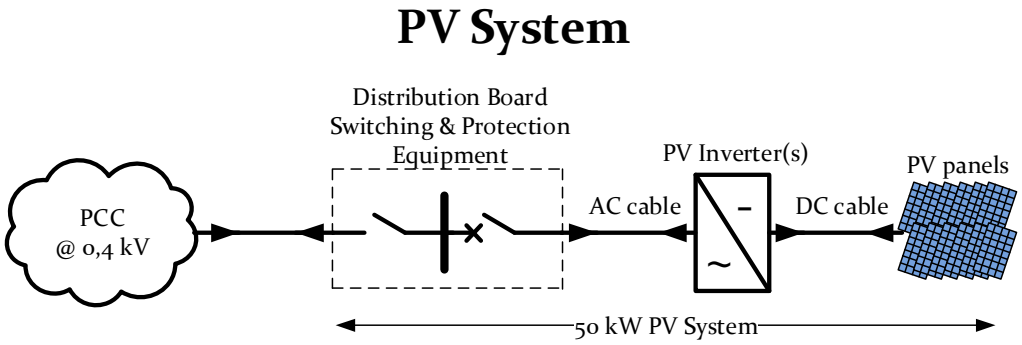

Figure 5.12 Block diagram of the PV plant on the Radiology clinic roof

PV strings, i.e. a series of the PV panels, are directly connected to three-phase inverter unit(s) which transform the DC voltage from the output of PV strings to AC voltage. The DC cables that connect PV strings with the inverters are planned for external mounting. The inverter(s) have built-in DC/DC converters with the algorithm for the maximum power point tracking thus enabling highly efficient energy conversion. Other electrical equipment such as protective and switch devices are placed inside the distribution board. The point between the board and the distribution power grid is called the point of common coupling (PCC) and the voltage level in the PCC is 0.4 kV. Using the PVGIS software tool, it is possible to predict the total monthly electrical energy production of the PV plant and this projection is depicted in Figure 5.13. The total estimated value of the energy produced annually is 51.36 MWh.

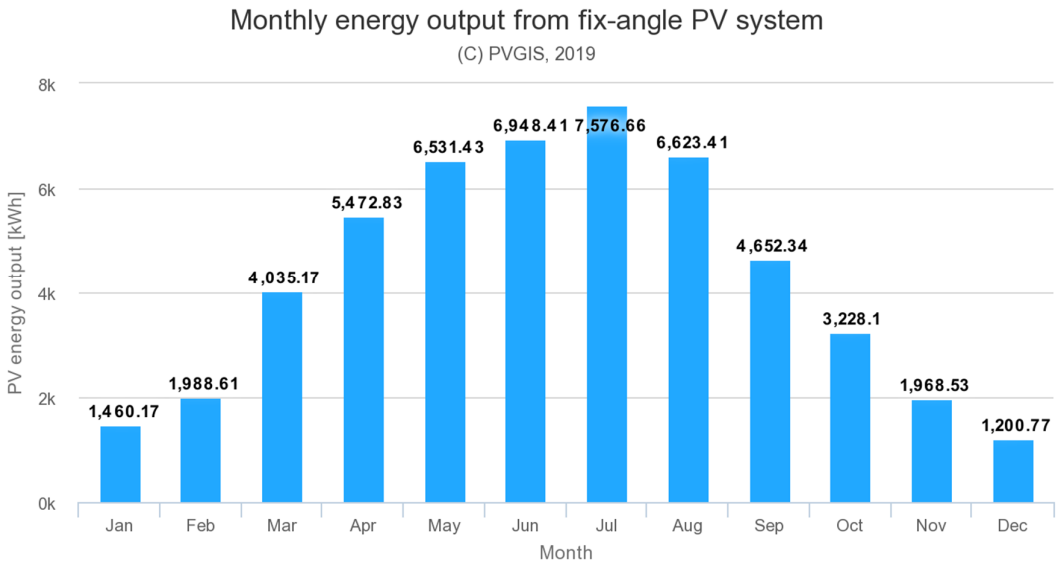

Figure 5.13 Estimated electrical energy production of the PV plant, located on the Radiology clinic rooftop.

Emergency center has flat roof making the PV power plant construction and utilization completely justified. The installed power of the PV plant is 50 kW, the panel slope is 10 degrees and azimuth angle is 90 degrees. The block diagram of the PV system on the rooftop of the Emergency center is given in Figure 5.14. PV strings, i.e. a series of the PV panels, are directly connected to three-phase inverter unit(s) which transform the DC voltage from the output of PV strings to AC voltage. The DC cables that connect PV strings with the inverters are planned for external mounting. The inverter(s) have built-in DC/DC converters with the algorithm for the maximum power point tracking thus enabling highly efficient energy conversion. Other electrical equipment such as protective and switch devices are placed inside the distribution board. The point between the board and the distribution power grid is called the point of common coupling (PCC) and the voltage level in the PCC is 0.4 kV.

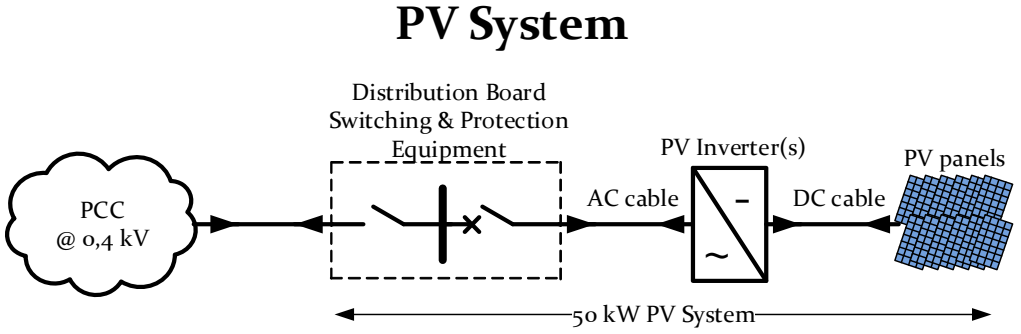

Figure 5.14 Block diagram of the PV plant on the Emergency center rooftop

Using the PVGIS software tool, it is possible to predict the total monthly electrical energy production of the PV plant and this projection is depicted in Figure 5.15. The total estimated value of the energy produced annually is 51.38 MWh.

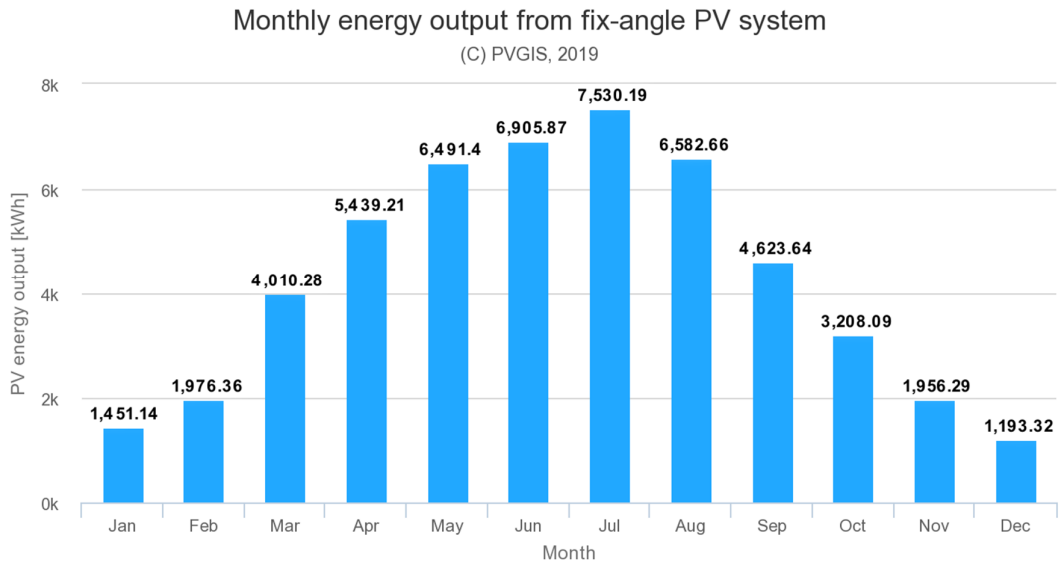

Figure 5.15 Estimated electrical energy production of the PV plant, located on the Emergency center rooftop

For the PV power plant on the parking inside KCV complex the supporting structure needs to be constructed, so that passenger vehicles can park below the PV plant but also the construction must withstand different weather conditions like strong wind etc. Supporting structure will be set so that the utilization of the PV panels is maximized. The installed power of the PV plant is 150 kW, the panel slope is 10 degrees and azimuth angle is 90 degrees. The block diagram of the PV system on the parking is given in Figure 5.16.

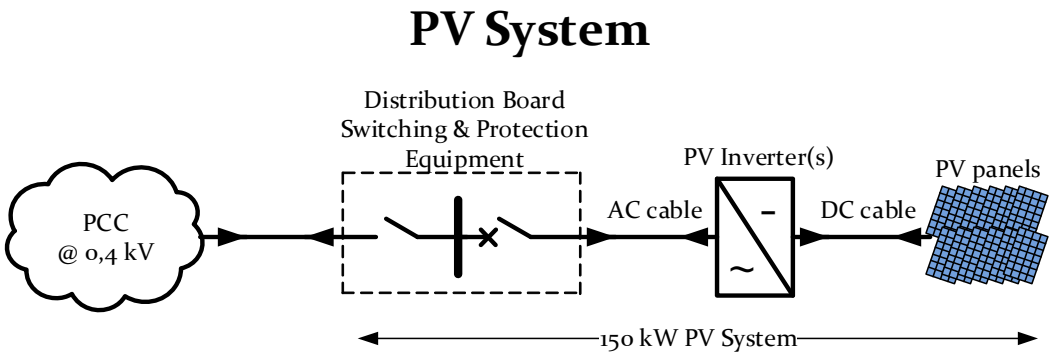

Figure 5.16 Block diagram of the PV plant on KCV parking

PV strings, i.e. a series of the PV panels, are directly connected to three-phase inverter unit(s) which transform the DC voltage from the output of PV strings to AC voltage. The DC cables that connect PV strings with the inverters are planned for external mounting.

The inverter(s) have built-in DC/DC converters with the algorithm for the maximum power point tracking thus enabling highly efficient energy conversion. Other electrical equipment such as protective and switch devices are placed inside the distribution board. The point between the board and the distribution power grid is called the point of common coupling (PCC) and the voltage level in the PCC is 0.4 kV. Using the PVGIS software tool, it is possible to predict the total monthly electrical energy production of the PV plant and this projection is depicted in Figure 5.17. The total estimated value of the energy produced annually is 155.14 MWh.

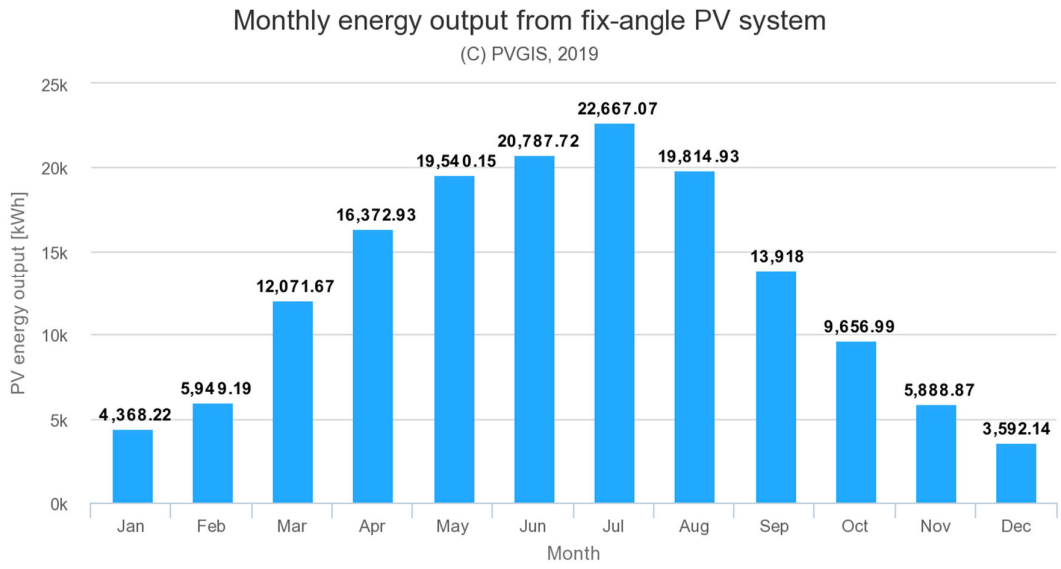

Figure 5.17 Estimated electrical energy production of the PV plant, located on the KCV parking

During the power consumption analysis it is confirmed that this facility has a huge need for energy that is used for heating water mainly in swimming pools and equipment used for rehabilitation. However, current system uses different previously described methods for heating water, which is rendered as inefficient and non-environmental friendly. On the other hand, analysis of the solar potential has confirmed that the location of this facility hold great solar potential thus the conclusion to install a 30 kW solar-thermal system on the rooftop of this facility is completely justified. In Figure 5.18, the average monthly solar irradiance that is expected on the location of this facility is shown, whereby in Figure 5.19 a block diagram of the solar-thermal system planned to be installed on the facility rooftop, is shown. As can be observed in Figure 5.19, solar-thermal system has classical configuration. The cold water is pumped through the boiler where it is heated and then returned to the swimming pool. The heat energy is generated by the solar collector located on the rooftop of the building.

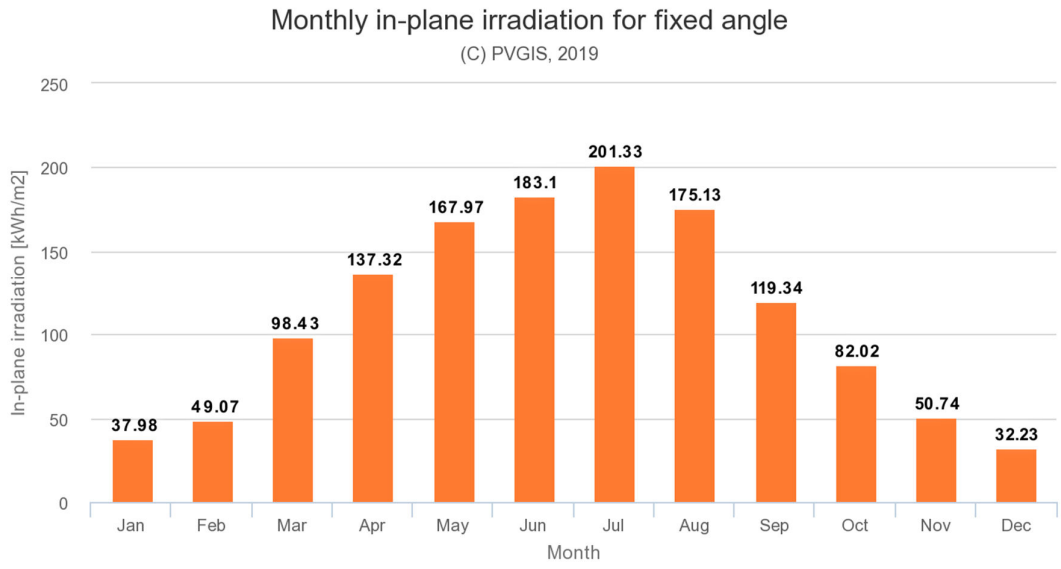

Figure 5.18 Monthly solar irradiance on the location of the Medical Rehabilitation Clinic

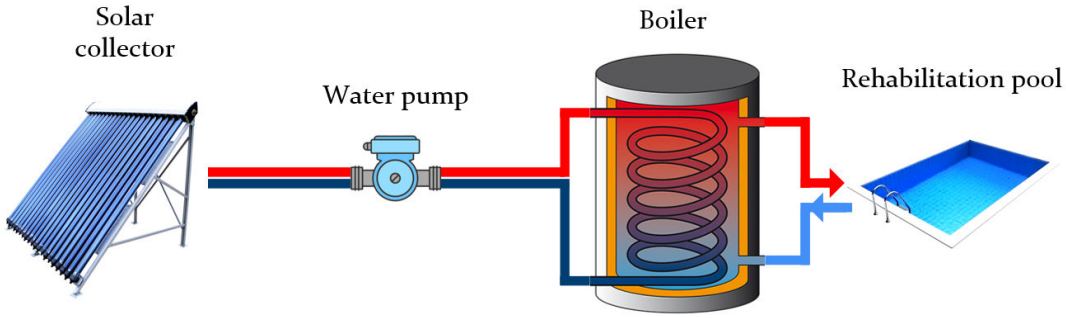

Figure 5.19 Block diagram of solar thermal system located on Medical Rehabilitation clinic roof

Based on the available software for solar thermal system performance prediction and available weather data for the location and heat demand of the Medical Rehabilitation Clinic values shown in Table 5.1 and Table 5.2 are obtained. Solar thermal energy (Q_{sol}) delivered to the system on a monthly basis is shown in Figure 5.20, and it can be inferred that highest energy delivery occurs in May and Jun and lowest in November and December.

Table 5.1 Solar thermal system properties

Parameter	Value
Number of collectors	20
Number of arrays	1
Tilt angle	45°
Orientation	0°
Collector field yield	19991.1 kWh
Temperature setting	45°C

Table 5.2 Overview of solar thermal energy (annual values)

Parameter	Value
Collector area	51.6 m2
Solar fraction total	43.5%
Total annual field yield	19991.1 kWh
Collector field yield relating to gross area	387,4 kWh/m2/Year
Collector field yield relating to aperture area	442.3 kWh/m2/Year
Max. energy savings	23519 kWh
Max. reduction in CO2 emissions	7072 kg

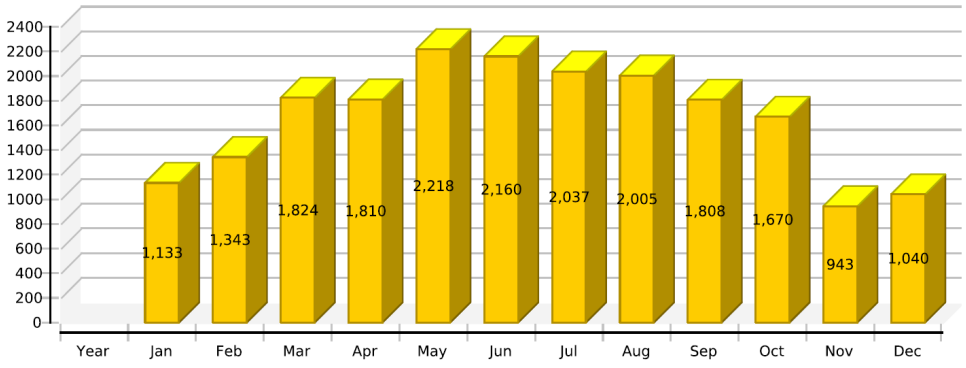

Figure 5.20 Solar thermal energy delivered to the system [kWh]

As previously described waste oil is one of the waste products of hospital kitchen operation, a proper environmental friendly disposal of the waste oil is expensive and relatively complicated therefore a system that enables the waste oil recycling and reusing is completely justified. The principal scheme of the waste oil processing system is shown in Figure 5.21. It employs standard industrial waste oil processor that is available on the market and as a result, a biodiesel fuel is obtained. This biodiesel fuel can be used either for vehicles like emergency vans or for diesel generators in KCV complex that operate during partial or complete power failure.

Figure 5.21 System for bio-diesel production from waste oil

This system offers a viable solution for waste oil disposal as well as for supplying all consumers that require fuel for its operation. It is estimated that the amount of waste oil produced at hospital kitchen is sufficient to ensure a steady amount of waste oil for constant bio fuel production.

When it comes to the KCV complex, and more precisely hospital kitchen the consumption of cooking oil is estimated to be between 150 and 160 liter per month. At the same time this is roughly the amount of the waste oil that is generated on monthly bases that if not recycled must be properly stored or disposed. Therefore recycling of the waste oil and converting it to biodiesel has two fold positive impact which is firstly elimination of the necessity for storage of expensive and complicated disposal procedures and secondly replacing the regular diesel fuel that is used on daily bases in KCV with more environmental friendly biodiesel.

The amount of the biodiesel produced is sufficient for normal operation of the backup generators with the power of the 2x250 kW.

5.3. FERIT renewable energy systems

According to the analysis of the renewables potential of the exemplary objects of the FERIT, following systems are going to be constituted:

- 80 kW photovoltaic (PV) systems in Trpimirova street consisting of 75 kW PV system on the roof/wall of building and 5 kW PV based e-bike charging station in the yard
- 40 kW PV systems in Cara Hadrijana street consisting of 35 kW PV system on the roof/wall of building and 5 kW PV based e-bike charging station in the yard
- Minimally 20 kW renewable energy storage/supply system in building in Trpimirova street;
- 6 kW wind energy system in building yard in Trpimirova street;

5.3.1. Photovoltaic systems on the buildings roofs

PV systems utilize solar irradiation for direct conversion of solar energy into electricity. There are two basic elements of PV systems, PV array and inverter on which PV modules are connected.

PV array consists of series-parallel connected PV modules which topology depends on the size of the array and inverter characteristics. Since output of the PV modules is DC electricity, in order to integrate PV systems into AC power grid, converter unit is necessary. This unit is called inverter which is power electronics device that converts DC electricity into AC electricity suitable for the power grid. The DC cables that connect PV strings with the inverters are planned for external mounting. Other electrical equipment such as protective and switching devices are placed inside the distribution board. The point between the board and the distribution power grid is called the point of common coupling (PCC) and the voltage level in the PCC is 0.4 kV.

Proposed PV systems for FERIT project partner have nominal power of 120 kW. This power will be distributed on two FERIT buildings roofs located in Trpimirova and Cara Hadrijana street. Preliminary design of the systems proposed that system with nominal power of around 80 kW will be installed on building in Trpimirova street and around 40 kW on building in Cara Hadrijana.

80 kW PV systems in Trpimirova street

75 kW PV system is planned to be installed on South-oriented roof/wall surfaces on different angles, depending on the roof/wall section. Azimuth of the building is 0 ° (South is reference). Tilt angle of the roof section on which PV modules will be installed varies from 20 ° to 30°. Block diagram of 75 kW PV system is given in Figure 5.22 while 3D model of the system is given in Figure 5.23.

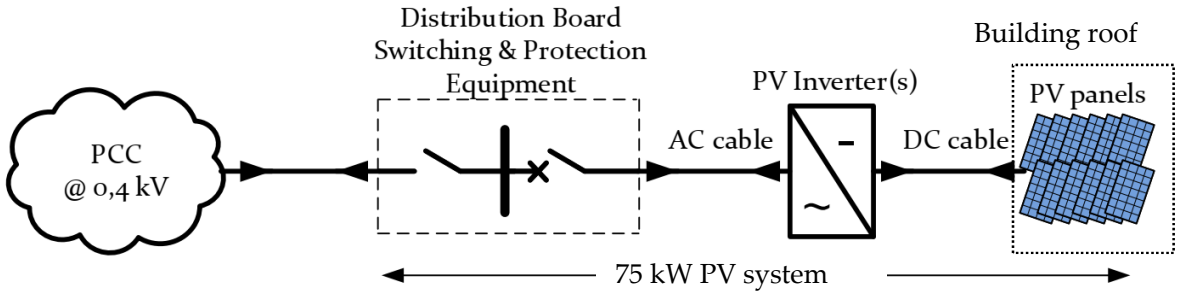

Figure 5.22 Block diagram of 75 kW PV system on building in Trpimirova street

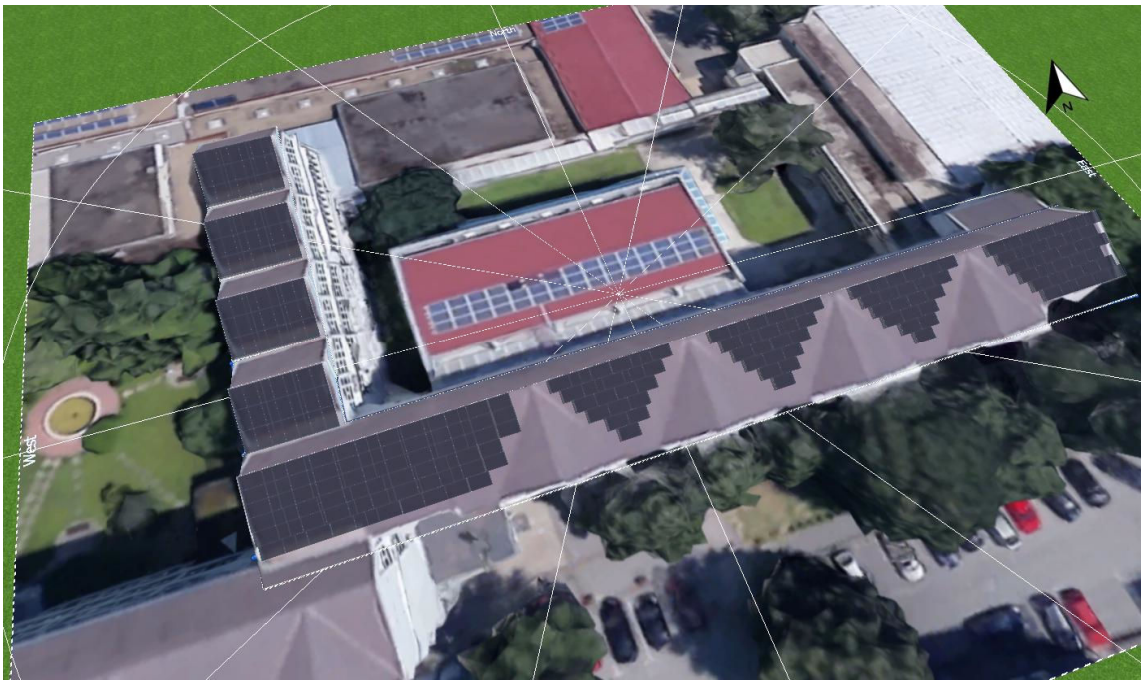

Figure 5.23 Preliminary 3D model of 75 kW PV system on building roof in Trpimirova street (with possible wall-mounted modules depending on roof shading)

The global e-bike market is expected to grow at a CAGR of 6.39%, during the forecast period, i.e. 2019-2024, according to [25]. Apart from the growing consumer preference toward recreational and adventure activities, the adoption of e-bike applications in several sectors, like logistics and e-bike rental services, is expected to drive the market studied during the forecast period. This is affordable and efficient transportation to the masses. Assuming that the number of electric bicycles is going to grow and considering that there is a large number of students and employees at the Faculty that may use this attractive technology, electric bike and assistive device (such as mobile phone) charging station is going to be constructed. This charging station is powered with solar energy and eco-friendly.

The e-bike charging station is going to be a part of 80 kW PV system located at the building in Trpimirova street. PV panels are going to be placed on a charging station roof since it is aesthetically attractive, enhances the landscape and architecture and yet behaves as a functional power generator.

The installed power of the PV based e-bike charging station is 5 kW and will be mounted on PV trackers in order to maximize PV electricity production during working hours. The block diagram of this system is depicted in Figure 5.24.

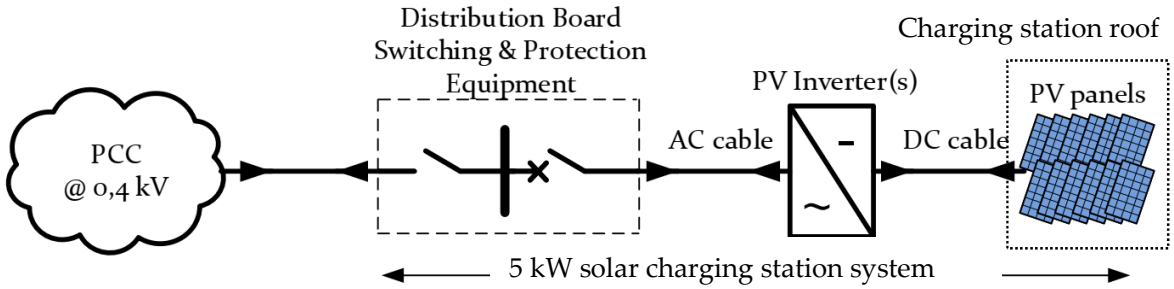

Figure 5.24 Block diagram of 5 kW PV based e-bike charging station.

The PV system is directly connected to the inverter unit that transforms the DC voltage from the output of PV panels placed on the solar tree to AC voltage. Electrical equipment such as protective and switching devices are placed inside the distribution board. The voltage level in the PCC is 0.4 kV.

If we assume to use monocrystalline silicon modules SUNCECO SEM 300W-HE, which technical characteristics are given in Table 5.3, for the PV modules of the system, PV array will consists of around 267 PV modules with nominal power of 300 W which results in total output power of 80.1 kW at the DC side of the system.

Table 5.3 – Technical characteristics of PV modules [26].

SUNCECO SEM 300W-HE			
Nominal power	P_{max}	300	W
Maximum power point voltage	U_{MPP}	32.9	V
Maximum power point current	U_{MPP}	9.12	A
Short-circuit current	U_{OC}	9.58	A
Open-circuit voltage	I_{SC}	39.7	V
Efficiency	η	18.3	%
Maximum system voltage		1000	V
Dimensions		1650 x 992 x 35	mm
Weight		18,5	kg
Operating temperature		-40 do +85	°C
Number of cells		60	pcs.

Based on Solar energy potential for Osijek, monthly forecast of electricity production for 80 kW (75 kW + 5 kW) PV systems is determined using PVSOL Premium software package and given in Figure 5.25. Total annual production of the PV system is around 95 MWh.

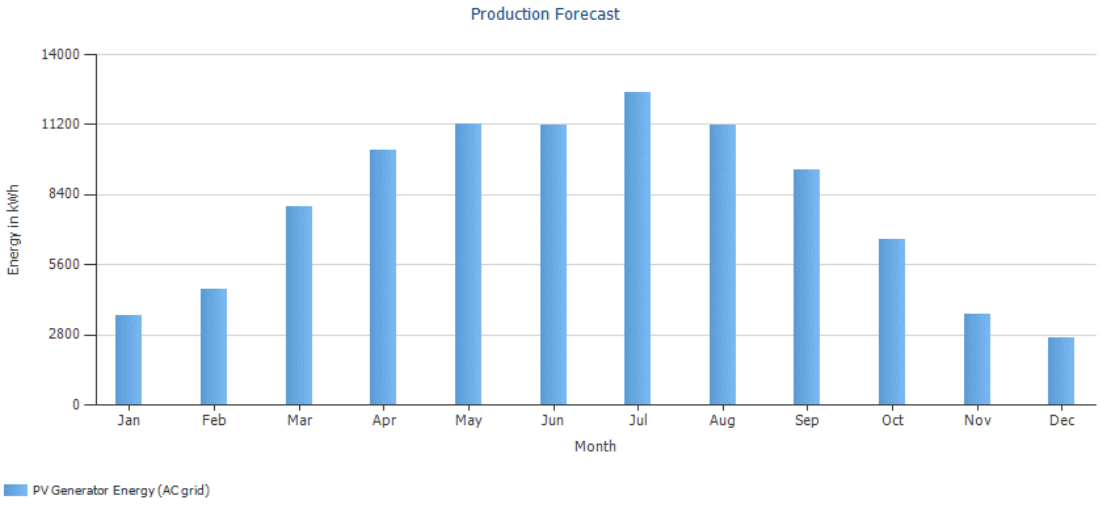

Figure 5.25 Estimated electricity production of 80 kW PV systems on building in Trpimirova street

40 kW PV system on building in Cara Hadrijana street

35 kW PV system is planned to be installed on South-oriented roof surfaces on different angles, depending on the roof section. Azimuth of the building is 19 ° to West (South is reference). Tilt angle of the roof section on which PV modules will be installed varies from 0 ° to 20°. Block diagram of 35 kW PV system is given in Figure 5.26 while 3D model of the system is given in Figure 5.27.

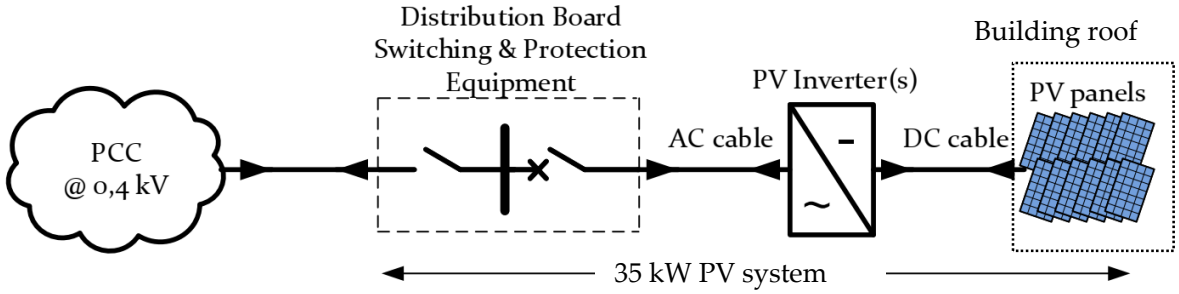

Figure 5.26 Block diagram of 35 kW PV system on building in Cara Hadrijana street

Figure 5.27 Preliminary 3D model of 35 kW PV system on building roof in Cara Hadrijana street

Similar to PV system in Trpimirova street, the e-bike charging station is going to be a part of 40 kW PV system located at the building in Cara Hadrijana street. PV panels are going to be placed on a charging station roof since it is aesthetically attractive, enhances the landscape and architecture and yet behaves as a functional power generator.

The installed power of the PV based e-bike charging station is 5 kW and will be mounted on PV trackers in order to maximize PV electricity production during working hours. The block diagram of this system is depicted in Figure 5.28.

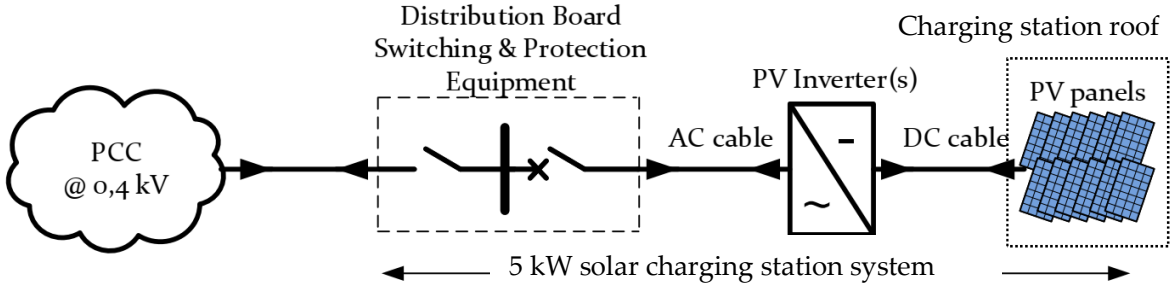

Figure 5.28 Block diagram of 5 kW PV based e-bike charging station.

The PV system is directly connected to the inverter unit that transforms the DC voltage from the output of PV panels placed on the solar tree to AC voltage. Electrical equipment such as protective and switching devices are placed inside the distribution board. The voltage level in the PCC is 0.4 kV.

If we assume to use monocrystalline silicon modules SUNCECO SEM 300W-HE, which technical characteristics are given in Table 5.3, for the PV modules of the system, PV array will consists of around 134 PV modules with nominal power of 300 W which results in total output power of 40.2 kW at the DC side of the system.

Based on Solar energy potential for Osijek, monthly forecast of electricity production for the proposed 40 kW (35 kW + 5 kW) PV systems is determined using PVSOL Premium software package and given in Figure 5.29. Total annual production of the PV system is around 40 MWh.

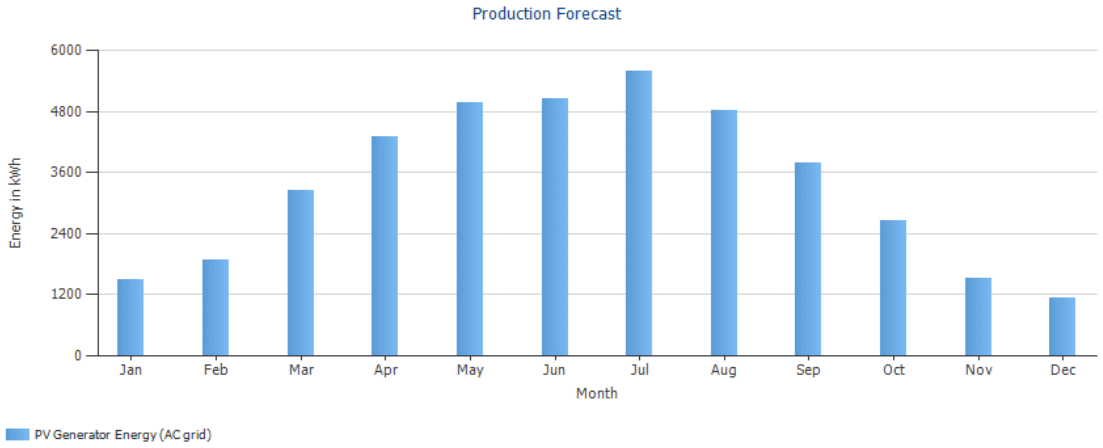

Figure 5.29 Estimated electricity production of 40 kW PV systems on building in Cara Hadrijana street

5.3.2. Renewable energy storage/supply system

Energy storage/supply technologies are used in modern grids in order to enhance the reliability of renewable energy sources, improve the resilience of the grid and resolve its issues, as well as realize the benefits of smart grids and optimizing generation to suit demand. They are usually accompanied by renewable energy sources. Due to the highly intermittent nature of the renewables, sometimes it is possible that consumers do not need all the energy produced by the source or there is not enough energy as required. Therefore, energy storage/supply systems can be used to store energy when the amount generated exceeds the demand and inject power into the system during shortages. Furthermore, they can be used for the peak shaving application, i.e. to cover the peak load.

Therefore, a renewable energy storage/supply system is going to be installed at the exemplary object in Trpimirova street in order to provide stabilizing the power output while also enhancing the reliability of the system. The block diagram of the energy storage/supply system is given in Figure 5.30. The bi-directional power converter is used as an interface between the storage/supply system and the grid. Switching and protection equipment is placed in the distribution board. The installed power of the bi-directional converter used in the system is minimum 20 kW, depending on financial resources of the project. The storage/supply comprises the battery storage system, as well as the supercapacitor system. Batteries present an advanced technique for storing electrical energy in electrochemical form and have a wide range of use. Supercapacitors have a high energy storage capacity due to their high-power ability and since the stored energy has to be used very quickly, they are able to provide peak shaving and thus improve the power profile.

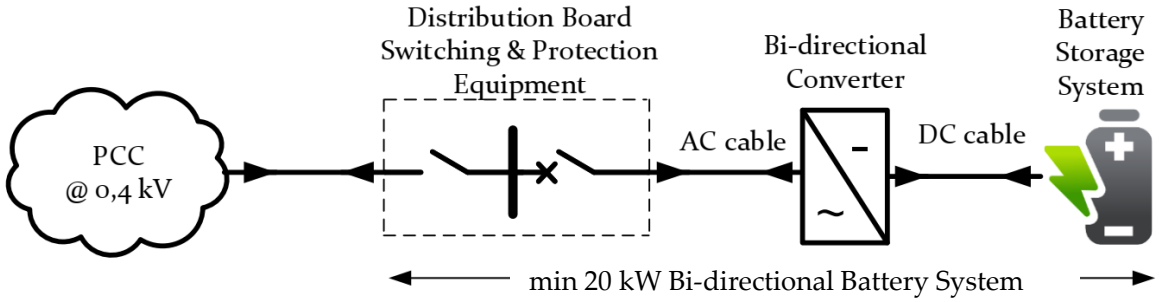

Figure 5.30 Block diagram of the energy storage/supply system.

The battery of the electric vehicles can also be used as a storage/supply unit and can enable different grid support functionalities. This is a state-of-art concept that is very interesting to the researches and certainly could become a new tool for electric utilities in the next decade.

5.3.3. Wind energy system

The exemplary public building is in the region with moderate potential for wind energy development, especially in higher height levels. However, since the area is urbanized, there are limited options when it comes to wind energy due to the surrounding buildings, trees and other obstacles. Another important issue is the size of the wind turbine. Wind turbines can be noisy and require consistent, non-turbulent winds of certain speeds that are uncharacteristic of urban environments. However, due to the technology improvements wind turbines should be self-starting, ultra-quiet, provide smooth torque, and be highly efficient so usable energy can be delivered at modest wind speeds.

Therefore, a small wind power system is planned to be constructed in the yard of the building in Trpimirova street. The installed power of the system is 6 kW. The block diagram of the wind power system is given in Figure 5.31.

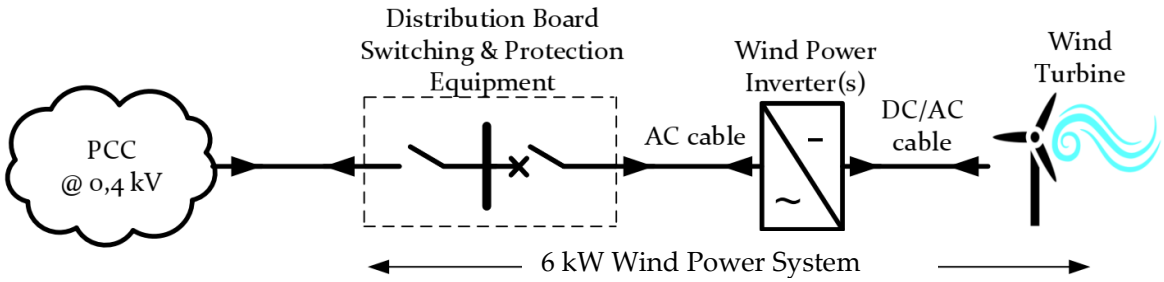

Figure 5.31 Block diagram of the wind power system.

The wind turbine(s) is(are) directly connected to the three-phase inverter unit(s) which transforms the DC voltage from the output of wind turbine to AC voltage. Protective and switching devices are placed inside the distribution board. The voltage level in the PCC is 0.4 kV.

A HOMER Pro software tool [27] is used to estimate the amount of electricity that can be generated by a wind turbine with 6 kW nominal output power and with wind energy potential of Osijek. Monthly forecast of electricity production by such wind energy system is given in Figure 5.32. The prediction is that the energy produced annually is 4.431 MWh.

However, the final decision on number and type of small wind turbine(s) that will be installed with total rated power of 6 kW will be determined depending on market research and availability.

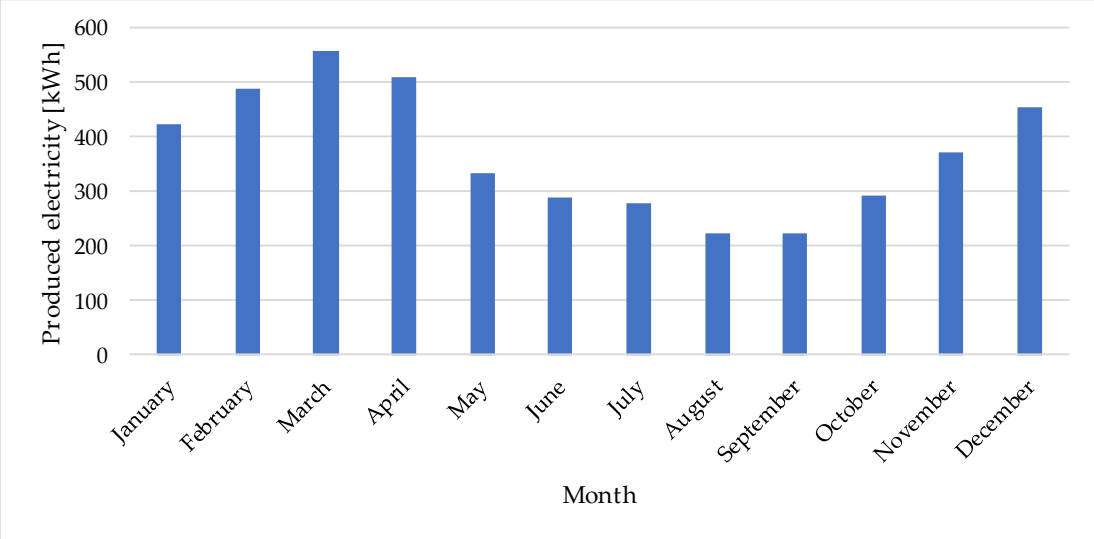

Figure 5.32 Estimated electricity production of 6 kW wind energy system located at the exemplary object in Trpimirova street.

5.4. KBCO renewable energy systems

According to the analysis of the renewables potential of the exemplary objects of KBCO, the following systems are going to be constituted:

- 110 kW photovoltaic (PV) system on the roof of central kitchen;
- 120 kW PV system on the roofs of Department of Oncology and Department of Diagnostical and Interventional Radiology;
- 125 kW biodiesel generator and biodiesel production system for additional 125 kW;

5.4.1. Photovoltaic systems on the buildings roofs

PV systems utilize solar irradiation for direct conversion of solar energy into electricity. There are two basic elements of PV systems, PV array and inverter on which PV modules are connected.

PV array consists of series-parallel connected PV modules which topology depends on the size of the array and inverter characteristics. Since output of the PV modules is DC electricity, in order to integrate PV systems into AC power grid, converter unit is necessary. This unit is called inverter which is power electronics device that converts DC electricity into AC electricity suitable for the power grid. The DC cables that connect PV strings with the inverters are planned for external mounting. Other electrical equipment such as protective and switching devices are placed inside the distribution board. The point between the board and the distribution power grid is called the point of common coupling (PCC) and the voltage level in the PCC is 0.4 kV.

Proposed PV systems for KBCO project partner have nominal power of 230 kW. This power will be distributed on three KBCO buildings roofs located in Huttler street. Preliminary design of the systems proposed that system with nominal power of around 110 kW will be installed on building central kitchen and around 120 kW on buildings of Department of Oncology and Department of Diagnostical and Interventional Radiology.

110 kW PV system on building of central kitchen

110 kW PV system is planned to be installed on horizontal roof surface. Azimuth of the building is 3 ° to East (South is reference). PV modules will be installed under optimal annual inclination angle of 35°. Block diagram of the PV system is given in Figure 5.33 while 3D model of the system is given in Figure 5.34.

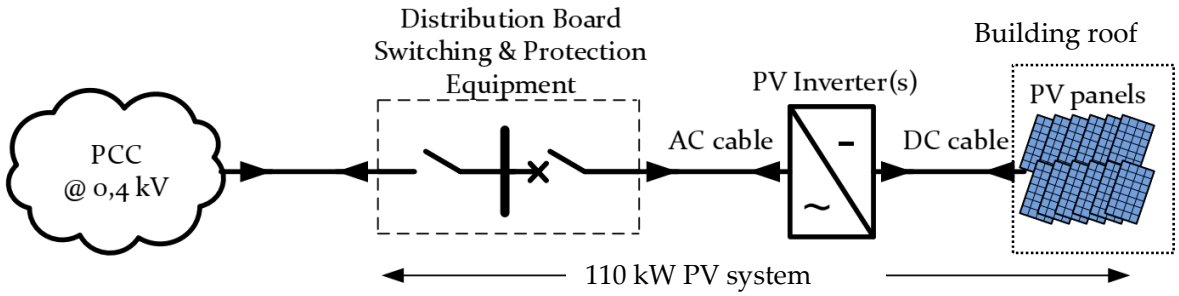

Figure 5.33 Block diagram of the PV systems on building of central kitchen

Figure 5.34 3D model of PV system on building of central kitchen

If we assume to use monocrystalline silicon modules SUNCECO SEM 300W-HE, which technical characteristics are given in Table 5.4, for the PV modules of the system, PV array will consists of around 367 PV modules with nominal power of 300 W which results in total output power of 110.1 kW at the DC side of the system.

Table 5.4 Technical characteristics of PV modules [26].

SUNCECO SEM 300W-HE			
Nominal power	P_{max}	300	W
Maximum power point voltage	U_{MPP}	32.9	V
Maximum power point current	U_{MPP}	9.12	A
Short-circuit current	U_{OC}	9.58	A
Open-circuit voltage	I_{SC}	39.7	V
Efficiency	η	18.3	%
Maximum system voltage		1000	V
Dimensions		1650 x 992 x 35	mm
Weight		18,5	kg
Operating temperature		-40 do +85	°C
Number of cells		60	pcs.

Based on Solar energy potential for Osijek, monthly forecast of electricity production for the proposed PV system is determined using PVSOL Premium software package and given in Figure 5.35. Total annual production of the PV system is around 117 MWh.

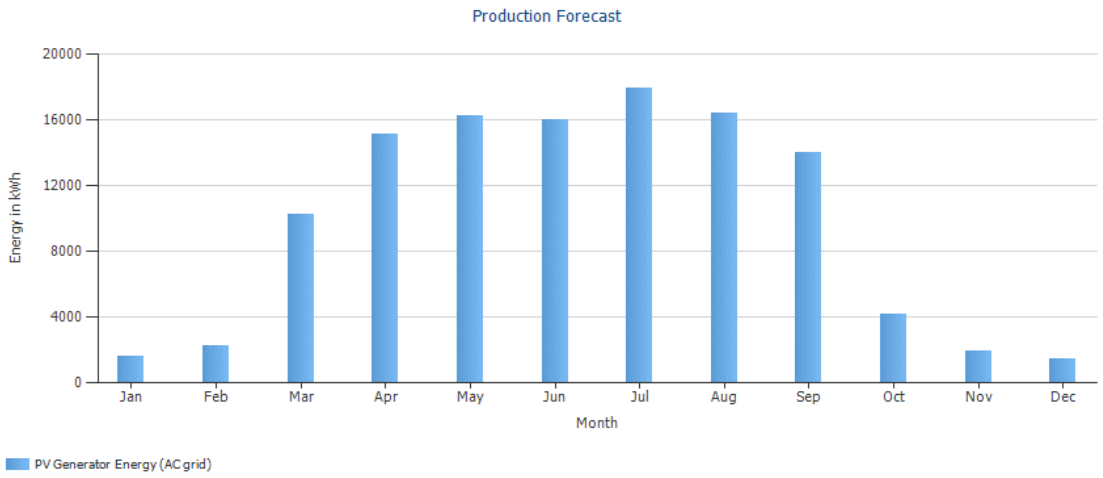

Figure 5.35 Estimated electricity production of 110 kW PV system of central kitchen

120 kW PV system on buildings of Department of Oncology and Department of Diagnostical and Interventional Radiology

120 kW PV system is planned to be installed on roof surfaces on different angles, depending on the roof section. First part of PV array will be installed on horizontal surface

of building of Department of Oncology under optimal inclination angle of 34°. Azimuth of the building is 1° to the West (South is reference). Second part of PV array will be installed on horizontal and tilted surfaces of building of Department of Diagnostical and Interventional Radiology under various tilt angles. Part of the photovoltaic array will be installed on horizontal surface under optimal tilt angle of 34° while the rest will be installed on tilted roof surfaces under 32° tilt angle. Azimuth of the building is 2° to the West (South is reference). Block diagram of the PV system is given in Figure 5.36 while 3D model of the system is given in Figure 5.37.

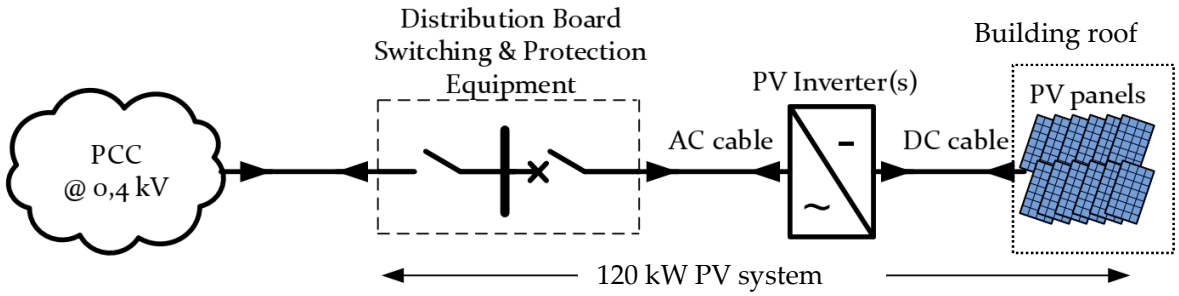

Figure 5.36 Block diagram of the PV system on buildings of Department of Oncology and Department of Diagnostical and Interventional Radiology

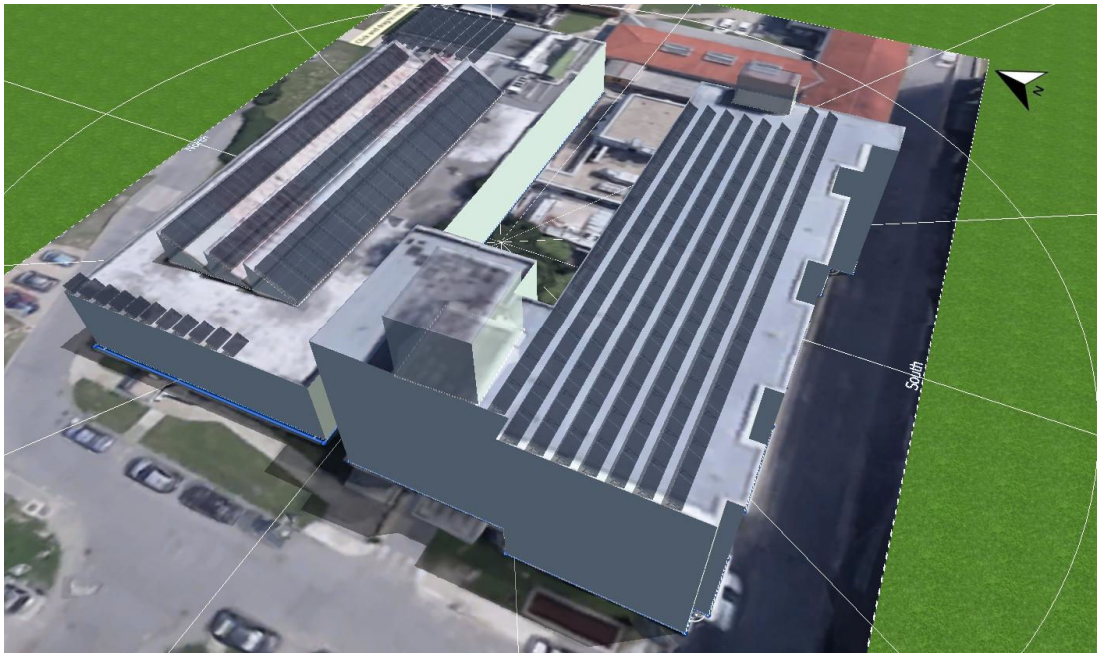

Figure 5.37 3D model of PV system on buildings of Department of Oncology and Department of Diagnostical and Interventional Radiology

If we assume to use monocrystalline silicon modules SUNCECO SEM 300W-HE, which technical characteristics are given in Table 5.4, for the PV modules of the system,

PV array will consists of 400 PV modules with nominal power of 300 W which results in total output power of 120 kW at the DC side of the system.

Based on Solar energy potential for Osijek, monthly forecast of electricity production for the proposed PV system is determined using PVSOL Premium software package and given in Figure 5.38. Total annual production of the PV system is around 130 MWh.

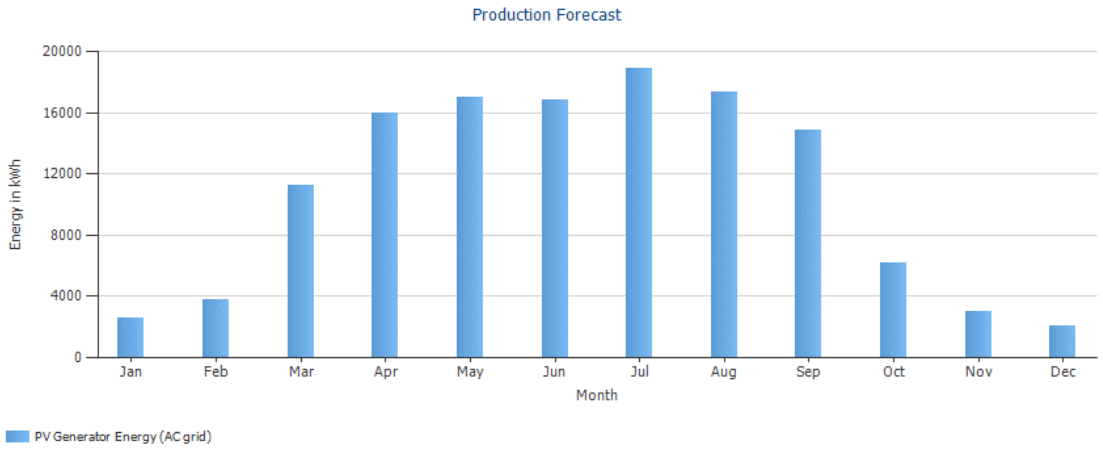

Figure 5.38 Estimated electricity production of PV system on building in Cara Hadrijana street

5.4.2. Biodiesel generator and biodiesel production system

As previously described, waste oil is one of the waste products of KBCO central kitchen operation. Proper environmentally friendly disposal of the waste oil is expensive and relatively complicated, therefore, a system that enables the waste oil recycling and reusing is completely justified. The principal scheme of the waste oil processing system is shown in Figure 5.39. It employs standard industrial waste oil processor that is available on the market and as a result of a biodiesel fuel is obtained. This biodiesel fuel can be used either for vehicles like emergency vans or for diesel and biodiesel generators in KBCO complex that operate during partial of complete blackout of electric power supply.

Figure 5.39 Principal schematic of system for biodiesel production from waste oil

This system offers a viable solution for waste oil disposal as well as for supplying all consumers that require fuel for its operation. It is estimated that the amount of waste oil produced at KBCO central kitchen is enough to ensure a steady amount of waste oil for constant biofuel production.

By analyzing the consumption of cooking oil used by KBCO central kitchen, it has been found out that 1000 liters of waste oil is generated on an annual basis. At the same time, this is roughly the amount of the waste oil that is generated on monthly basis that is not recycled and must be properly stored or disposed. Therefore, recycling of the waste oil and converting it to biodiesel has twofold positive impact which is elimination of necessity for storage of expensive and complicated disposal procedures and replacing the regular diesel fuel that is used on daily basis in KBCO with more environmentally friendly biodiesel fuel.

Furthermore, new 125 kW biodiesel generator will be installed in order to fully utilize biodiesel production potential. Generator will serve as a backup electricity supply during partial or total blackouts. Block diagram of the PV system is given in Figure 5.40.

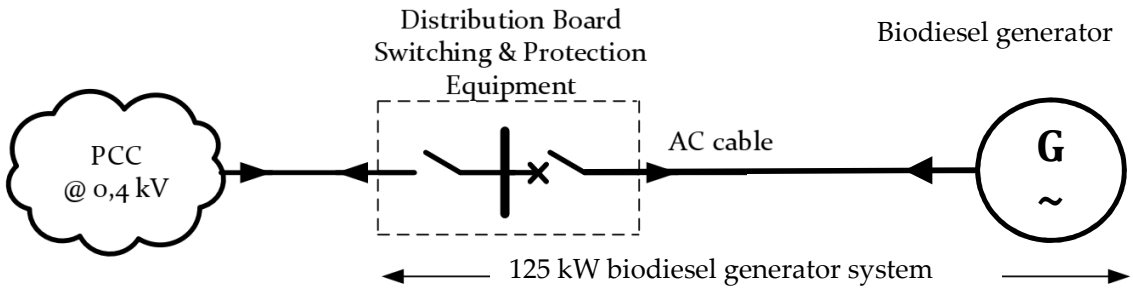

Figure 5.40 Block diagram of biodiesel generator system

5.5. UNISB renewable energy systems

5.5.1. Solar-Thermal systems

In order to increase energy efficiency through the use of renewable energy sources, the construction of a thermo-technical system from hot-water solar collectors, an air-to-water heat pump and a condensation flow apparatus with natural gas propulsion is envisaged. Electricity supply will be provided through a photovoltaic system by absorbing solar radiation. The customized method of installation on the building and the construction of the installation will retain the external architectural form with optimal year-round utilization of external energy potential (outdoor air, solar insulation). The fan / convector will use heat / cooling energy to heating / cooling certain rooms in the building. The installed thermal power of the solar collectors is 25 kW and the heat pumps total ≥ 60 kW at appropriate external microclimate conditions and solar insulation at the location. The

thermotechnical system will be properly dimensioned, thermally and hydraulically balanced with very little heat loss of energy transfer. The maximum hot water temperature will be up to 80° C and the cold water operating mode 7/12°C. Technical connectivity and appropriate drive and control elements and circuits, as well as custom software support, will enable thermo-technical functionality, optimal energy efficiency and monitoring of relevant thermo-technical parameters during use. Consumers' energy needs (thermal / cooling) will be continually adjusted and supplemented according to the available state of the renewable energy source (1. Solar collectors, 2. Heat pump, 3. Gas-fired condensing circulation apparatus), depending on the external microclimatic conditions and solar insolation.

5.5.2. Photovoltaic systems

Photovoltaic systems utilize solar irradiation for direct conversion of solar energy into electricity. There are two basic elements of photovoltaic systems, photovoltaic array and inverter on which photovoltaic modules are connected.

Photovoltaic array consists of series-parallel connected photovoltaic modules which topology depends on the size of the array and inverter characteristics. Since output of the photovoltaic modules is DC electricity, in order to integrate photovoltaic systems into AC power grid, converter unit is necessary. This unit is called inverter which is power electronics device that converts DC electricity into AC electricity suitable for the power grid.

Proposed roof photovoltaic systems for UNISB project partner have minimum nominal power of 60-64 kW. This power will be distributed on UNISB building located in Ivan Gundulić Street. This system will be described in this section. Final distribution of power and topology of the photovoltaic systems will be determined in the main electrical engineering project.

Mostly, PV modules will be mounted on the south side of the roof of the object. One section of the PV modules will be added to façade of the building and one section will be on tracker construction in the yard of the building.

Photovoltaic system is planned to be installed on South-oriented roof surfaces on different angles, depending on the roof section. Azimuth of the building is 0° (South is reference). Tilt angle of the roof section on which photovoltaic modules will be installed varies from 14° (roof) to 61° (façade). Conceptual design of the roof PV system proposed nominal output power of photovoltaic array of 60-64 kW while nominal output power of the inverters is approximately 65 kW. Total area of photovoltaic array is 407 m^2. 3D model of the proposed photovoltaic system is given in Figure 5.41.

Figure 5.41 3D model of photovoltaic and solar-thermal system on building in I. Gundulić Street

Photovoltaic roof arrays consist of approximately 200-220 photovoltaic modules with nominal power of 300 - 320 W which results in total output power of 60 - 64 kW at the DC side of the system. Façade PV system consists of 20 modules.

Proposed photovoltaic modules are monocrystalline silicon modules SUNCECO SEM 300W-HE which technical characteristics are given in Table 5.5.

Table 5.5 Technical characteristics of photovoltaic modules SUNCECO SEM 300W-HE

SUNCECO SEM 300W-HE			
Nominal power	P_{max}	300	W
Maximum power point voltage	U_{MPP}	32,9	V
Maximum power point current	U_{MPP}	9,12	A
Short-circuit current	U_{OC}	9,58	A
Open-circuit voltage	I_{SC}	39,7	V
Efficiency	η	18,3	%
Maximum system voltage		1000	V
Dimensions		1650 x 992 x 35	mm
Weight		18,5	kg
Operating temperature		-40 do +85	°C
Number of cells		60	pcs.

Conceptual design of the roof system proposed that photovoltaic array consists of 8 photovoltaic strings connected to 4 equally rated inverters. Each inverter has two photovoltaic strings connected at its inputs. Six photovoltaic strings consist of 22 series-connected photovoltaic modules installed on 4 equal roof surfaces at 14° angle. Last two photovoltaic strings consist of 2 parallel-connected branches of 22 and 23 series-connected photovoltaic modules. During the design of photovoltaic array, technical characteristics of the inverters are considered as well as lowest possible probability of shading occurrence during the year. Facade PV system consists of a string with 20 series connected PV modules and inverter 10 kW.

5.6. Building energy management systems

Building energy management system represents superior control and management system for sources of electricity alongside with electric loads into one fully controllable unit. This is realised with Supervisory Control and Data Acquisition System (SCADA) which is computer-based system for control and management of processes. In our case, sources of electricity are renewable energy-based while the electric loads represent building loads. In the area of electrical engineering, this unit represents microgrid which is an emerging concept while its SCADA system represents its superior control and management system.

SCADA system consists of fully coordinated ICT systems that supervise and control every element in the microgrid.

Basic block diagram of building energy management system for FTN buildings is given in Figure 5.42, for KCV buildings in Figure 5.43, for FERIT building in Trpimirova street in Figure 5.44, for KBCO buildings in Figure 5.45 while for UNISB.

At the PCC point of all of these systems smart meters will be placed and collect information about electrical quantities and consequently reconstruct the power quality, production and consumption. Sensing devices are going to be placed in all systems to monitor environmental variables such as solar irradiance, temperature, humidity, air speed and direction, etc. This data is sent to the BEMS system and processed. Based on all inputs, BEMS provides outputs – control signals for controllers so that the automation of all ongoing processes is possible regarding the energy efficiency maximization. In this manner, the maximal energy efficiency should be realized, as well as optimal and coordinate operation of all units.

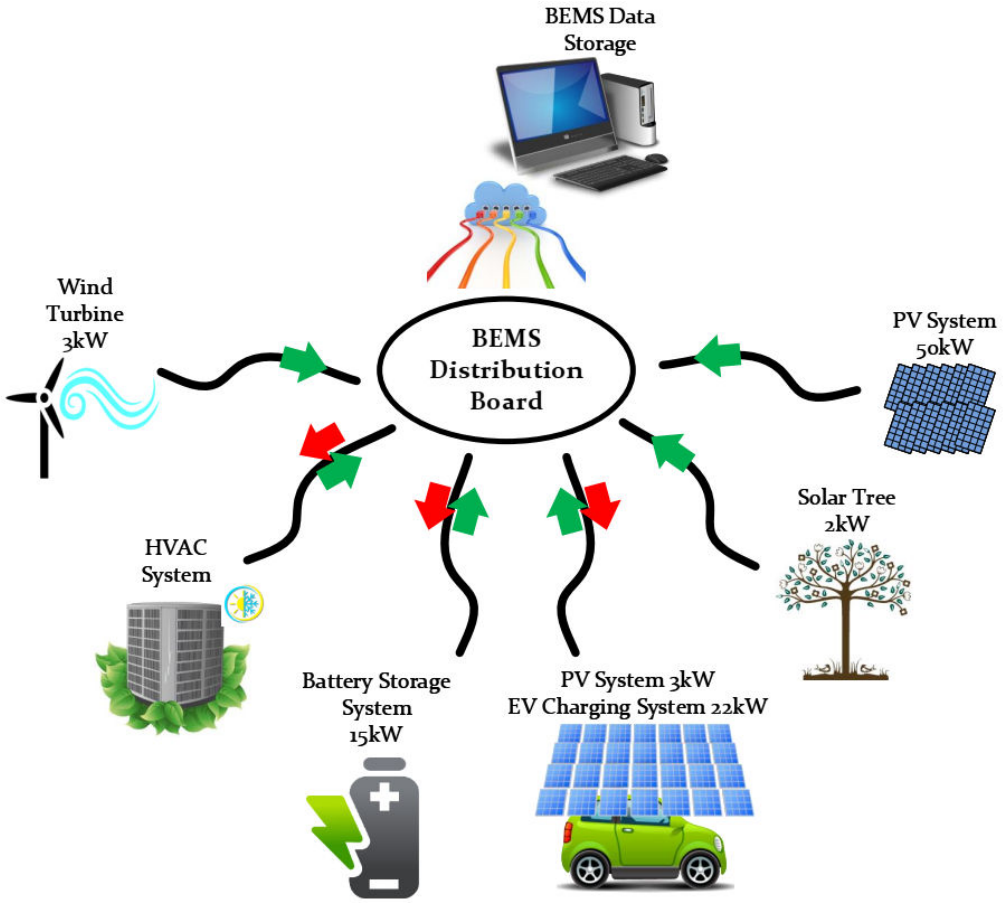

Figure 5.42 Basic block diagram of building energy management system for FTN

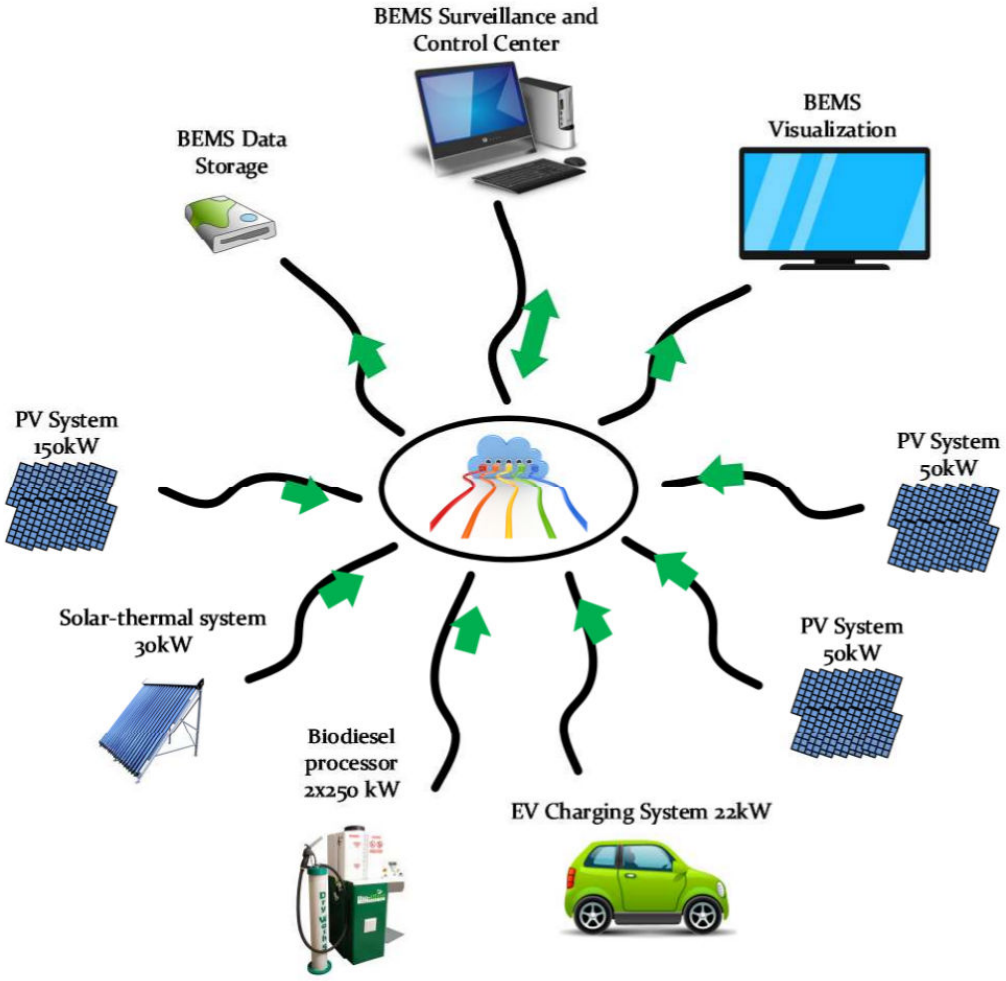

Figure 5.43 Basic block diagram of building energy management system for KCV

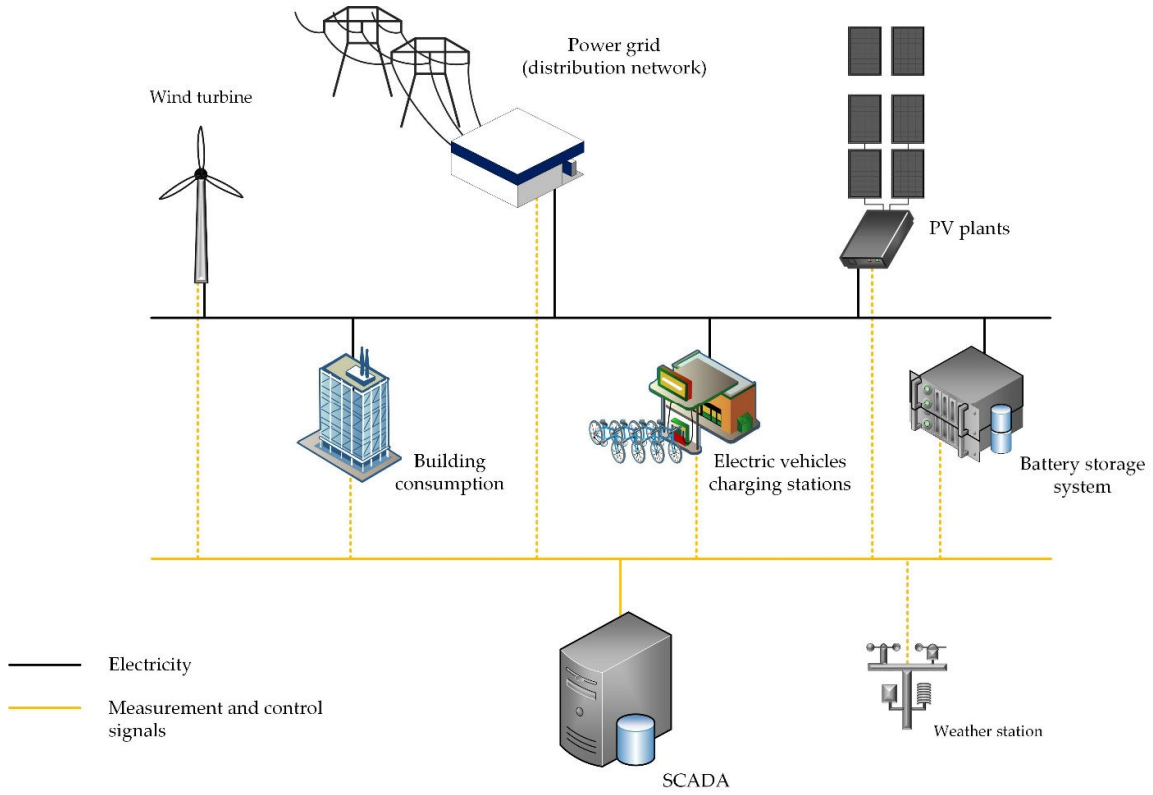

Figure 5.44 Basic block diagram of building energy management system for FERIT building in Trpimirova street

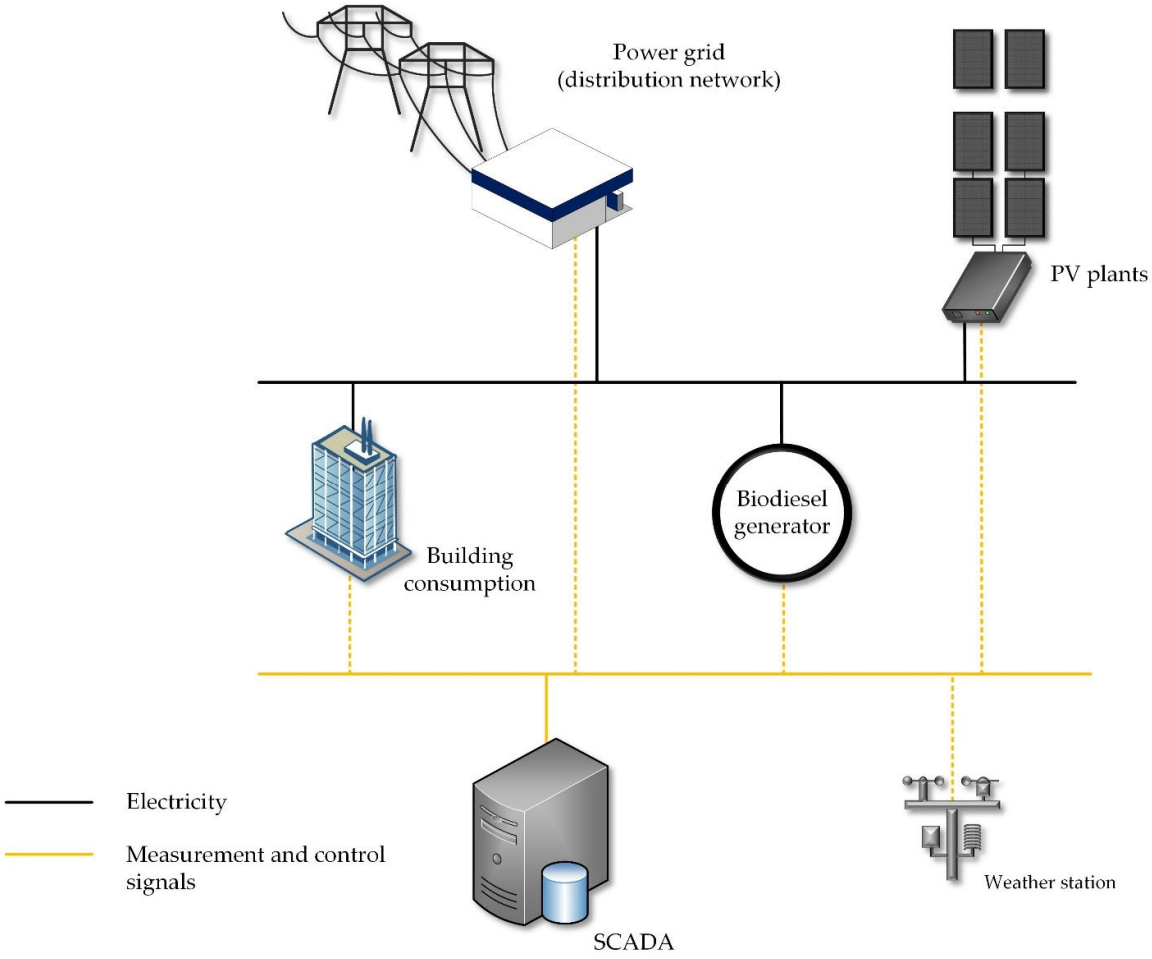

Figure 5.45 Basic block diagram of KBCO building energy management system

6. Installed renewable energy systems for the exemplary facilities

6.1. FTN renewable energy systems

In accordance with described renewable energy potential given in section 4.1 and renewable energy implementation plan presented in section 5.1**Error! Reference source not found.**, the following systems have been installed:

- Photovoltaic system;
- Solar tree;
- Photovoltaic based electric vehicle charging station;
- Renewable energy storage/supply system;
- Wind energy system;
- Heating, ventilation and air conditioning (HVAC) system.

6.1.1. Photovoltaic system

A photovoltaic system is installed on the rooftop of one of the sectors of the “Masinski institut” building, shown in Figure 6.1 .

Figure 6.1 PV plant on the rooftop of the FTN building

PV strings, i.e. a series of the PV panels, are directly connected to three-phase inverter unit. There are 180 PV panels Luxor Solar LX-285P in total, with the peak power 285 Wp. Table 6.1 shows technical data related to the selected PV moduls.

Table 6.1 PV modules technical data

Electrical data at STC	
Rated power Pmpp [Wp]	285.00

Pmpp range to	291.49
Rated current Impp [A]	8.94
Rated voltage Vmpp [V]	31.92
Short-circuit current Isc [A]	9.46
Open-circuit voltage Uoc [V]	39.17
Efficiency at STC up to	17.54%
Efficiency at 200 W/m2	16.96%
Electrical data at NOCT	
Power at Pmpp [Wp]	211.77
Rated current Impp [A]	7.15
Rated voltage Vmpp [V]	29.61
Short-circuit current Isc [A]	7.64
Open-circuit voltage Uoc [V]	36.17
Limiting values	
Max. system voltage [V]	1000 V oder 1500 V
Max. return current [I]	25 A
Operating Temperature	- 40 to 85°C
Safety class	II
Max. tested pressure load [Pa]2	5400
Max. tested tensile load [Pa]2	2400

The ABB solar inverter PVS-50-TL has built-in DC/DC converters with the algorithm for the maximum power point tracking. The installed inverter is depicted in Figure 6.2.

Figure 6.2 ABB solar inverter

Technical data of the ABB solar inverter is summarized in Table 6.2.

Table 6.2 ABB PVS-50-TL solar inverter technical characteristics

Table: Technical Data	PVS-50-TL
Input	
Absolute Maximum Input Voltage (Vmax,abs)	1000 V
Input start-up voltage (Vstart)	420…700 V (default 420 V)
DC Input operating interval (Vdcmin...Vdcmax)	0.7xVstart ...950 V (min 300 V)
Rated DC Input Voltage (Vdcr)	610 Vdc
DC Input Nominal Power(Pdcr)	52000 W
Number of Independent MPPT	3 (-SX and -SX2 version) / 1 (standard and -S version)
Max DC Input power for each MPPT (PMPPT,max)	19300W@30°C/17500 W@45°C
MPPT DC Voltage Range (VMPPTmin ... VMPPTmax) to Pacr	480-800 Vdc
Maximum DC Input Current (Idcmax) for each MPPT	36 A
Maximum Return current (AC side vs DC side)	Negligible in normal operating conditions (3)
Max short circuit current (Iscmax) for each MPPT	55 A (165A in case of parallel MPPTs)
Number of DC Connection Pairs for each MPPT	5 (-SX and -SX2 versions)
Type of Input DC Connectors	Screw terminal block max. cross-section 95mm2 (Standard and -S version) PV quick fit connector (4) (-SX and -SX2 version)
Type of photovoltaic panels that can be connected at input according to IEC 61730	Class A
Input protection	
Reverse Polarity Protection	Yes, from current limited source
Input overvoltage protection for each MPPT - SPD	Yes, 1 for each MPPT
Input overvoltage protection for each MPPT - surge arrester	Type II/Type I+II (optional)
Isolation Check	Complying with the local standard
Characteristics of DC disconnect switch for each MPPT (versions with	1000 V / 60 A for each MPPT (180 A in case of parallel MPPTs)

DC disconnect switch)	
String fuses (-SX/-SX2 versions)	15A (gPV / 1000Vdc) (6)
Output	
AC Connection to the grid	3W + GND (no N connection) or 4W + GND (with N connection), Grounded WYE system only
Nominal AC Output Power (Pacr @cosφ=1)	50000 W
Maximum AC Output Power (Pacmax @cosφ=1)	55000 W up to 30°C
Maximum apparent Output power (Smax)	55000 VA up to 30°C
Rated AC Output Voltage (Vacr)	400 V
Output voltage range (Vacmin...Vacmax)	320...480 V (1)
Maximum output current (Iacmax)	80 A
Contribution to short-circuit current	92 A
Rated Output Frequency (fr)	50 Hz / 60 Hz
Output Frequency Range (fmin...fmax)	47...53 Hz / 57…63 Hz (2)
Nominal power factor and setting interval	> 0.995, 0...1 inductive/capacitive with maximum Smax
Total harmonic distortion of current	<3%
Max AC cable cross section accepted	95 mm2 copper copper/aluminum
AC Connections Type	Screw terminal block - single AC cable gland M63
Output protection	
Anti-islanding Protection	Complying with the local standard (active frequency drift combined with RoCoF techniques)
Maximum external AC overcurrent protection	100 A
Output overvoltage protection - SPD	Yes
Table: Technical Data	PVS-50-TL
Output overvoltage protection - Modular surge arrester	Type II
Operating performance	
Maximum Efficiency (ηmax)	98.4%
Weighted Efficiency (EURO/CEC)	98.2% / -
Communication	

Embedded communication interface	2x RS485, 2x Ethernet (RJ45), WLAN (IEEE802.11 b/g/n @ 2,4 GHz)
Communication protocol	Modbus RTU / TCP (Sunspec compliant); Aurora Protocol
Remote Monitoring services	Standard level access to Aurora Vision monitoring portal
Advanced features	Integrated Web User Interface; Display (option); Embedded logging and direct transferring of data to Cloud
Environmental	
Ambient temperature range	-25...+60°C (-13...140°F) with derating over 45°C (113°F)
Relative Humidity	4…100 % condensing
Typical noise emission pressure	75 dB(A) @ 1 m
Maximum operating altitude	4000 m (13123 ft) with derating above 2000 m / 6561 ft
Environmental pollution degree classification for external environments	3
Environmental class	Outdoor
Physical	
Environmental Protection Rating	IP 65 (IP54 for the cooling section)
Cooling System	Forced air
Dimensions (H x W x D)	750 mm x 1100 mm x 257 mm / 29.5” x 43.3” x 10.12”
Weight	70 kg / 154 lbs (SX version)
Assembly System	Mounting bracket (vertical or horizontal)
Overvoltage rating as per IEC 62109-1	II (DC input) III (AC output)
Safety	
Safety class	I
Isolation Level	Transformerless (TL)
CE Marking	CE (5)
Safety and EMC Standards	IEC/EN 62109-1, IEC/EN 62109-2, EN 61000-6-2, EN 61000-6-3, EN 61000-3-11, EN 61000-3-12
Grid standard (check the availability with your sales channel)	CEI 0-21, CEI 0-16, DIN V VDE V 0126-1-1, VDE-AR-N 4105, G59/3, EN 50438 (not for all national appendices), RD 1699, RD 413, RD 661, P.O. 12.3, AS 4777, BDEW, NRS-097-2-1, MEA, PEA, IEC 61727, IEC 60068, IEC 61683, VFR-2014, IEC 62116
Accessories	
PVS-50/60-GROUNDING KIT	Allows to connect the negative input pole to ground
DISPLAY	Display is available as optional by dedicated part

	number

6.1.2. Solar tree

The installed power of the solar tree system is 2 kW. Installed solar tree is depicted in Figure 6.3.

Figure 6.3 Installed solar tree

The solar tree is directly connected to the inverter unit GROWATT mic3000tl-x (shown in Figure 6.4) that transforms the DC voltage from the output of PV panels placed on the solar tree to AC voltage. Electrical equipment such as protective and switching devices is placed inside the distribution board. The voltage level in the PCC is 0.4 kV. The technical specification of the used PV panels is given in Table 6.3.

Figure 6.4 GROWATT mic3000tl-x inverter

Table 6.3 Technical specification for PV modules used to build the solar tree

Peak Power (PMP)	40Wp
Production Tolerance	±3%
Open-Circuit Voltage (VOC)	21.6V
Maximum Power Current(IMP)	2.2A
Short-Circuit Current (ISC)	2.3A
Maximum Power Voltage (VMP)	18.0V
Maximum System Voltage	1000VDC
Cell Technology	monocrystalline silicon
Module Dimension	540x510x18mm
Module	MONO
Name	M-40Wp
Cell area (mm)	125*125(mm)
Cell parallel	4*9
Ambient temp (℃)	25℃
Irradiance (W/m2))	1000(W/㎡)
Vmp (V)	18.00V
Power current (IMP)	2.20 A
Voc (V)	21.60V
Short circuit current	2.30A
Peak power	48. 3Wp
F.F	75.7686
Module eff.(%)	17.6%
Est.series resistance (ohm)	0.1665Ω
V_Load (V)	19.80V

The technical specification of the used inverter is given in 0.

Table 6.4 Technical specification for inverter unit within solar tree system

Input	
Maximum input power	4200W
Maximum DC voltage	550V
MPPT voltage range	65V-550V /360V
Maximum input current per MPPT	13A
Maximum short-circuit current per MPPT	16A
Number of MPPTs/inputs per MPPT	1/1
Output	
Nominal AC active power output	3000W
Maximum AC apparent power output	3000VA
Maximum AC output current	14.3A
Nominal voltage	Default: 240V split phase, optional: 208V & 240V single-phase, 183-228@208V 211-264@240V
Frequency range	50Hz/60Hz,±5Hz
Power factor range	0.8 leading 0.8 lagging
THDi	<3%
Connection	Single-phase
Efficiency	
Maximum efficiency	97.60%
European efficiency	97.10%
General data	
Dimensions	74/254/138mm
Mass	6.2kg
Temperature range	–25°C ... +60°C(-13 +140°F)
Protection	IP65

6.1.3. Photovoltaic based electric vehicle charging station

The charging station is powered by a PV system on the rooftop of the station and shown in Figure 6.5.

Figure 6.5 Solar powered EV charging station

The installed power of the EV charging station is 3 kW. The EV charger is a ABB power converter with a nominal power of 22 kW, shown in Figure 6.6. Technical data related to the ABB charger are listed in Figure 6.7.

Figure 6.6 EV charger

General Information

Extended Product Type	TAC-W22-G5-R-C-0
Product ID	6AGC082157
ABB Type Designation	Terra AC
EAN	8719874450959
Alternative Product Reference	3Q510002000A
Catalog Description	TAC-W22-G5-R-C-0 Terra AC wallbox type 2, cable 5m, three phase/32A, with RFID and 4G
Long Description	TAC-W22-G5-R-C-0 AC wallbox type 2, cable 5m, three phase/32A, with RFID and 4G

Technical

EV Connectors	(AC Type 2) 1 piece
Number of Socket Outlets	No socket outlet
Cable Length	5 m
Output Power	AC 22 kW
Output Voltage (U_{out})	AC 3-phase 380 ... 415 V
Output Current	3 phase 32 A
Connection Power	Nominal 22 kW
Supply Voltage	AC 3-phase 380 ... 415 V
Input Current	3 phase 32 A
Operating Frequency (f_{sw})	50 ... 60 Hz
Number of Phases	3
Connection Configuration	TT, TN
Number of RCDs Electric Vehicle Supply Equipment	Resid. Curr. Monitor
Number of Miniature Circuit Breakers (MCBs)	0
Overvoltage Category	III
Overload Protection	Overcurrent protection at 40 A
Ambient Air Temperature	Operation -30 ... +50 °C Storage -50 ... +80 °C
Maximum Operating Altitude Permissible	2000 m
Communication Interface	Wi-Fi Bluetooth 4G
Authentication Method	RFID
Energy Meter Type	AC
Enclosure Type	indoor, outdoor
Mounting Type	Wall mounting
Degree of Protection	acc. to IEC 60529 IP54
Impact Resistance Rating	IK08

Figure 6.7 EV charger technical data

PV system used to power an electric vehicle is directly connected to the Fronius SYMO inverter unit, shown in Figure 6.8. The voltage level of the point of common coupling is 0.4 kV.

Figure 6.8 The inverter unit that connects PV system for EV charging station to the grid

6.1.4. Renewable energy storage/supply system

The storage/supply comprises the battery storage system (Victron 12,8V, 220Ah Lithium-Iron-Phosphate Battery) and the supercapacitor system.

Custom-made bi-directional power converter is used as an interface between the storage/supply system and the grid. The installed power of the bi-directional converter used in the system is 35 kW. Supercapacitors and battery are depicted in Figure 6.9 and Figure 6.10, respectively, while all important technical data are presented in 0 and 0.

Figure 6.9 Supercapacitors within storage-supply system

Table 6.5 Technical data about supercapacitor system

Symbol	Parameter	Conditions	Min	Typical	Max	Unit
Electrical						
C_R	Initial Rated Capacitance	Note 1	5.8	6.1	–	F
	Initial Capacitance Range/Box	3 modules per box	–	±0.05	–	F
R_S	Initial Equivalent Series Resistance (ESR)	Note 1	–	188	240	mΩ
V_R	Maximum Rated Voltage		–	–	160	V
V_{MAX}	Absolute Maximum Voltage	Non-repeated. Not to exceed 1 second	–	170	–	V
–	Maximum String Voltage	For series of modules	–	750	–	V
I_{DCMAX}	Maximum Continuous Current	$\Delta T_{CELL} = I_{RMS} \times R_S \times R_{th}$ - ΔT = 15°C - ΔT = 40°C	– –	7 12	– –	A_{RMS}
I_{ACMAX}	Maximum Peak Current		–	170	–	A
I_{SHORT}	Short Circuit Current	Calculated from V_R and R_S Do not use as operating current	–	670	–	A
I_{LEAK}	Leakage Current	After 72 hours at 25°C	–	–	25	mA
Life						
t_{AGING}	Accelerated Aging	At V_R = 160V and T_A = 65°C (Note 1) Capacitance change ΔC from C_R Resistance change ΔR from R_S	– – –	2,000 20 100	– – –	hours % %
t_{LIFE}	Projected Life Time	At V_R = 160V and T_A = 25°C (Note 1) Capacitance change ΔC from C_R Resistance change ΔR from R_S	– – –	10 20 100	– – –	years % %
n_{LIFE}	Projected Cycle Life	At V_R = 160V and T_A = 25°C (Note 1) Capacitance change ΔC from C_R Resistance change ΔR from R_S	– – –	500,000 20 100	– – –	cycles % %
t_{SHELF}	Shelf Life	Stored uncharged at 25°C	–	4	–	years
Power & energy						

P_d	Usable Specific Power	Per IEC 62391-2, $P_d = \frac{0.12 \cdot V^2}{ESR_{DC0} \cdot Mass}$	–	2,500	–	W/kg
P_{MAX}	Impedance Match Specific Power	$P_{MAX} = \frac{V^2}{4 \cdot ESR_{DC0} \cdot Mass}$	–	5,200	–	W/kg
E_{MAX}	Specific Energy	$E_{MAX} = \frac{\frac{1}{2}CV^2}{3{,}600 \cdot Mass}$	–	4.0	–	Wh/kg
E_{STORED}	Stored Energy	$E_{STORED} = \frac{\frac{1}{2}CV^2}{3{,}600}$	–	20.6	–	Wh
Temperature						
T_A	Operating Temperature	Cell Case Temperature	-40	–	65	°C
T_{STG}	Storage Temperature	Stored Uncharged @< 50% Relative humidity (RH)	–	–	25	°C
R_{th}	Thermal Resistance		–	1.1	–	°C/W
C_{th}	Thermal Capacitance		–	4,800	–	J/°C
–	Cooling		Natural Convection			–

Figure 6.10 Battery within storage-supply system

Technical data regarding battery operation are shown in 0.

Table 6.6 Technical data about battery system.

Battery specification	
VOLTAGE AND CAPACITY	LFP- Smart 12,8/200
Nominal voltage	12,8V
Nominal capacity @ 25°C*	200Ah
Nominal capacity @ 0°C*	160Ah
Nominal capacity @ -20°C*	100Ah
Nominal energy @ 25°C*	2560Wh
CYCLE LIFE (capacity ≥ 80% of nominal)	
80% DoD	2500 cycles
70% DoD	3000 cycles
50% DoD	5000 cycles
Discharge	
Maximum continuous discharge current	400A
Recommended continuous discharge current	≤200A
End of discharge voltage	11,2V
Internal resistance	0,8mΩ
Operating conditions	
Operating temperature	Discharge: -20°C to +50°C, Charge: +5°C to +50°C
Storage temperature	-45°C to +70°C
Humidity (non-condensing)	Max. 95%
Protection class	IP 22
Charge	
Charge voltage	Between 14V/28V and 14,4V/28,8V (14,2V/28,4V recommended)
Float voltage	13,5V/27V
Maximum charge current	400A
Recommended charge current	≤100A
Other	
Max storage time @ 25°C*	1 year
BMS connection	Male + female cable with M8 circular connector, length 50cm
Power connection (threaded inserts)	M8
Dimensions (hxwxd) mm	237 x 321 x 152
Weight	20kg

6.1.5. Wind energy system

The small wind power system is constructed on the rooftop of the FTN building, to prevent noise and vibrations, as shown in Figure 6.11. Since the wind power system is elevated above the ground, better potential for wind energy development can be achieved, even in such an urban environment. The installed power of the system is 2kW. The wind turbine is directly connected to the three-phase inverter unit. Both turbine and

inverter are produced by the same company - Wuxi Flyt FS 2000. Technical data about this system can be found in 0. The voltage level of the point of common coupling is 0.4 kV.

Figure 6.11 Installed wind system at the rooftop of the building

Table 6.7 Wind system technical specification

2kw wind turbine	
items	**FS-2000**
Started wind speed (m/s)	1.5m/s
Cut-in wind speed (m/s)	3m/s
Rated Wind speed (m/s)	11m/s
Rated voltage(AC)	48v/96v
Rated power(W)	2000w
Max power(W)	2100w
Rotor Diameter of Blades(m)	0.8m
Product assembly weight (Kg)	<80Kg
Blades height(m)	2m
Safe wind speed (m/s)	≤40m/s
Blades quantity	2
Blade material	glass/basalt
Generator	Three phase permanent magnet suspension motor
Control System	Electromagnet
Mount Height(m)	7~12m (9m)
Generator protection grade	IP54
Work environment temperature	-25~+45ºC,
Work environment humidity	≤90%,
Altitude:	≤4500m
Overspeed protection	Electromagnetic brake
2000w 48v on grid Inverter	
Input data (DC)	**SUN-2000GTIL2-WAL-LCD**
Input voltage range	45-90VDC
Maximum input DC voltage	90V
Peak power tracking voltage	50V - 90V
Operating DC voltage range	45V - 90V
Start-up voltage	49V
Output data (AC)	
Maximum output power	2000W
Nominal voltage	230VAC
Nominal voltage range	185-265V
Frequency range	47.5-51.5 for 50Hz, 59.3-60.5 for 60Hz
Power factor	>0.95
Output waveform	Pure sine wave
Characteristic data	
MPPT efficiency	99%
Over current protection	Yes
Over temperature protection	Yes

Reverse polarity protection	Yes
Anti-Island protection	Yes
Stackable	Just for AC output
Operating temperature range	-20°C ~ 45°C
Storage temperature range	-40°C ~ 85°C
Current THD	<5%
Voltage THD	<5%
Standard	CE,EN50438
Efficiency	92%
Features	
Net Weight	5.8kg
Gross weight	7.0kg
Dimensions (package)	540mm x 310mm x 160mm

6.1.6. Heating, ventilation and air conditioning (HVAC) system

In order to improve thermal comfort and indoor air quality, HVAC (Gree GMV5 Solar) system was installed. The installed power of the HVAC system is 55 kW. This will result in significant energy savings related to the heating of the part of the exemplary object. One of two installed HVAC units is depicted in Figure 6.12.

Figure 6.12 Installed HVAC unit

By adopting advanced photovoltaic direct-driven technology, the system can achieve power generation by utilizing solar power while consuming electricity and ensure utilization of photovoltaic power in priority; compared with traditional photovoltaic system, energy wastage during multiple commutation of alternating current and direct current is

eliminated, with energy efficiency improved by 6%-8% and photovoltaic utilization ratio up to 99%. Besides, the innovative MPPT (Maximum Power Point Tracking) technology can track and control the maximum power point status of photovoltaic power generation, so as to achieve maximum utilization of photovoltaic power.

In summer, power consumption of air conditioner is large and photovoltaic power generation is relatively large as well. Gree Photovoltaic Direct- driven Inverter Multi VRF System, combining the characteristics of photovoltaic power, makes sure that the consumed electricity of units matches with the photovoltaic power generation so as to achieve zero electricity charge.

In rated engineering proportion, the power amount that Photovoltaic Direct-driven Inverter Multi VRF System gets from the grid is balanced with the power amount that the system delivers to the grid in each day, each month, each quarter and each year. Generally, power consumed from the grid is zero.

Technical data for the Gree photovoltaic direct-driven inverter multi VRF system are listed in 0.

Table 6.8 Technical specification for installed HVAC system

Model			GMV-Y224WM/C-X*
Capacity range		HP	8
Capacity	Cooling	kW	22.40
	Heating	kW	25.00
Cooling power input		kW	5.7
Heating power input		kW	5.5
EER/COP		kW/kW	3.93/4.24
Air flow volume		m3/h	11400
Power supply		V/Ph/Hz	380-415V-3Ph~50/60Hz
Range of allowable open circuit input voltage		V	1000
Range of input operating voltage		V	560~780
Max. solar short circuit current		A	39
Recommended quantity of PV module base on Gree Module GIE-M60/290		/	22/44/66/88
Maximum drive IDU NO.		unit	13
Refrigerant charge volume		kg	5.9
Sound pressure level		dB(A)	60
Connecting pipe	Liquid	inch(mm)	Φ3/8(9.52)
	Gas	inch(mm)	Φ3/4(19.05)
Dimension (WxDxH)	Outline	mm	930×765×1605
	Package	mm	1010×840×1775
Net weight/Gross weight		kg	266/278
Loading quantity	40’ GP	set	24
	40’ HQ	set	24

6.2. KCV renewable energy systems

PV system on the Radiology clinic roof during and after montage is shown in Figure 6.13. Number of PV panels that were laid is around 130. Used PV module are Luxor Monocrystalline Eco Line Half Cell M120 type. Technical data of the used modules is shown in Figure 6.14.

Figure 6.13 PV system on the Radiology clinic roof

Monocrystalline module family	Module type LX - XXXM/166-120+ | XXX = Rated power Pmpp				
Electrical data at STC					
Rated power Pmpp [Wp]	365.00	370.00	375.00	380.00	385.00
Pmpp range to	371.49	376.49	381.49	386.49	391.49
Rated current Impp [A]	10.69	10.74	10.81	10.88	10.94
Rated voltage Vmpp [V]	34.17	34.48	34.72	34.96	35.21
Short-circuit current Isc [A]	11.27	11.34	11.41	11.49	11.55
Open-circuit voltage Uoc [V]	40.76	41.04	41.33	41.62	41.91
Efficiency at STC up to	20.39%	20.67%	20.94%	21.22%	21.49%
Efficiency at 200 W/m²	19.80%	20.07%	20.34%	20.62%	20.88%
Electrical data at NOCT					
Power at Pmpp [Wp]	270.70	274.76	278.86	283.01	286.95
Rated current Impp [A]	8.53	8.59	8.66	8.73	8.78
Rated voltage Vmpp [V]	31.73	31.98	32.21	32.43	32.66
Short-circuit current Isc [A]	9.09	9.15	9.22	9.28	9.33
Open-circuit voltage Uoc [V]	37.62	37.90	38.17	38.45	38.74

Specification as per STC (Standard test conditions): irradiance 1000W/m² | module temperature 25°C | Air Mass = 1.5
NOCT (nominal operating cell temperature): irradiance 800W/m² | wind speed 1m/sec | ambient temperature 20°C | cell operating temperature 45 +/-2°C | Air Mass = 1.5

Figure 6.14 Luxor M120 PV module technical data

For purposes of interconnecting PV plant with electric power grid inside KCV complex, the adequate solar inverter is used. For the Radiology clinic PV plant ABB PVS-50-TL solar inverter, shown in Figure 6.15, is used. In addition, the appropriate electric cabinet for interconnection and monitoring is assembled. This electric cabinet is shown in Figure 6.16.

Figure 6.15 ABB PVS-50-TL solar inverter

Figure 6.16 Electric cabinet for interconnection and monitoring of Radiology clinic PV plant

PV system on the Emergency center roof during and after montage is shown in Figure 6.17. Number of PV panels that were laid is around 160. Used PV module are Luxor Monocrystalline Eco Line Half Cell M120 type. Technical data of the used PV modules are the same as in case of Radiology clinic. For purposes of interconnecting PV plant with electric power grid inside KCV complex, the adequate solar inverter is used. For the Emergency center PV plant ABB PVS-50-TL solar inverter, shown in Figure 6.15, is used. In addition, the appropriate electric cabinet for interconnection and monitoring is assembled. This electric cabinet is shown in Figure 6.16.

Figure 6.17 PV system on the Emergency center roof

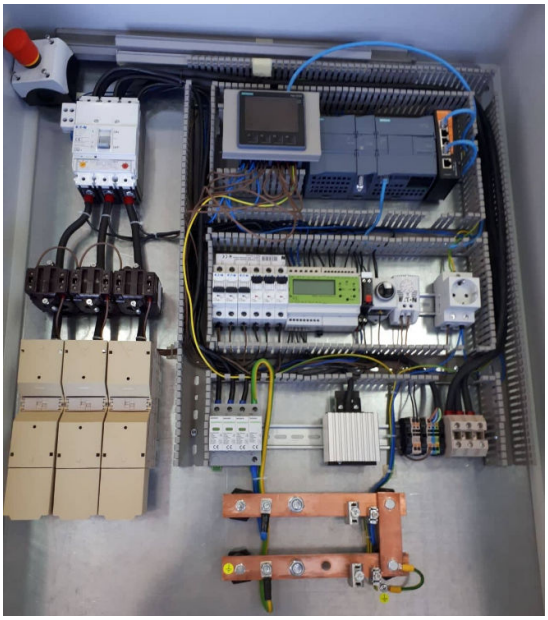

Figure 6.4 Electric cabinet for interconnection and monitoring of Emergency center PV plant

PV system on the parking inside KCV complex during and after montage is shown in Figure 6.18. Number of PV panels that were laid is around 380. Used PV module are Luxor Monocrystalline Eco Line Half Cell M108 type. Technical data of the used PV modules is shown in Figure 6.14.

Figure 6.18 PV plant on the KCV parking

Monocrystalline module family	Module type LX - XXXM/182-108+ | XXX = Rated power Pmpp				
Electrical data at STC					
Rated power Pmpp [Wp]	390.00	395.00	400.00	405.00	410.00
Pmpp range to	396.49	401.49	406.49	411.49	416.49
Rated current Impp [A]	12.71	12.78	12.85	12.92	12.99
Rated voltage Vmpp [V]	30.71	30.93	31.14	31.36	31.58
Short-circuit current Isc [A]	13.42	13.50	13.57	13.64	13.72
Open-circuit voltage Uoc [V]	36.56	36.82	37.08	37.34	37.60
Efficiency at STC up to	20.28%	20.54%	20.79%	21.05%	21.30%
Efficiency at 200 W/m²	19.72%	19.97%	20.22%	20.47%	20.72%
Electrical data at NOCT					
Power at Pmpp [Wp]	289.54	293.25	296.96	300.67	304.38
Rated current Impp [A]	10.27	10.32	10.38	10.44	10.49
Rated voltage Vmpp [V]	28.20	28.40	28.61	28.81	29.01
Short-circuit current Isc [A]	10.83	10.89	10.96	11.02	11.08
Open-circuit voltage Uoc [V]	33.75	34.00	34.24	34.50	34.75

Specification as per STC (Standard test conditions): irradiance 1000 W/m² | module temperature 25°C | Air Mass = 1.5
NOCT (nominal operating cell temperature): irradiance 800 W/m² | wind speed 1 m/sec | ambient temperature 20°C | cell operating temperature 45 +/-2°C | Air Mass = 1.5

Figure 6.2 Luxor M108 PV module technical data

For purposes of interconnecting PV plant with electric power grid on the parking inside KCV complex, the adequate solar inverter is used. For the PV plant on the KCV parking ABB PVS-50-TL solar inverter, shown in Figure 6.15, is used. In addition, the appropriate electric cabinet for interconnection and monitoring is assembled.

Solar-thermal system on the roof of the Medical Rehabilitation clinic during and after montage is shown in Figure 6.19. Used modules are Bosch Flat-Plate Solar Collectors and technical data for these modules is shown in 0. Number of solar collector modules that were installed is 25.

Figure 6.19 Solar-thermal system on the Medical Rehabilitation clinic roof

Solar-Lifestyle	
Certificates	CE
Length	2017 mm
Width	1175 mm
Height	87 mm
Clearance between collectors	25 mm
Collector connection (in the shape of a nozzle)	23 mm
Absorber capacity, portrait (V_f)	0.94 l
Absorber capacity, landscape (V_f)	1.35 l
External area (gross area, A_G)	2.37 m^2
Absorber area (net area, A_A)	2.18 m^2
Aperture area (A_a)	2.25 m^2
Net weight, portrait version	40 kg
Net weight, landscape version	41 kg
Permissible operating pressure collector (p_{max})	6 bar
Max. stagnation temperature	199 °C

Figure 6.20 Technical data for Solar collectors on the Medical Rehabilitation clinic roof

The solar-thermal system was interconnected with existing heating installation that is mainly used for heating the water in medical rehabilitation pools. The interconnection between solar-thermal and existing heating system is shown in Figure 6.21.

Figure 6.21 Interconnection between solar-thermal and existing heating system

Bio-diesel production system was installed and is shown in Figure 6.22. This system produces the bio-diesel which is later used for running diesel generator system shown in Figure 6.23. Bio-diesel system is used to convert waste oil which is obtained from KCV kitchen.

Figure 6.22 Bio-diesel production system

Figure 6.23 Diesel generator system in KCV complex

System for bio-diesel production is supplied by electric power from electric cabinet shown in Figure 6.24. Production capacity of the used bio-diesel system is around 960 liters per day, whereas the nominal consumption of electric power is around 5 kW. The process of obtaining the bio-diesel fuel last around 6 hours, during which around 160 liters of fuel can be expected.

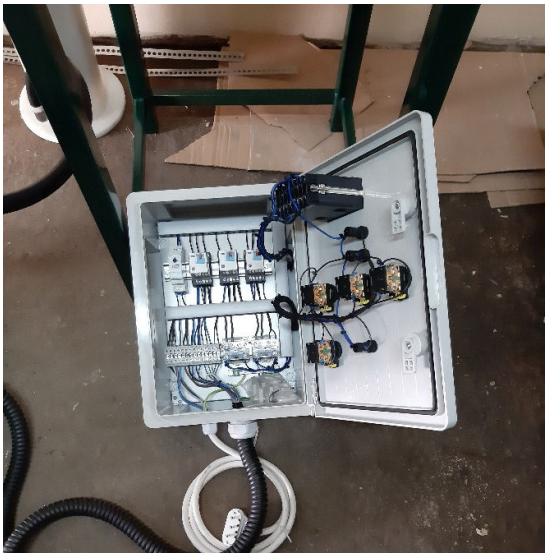

Figure 6.24 Electric cabinet for supplying the bio-diesel production system

6.3. FERIT renewable energy systems

6.3.1. Photovoltaic systems on the buildings roofs

Total installed power of the photovoltaic systems on FERIT buildings is 125 kW. Installed power of the photovoltaic system on building roof in Trpimirova street is 85 kW while installed power of the photovoltaic system in Cara Hadrijana street is 40 kW.

Block schematic of the FERIT building power system in Trpimirova street is given in Figure 6.25. FERIT building power system in Trpimirova street consists of photovoltaic systems on building roof along with storage system, building consumption and old 10 kW photovoltaic system. Photovoltaic system and storage systems are connected in RO-SE1 and RO-SE2 cabinets located in room 3-40 (Figure 6.26). Great hall air-conditioning system as a part of building consumption is connected directly to the RO-SE2 cabinet. Storage systems, which are integral part of the photovoltaic systems, are described in chapter 6.3.2.

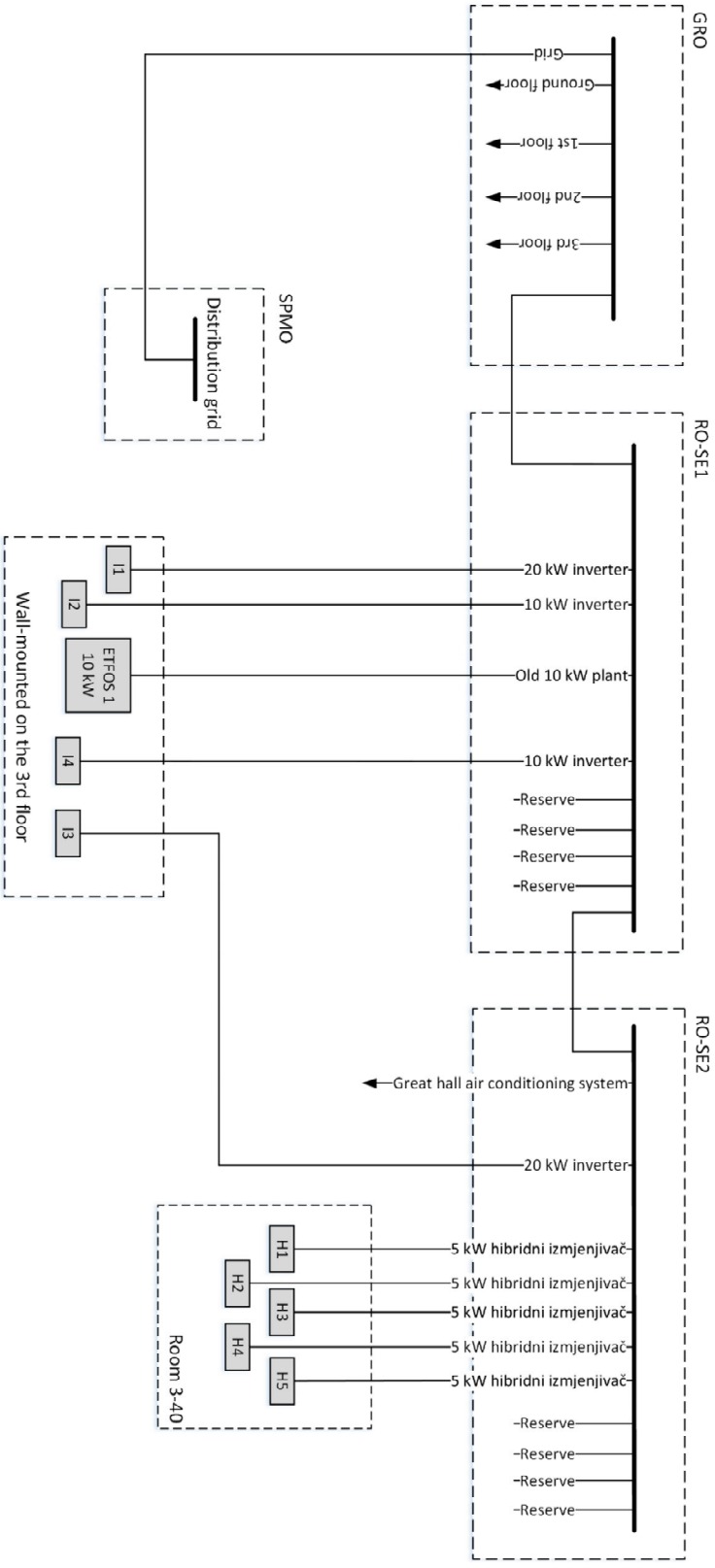

Figure 6.25 Block schematic of FERIT building power system in Trpimirova street

Figure 6.26 Room 3-40 along with RO-SE1, RO-SE2 cabinets and hybrid invertes with lithium battery packs

Photovoltaic system building roof in Trpimirova street (Figure 6.27) consists of nine inverters, two Growatt MID 20KTL3-X inverters with nominal power of 20 kW each, two Growatt 10000TL3-S inverters with nominal power of 10 kW each, five Growatt SPH 5000TL3-BH hybrid inverters with nominal power of 5 kW each and 298 monocrystalline silicon photovoltaic modules Luxor EcoLine M60/320W with nominal power of 320 Wp. Wall-mounted inverters on the 3rd floor of FERIT building in Trpimirova street are given in Figure 6.28.

Figure 6.27 FERIT photovoltaic system modules on building roof in Trpimirova street

Figure 6.28 Wall-mounted inverters at the 3rd floor of FERIT building in Trpimirova street

Block schematic of the FERIT building power system in Cara Hadrijana street is given in Figure 6.29. FERIT building power system in Cara Hadrijana street consists of photovoltaic systems on building roof along with building consumption.

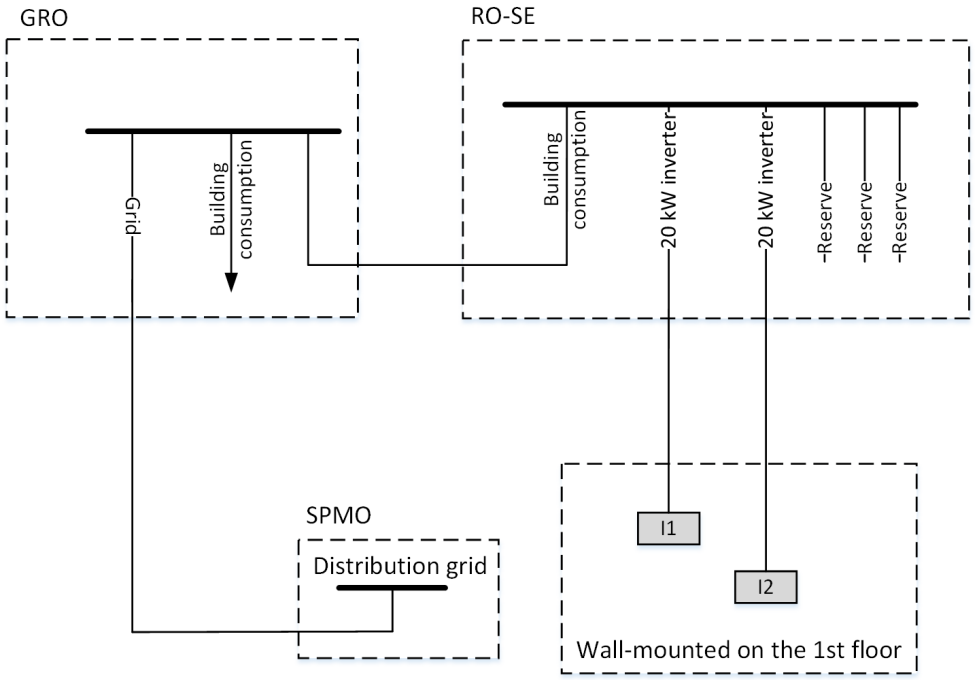

Figure 6.29 Block schematic of FERIT building power system in Cara Hadrijana street

Photovoltaic system on building roof in Cara Hadrijana street (Figure 6.30) consists of two inverters Growatt MID 20KTL3-X inverters with nominal power of 20 kW each and 128 monocrystalline silicon photovoltaic modules Luxor EcoLine M60/320W with nominal power of 320 Wp. Wall-mounted inverters at the 1st floor of FERIT building in Cara Hadrijana street are given in Figure 6.31.

Figure 6.30 FERIT photovoltaic system modules on building roof in Cara Hadrijana street

Figure 6.31 Wall-mounted inverters at the 1st floor of FERIT building in Cara Hadrijana street

Technical characteristics of Growatt MID 20KTL3-X inverters are given in 0, technical characteristics of Growatt 10000TL3-S inverters are given in 0, technical characteristics of Growatt SPH 5000TL3-BH hybrid inverters are given in 0 while Table 6.12 gives technical characteristic of photovoltaic modules Luxor EcoLine M60/320W.

Table 6.9 Technical characteristics of Growatt MID 20KTL3-X inverters [28]

DC side	
Maximum DC power	30 kW
Maximum input voltage	1100 V
MPP voltage range*	160 V to 1000 V
Maximum input current	30 A
Number of MPPT / inputs per MPPT**	2/2
AC side	
Nominal power	20 kW
Maximum apparent AC power	22000 kVA
AC nominal voltage	230 V / 400 V
Nominal frequency	50/60 Hz
Maximum output current	31.9 A
THD***	< 3 %
Adjustable power factor	0.8 leading to 0.8 lagging
General data	
Efficiency / European efficiency	98.75 % / 98.6 %
Degree of protection	IP65

*MPP – maximum power point

**MPPT – maximum power point tracker

*** THD – total harmonic distortion

Table 6.10 Technical characteristics of Growatt 10000TL3-S inverters [29]

DC side	
Maximum DC power	12 kW
Maximum input voltage	1000 V
MPP voltage range*	450 V to 850 V
Maximum input current	13 A
Number of MPPT / inputs per MPPT**	2/1
AC side	
Nominal power	10 kW
Maximum apparent AC power	11 kVA
AC nominal voltage	230 V / 400 V
Nominal frequency	50/60 Hz
Maximum output current	16.7 A
THD***	< 3 %
Adjustable power factor	0.8 leading to 0.8 lagging
General data	
Efficiency / European efficiency	98.4 % / 98 %
Degree of protection	IP65

*MPP – maximum power point

**MPPT – maximum power point tracker

*** THD – total harmonic distortion

Table 6.11 Technical characteristics of Growatt SPH 5000TL3-BH hybrid inverters [30]

PV side (DC)	
Maximum DC power	6.5 kW
Maximum input voltage	1000 V
MPP voltage range*	160 V to 1000 V
Maximum input current	15 A
Number of MPPT / inputs per MPPT**	2/1
Battery side (DC)	
Battery voltage range	100 V to 550 V
Max charging and discharging current	25 A
Continuous charging and discharging power	5 kW
Type of battery	Lithium battery
Output data (AC)	
Nominal power	5 kW
Maximum apparent AC power	5 kVA
AC nominal voltage	230 V / 400 V
Nominal frequency	50/60 Hz
Maximum output current	7.6 A
THD***	< 3 %
Adjustable power factor	0.8 leading to 0.8 lagging
Backup power (AC)	
Maximum AC output power	5 kW
Maximum AC apparent power	5 kVA
Maximum output current	7.6 A
AC nominal voltage	230 V / 400 V
THD***	< 3 %
Switch time	< 0.5 s
General data	
Efficiency / European efficiency	97.8 % / 97.2 %
Degree of protection	IP65

*MPP – maximum power point

**MPPT – maximum power point tracker

*** THD – total harmonic distortion

Table 6.12 *Technical characteristics of photovoltaic modules Luxor EcoLine M60/320W [31]*

Nominal power	320 W
Short-circuit current	10.05 A
Open-circuit voltage	39.56 V
MPP current	9.59 A
MPP voltage	33.45
Efficiency	20.07
Current temperature coefficient	0.06 %/°C
Voltage temperature coefficient	-0.3 %/°C
Power temperature coefficient	-0.4 %/°C
Dimensions	1640x992x35 mm

All data is given for standard test conditions (STC)

** MPP – maximum power point

6.3.2. Renewable energy storage/supply system

Energy storage/supply system is an integral part of the photovoltaic system in building in Trpimirova street. Hybrid inverters Growatt SPH 5000TL3-BH, connected to the RO-SE2 cabinet visible on block schematic of building power system in Figure 6.25, have connected lithium-ion battery pack on their DC side.

Battery pack needs to be compatible with hybrid inverters for which technical characteristics are given in 0. First 4 hybrid inverters (H1, H2, H3 and H4) are equipped with H48050 lithium-ion battery pack with energy capacity of 9.6 kWh (Figure 6.33 right) while 5th hybrid inverter (H5) use ARK 7.6H-A1 lithium-ion battery pack with energy capacity of 7.68 kWh (Figure 6.33 right). Along with normal grid-connected operation, hybrid inverter enables emergency supply of loads in case of grid blackout through the EPS output. Wiring of the hybrid inverter Growatt SPH 5000TL3-BH along with battery pack is given in Figure 6.32.

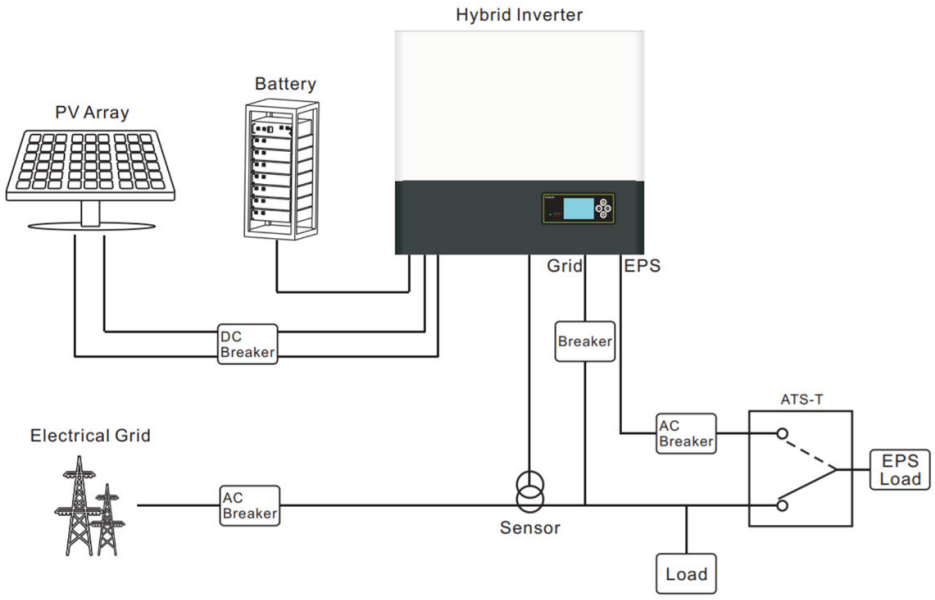

Figure 6.32 Wiring diagram of hybrid inverter Growatt SPH 5000TL3-BH with battery pack

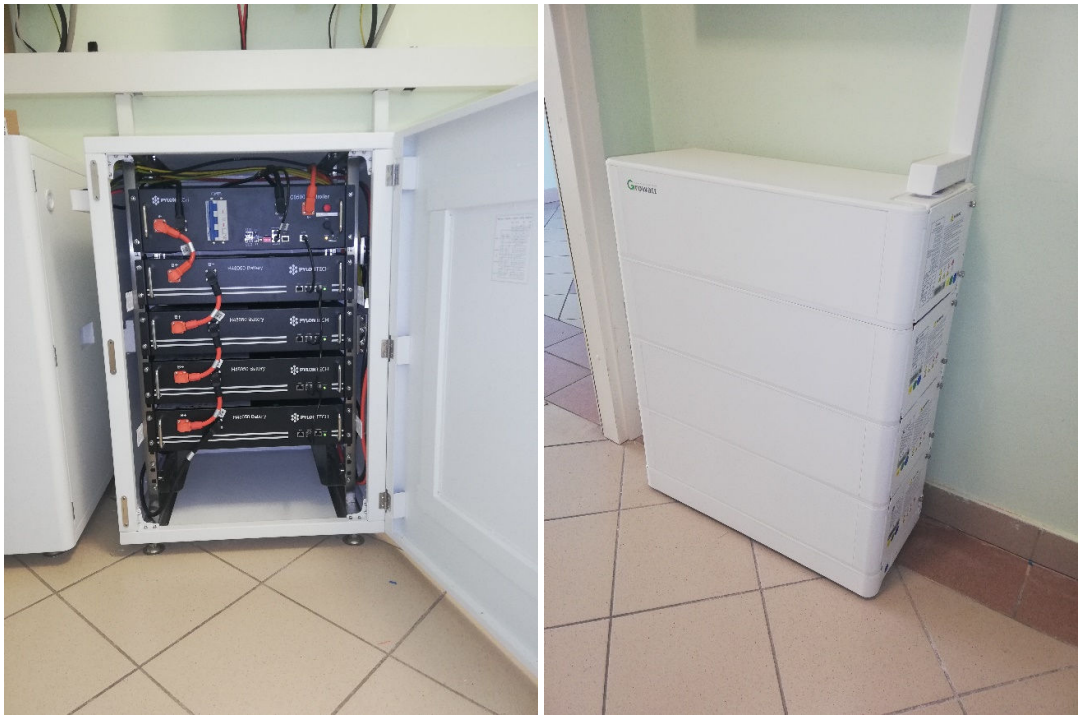

Figure 6.33 H48050 lithium-ion battery pack with energy capacity of 9.6 kWh (left) and ARK 7.6H-A1 lithium-ion battery pack with energy capacity of 7.68 kWh (right) installed at the DC side of the hybrid inverter Growatt SPH 5000TL3-BH in the room 3-40 of FERIT building in Trpimirova street

Technical characteristic of H48050 lithium-ion battery pack with energy capacity of 9.6 kWh is given in Table 6.13 while Table 6.14 gives technical characteristics of ARK 7.6H-A1 lithium-ion battery pack with energy capacity of 7.68 kWh.

Table 6.13 Technical characteristics of 9.6 kWh lithium-ion battery pack H48050 [32]

Battery pack energy capacity	9.6 kWh
Number of battery modules	4
Battery module energy capacity	2.4 kWh
Battery module nominal voltage	48 V
Battery module operating voltage	45 V to 54 V
Battery module charge/discharge current	25 A (normal) 50 A (maximum)

Table 6.14 Technical characteristics of 7.68 kWh lithium-ion battery pack ARK 7.6H-A1 [33]

Battery pack energy capacity	7.68 kWh
Number of battery modules	3
Battery module energy capacity	2.56 kWh
Battery module nominal voltage	51.2 V
Battery module operating voltage	47.2 V to 56.8 V
Battery module charge/discharge current	25 A (normal) 50 A (maximum)

6.4. KBCO renewable energy systems

6.4.1. Photovoltaic systems on the buildings roofs

Total installed power of the photovoltaic systems on the buildings of central kitchen and Department of Oncology and Department of Diagnostical and Interventional Radiology is 230 kW. Photovoltaic systems consist of six inverters, four SMA Sunny Tripower CORE1 inverters with nominal power of 50 kW each and two SMA Sunny Tripower 20000TL inverters with nominal power of 20 kW each. Technical characteristics of the SMA Sunny Tripower CORE1 inverters are given in 0 while 0 gives technical characteristics of SMA Sunny Tripower 20000TL inverters.

Table 6.15 Technical characteristics of SMA Sunny Tripower CORE1 inverters [34]

DC side	
Maximum DC power	51 kW
Maximum input voltage	1000 V
MPP voltage range*	150 V to 1000 V
Maximum input current	30 A
Number of MPPT / inputs per MPPT**	6/2
AC side	
Nominal power	50 kW
Maximum apparent AC power	50 kVA
AC nominal voltage	230 V / 400 V
Nominal frequency	50 Hz
Maximum output current	72.5 A
THD***	3 %
Adjustable power factor	0 leading to 0 lagging
General data	
Efficiency / European efficiency	> 98 % / > 98 %
Degree of protection	IP65

*MPP – maximum power point

**MPPT – maximum power point tracker

*** THD – total harmonic distortion

Table 6.16 Technical characteristics of SMA Sunny Tripower 20000TL inverters [35]

DC side	
Maximum DC power	20440 kW
Maximum input voltage	1000 V
MPP voltage range*	320 V to 800 V
Maximum input current	33 A
Number of MPPT / strings per MPPT**	2/3
AC side	
Nominal power	20 kW
Maximum apparent AC power	20 kVA
AC nominal voltage	230 V / 400 V
Nominal frequency	50 Hz
Maximum output current	29 A
THD***	≤ 3 %
Adjustable power factor	0 leading to 0 lagging
General data	
Efficiency / European efficiency	98.4 % / 98 %
Degree of protection	IP65

*MPP – maximum power point

**MPPT – maximum power point tracker

*** THD – total harmonic distortion

Total number of 767 monocrystalline silicon photovoltaic modules SOLVIS SV60-300E with nominal power of 300 W are installed on the roofs which technical characteristics are given in 0.

Table 6.17 *Technical characteristics of photovoltaic modules SOLVIS SV60-300E [36]*

Nominal power	300 W
Short-circuit current	9.73 A
Open-circuit voltage	40.14 V
MPP current	9.13 A
MPP voltage	33.03
Efficiency	18.44
Current temperature coefficient	0.05 %/°C
Voltage temperature coefficient	-0.33 %/°C
Power temperature coefficient	-0.42 %/°C
Dimensions	1640x992x40 mm

All data is given for standard test conditions (STC)

** MPP – maximum power point

Photovoltaic systems are connected to the KBCO complex power system at the substation TS 10/0.4 kV Bolnica 3 (Maternite/Ginekologija) visible on Figure 3.19. Single line diagram of the TS 10/0.4 kV Bolnica 3 (Maternite/Ginekologija) is given in . Single line diagram of the photovoltaic system connected to the low voltage bus at the TS 10/0.4 kV Bolnica 3 (Maternite/Ginekologija) is given in Figure 6.35.

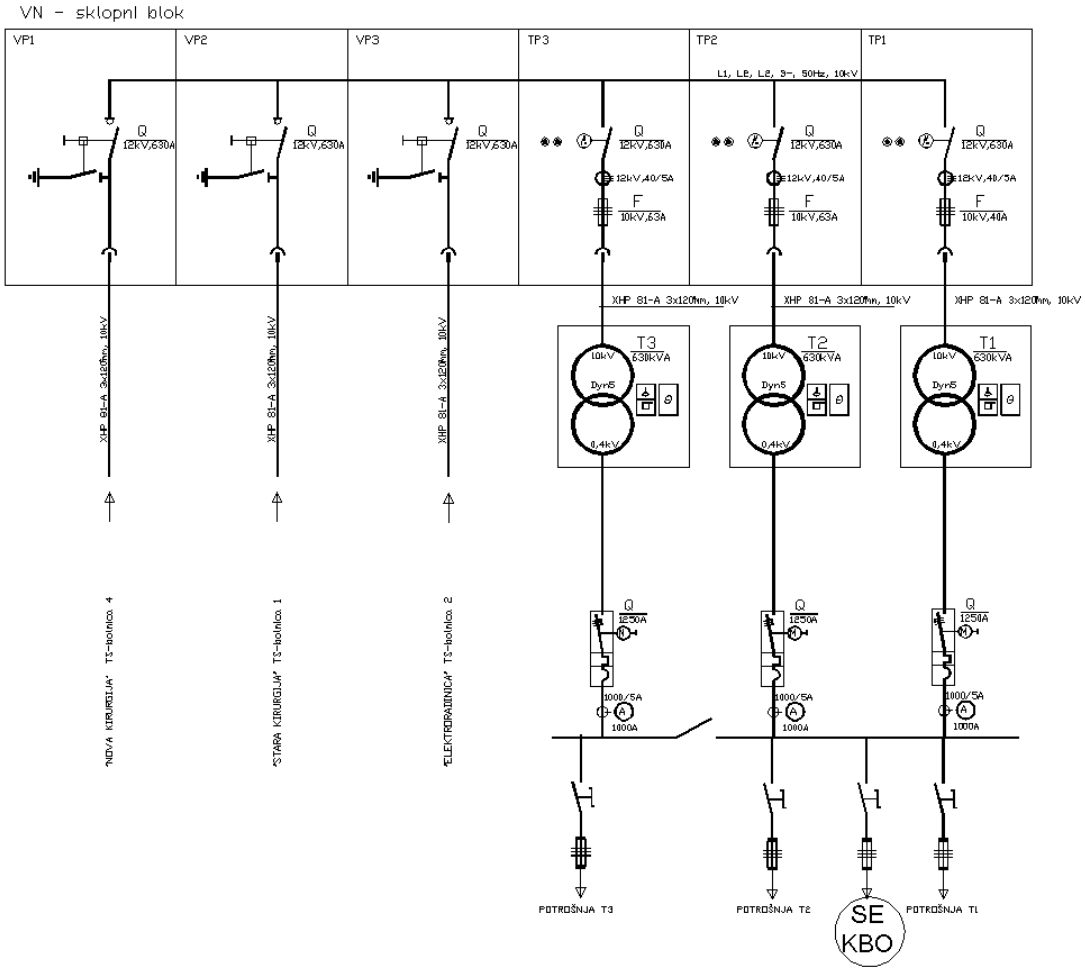

Figure 6.34 Single line diagram of the substation TS 10/0.4 kV Bolnica 3 (Maternite/Ginekologija) in KBCO [16]

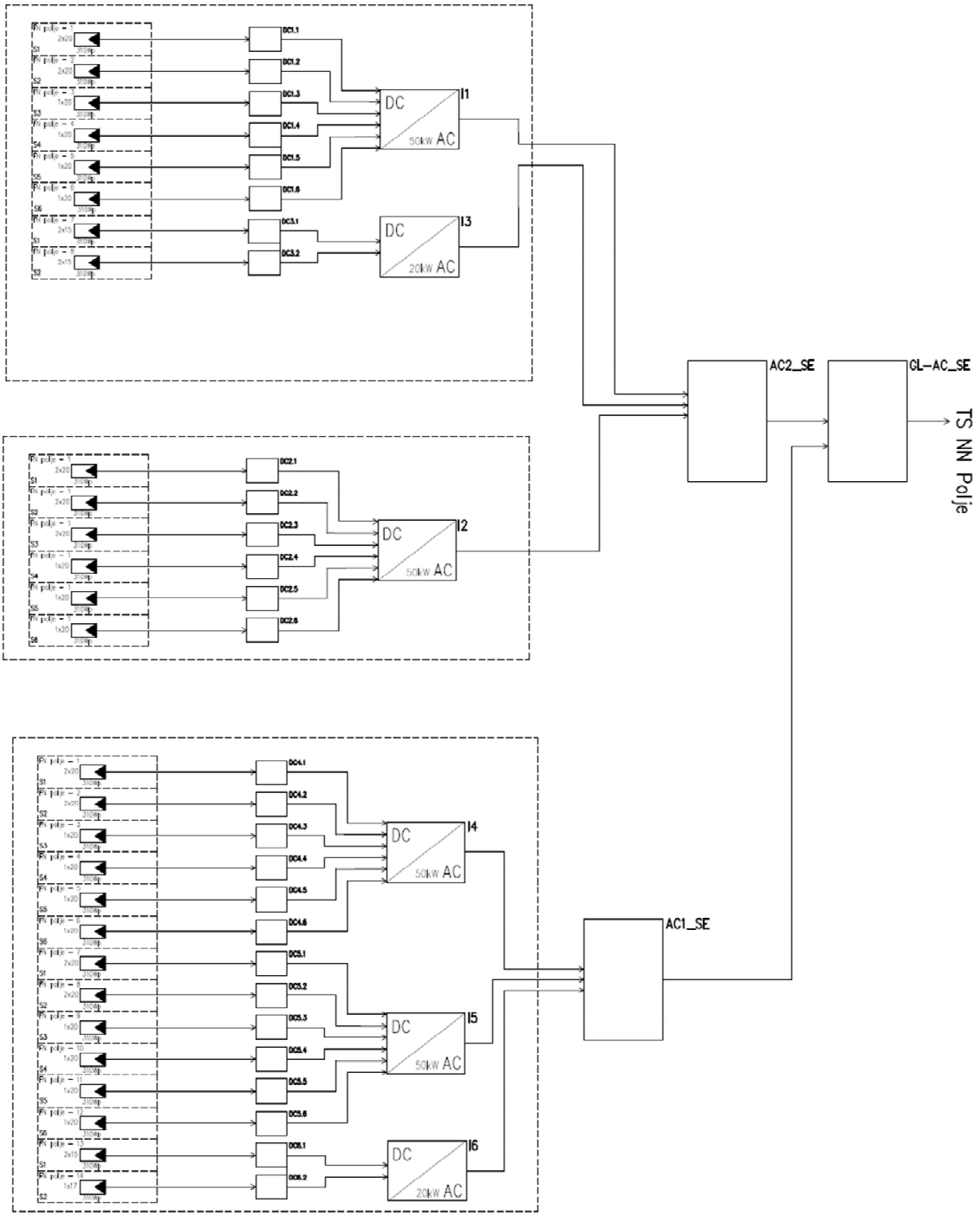

Figure 6.35 Single line diagram of the KBCO photovoltaic systems [16]

Placement of the photovoltaic modules on the Central kitchen and Department of Oncology and Department of Diagnostical and Interventional Radiology building roof is given in Figure 6.36.

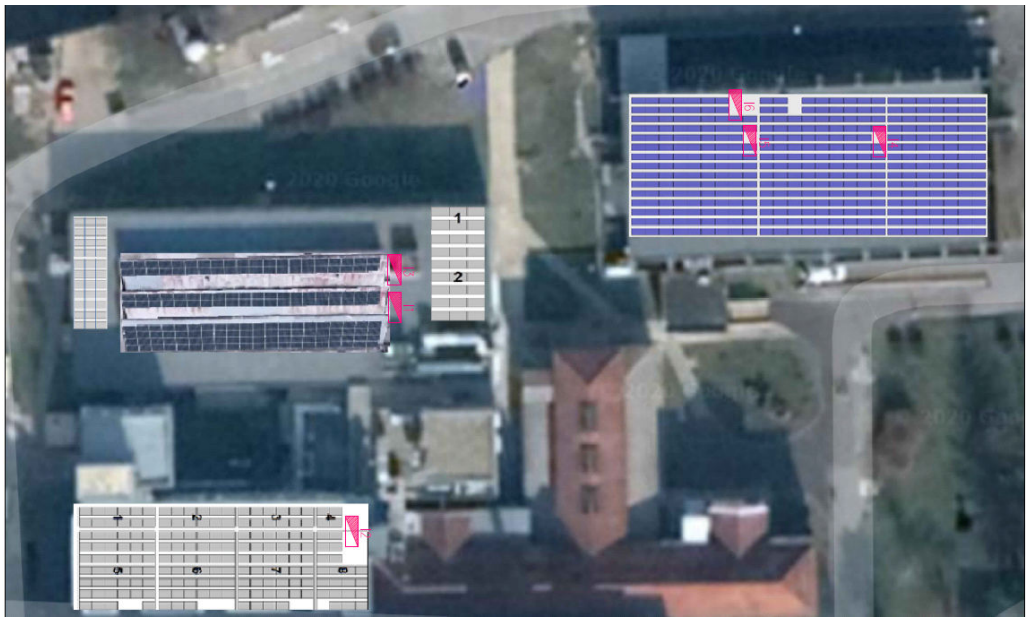

Figure 6.36 Placement of the photovoltaic modules on the Central kitchen and Department of Oncology and Department of Diagnostical and Interventional Radiology building roof at KBCO [16]

Photographs of the photovoltaic system on the central kitchen is given in Figure 6.37 while Figure 6.38 shows photovoltaic system on Department of Oncology and Department of Diagnostical and Interventional Radiology building roof.

Figure 6.37 KBCO photovoltaic system on central kitchen building roof

Figure 6.38 KBCO photovoltaic system on Department of Oncology and Department of Diagnostical and Interventional Radiology building roof

6.4.2. Biodiesel generator and biodiesel production system

As planned, KBCO installed biodiesel generator with nominal power of 125 kVA (kW), given in Figure 6.39, that operate during partial of complete blackout of electric power supply enhancing reliability of power supply overall. Biodiesel generator uses biodiesel fuel generated by the biodiesel production system that uses waste oil from the central kitchen given in Figure 6.40.

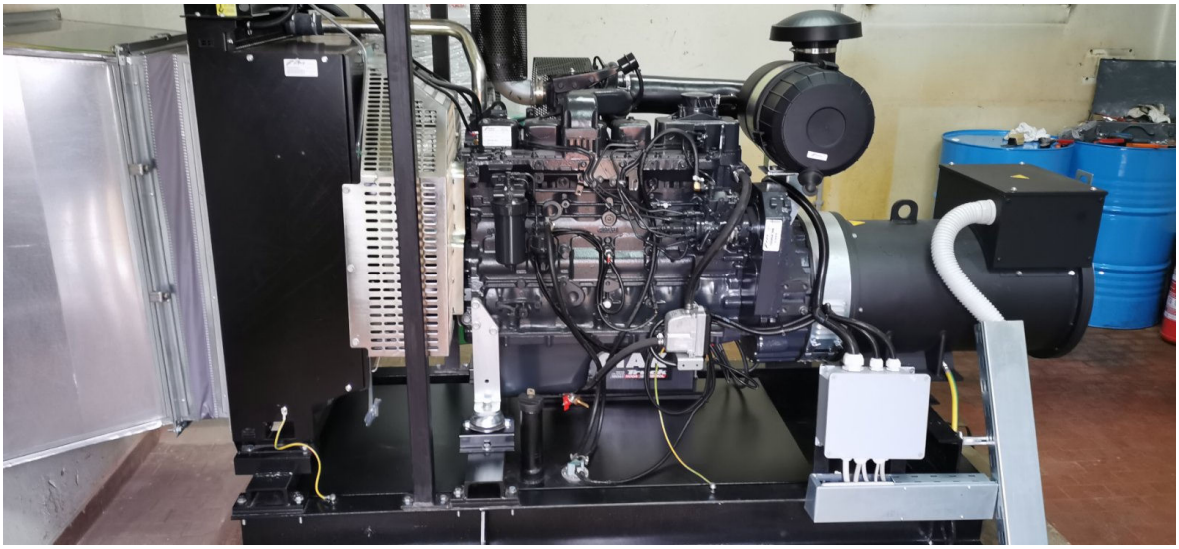

Figure 6.39 KBCO 125 kW biodiesel generator

Figure 6.40 KBCO biodiesel production system from waste oil

6.5. UNISB renewable energy systems

6.5.1. Technical description of Photovoltaic power plant UNISB, Gunduliceva 20A

General data

The purpose of the power plant is the generation of electricity for its own needs of the facility where the solar power plant is located with the possibility of handing over the produced surplus electricity to the grid. The power of the built solar power plant is 64 kW. The power plant is located on the tin roof of the building and is divided into rows of photovoltaic modules as shown in the drawings and single-pole scheme. The power plant is installed in a way that follow the slope of the roof which is about 14°.

Connections (cables)

Electricity (DC voltage, DC current) generated in solar cells is sent by PV wire red / blue 6 mm2 conductors to an inverter that converts DC voltage and current to AC. DC cables are routed in protective perforated tin galvanized channels (ducts) and protective tubes of the plastic kaoflex type. Growatt's built-in MID and SPH inverters are equipped with surge, overcurrent and reverse current protection devices at the inlet to the inverter. From the inverter, the FG16OR 5x10 mm^2 conductors send the alternating components of electricity (voltage and current) to the distribution cabinet of the R-FNE power plant, which includes four-pole RCD switches type A, three-pole circuit breakers, surge

protectors, surge protection switches and other equipment, all according to the single-pole scheme in the appendix. From the R-FNE, electricity (alternating voltage and current) is sent via cable XP00 4x70 mm^2 + FG16OR 1x35 mm^2 to the main distribution cabinet SSRO1, which contains disconnectors for both the power plant and the main distribution to the facility and other consumers. The main power cable of the building type NAYY 4x150 mm^2 is laid in the cable trench from the position SSRO1 to the position of the measuring cabinet SPMO near the transformer substation. Wires and connectors for connecting photovoltaic modules Special guides for solar power plants have been installed. These are PV WIRE (PhotoVoltaic Wire) conductors. These are special, double-insulated, tinned copper conductors designed to withstand relatively high DC voltages (up to 1000 VDC). RED / BLUE labels are wire color labels that serve to make it easier to distinguish a positive (+) conductor from a negative (-) conductor. Conductors such as Schrack, type PV-1, cross section 6 mm2 are installed. DC conductor connectors are specially designed for the purpose of connecting photovoltaic equipment, withstand voltages up to 1000 VDC, and direct current up to 25 A. They are resistant to moisture, dust and other external influences (appropriate IP protection). MultiContact connectors are installed.

Photovoltaic modules

For the construction of the solar power plant, 216 photovoltaic modules with a nominal power of 320 W were installed. Luxor EcoLine HalfCell M120 / 320 photovoltaic modules of the German manufacturer Luxor Solar GmbH were installed. The photovoltaic module consists of 120 serial monocrystalline silicon cells, dimensions of cells are 79 × 158 mm which are soldered together with copper tin conductors and laminated with ethylene vinyl acetate, between 3.2 mm thick tempered solar glass with excellent optical and mechanical properties, front and composite polyester protective foils on the back. The frame of the module is made of anodized aluminum and is made so that it has double walls and holes for drainage. The cells are soldered to each other with copper tin conductors and laminated between glass of excellent optical and mechanical properties on the front and a polymer protective white film on the back. The nominal power of the module is 320 Wp, the dimensions of the module are 1984 × 1002 × 35 mm, and the weight of the module is 19 kg. The photovoltaic field contains 216 modules, divided into 13 arrays, as shown in the drawings. Photovoltaic modules are connected in series, and the connection cables are type PV-1 6 mm^2. Cables such as Schrack PV-1 6mm2 were used. Photovoltaic modules are installed at an angle of about 14°. The solar cable that goes with the junction box is 4 mm^2 in cross section, 1 m long, while the connectors are MC4 type. Figure 6.41 shows Luxor EcoLine HalfCell M120 / 320W on SE UNISB.

Figure 6.41 Photovoltaic power plant on UNISB building in I. Gundulić Street

Inverter

The inverters, with their input voltage and current limits, cover the working area of the photovoltaic field in all conditions. A total of 4 Growatt inverters have been installed. Three MID20KTL3-X type inverters with a nominal power of 20 kW have been installed, as well as a total of 1 hybrid inverter type SPH5000TL3 BH with a nominal power of 5 kW, which is software limited to an output power of 4 kW. A 2 x 9.6 kWh battery system is connected to the hybrid inverter. Built-in inverters are without transformers, total output power 64 kW. They have built-in very advanced security systems for protection against island operation, as well as overcurrent and overvoltage protection. The inverters have a built-in maximum power field tracking system (MPPT) of the photovoltaic field. Exchangers are installed on the inner wall of the building, as shown in the drawings and figure.

The inverters, with their input voltage and current limits, cover the working area of the photovoltaic field in all conditions. Growatt inverters on Solar power plant UNISB are presented on Figure 6.42.

Figure 6.42 Inverters of Photovoltaic power plant on UNISB building in Laboratory for renewable energy sources

Lightning, overvoltage and surface protection

Class II surge arresters are installed inside the DC protection cabinets, which protect the inlet side of the inverter, and through them DC circuits are protected from overvoltage. The R-FNR distribution cabinet has built-in surge protection class C 20 kA. For the purpose of grounding the solar power plant, the tin cover of the building was used, which was grounded, and an additional lightning protection installation was installed. Overcurrent protection is provided by cylindrical fuses gPV characteristics 1000 V / 16 A for DC circuits, while the protection of the AC side is performed by a circuit breaker type B. A four-pole RCD switch type A is also installed.

Construction

The construction for photovoltaic modules mounting is made of aluminum. A total of 216 photovoltaic modules, with a total weight of about 4100 kg, were installed on the roof (Figure 6.43). The construction of the manufacturer K2 Systems, type MiniRail, was installed. The load-bearing structural elements are fastened to the metal roof of the building by means of 4 sheet metal screws.

Plant diagrams available from main electrical design project are visible in Figure 6.44, Figure 6.45, Figure 6.46, Figure 6.47, Figure 6.48, Figure 6.49, Figure 6.50, Figure 6.51, Figure 6.52 and Figure 6.53.

Figure 6.43 Base roof construction (K2 Systems) of Photovoltaic power plant on UNISB building in I. Gundulić Street

REPUBLIKA HRVATSKA
DRŽAVNA GEODETSKA UPRAVA
PODRUČNI URED ZA KATASTAR SLAVONSKI BROD

NESLUŽBENA VERZIJA

K.o. SLAVONSKI BROD, 328758
k.č. br.: 3254/1

IZVOD IZ KATASTARSKOG PLANA

Približno mjerilo ispisa 1: 1000
Izvorno mjerilo plana 1:1000

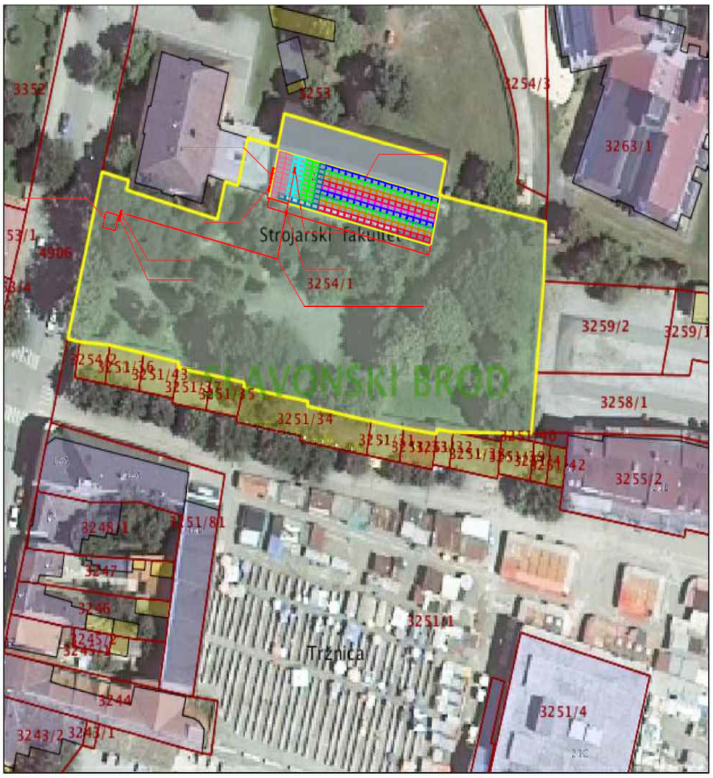

Datum ispisa: 13.01.2021

Figure 6.44 Situation map of Photovoltaic power plant on UNISB building

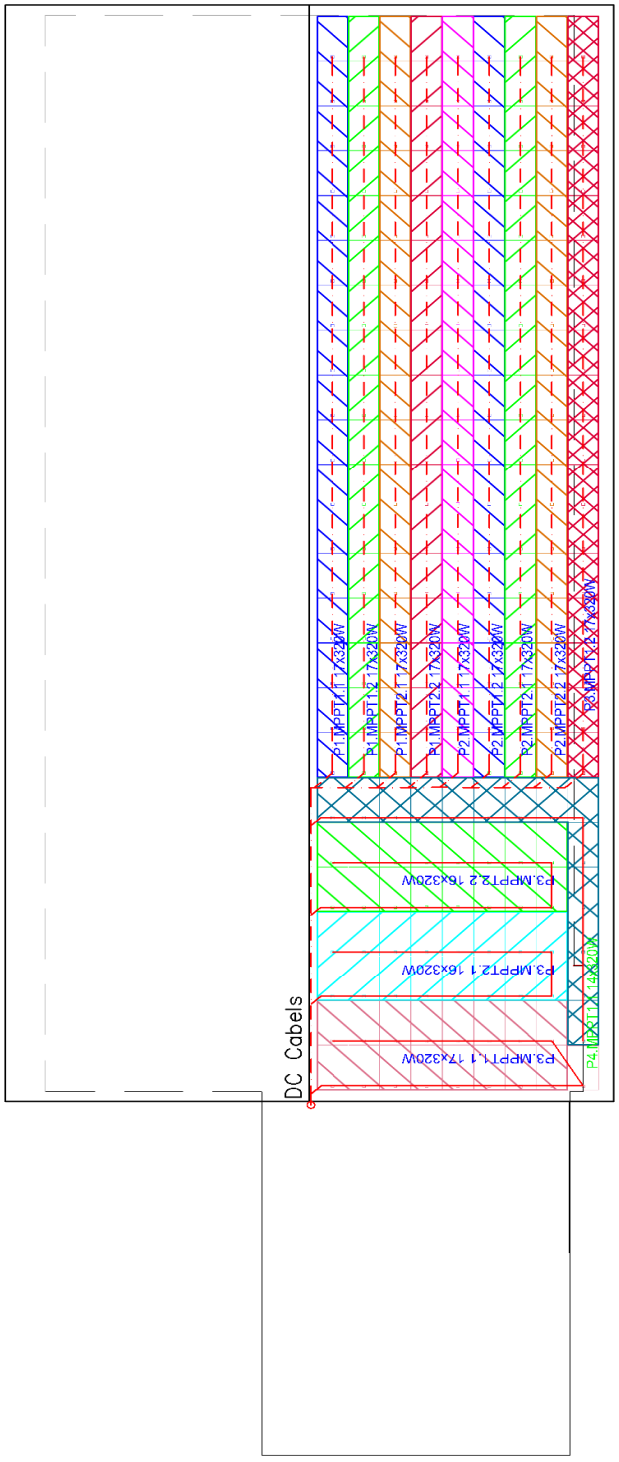

Figure 6.45 PV arrays of Photovoltaic power plant on UNISB building in I. Gundulić Street (ground plan)

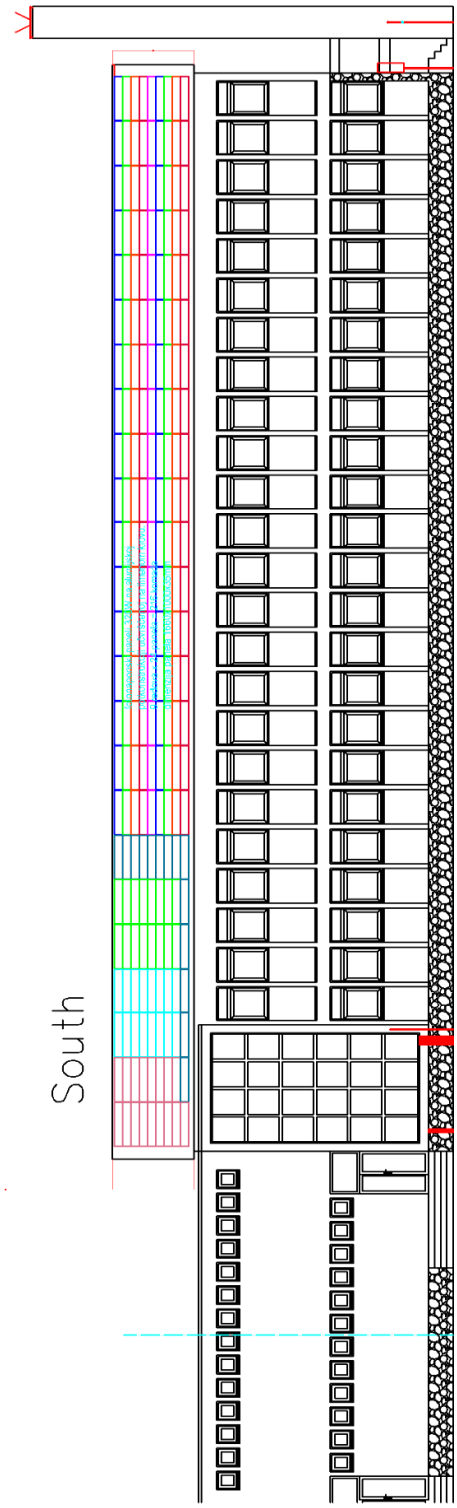

Figure 6.46 PV arrays of Photovoltaic power plant on UNISB building in I. Gundulić Street (front plan, south side)

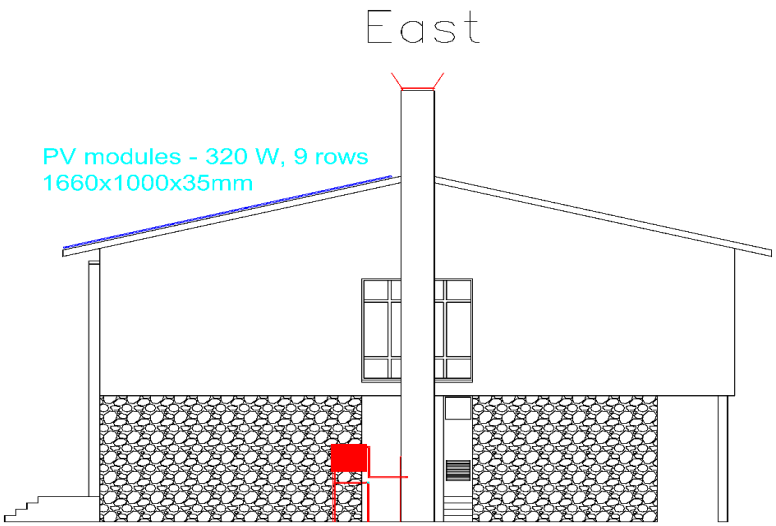

Figure 6.47 PV arrays of Photovoltaic power plant on UNISB building in I. Gundulić Street (front plan, east side)

Figure 6.48 Inverters of Photovoltaic power plant on UNISB building in Laboratory for renewable energy sources

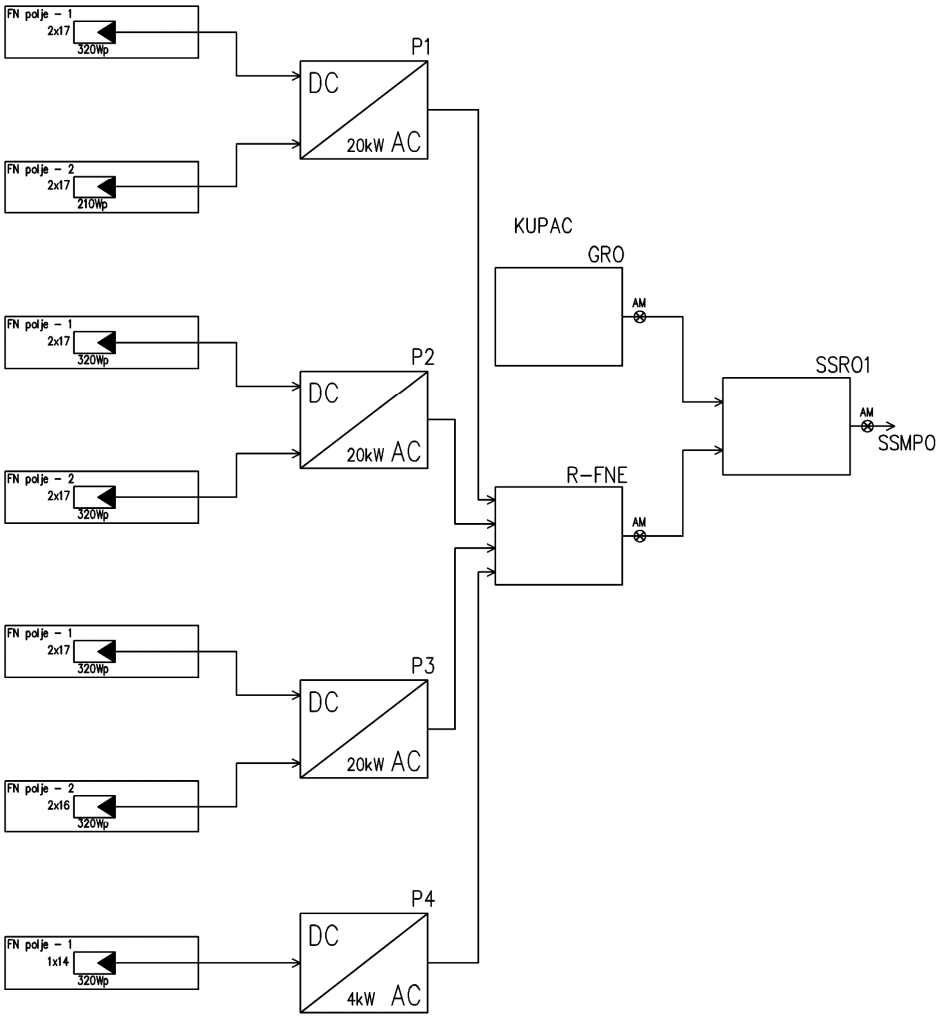

Figure 6.49 Connection scheme of Photovoltaic power plant of UNISB building

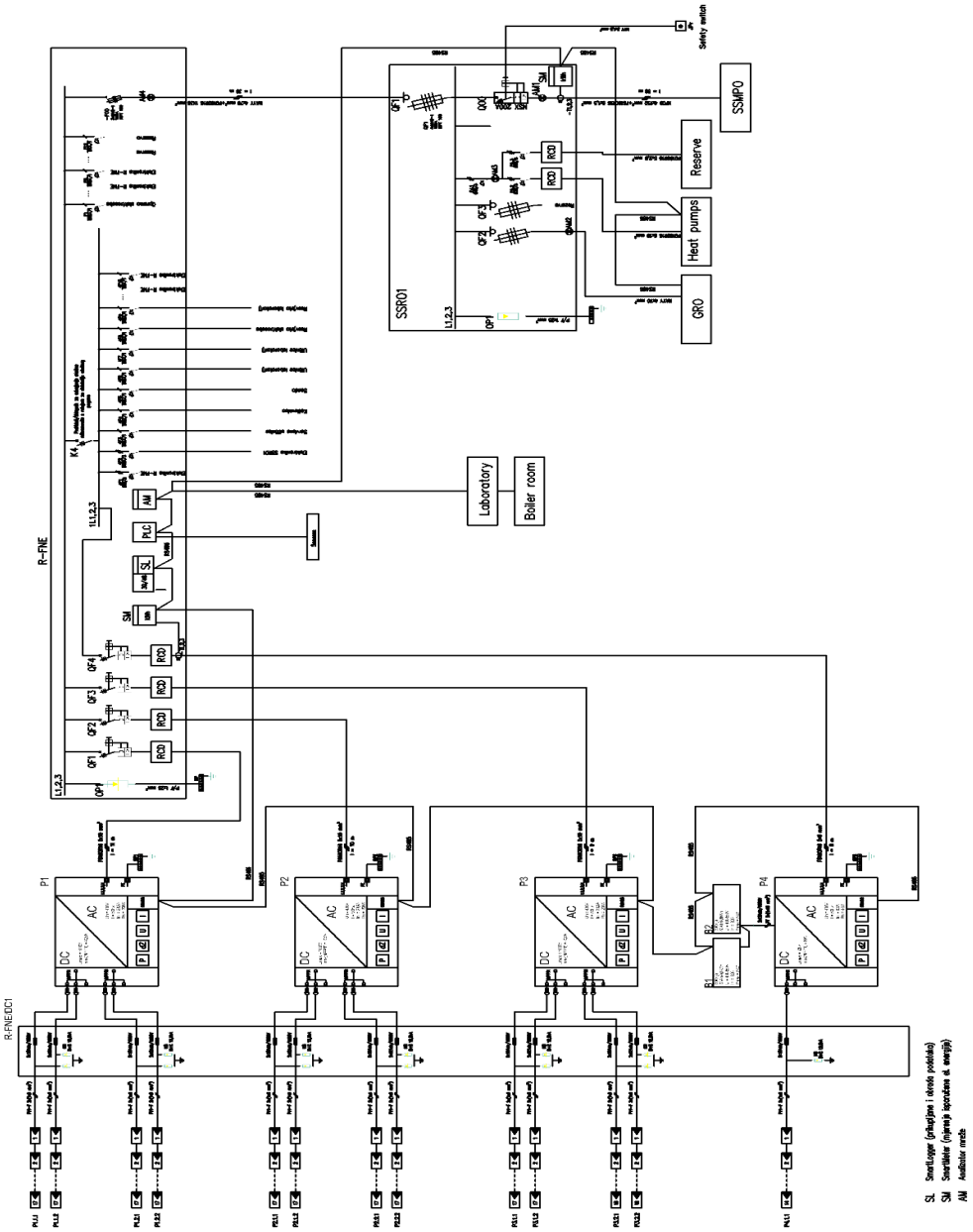

Figure 6.50 Single-pole electric scheme of main cabinet of Photovoltaic power plant UNISB

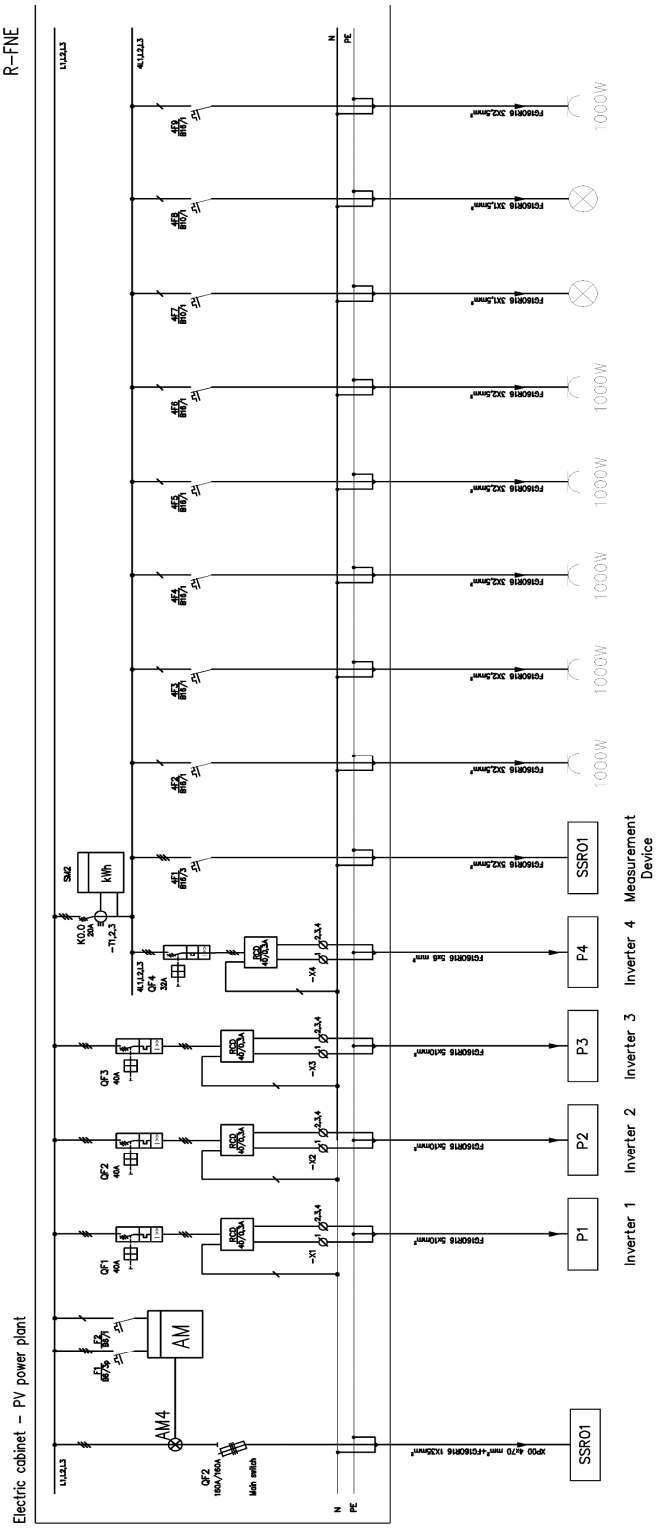

Figure 6.51 Single-pole electric scheme of main cabinet of Photovoltaic power plant UNISB

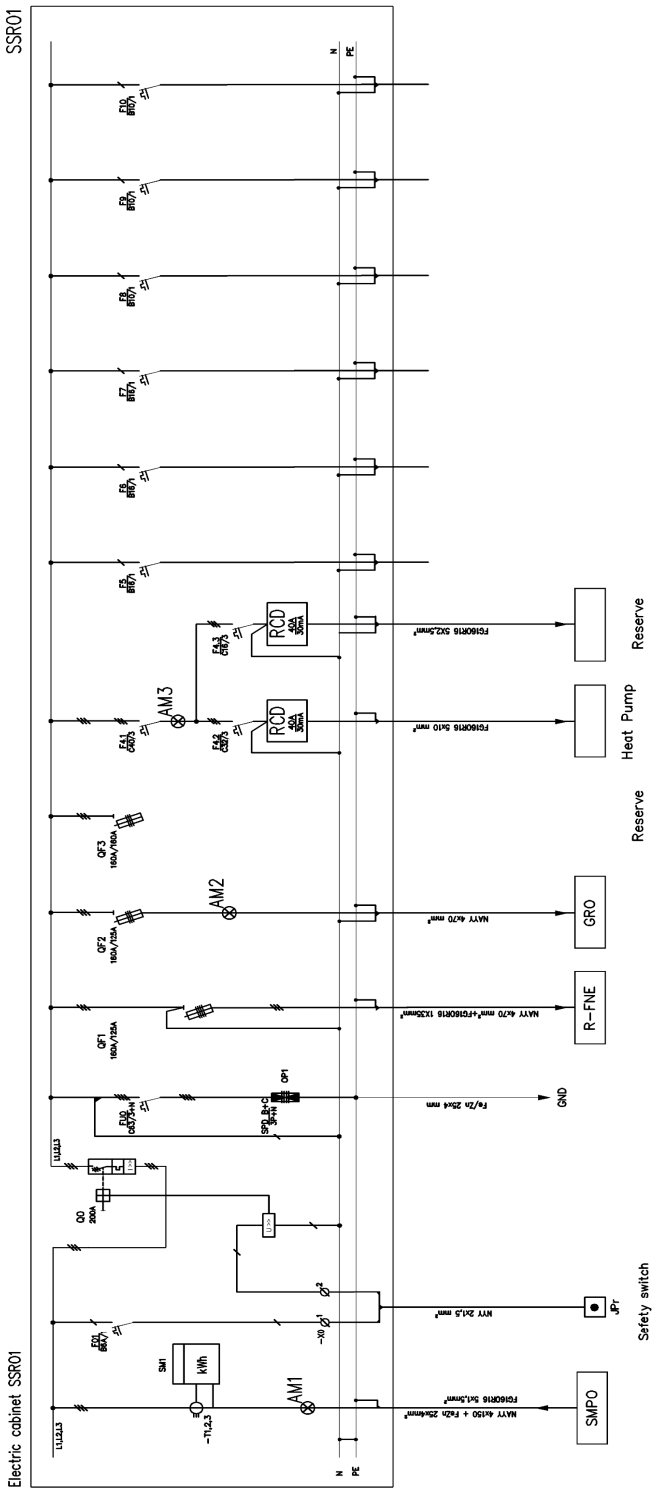

Figure 6.52 Single-pole electric scheme of main outdoor cabinet (SSRO1) of UNISB building

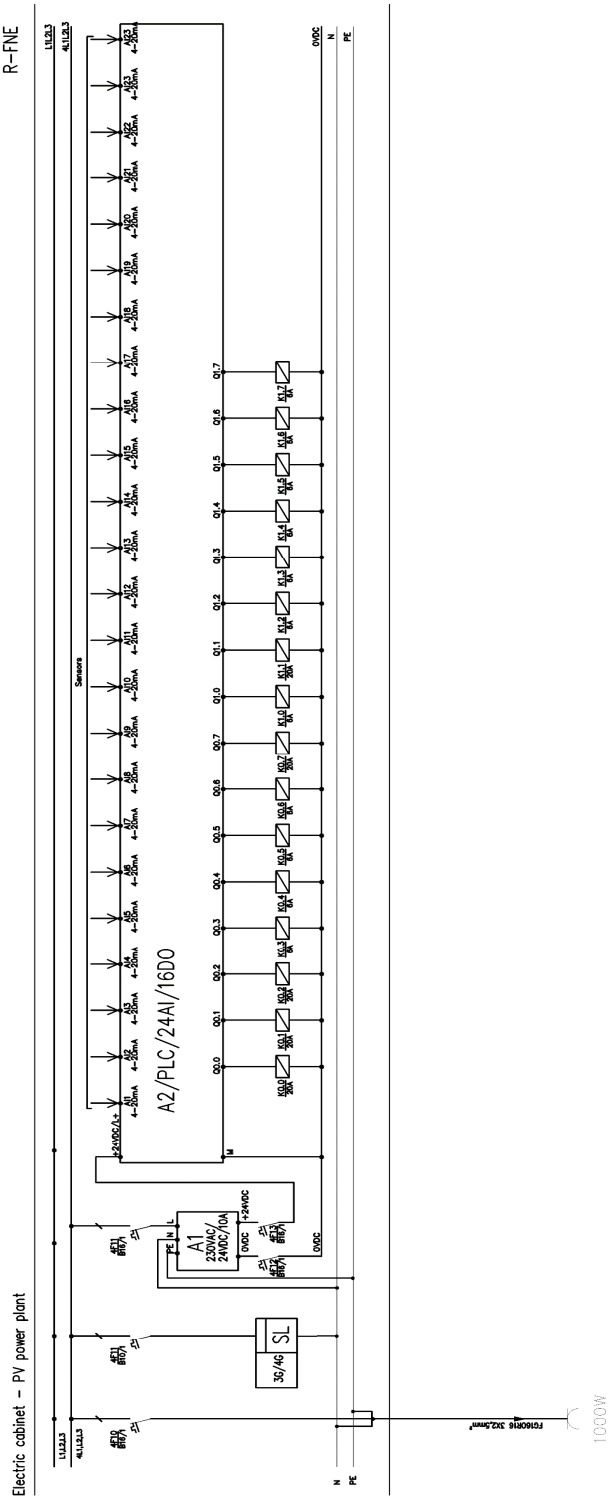

Figure 6.53 Single-pole electric scheme of hardware for BEMS (PLC) - UNISB building

6.5.2. Technical description of thermotechnical system with heat pump and solar collectors at UNISB, Gunduliceva 20A

General data

The thermo-technical system is intended for heating / cooling part of the rooms on the first floor in the building of the Faculty of Mechanical Engineering in Slavonski Brod Gundulićeva 20A. The basic components of the thermo-technical system, heat / cooling energy sources, are plate solar collectors and air-water heat pumps. The nominal output power of the four heat pumps heating is 64 kW and the nominal output power of the four heat pumps cooling is 56 kW. Heat pumps are placed next to the building on the south side on a suitable solid concrete base in accordance with applicable regulations and safety measures. 18 solar panel collectors were installed vertically in one row at an angle of 63°. Heating / cooling of individual rooms in the building is provided by floor and ceiling fan coils connected by a four-pipe heat / cooling energy supply system. For higher energy efficiency, a vertical insulated storage tank with a volume of V = 1000 litres with two tubular heat exchangers installed, with the purpose of accumulation - compensatory action during the year - round production and consumption of heat / cooling energy.

Devices and assemblies of thermo-technical system

18 plate solar collectors (2005 x 1005 x 85 mm) with an area of 2.02 m^2 were installed vertically in one row at an angle of 63°. The maximum operating pressure is 10 bar and the maximum idle temperature is 213° C.

Four air-to-water heat pumps have been installed. Each rated heating output 16 kW (A7 / W35) at COP = 4.42 and rated cooling output 14 kW (A35 / W18) at EER = 4.27. The working substance is R32. The operating ambient temperature for heating is - 25 - 35° C, and for cooling 10 - 46° C. The leaving water temperature is 15 - 65° C when heated and 5 - 25 ° C when cooled.

An integral part of the heat pump is an insulated storage - compensation tank with a volume of 80 litres and a circulation pump for the distribution of heating / cooling medium to the heat exchanger for heating / cooling the water in the tank.

The insulated heat storage tank with a volume of 100 litres is equipped with a pipe exchanger, ribbed pipes, all connections, sensors and control elements.

Fan convector with all associated control and management elements and protective mask and with thermostatic control devices with several fan coils in one room and are four-pipe versions. Five fan coil units are of the ceiling version and two floor fan coil units.

All heating medium distribution pipelines to the consumer are designed in a way that each collector and each heat exchanger have approximately the same hydraulic energy distribution conditions. The distribution of the heating medium from the solar collectors to the consumers will be carried out by a circulating pump with all the associated elements.

The heating medium from each heat pump will be distributed to the heat exchanger by a circulating pump.

In each circulation circuit of the heating medium of the installation, a closed membrane expansion vessel maintains the static pressure in the installation and accept thermal dilatations due to temperature changes of the heating medium. The static pressure of the heating medium in the circulation circuit of the heat pump is p = 1.5 - 1.8 bar, in the circulation circuit of the heating medium of the solar installation p = 4 - 4.5 bar and in the circulation circuit of the heat / cooling energy consumer 1.5 - 2 bar.

Electrical installation with all necessary technical and safety protective elements is designed in accordance with applicable regulations and standards. Earthing of all metal surfaces were performed in accordance with the rules of technical practice, standards and applicable regulations.

Functionality and regulation of heating and cooling

The speed of heating / cooling in the building is harmonized with the cascade switching of drive devices with the lowest possible frequency of peak energy loads.

Solar collectors and heat pumps participate in the regulation and management, conditioned by the leading variables (indoor and outdoor air temperature), the order of priorities and supplementing energy needs, in creating thermal balance.

Primary heating of water in the tank is carried out using solar collectors. If the temperature of the heating medium in the supply line of the solar collector circuit determined by the bearing sensor on the pipeline is about 10 - 15° C higher than the water temperature in the tank, the water is heated by solar collectors and the solar circuit circulating pump distributes the heating medium to the heat exchanger until the set water temperature in the tank is reached. If this condition is not met or this temperature difference cannot be fully achieved until the set water temperature, the heat pumps start to function.

Room heating by means of a fan coil is switched on by a thermostat with adjustable values of the room air temperature. The thermostats in both rooms are placed at the reference points of the sensitivity of the internal air temperature without the direct influence of other heat sources on the sensing device.

Maintaining the set room air temperature in winter and summer is carried out by achieving the appropriate temperature of hot water or cold water in the circulation circuits. Comparing the outdoor air temperature with the set value of the indoor air temperature, the temperature of hot or cold water in the flow line of each circulation system is maintained by the action of a three-way mixing electric motor control valve installed in front of the circulation pump. Depending on the winter or summer period, the corresponding circulation pump or the corresponding control circuit will be in operation.

The functionality of room heating or cooling control circuits is directly related to the storage tank of heat / cooling energy of a certain water temperature and the function of

individual heat sources in accordance with the envisaged priority of switching on and using renewable energy sources.

Main parts of thermotechnical system along with schematics are given in Figure 6.54, Figure 6.55, Figure 6.56, Figure 6.57, Figure 6.58, Figure 6.59, Figure 6.60, Figure 6.61 and Figure 6.62.

Figure 6.54 Heat pumps installed in front of the UNISB building

Figure 6.55 Vertical insulated storage tank in the UNISB building

Figure 6.56 Devices of thermo-technical system in the UNISB building

Figure 6.57 Fan converters of thermo-technical system in the UNISB building, G111

Figure 6.58 Fan converters of thermo-technical system in the UNISB building, corridor

Figure 6.59 Outdoor thermo-technical system of the UNISB building

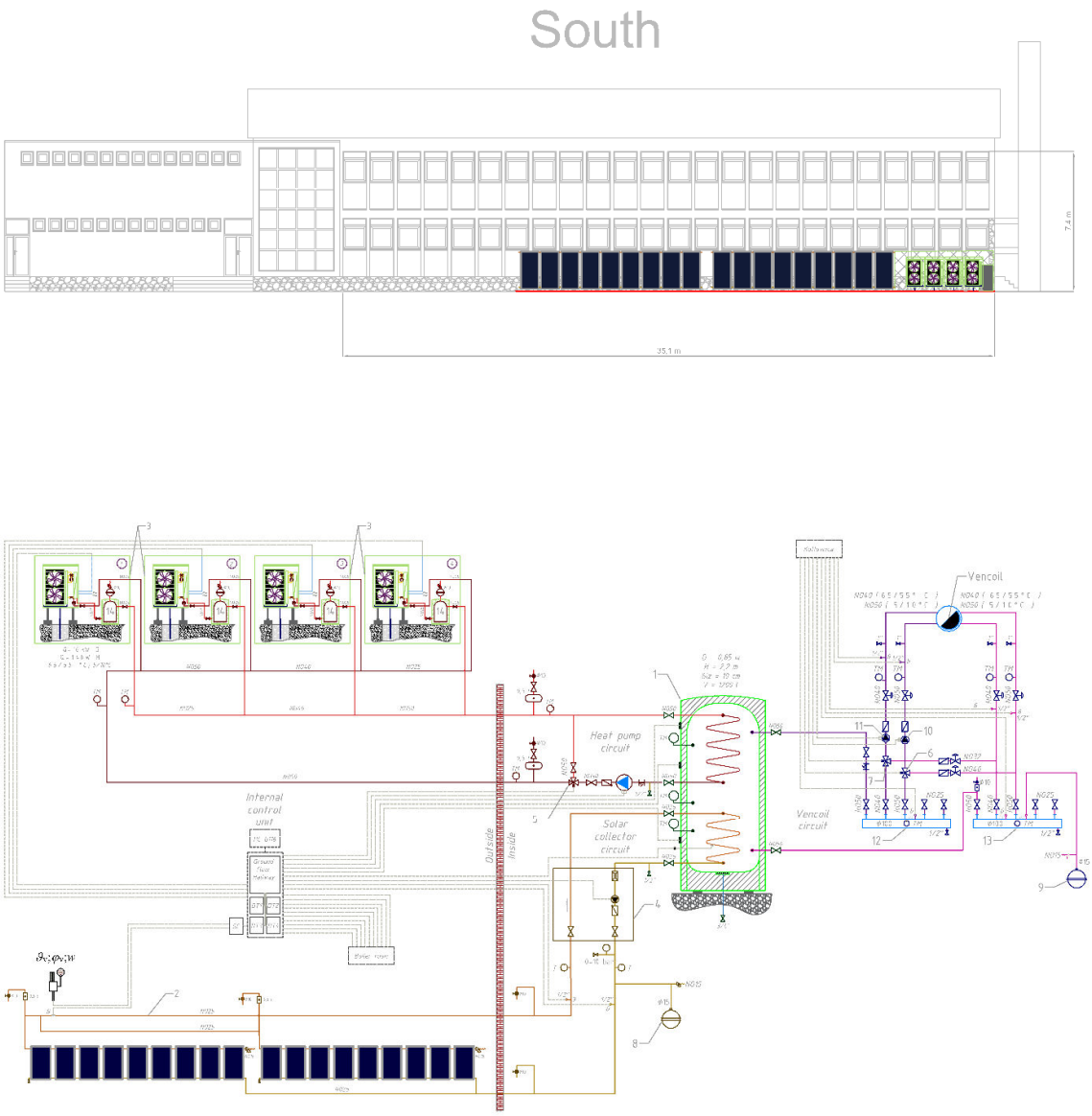

Figure 6.60 Scheme of thermo-technical system of the UNISB building

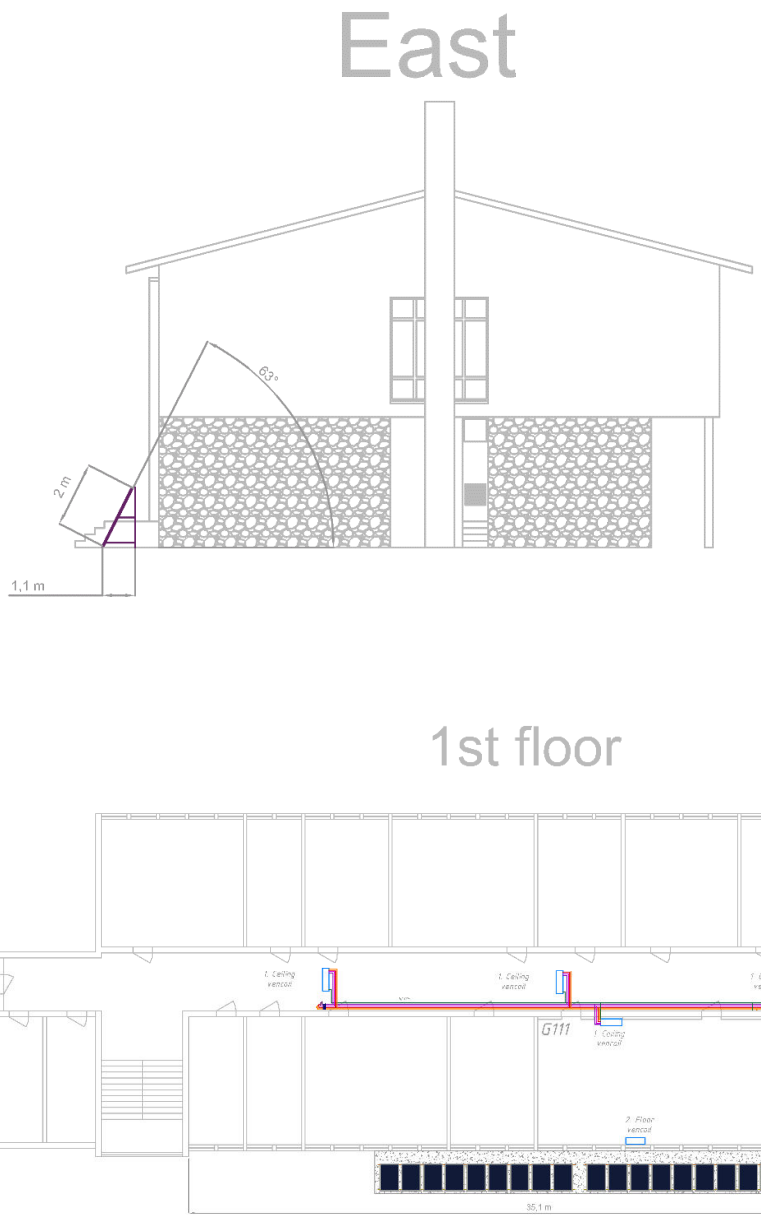

Figure 6.61 Fan converters inside the UNISB building

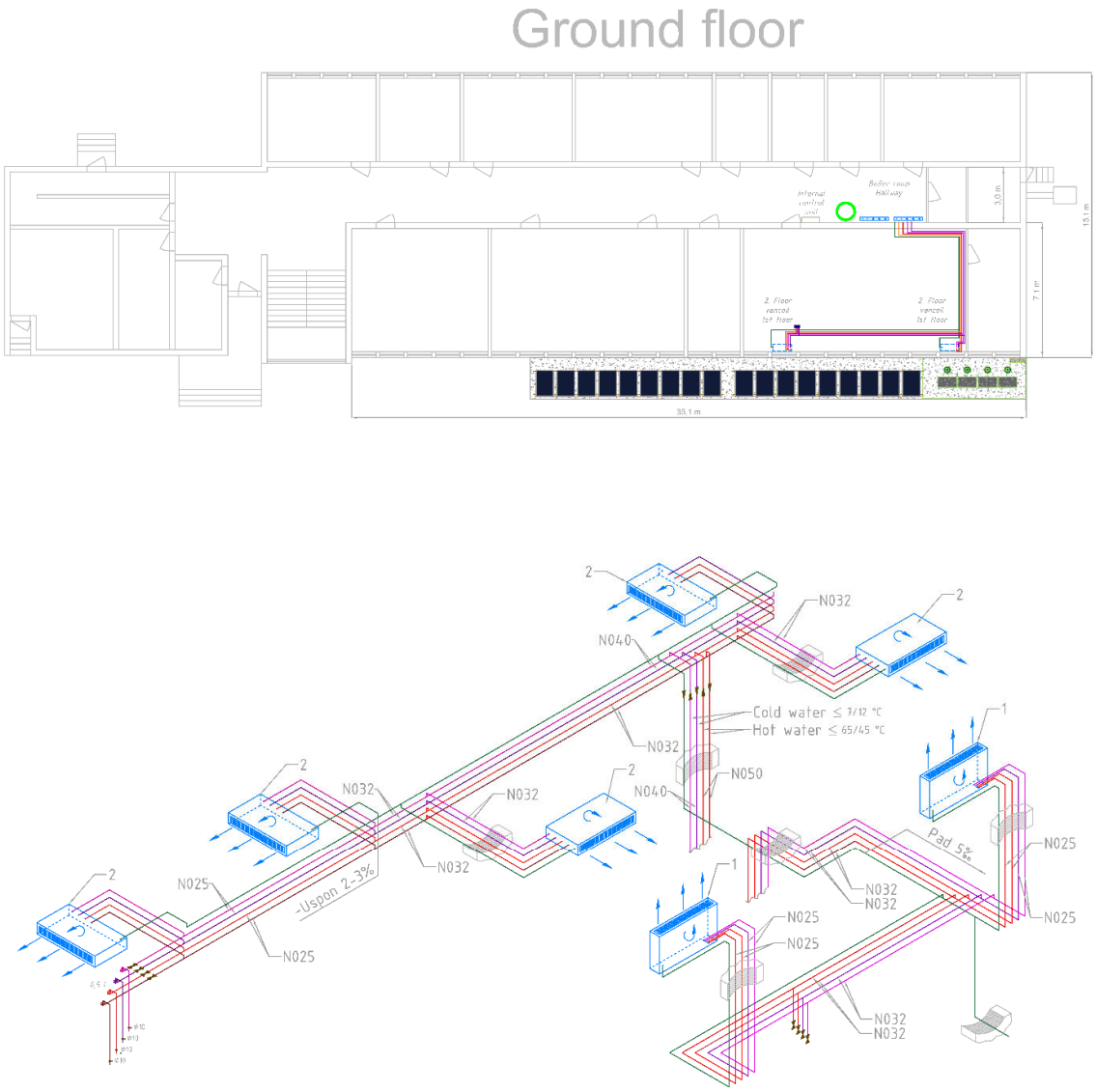

Figure 6.62 Connection scheme of fan converters inside the UNISB building

7. Building energy management systems for the exemplary facilities

7.1. FTN building energy management system

Building energy management system controls and monitors mechanical and electrical equipment in the “Mašinski institut” building in order to provide optimal control of all subsystems, with special emphasis on finding the optimal energy management strategy. To achieve this, real-time measurements of important data are necessary. This is usually done using smart meters. Collected data are saved both on the local data center and on the cloud-based repository system. Traditionally, PC-based SCADA systems are used to locally control and monitor all important parameters in real-time.

Two types of smart power meters are used - Siemens Sentron PAC 3220 and PAC 4200, shown in Figure 7.1. These smart meters are reliable industrial devices that meet all requirements for adequate BEMS operation. These PAC devices have Modbus TCP/IP communication capabilities and therefore enable easy, reliable and real-time data transfer. PAC devices are connected to the PLC units that preform the data requests, gather data, perform necessary calculations, log data locally and to the cloud-based repository system, and display real-time data on SCADA interface. One PLC unit, with signal boards with additional inputs and outputs, is shown in **Error! Reference source not found.**.

Figure 7.1 Installed Siemens Sentron smart power metes.

Figure 7.2 Installed PLC unit with additional signal boards.

Operational data are measured by installed sensing equipment or provided by installed power electronic devices. Regardless, all these devices communicate through Ethernet, Profinet, Profibus or Modbus protocols.

SCADA system was developed using latest Siemens WinCC RT software. Since both hardware and software are from the same manufacturer, easy commissioning and fault-free operation is expected. Besides, real-time monitoring and logging developed SCADA system enables active control over the systems. This means that SCADA system enables operation control, turning the system on or off as necessary, monitoring and dealing with warnings and alarms, without the necessity for physical contact with the systems. Working station from which the SCADA system is used is shown in Figure 7.3.

Figure 7.3 SCADA system working station.

Two different SCADA systems were implemented – one is based on the Siemens software, as mentioned previously, while the other is based on the inVIEW SCADA platform and displayed in web browser. inVIEW Web SCADA allows end-users to easily and efficiently develop applications for remote monitoring and control of industrial systems. Main screens of these two SCADA systems are shown in Figure 7.4 and Figure 7.5, respectively.

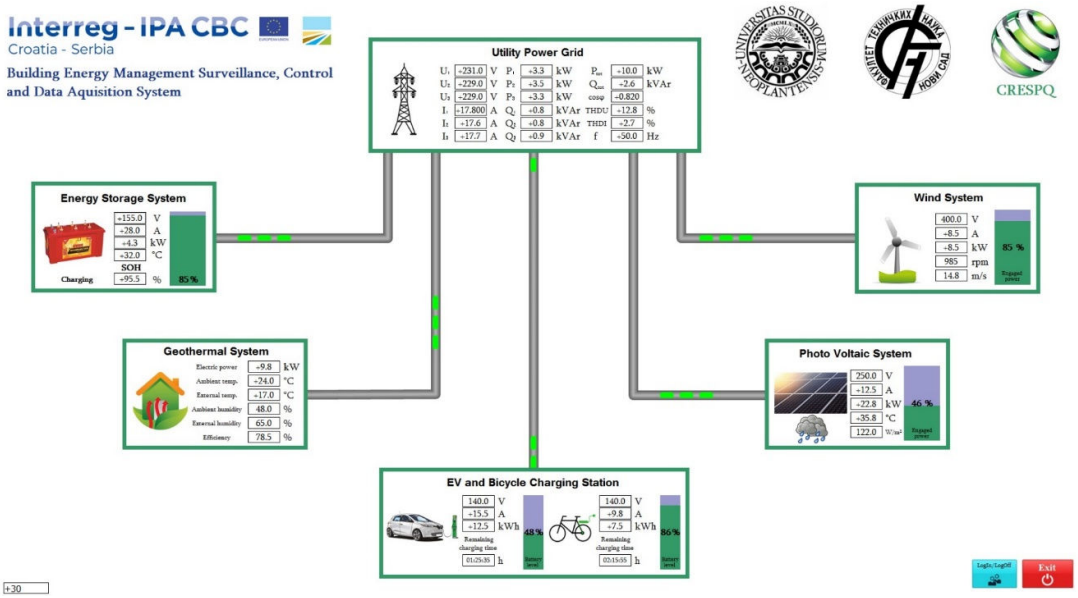

Figure 7.4 Main screen in Siemens SCADA system.

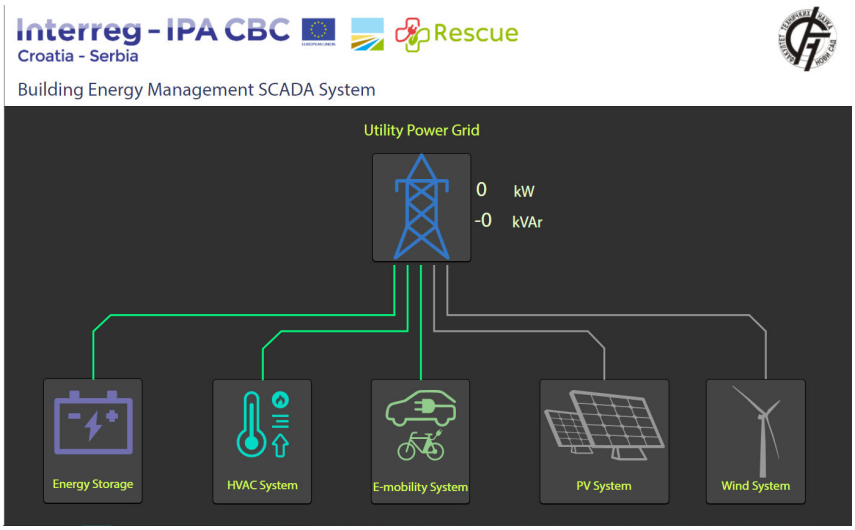

Figure 7.5 . Main screen in inVIEW Web SCADA system.

7.2. KCV building energy management system

Building Energy Management system for KCV complex is mainly based on active, real-time measurement of electric and other parameters by using smart, industrial grade meters. The measured information is then gathered and logged on the local data center, but also the logged data is saved on the internet based storage system. The operational parameters of all systems can be monitored locally in real-time through the use of developed PC based SCADA system.

For measuring electrical parameters of the systems inside KCV complex Siemens Sentron PAC 3200 and PAC 4200 smart power meters are used. Exemplary PAC unit is shown in Figure 7.6. These PAC devices have Modbus TCP/IP communication capabilities thus enabling easy, reliable and real-time data transfer.

Figure 7.6 Siemens Sentron smart power meter

Used configuration assumes a number of PAC devices being connected with PLC unit though industrial switch. The PLC unit preforms the data requests, gathers data, performs necessary calculations, logs data locally and in internet based storage, and displays real-time data on SCADA interface.

Other types of data, like insolation, flow, pressure and temperature are obtained either from dedicated sensors or for example from inverters containing the necessary process information. Again all these devices are in terms of communication connected with PLC through Ethernet, Profinet, Profibus or Modbus protocols.

Developed SCADA interface is shown in Figure 7.7, where it can be seen that all systems developed at the KCV complex are visible together with real time process data. SADA system was developed using latest Siemens WinCC RT software for real-time SCADA development. Since both hardware and software are from the same manufacturer easy commissioning and fault-free operation is expected. Besides real-time monitoring and logging developed SCADA system enables active control over the systems. This means that SCADA system enables operation control, turning the system on or off as necessary, monitoring and dealing with warnings and alarms, without the necessity for physical contact with the systems. Working station from which the SCADA system can be used is shown in Figure 7.8.

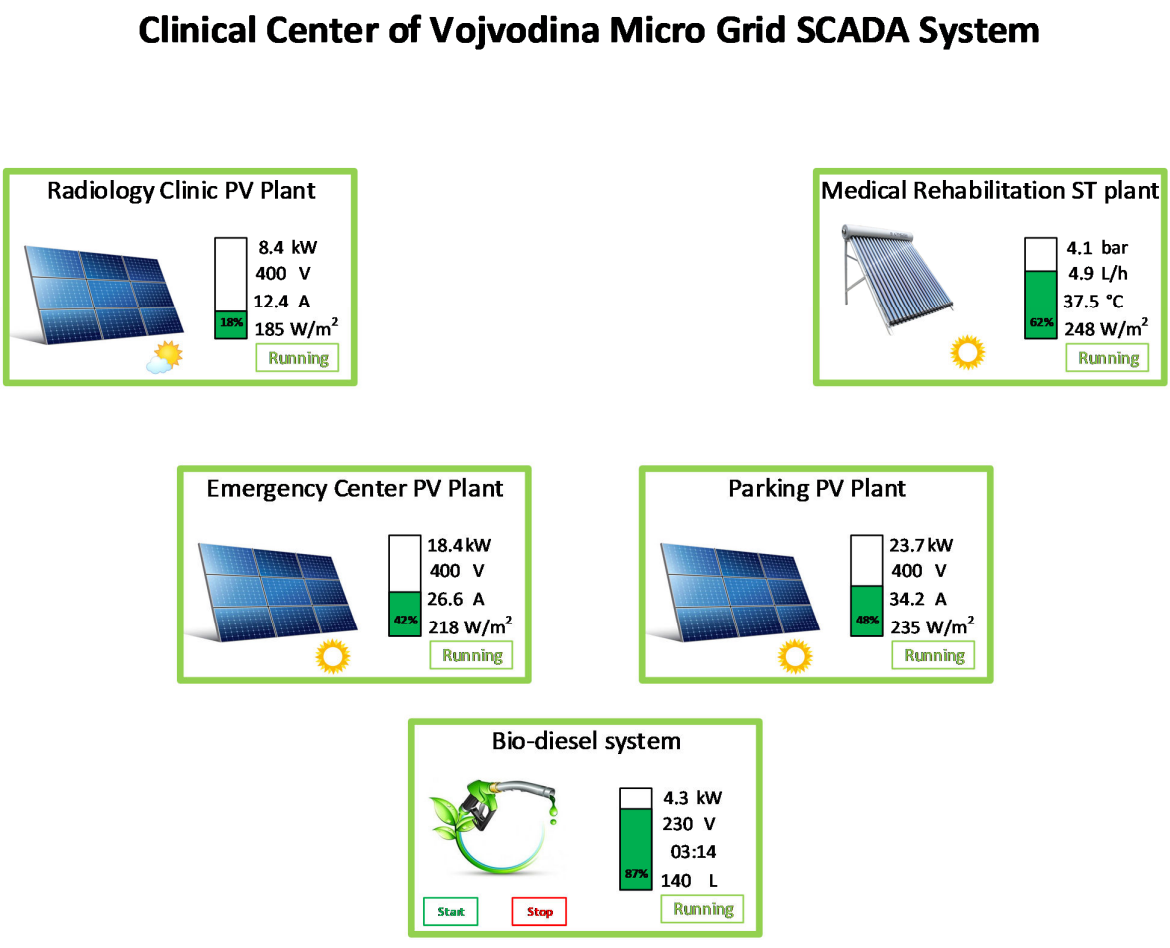

Figure 7.7 SCADA system for monitoring and control of KCV systems

Figure 7.8 SCADA system working station

7.3. FERIT building energy management system

FERIT building energy management system continuously monitors current meteorological parameters at the microlocation of FERIT buildings, generation of electricity by the renewable energy systems and building consumption. General schematic of the building energy management system is given in Figure 7.9. Building energy management system uses Growatt ShineMaster data logger (Figure 7.10). Growatt ShineMaster serves as a central data logger in the system that enables to monitor, analyze, parameterize all managing systems. Data logger enables communication with up to 64 inverters and smart meters over RS485 protocol. Photovoltaic inverters Growatt MID 20KTL3-X and Growatt 10000TL3-S, Growatt smart meters and Growatt weather station is connected to data logger via RS485 communication interface while Growatt SPH 5000TL3-BH hybrid inverters are connected via WiFi interface. Growatt ShineMaster is installed along with ProzaNET SCADA on server. Current meteorological parameters (solar irradiance, ambient temperature, wind speed and module temperature) are measured with Growatt Weather Station installed at the FERIT building roofs.

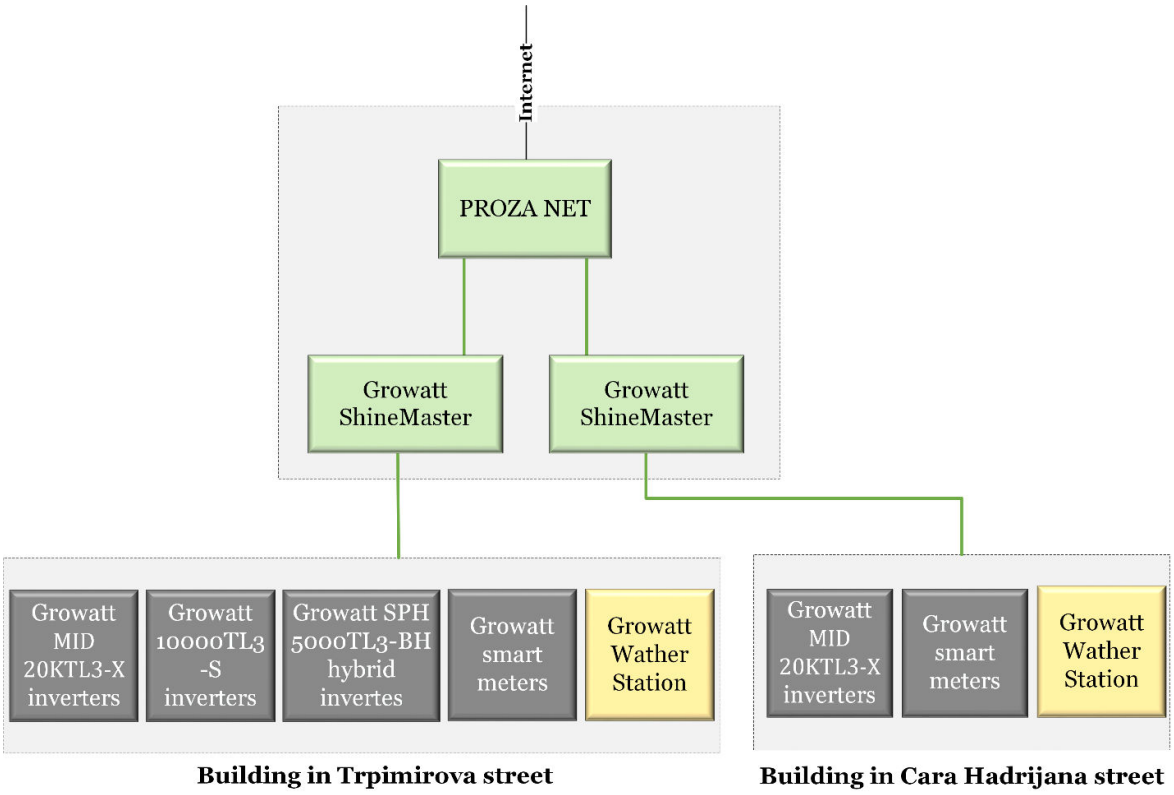

Figure 7.9 FERIT building energy management system schematic

Figure 7.10 FERIT data logger Growatt ShineMaster

Building energy management system also continuously monitors power quality. Monitoring of power quality in FERIT building in Trpimirova street is performed using network analyser PQube 3. This instrument is for both monitoring and diagnosing issues with electric power systems and sensing environmental conditions, helping to quickly solve problems that impact the quality and reliability of product or process. This compact instrument is the power monitor and real-time sensor. It records every type of AC power disturbance - including 4 MHz sampling of impulses - and it is an IEC 61000-4-30, edition 3 Class A certified, ultra-precise energy meter. It monitors up to two three-phase loads, or eight single-phase loads with a single instrument. Records environmental data - such as temperature, humidity and barometric pressure, vibration, 3-axis acceleration - as well as process parameters, including torque, RPM, fuel level, water flow, and more. It is a unique combination of the best features of a power disturbance monitor, a power/energy meter, a process and environmental data logger, and a digital fault recorder. It's easy to install, easy use.

FERIT building in Trpimirova street installed three the network analyzer PQube 3. These measurement devices are placed around in the building to collect information about electrical quantities, power quality, production and consumption. The exact position of the measuring points is shown in the single-line diagram in Figure 7.11.

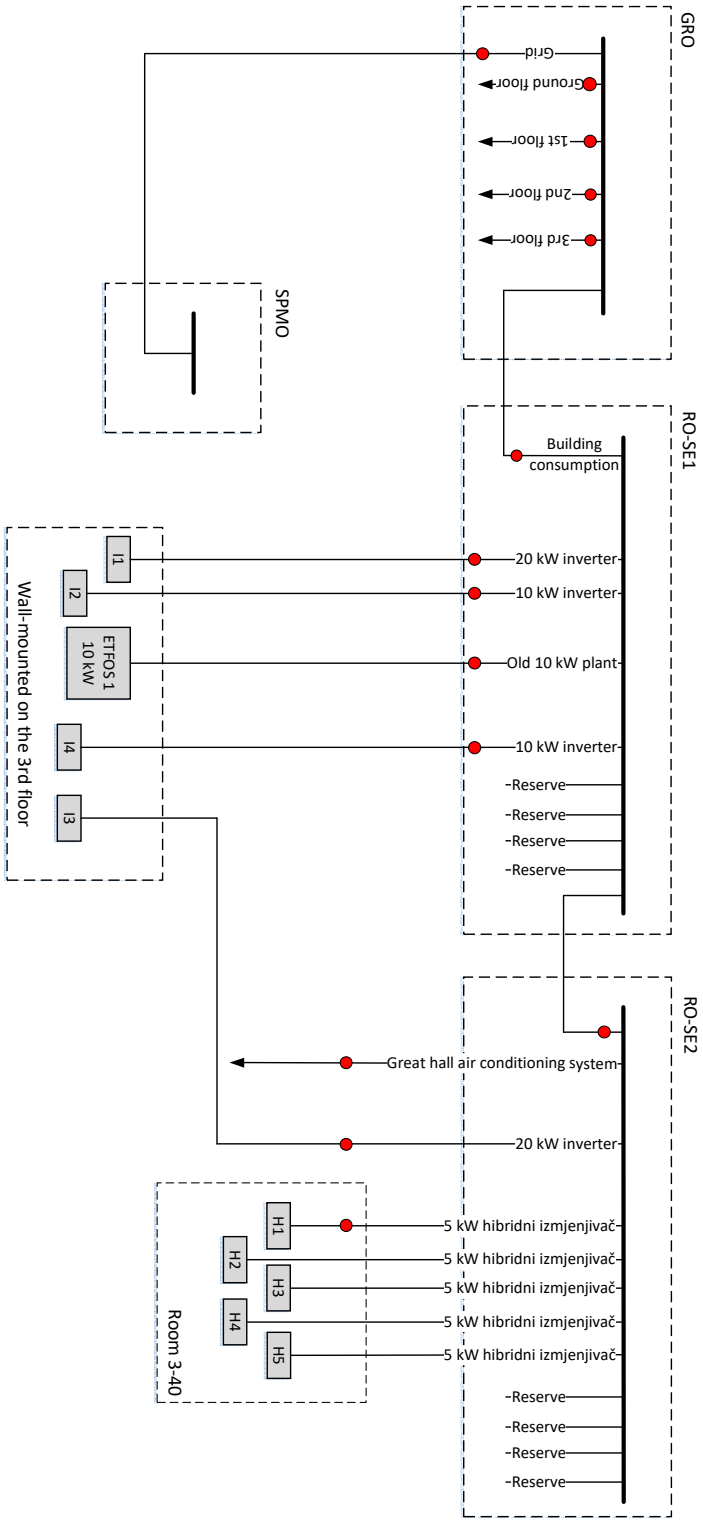

Figure 7.11 Single-line diagram of power quality monitoring in FERIT building in Trpimirova street

Single line diagram represents all power quality measurements point in FERIT building. Respectively, PQ 1 is installed in a separate electrical switchboard (GRO) and is used for measurement:

- Total energy consumption from utility grid: at this measurement point device records all power quality data of electricity we export to the public utility grid or import from the grid.
- Total energy produced: at this measurement point, device records the production power quality of electricity from photovoltaic systems and from the renewable energy storage system.
- Total energy consumption of the FERIT building: the device at this measurement point records the production power quality of electricity total energy consumption, more precisely, the device measures what power quality of electricity it takes from the grid. In this point the total energy is the sum of energy from the utility network and the energy produced by the photovoltaic systems or renewable energy storage system.

PQ2 is installed in an electrical switchboard RO-SE1 and he are used for measurement total energy produced by photovoltaic system inverters I_1, I_2, I_3 and $ETFOS_1$. Network analyser PQ 3, installed in electrical switchboard RO-SE2, is used for measurement the point between the microgrid (Figure 7.12) and the distribution power grid. That point we also called the point of common coupling (PCC). Furthermore, the network analyser measures the production of the I_3 hybrid inverter and the consumption of great hall air conditioning system.

Figure 7.12 PQ3 in electrical switchboard RO-SE2

7.4. KBCO building energy management system

KBCO simultaneously monitors current meteorological parameters at the microlocation of the KBCO complex, generation of electricity by the photovoltaic systems and total consumption of the complex. General schematic of the building energy management system is given in Figure 7.13. Generation of the photovoltaic system uses SMA Data Manager M (Figure 7.14) as a central data logger in the system that enables to monitor, analyze, parameterize and manage photovoltaic systems. Photovoltaic inverters and data logger are connected over Ethernet communication interface, even though other interfaces like WLAN and RS485 are available. SMA Data Manager M data logger enables to connect up to 50 inverters with nominal power up to 2.5 MVA. SMA Data Manager M is installed along with Movicon 11 SCADA on server at the TS 10/0.4 kV Bolnica 3 (Maternice/Ginekologija) substation. Consumption of the KBCO complex is monitored at the energy meter location with power analyzer SENECA S711-E power meter installed at TS 10/0.4 kV Bolnica 2 substation connected with Ethernet to the SCADA. Current meteorological parameters (solar irradiance, ambient temperature, wind speed and module temperature) are measured with SMA Sunny Sensorbox installed at the Department of Diagnostical and Interventional Radiology building roof also connected to the SMA Data Manager M.

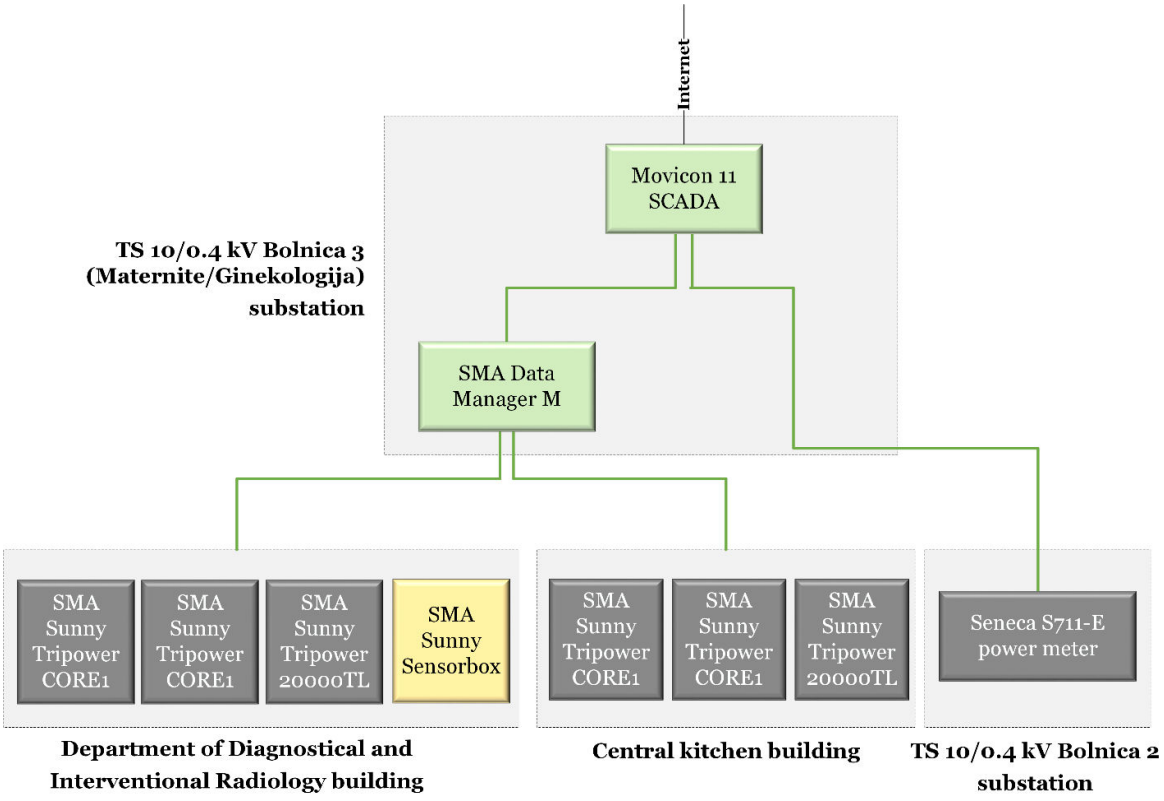

Figure 7.13 KBCO building energy management system schematic

Figure 7.14 KBCO data logger SMA Data Manager M

7.5. UNISB building energy management system

BEMS (Building energy management system) of UNISB building consists of 3 parts: the first part is based on GROWAT's inverter and photovoltaic monitoring system together with battery controller, power quality analyzer and data loggers - in general it is a monitoring system of the electrical part of renewable energy sources and meteorological (outdoor) conditions; the second part displays and stores measurement data on a computer (internal conditions of individual rooms) via temperature sensors in several characteristic offices/classrooms of the building together with PLC and the third part consists of a measurement system that measures, displays and stores basic parameters of thermo-technical system (Figure 7.15).

Figure 7.15 Electric cabinets: PV system (left) and Thermo-technical system (right)

7.6. Results

Since all exemplary objects contain building energy management systems, it is impractical to present all available measurements and results. Figure 7.16 and Figure 7.17 some results of KBCO BEMS, Figure 7.18 and Figure 7.19 present results of FERIT BEMS while Figure 7.20, Figure 7.21, Figure 7.22, Figure 7.23, Figure 7.24, Figure 7.25, Figure 7.26, Figure 7.27, Figure 7.28, Figure 7.29, Figure 7.30 and Figure 7.31 give an overview of UNISB BEMS results.

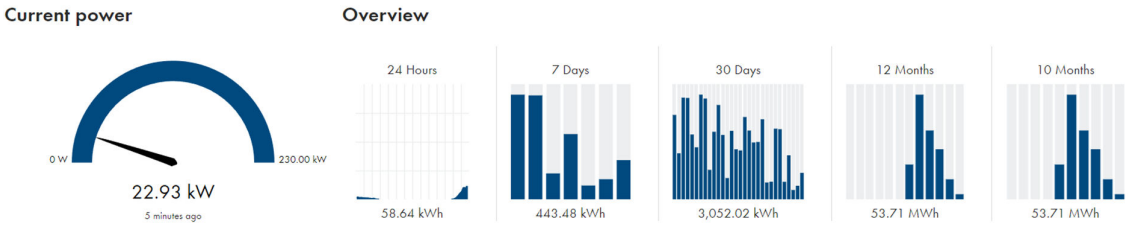

Figure 7.16 KBCO PV systems overview

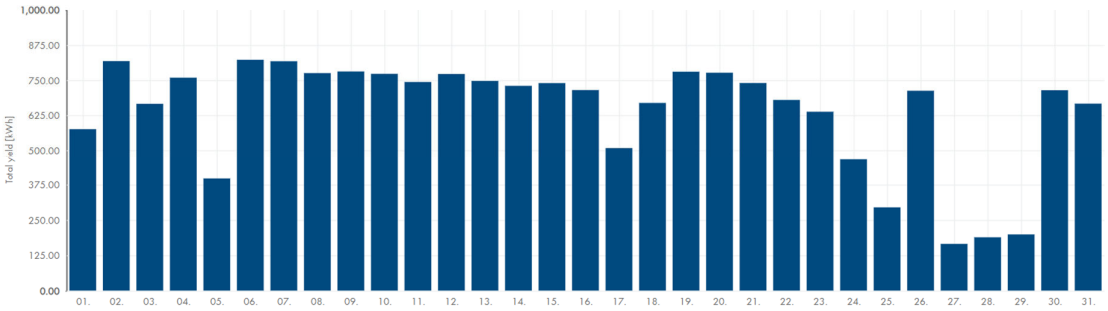

Figure 7.17 KBCO total yield of PV systems in August 2021

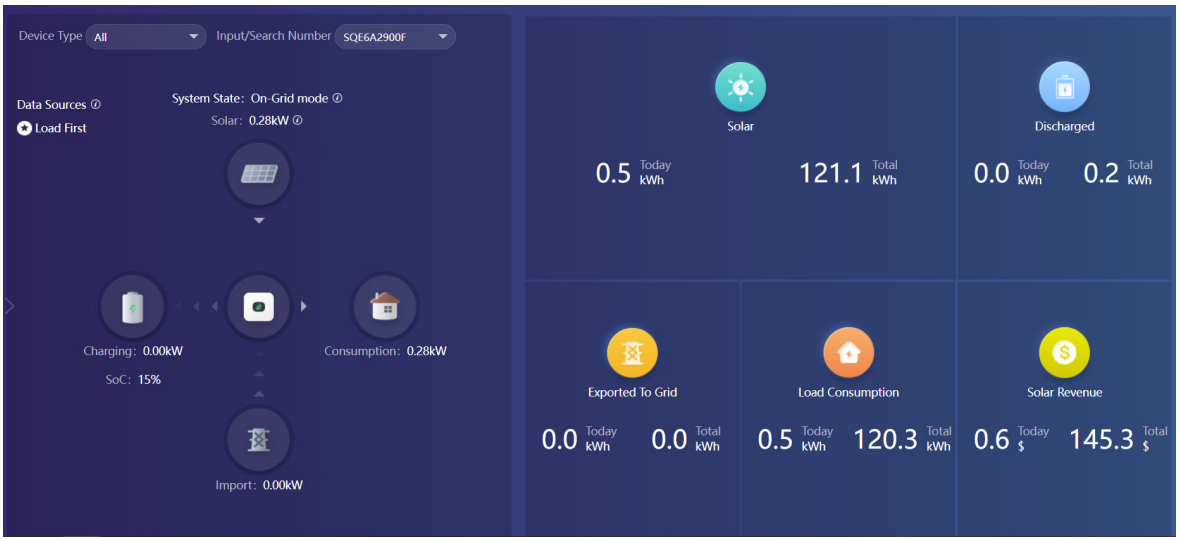

Figure 7.18 FERIT overview of hybrid inverter equipped with renewable energy storage

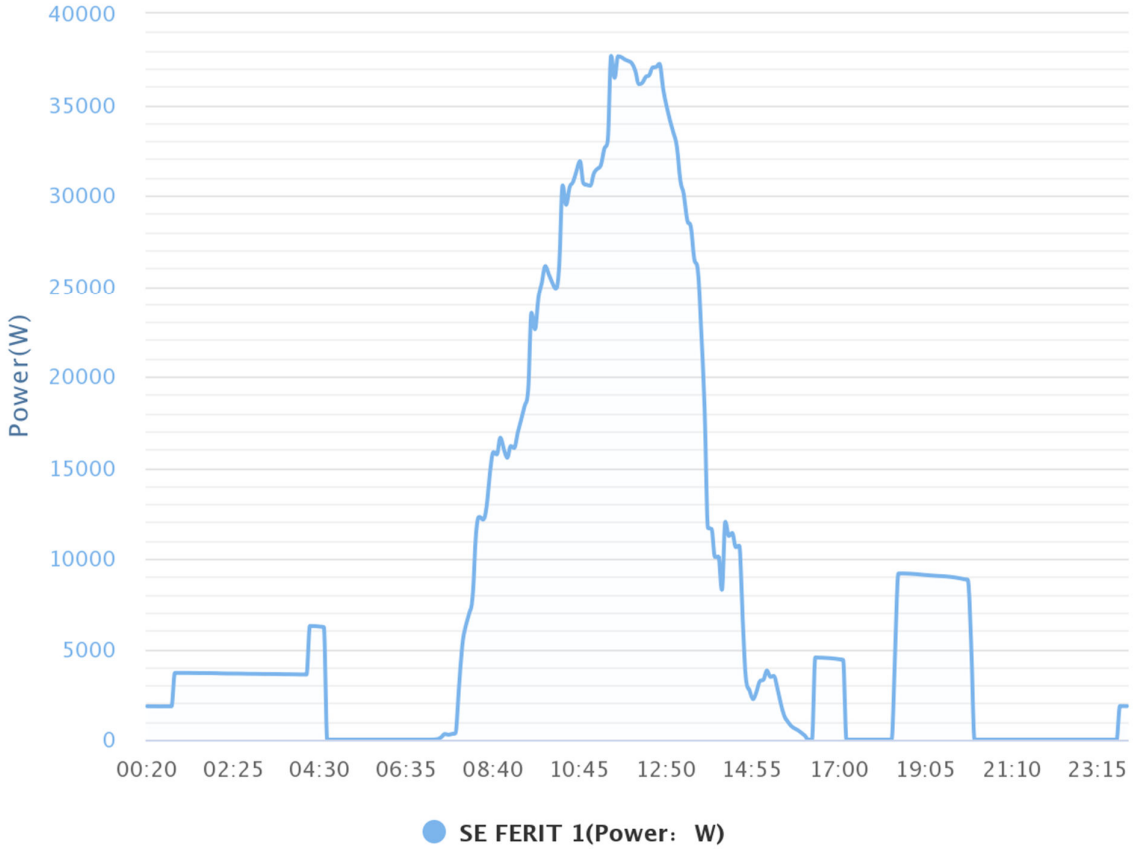

Figure 7.19 FERIT PV system generation profile installed on building on December 20 2021

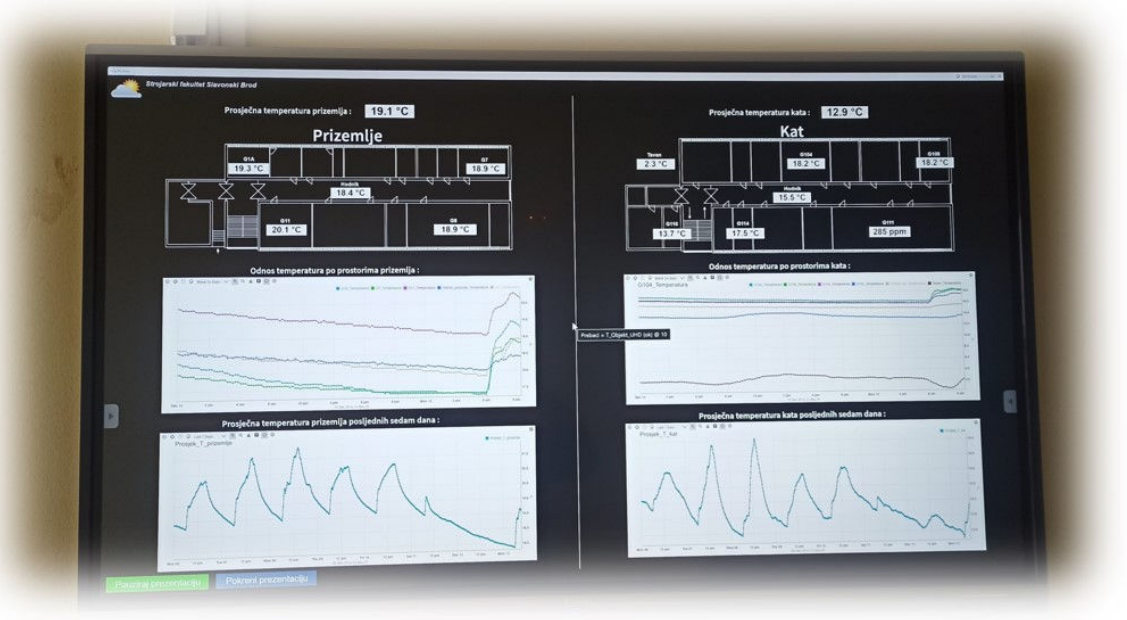

Figure 7.20 Location of temperature sensors inside the UNISB building and their weekly measured data

Figure 7.21 Output power of UNISB PV power plant during cloudy day

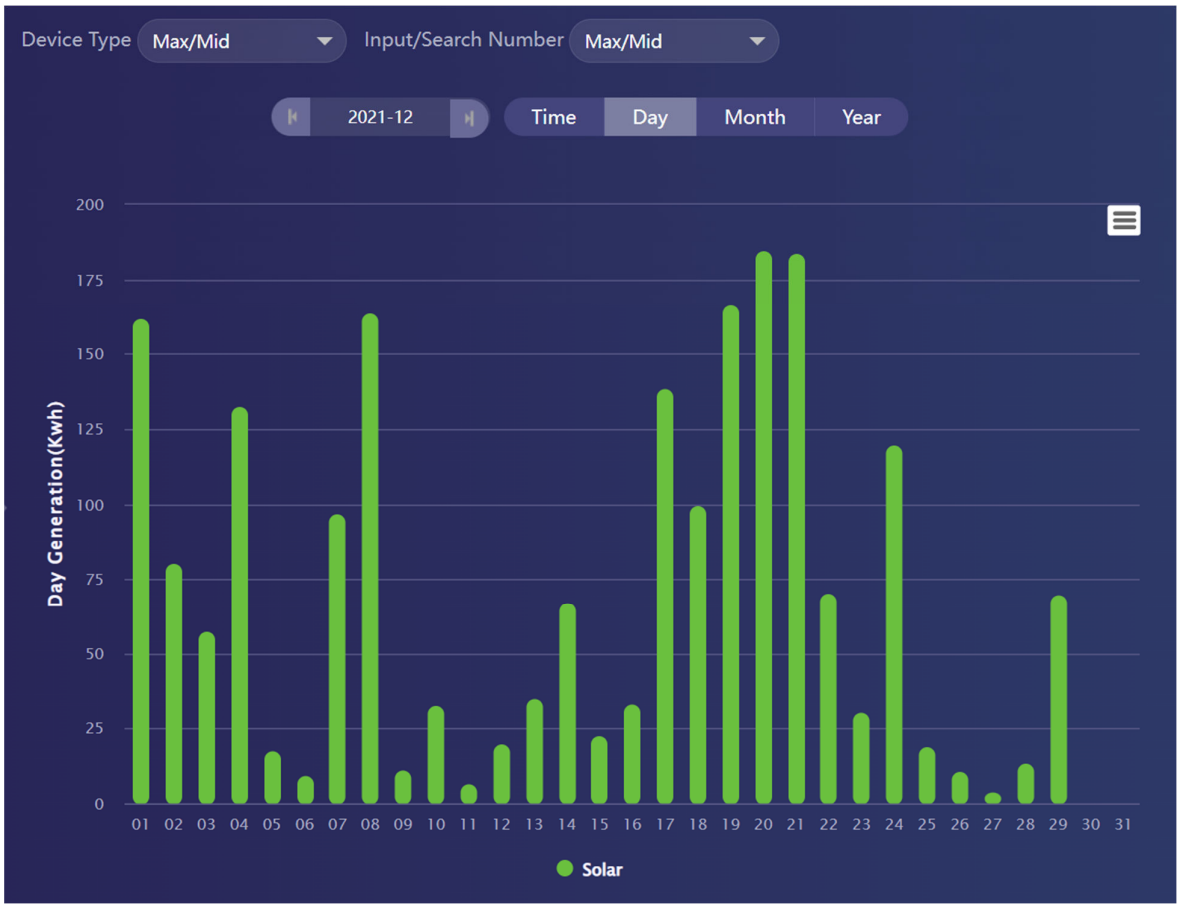

Figure 7.22 Daily generated electric energy of UNISB PV power plant during December 2021

Figure 7.23 Monthly generated electric energy of UNISB PV power plant during 2021.

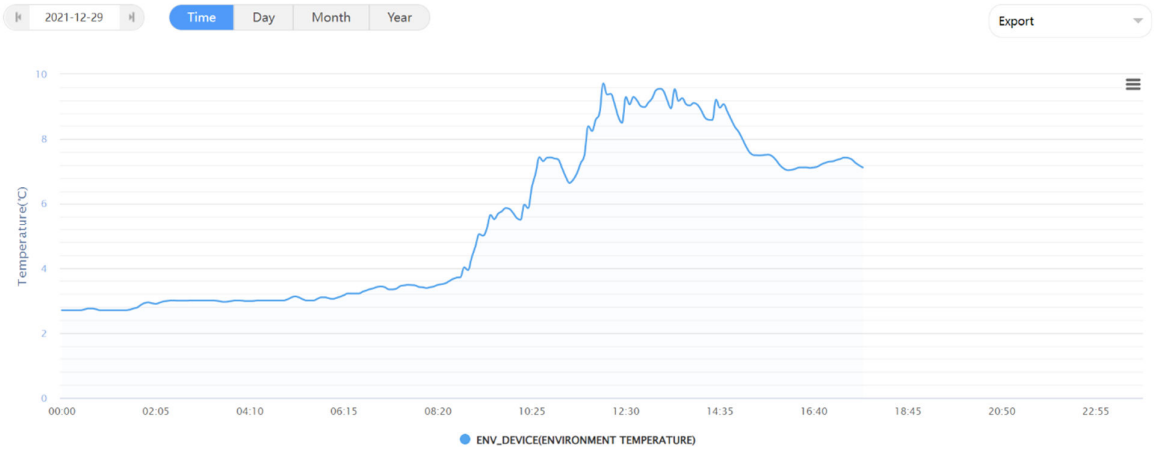

Figure 7.24 Continuosly measured data of outside temperature at the UNISB building during the day

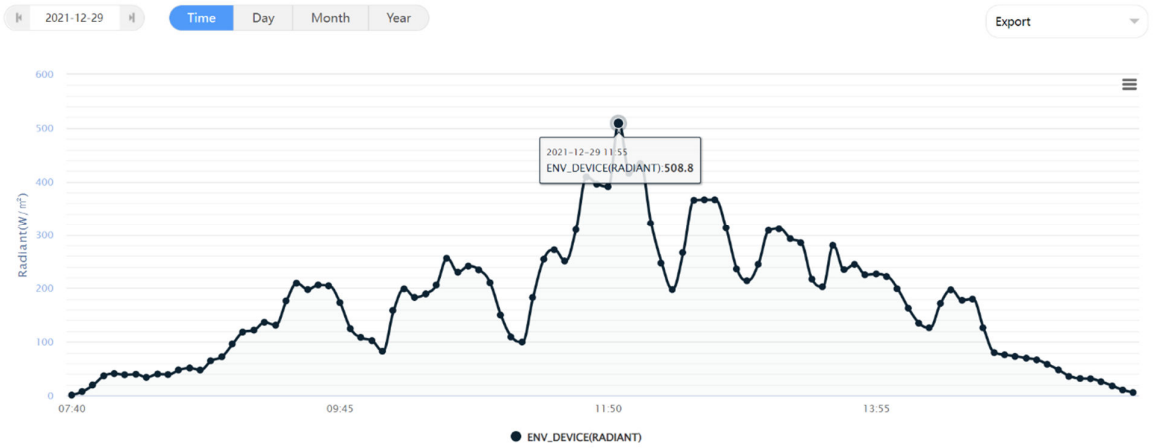

Figure 7.25 Continuosly measured data of insolation at UNISB building during the day

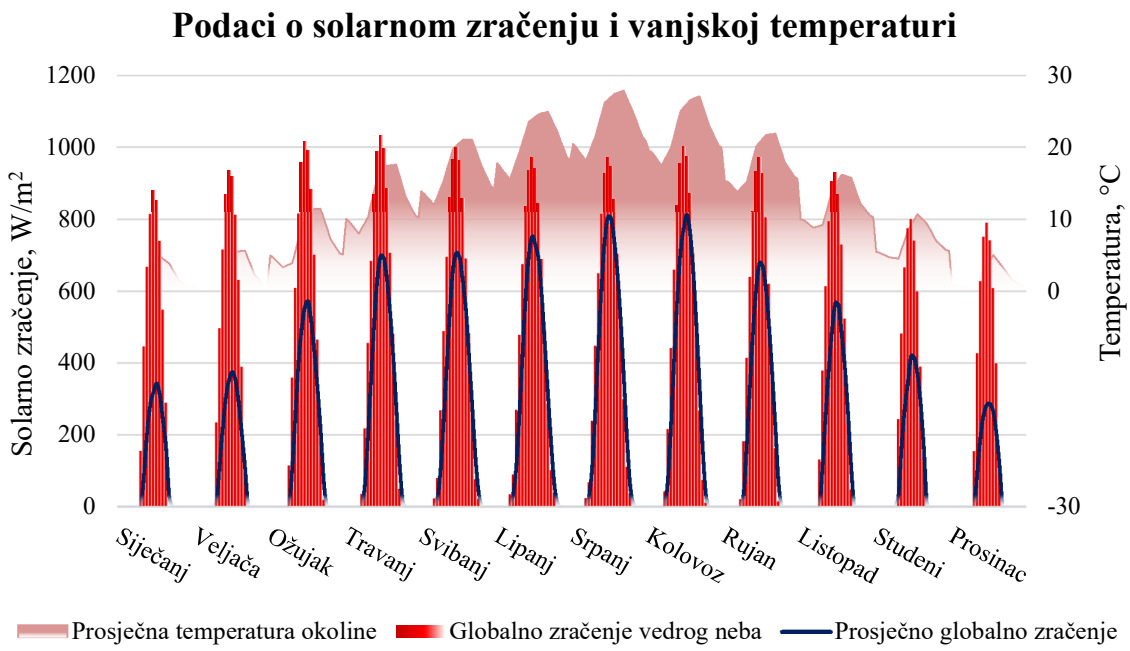

Figure 7.26 Monthly average measured data of insolation and temperature at UNISB building during 2021.

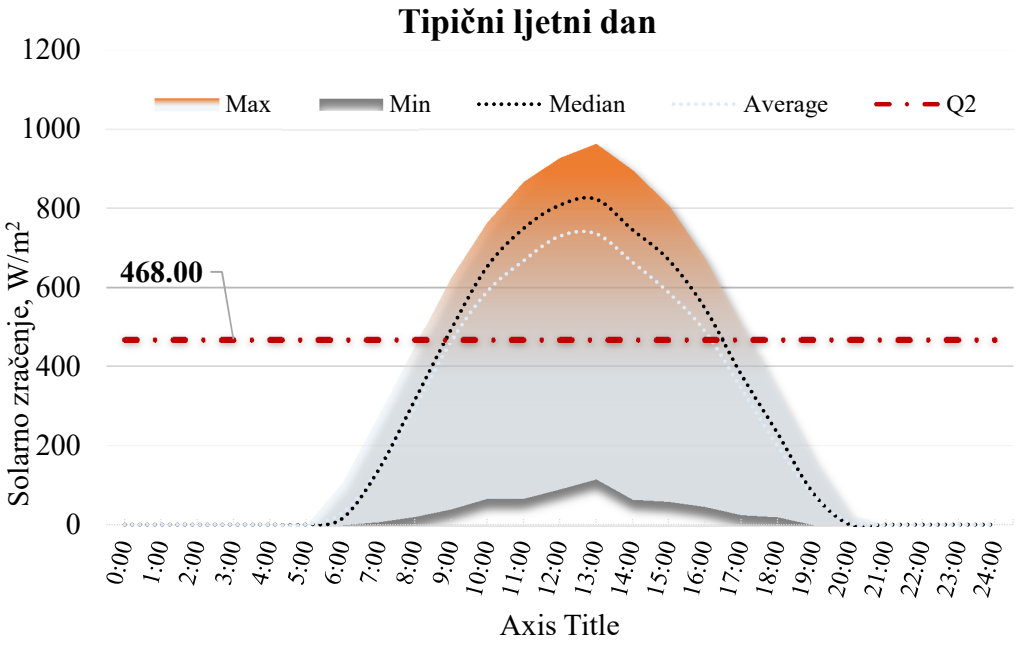

Figure 7.27 Insolation of typical summer day at UNISB building

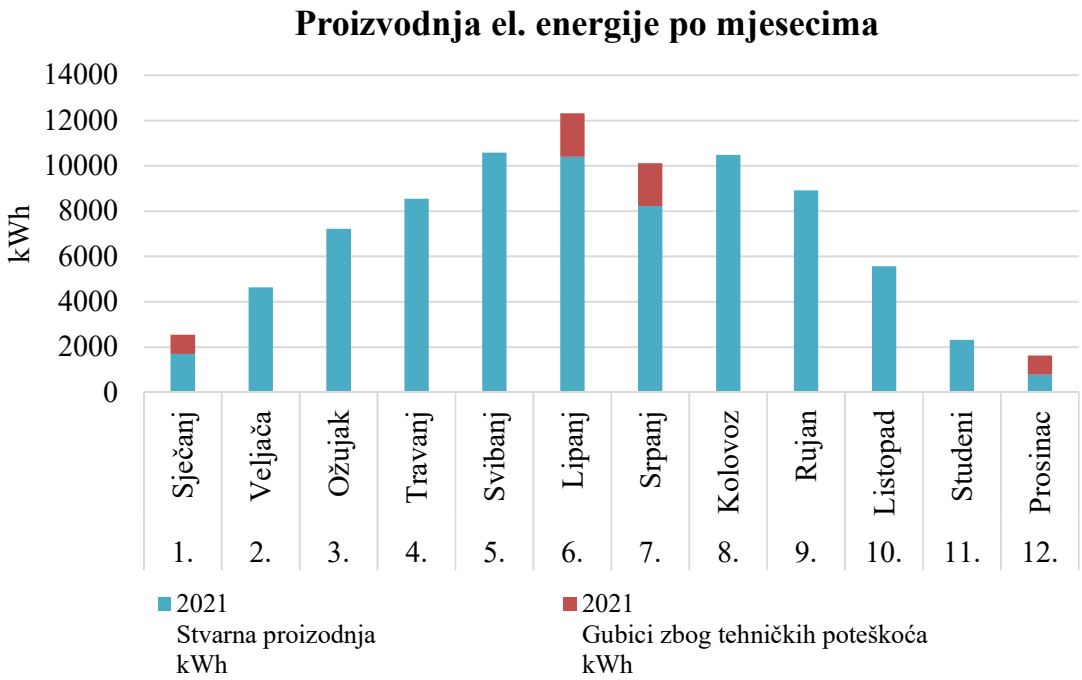

Figure 7.28 Monthly data of electricity generation of UNISB PV power plant measured by network analyzer

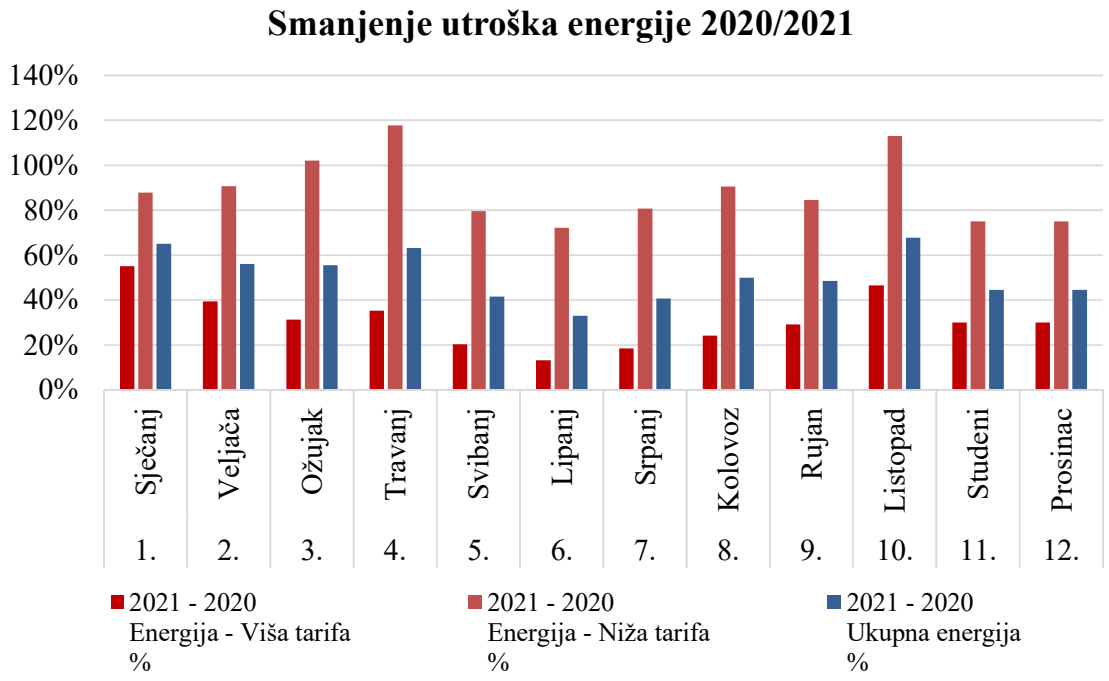

Figure 7.29 Energy percentage monthly savings between 2020. and 2021. (UNISB PV power plant in function)

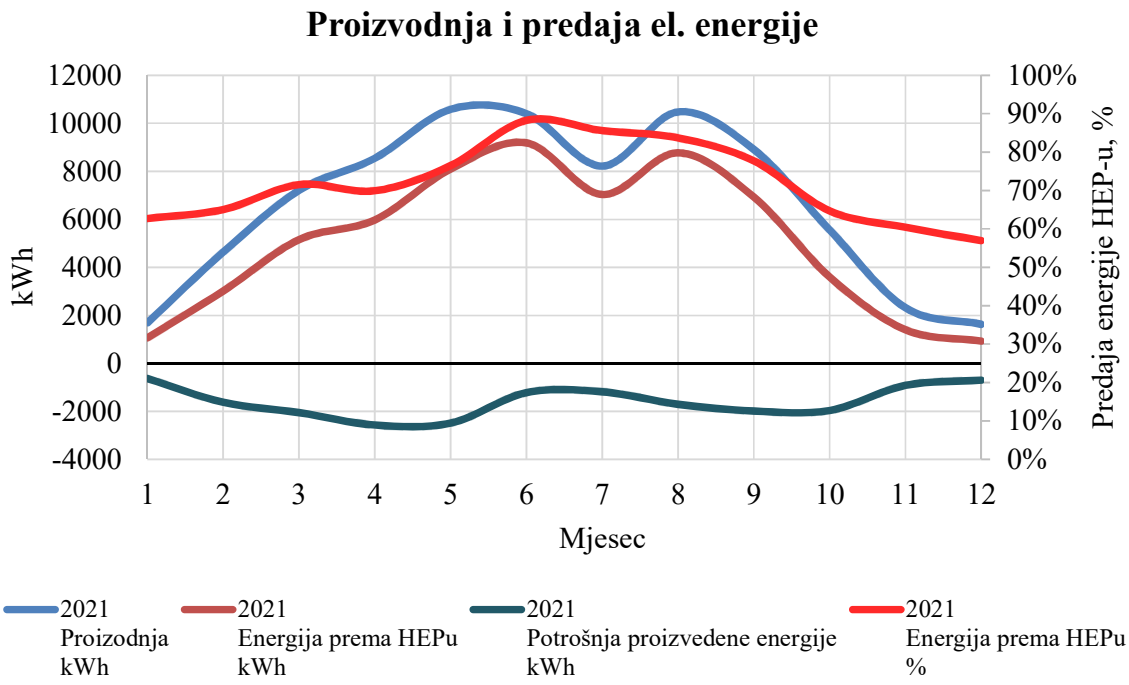

Figure 7.30 Energy monthly data during 2020. and 2021. (UNISB PV power plant in function)

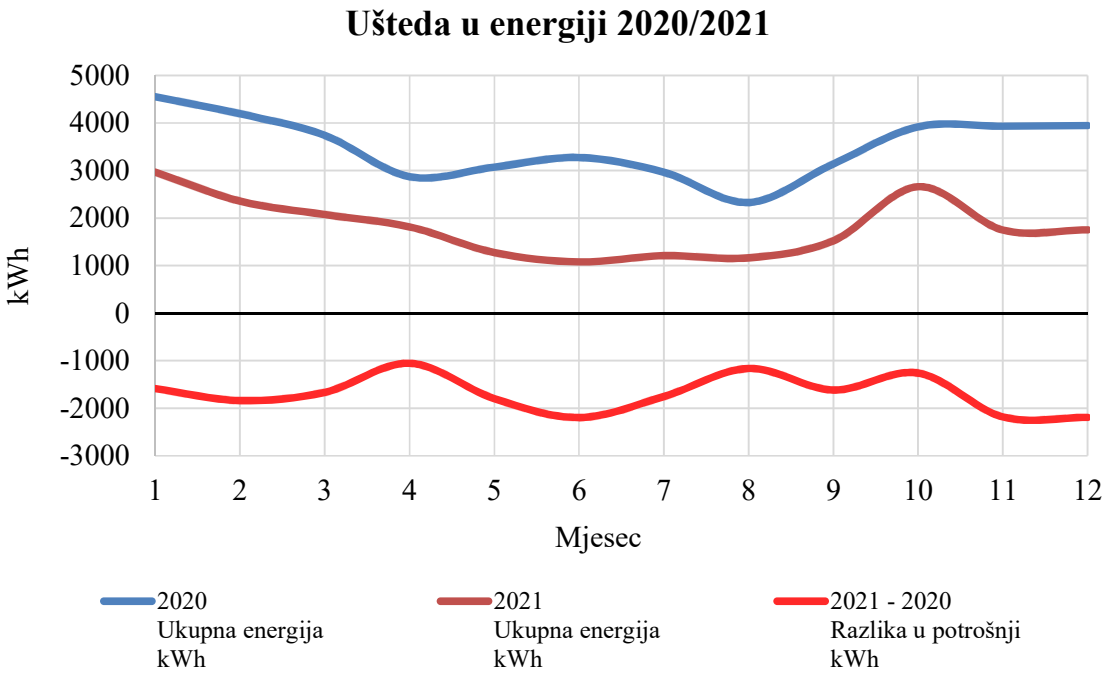

Figure 7.31 Energy monthly savings between 2020. and 2021. (UNISB PV power plant in function)

Conclusion

Realised renewable energy-based systems represent a diverse mix spanning from PV systems, renewable energy storage systems, charging stations, wind energy systems, HVAC systems, biodiesel generators and biodiesel generation systems, solar-thermal systems and heat-pump systems installed on exemplary facilities of project partners. BEMS developed enable continuous monitoring and control of the systems enabling the conversion to smart public buildings. The stored data from developed BEMS will enable the performance analysis of all installed renewable energy systems on the facilities, optimizing the work of individual subsystems, education of our students and experts with the new technologies of RES and performing of scientific researches.

8. References

[1] "When will fossil fuels run out? - Ecotricity." https://www.ecotricity.co.uk/our-green-energy/energy-independence/the-end-of-fossil-fuels (accessed Nov. 20, 2019).
[2] H. Ritchie and M. Roser, "CO_2 and Greenhouse Gas Emissions," *Our World Data*, May 2017, Accessed: Nov. 20, 2019. [Online]. Available: https://ourworldindata.org/co2-and-other-greenhouse-gas-emissions
[3] "The Cost of Energy, Environmental Impact — The National Academies." http://needtoknow.nas.edu/energy/energy-costs/environmental/ (accessed Nov. 20, 2019).
[4] A. Ç. Köne and T. Büke, "Forecasting of CO2 emissions from fuel combustion using trend analysis," *Renew. Sustain. Energy Rev.*, vol. 14, no. 9, pp. 2906–2915, Dec. 2010, doi: 10.1016/j.rser.2010.06.006.
[5] A.-C. Gaeta Hernández, "REDUCING HEALTHCARE'S CLIMATE FOOTPRINT," Dec. 2016. [Online]. Available: https://noharm-europe.org/sites/default/files/documents-files/4746/HCWHEurope_Climate_Report_Dec2016.pdf
[6] H. Ritchie and M. Roser, "Renewable Energy," *Our World Data*, Dec. 2017, Accessed: Nov. 20, 2019. [Online]. Available: https://ourworldindata.org/renewable-energy
[7] "Global Energy Transformation: A Roadmap to 2050 (2018 edition)," */publications/2018/Apr/Global-Energy-Transition-A-Roadmap-to-2050*. /publications/2018/Apr/Global-Energy-Transition-A-Roadmap-to-2050 (accessed Nov. 20, 2019).
[8] "International Energy Outlook 2019." https://www.eia.gov/outlooks/ieo/ (accessed Nov. 20, 2019).
[9] European Commission, "Energy efficiency directive." Accessed: Nov. 26, 2019. [Online]. Available: https://ec.europa.eu/energy/en/topics/energy-efficiency/targets-directive-and-rules/energy-efficiency-directive
[10] "DIRECTIVE (EU) 2018/ 2002 OF THE EUROPEAN PARLIAMENT AND OF THE COUNCIL - of 11 December 2018 - amending Directive 2012/ 27/ EU on energy efficiency," p. 21.
[11] *Directive 2010/31/EU of the European Parliament and of the Council of 19 May 2010 on the energy performance of buildings*, vol. OJ L. 2010. Accessed: Nov. 26, 2019. [Online]. Available: http://data.europa.eu/eli/dir/2010/31/oj/eng
[12] "Geoportal DGU." https://geoportal.dgu.hr/ (accessed Dec. 28, 2019).
[13] Croatian Meteorological and Hydrological Service, "Climate of Croatia - general characteristics." https://meteo.hr/klima_e.php?section=klima_hrvatska&param=k1 (accessed Dec. 28, 2019).
[14] Croatian Meteorological and Hydrological Service, "Climate of Croatia - wind atlas." https://meteo.hr/klima_e.php?section=klima_hrvatska&param=k1_8 (accessed Dec. 28, 2019).
[15] Croatian Meteorological and Hydrological Service, "Monthly values and extremes for Osijek." https://meteo.hr/klima.php?section=klima_podaci&param=k1&Grad=osijek (accessed Dec. 28, 2019).
[16] Marko Jazvić et. al., "Elaborat utjecaja sunčane elektrane KBC Osijek na elektroenergetsku mrežu Onkologija i radiologija," 2021.
[17] "Energy Sector Development Strategy of the Republic of Serbia for the period by 2025 with projections by 2030." Republic of Serbia, Ministry of Mining and Energy, Department for strategic planning in energy sector, 2016.
[18] "Photovoltaic Geographical Information System (PVGIS)." https://ec.europa.eu/jrc/en/pvgis
[19] "Global Solar Atlas." https://globalsolaratlas.info/map
[20] B. Nešić, "Upravljanje komunalnim otpadom i potencijali za reciklažu južne i jugoistočne Srbije." 2010.
[21] "Statistika otpada u Republici Srbiji 2010-2013." Republički zavod za statistiku, 2015.
[22] "JRC Photovoltaic Geographical Information System (PVGIS) - European Commission." https://re.jrc.ec.europa.eu/pvg_download/map_index.html (accessed Dec. 28, 2019).
[23] Energy Institute Hrvoje Požar, "Potencijal obnobljivih izvora energije u Osječko-baranjskoj županiji (Renewable energy sources potential in Osijek-Baranja county)." 2013.

[24] "Sonnenkraft Solar Calculator." [online], https://www.sonnenkraft.com/en/solar-calculator.html. [Online]. Available: https://www.sonnenkraft.com/en/solar-calculator.html
[25] "E-bike Market | Growth, Statistics, Industry Forecast 2019-2024." https://www.mordorintelligence.com/industry-reports/e-bike-market?gclid=EAIaIQobChMI0p3e28265gIVieR3Ch13pwbOEAAYASAAEgJQvPD_BwE (accessed Dec. 17, 2019).
[26] Sunceco, Inc., "SUNCECO SEM 300W-HE datasheet." 2019.
[27] "HOMER Pro - Microgrid Software for Designing Optimized Hybrid Microgrids." https://www.homerenergy.com/products/pro/index.html (accessed Dec. 28, 2019).
[28] GROWATT NEW ENERGY TECHNOLOGY Co.,LTD, "Growatt MID 20KTL3-X datasheet," 2021. Accessed: Dec. 14, 2021. [Online]. Available: https://www.ginverter.com/upload/file/contents/2021/03/6062c5092dd23.pdf
[29] GROWATT NEW ENERGY TECHNOLOGY Co.,LTD, "Growatt 10000TL3-S datasheet." Accessed: Dec. 14, 2021. [Online]. Available: https://www.4blue.nl/media/wysiwyg/Growatt_8000TL3S_-_11000TL3S.pdf
[30] GROWATT NEW ENERGY TECHNOLOGY Co.,LTD, "Growatt SPH 5000TL3-BH datasheet," 2021. Accessed: Dec. 14, 2021. [Online]. Available: https://www.ginverter.com/upload/file/contents/2021/01/6014b53817b25.pdf
[31] Luxor Solar GmbH, "Luxor EcoLine M60/320W datasheet," 2019. Accessed: Dec. 14, 2021. [Online]. Available: https://www.luxor.solar/files/luxor/solarmodule/datenblaetter/LX_DB_EcoLine_M60_300-320W_EN.pdf
[32] GROWATT NEW ENERGY TECHNOLOGY Co.,LTD, "H48050 Box-4," 2021. Accessed: Dec. 17, 2021. [Online]. Available: https://www.stralendgroen.nl/wp-content/uploads/2021/02/Datasheet_Growatt-H48050-BOX_2020_ENG.pdf
[33] GROWATT NEW ENERGY TECHNOLOGY Co.,LTD, "Residential Energy Storage Solutions," 2021. Accessed: Dec. 17, 2021. [Online]. Available: https://www.ginverter.com/upload/file/admin/2020/11/5fa395586de02.pdf
[34] SMA Solar Technology AG, "SMA Sunny Tripower CORE1 datasheet," 2021. Accessed: Dec. 14, 2021. [Online]. Available: https://files.sma.de/downloads/STP50-41-DS-en-14.pdf
[35] SMA Solar Technology AG, "SMA Sunny Tripower 20000TL datasheet," 2021. Accessed: Dec. 14, 2021. [Online]. Available: https://files.sma.de/downloads/STP15-25TL-30-DS-en-41.pdf
[36] Solvis d.o.o., "Solvis SV60-300E datasheet," 2019. Accessed: Dec. 14, 2021. [Online]. Available: https://solvis.hr/wp-content/uploads/2019/05/LQSOLVIS-DS-HR-SV60_E_5BB-1640x992x40-290-310-20190125.pdf